CHAPTER 1
INTRODUCTION

1.1 Background

Thermal Energy Storage (TES) tank is normally used to enhance utilization of thermal energy to meet the fluctuating demand in the supply of chilled water for air-conditioning systems. The advantage of TES tank is that it enables shifting of energy usage from off-peak demand to on-peak demand requirement. This is achieved by charging the tank during off-peak periods and discharging it during on-peak periods. The capability of increasing the thermal energy utilization has led TES tank to be incorporated to cogeneration plants, such as district cooling or heating, and some other plants that are involved in energy utilization.

In district cooling plant where electricity and cooling capacity are generated, TES tank could function in supporting chillers to meet cooling demand. The benefits of using TES tank incorporated to district cooling are [1]:

i. Reduces equipment size,
ii. Capital cost saving,
iii. Energy cost saving,
iv. Energy saving,
v. Improves chillers operation.

District cooling plant normally utilizes two types of chillers namely absorption and electric chillers. Absorption chillers are operated inexpensively by recovering waste heat from the gas turbines. Even though low in cost operation, absorption chillers are not utilized for charging of TES tank [2]. On the other hand, electric chillers are costly to operate, since they consume electricity. Thus, the current practises of charging TES tank using electric chillers could lead to cost reduction if absorption chillers are also used to charge the TES tank. Among the reason absorption chillers not being utilized for charging the TES tank is due to temperature limitation in the absorption chillers. The restriction is that the outlet charging temperatures during charging have to be maintained above the operation temperature limit of absorption chillers [3]. If the limitation can be solved, absorption chillers can be effectively used for charging the TES tank by utilizing waste heat from gas turbines. Thus, it would increase energy utilization of district cooling plant.

Important considerations to overcome temperature limitation in the charging of TES tank using absorption chillers involve two aspects namely identification of temperature distribution characteristics and determination of charging parameters. The first aspect is related to water temperature distribution in a stratified TES tank incorporated to cogeneration plant. Stratified TES tank has naturally separation mechanism in which water temperature forms a stratified formation. The water temperature distribution characteristic holds important role for evaluating charging performance. Besides reflecting cumulative cooling capacity, temperature distribution is also used to measure the important TES tank parameters such as mixing factor and separation performance [4].

The other aspect is determination of charging parameter of stratified TES tank. The charging parameter is required for enabling determination of charging duration as well as cumulative cooling capacity. Among the charging parameters, limit capacity is an important basis for determination of initial and final states charging stratified TES tank. Initial state of the charging has to be set properly to ensure supply cooling demand with proper temperature. Final state of the charging needs to be served effectively in achieving full capacity in the charging stratified TES tank. Determination of final state charging is also essential to avoid excessive partial load charging from the chillers [5].

This research focuses on the study of temperature distribution of charging stratified TES tank. The results of temperature distribution analysis are subjected to overcome temperature limitation of absorption chillers to complement electric chillers to charge stratified TES tank. In the purpose of identification and validation, historical data of operating TES tank were acquired in this study.

1.2 Problem Statement

The main consideration on the charging of stratified TES tank involving absorption chillers is solution of temperature limitation problem. Related to this consideration, two issues that were required to be resolved are as follows:

i. Temperature distribution has important role in the charging stratified TES tank characteristics. Intensive analysis of temperature distribution is required to determine charging parameters as well as identification of temperature distribution characteristic in the charging of stratified TES tank.

ii. Charging characteristic is significantly influenced by the working parameters of TES tank and chillers. Simulation model which covers TES tank and chillers parameters could assist in identification of charging characteristic under various temperature limitations in the charging stratified TES tank.

1.3 Objective of Study

The main objective of this study is to develop simulation models which incorporate absorption chillers in combination with electric chillers to charge stratified TES tank. This is to be achieved by developing single and two-stage charging models as follows:

i. Development of single and two-stage charging models in an open charging system that is capable of synthesizing temperature distribution characteristics and determining charging parameters using the stratified TES tank.

ii. Development of single and two-stage charging models using a close system that enable integrating of TES tank and chillers parameters.

1.4 Scope of Study

The scope of the study covers the following:

i. The TES used in this study is stratified cylindrical tank for storing of chilled water.

ii. The simulation charging models that were developed based on open charging system used temperature distribution analysis of stratified TES tank.

iii. The simulation charging models in close system were established on one dimensional conduction-convection equation based. Assumption of the model was due to conduction between cool-warm water and mixing effect factors. The conduction through the wall and heat loss to surrounding is assumed negligible.

1.5 Organization of Thesis

The organization of the thesis is as follows:

Chapter 1 contains a review of the research background, the problem statement, the dissertation objectives, the scope of study and the organization of thesis.

Chapter 2 reviews literatures related to the stratified TES tank. It contains introduction to TES system in cogeneration plant, water temperature distribution, charging cycle in stratified TES tank, simulation model of TES tank and its solution, chiller models and non linear regression fitting.

Chapter 3 explains the methodology used in developing single and two-stage charging models in open and close system. The models of the open charging system are developed based on temperature distribution analysis. In the water temperature distribution analysis, it involves defining parameters of temperature distribution profile and selecting the function with non linear regression fitting. Formulation of charging parameters of the models based on temperature distribution function. In the close charging system, the models are developed by integrating TES tank and chillers. For both open and close charging system, the models are developed for single stage and enhanced for two-stage charging model. The verification and validation is performed at the single stage charging model using historical data of operating TES system. Finally, comparison of the two models in open and close charging system is carried out through several simulation cases in single and two-stage charging stratified TES tank.

Chapter 4 contains the results and discussion of the work accomplished. The results is divided into three main parts : development of the single and two-stage charging models in open system, development of single and two-stage charging models in close charging system and comparison analysis of the models. It continues for its verification and validation using historical data of operating TES. The simulation of the single and two-stage of charging and comparison analysis of these two models are carried out. Summary is presented in the final section of Chapter 4.

Chapter 5 draws the overall conclusions and recommendations for future works, based on the findings of this research. These conclusions, contributions and recommendations address the objectives stated in the Section 1.3.

CHAPTER 2
LITERATURE REVIEW

This chapter reviews relevant literatures on stratified thermal energy storage (TES) tank incorporated to district cooling plant. The review covers TES tank in cogeneration plant, details of stratified TES tank, temperature distribution in the stratified TES tank, factors degrading stratification of temperature distribution, charging of stratified TES tank, models of stratified TES tank, chiller models and non linear regression fitting.

2.1 Thermal Energy Storage Systems in Cogeneration Plant

Cogeneration work as combined heat and power (CHP) plant which generate electricity and heat simultaneously [6]. The electricity is generated from mechanical works from turbine, while the heat is produced by utilizing waste heat of the turbine. The main advantage of cogeneration is that less consumed energy to generate heat for demand requirements. Utilizing cogeneration, it has benefit in reducing more than 35% electricity cost as well as plenty of free cooling and or heating [7]. An additional benefit of cogeneration is reducing of environment emissions and more economic operation.

The cogeneration is constructed as district heating or district cooling. For supplying heating demand, cogenerations are constructed as district heating. District cooling, on the other hand, is more suitable for tropical countries where substantial cooling is required. In the district cooling, absorption chiller is incorporated to the cogeneration plants. The absorption chiller generates cooling capacity that is obtained by utilizing waste heat from the turbine [8]. It offers benefit to supply the space cooling requirement of building in the residential, commercial and institutional sectors in tropical countries [9, 10].

In a district cooling system, chilled water is supplied from the chillers plant and transported to meet cooling demand. Several chillers can be used, including electrically driven vapor compression chillers and absorption chillers. Absorption chillers can operate on steam utilized from waste heat of gas turbine [11-14], hence increase the thermal efficiency of cogeneration plant [15, 16].

Beside implementing absorption chiller for utilizing waste heat, district cooling store excess thermal energy as chilled water in TES tank [17]. Having capability to store chilled water, the TES tank is efficient for shifting energy utilization from on-peak to off-peak demand periods. It is realized that if chilled water could be generated and stored during off-peak demand, more cooling capacity would be utilized later for on-peak demand [18]. Beside avoiding mismatch between cooling supply and demand, the TES tank also has advantages in meeting society's preference for more efficient and economic operation [19]. The TES tank can be implemented into two types of storage namely latent or sensible. In the latent storage, the tank use ice cool storage whereas in sensible storage uses chilled water [20]. The chilled water temperature in the sensible storage form stratified, therefore it is well known as stratified TES tank.

2.2 Stratified Thermal Energy Storage Tank

TES tank application was introduced in 1980's and become popular and widespread currently in response to the efforts of increasing of energy utilization [21]. TES tank has also been utilized for many years incorporated to district cooling plant as a load shifting cooling demand technology. This takes advantage from its capability to store cooling capacity during off-peak and supply it within on-peak demand periods, allowing it to make more effective utilization of meeting cooling requirement.

Several technologies for TES tank have been implemented to enhance its applications. The important factor of the TES tank is separation mechanism between cool and warm water [22]. This is obtained either by providing physical barrier inside tanks or using natural stratification. Physical barrier separation have been implemented with labyrinth, baffle and membrane, whereas natural is achieved in thermally stratified systems [22]. In the first case, separation is obtained with a maze mechanism, whereas in latter case separation is made by natural process of stratification that permit the warm water to float on the top of cool water [23]. Compared to the first case, naturally stratified tanks are simple, low cost, and equal or superior in thermal performance [24], therefore they have become a choice for many TES design.

Most stratified chilled-water storage tanks are cylindrical vessels provided with two nozzles installed at lower and upper parts of the tank [25]. Diffusers are provided at the end connection of the nozzles to preserve stratification by minimizing the disturbance caused by inlet and outlet water flows in the tank [26]. This configuration allows the TES tank to be operated either by charging or discharging. Charging is conducted during off-peak cooling demand while discharging during the on-peak cooling demand [27]. Charging is performed by introducing cool water into the lower nozzle while warm water is withdrawn from the upper nozzle of TES tank [28]. Reversely, discharging is carried out by withdrawing the cool water from the lower nozzle while warm water is introduced from the upper nozzle. Schematic flow diagram of charging and discharging stratified TES tank is presented in Figure 2.1.

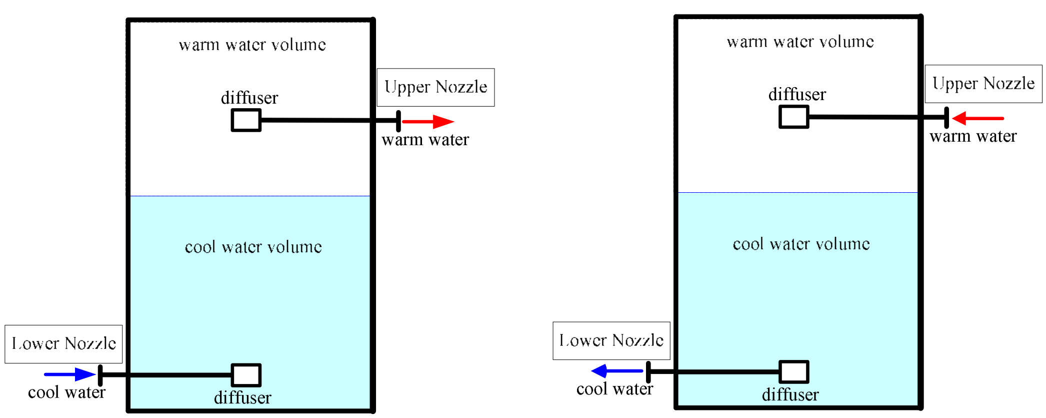

(a) Charging (b) Discharging

Figure 2.1 Schematic flow diagram of charging and discharging stratified TES

2.3 Water Temperature Distribution in the Stratified TES Tank

In a stratified TES tank, warm water resides above cool water without an intervening physical barrier. Separation is maintained by the natural density difference between the warm and cool water. The warm and cool layers are separated by a thin transition region namely thermocline. Temperature distribution form stratified layers similar to S-curve in which cool water settled in the lower part and warm water in the upper part, whereas thermocline settled in middle region [29]. This typical stratification temperature distribution were confirmed by some fundamental literatures [22, 30] and [28, 29, 31]. A typical temperature profile in a stratified TES tank is presented in Figure 2.2.

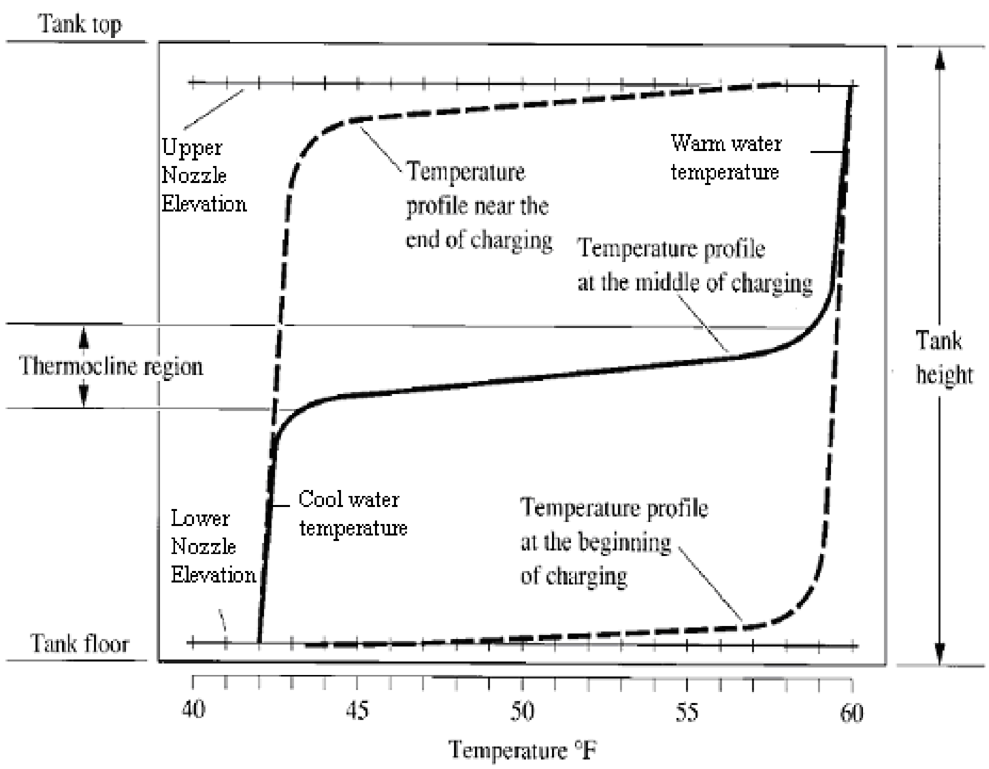

Figure 2.2 A typical temperature profile in stratified TES tank [29]

From Figure 2.2, it is inferred that cool water volume exists in the lower part of the TES tank, whereas warm water exists in the upper part. The boundary limit between cool and warm water volume is located at midpoint of thermocline thickness.

The cool water temperature has small difference and often has accounted exist at its average temperature, this also occurs at warm water temperature [32]. The inclined line of cool and warm water is assumed to be straight line which indicates the average temperature of that two water volume in the stratified TES tank.

2.3.1 Researches in Temperature Distribution of Stratified TES Tank

Temperature distributions have been a subject of number of researches, both for full scale and experimental measurements. This is important to identify not only cumulative cooling capacity but also its performance [33]. Temperature distribution was used to observe stratified TES tank in several purposes such as performance evaluations, parametric studies, characterization as well as determination of mixing effects. Observations were carried out using both field measurement and experimental approaches.

Musser and Bahnfleth [34] used temperature profile of a full scale stratified chilled water TES tank for determining thermocline thickness at various charging and discharging flow rate. The temperature was also carried out to evaluate the performance in term of half-cycle figure of merit. Half-cycle figure of merit is defined as a metric performance which measure lost capacity due to mixing and conduction between the cool and warm water volume in the stratified TES tank [35]. Bahnfleth, et al. [36] used temperature distribution to evaluate thermocline thickness on a full scale stratified TES tank with slotted pipe diffuser.

Temperature distribution was also used to conduct parametric study on special diffuser configuration of stratified TES tank. Musser and Bahnfleth [37, 38] utilized temperature distribution for radial diffuser configuration. In this work, temperature distribution was used for validation of a computational fluid dynamics (CFD) model of stratified TES tank. Parametric study was also performed by Jing Song and Bahnfleth [39] which utilized temperature distribution for single pipe diffuser in stratified chilled water storage tank.

Bahnfleth and Jing Song [40] conducted charging characterization of chilled water storage tank with double ring octagonal slotted pipe diffusers. This research was conducted in constant flow rate. Initial temperature distribution was at a relatively uniform temperature after being fully discharged. In this research, the performance was quantified using thermocline thickness and half-cycle figure of merit. Caldwell and Bahnfleth [41] used the temperature distribution data to validate one-dimensional model of TES tank that used to identify mixing effect in stratified chilled water storage tank.

The researches have also been conducted through experimental study related to temperature distribution in stratified TES tank. Nelson, et al. [42] conducted experimental studies on thermal stratification in chilled water storage system. The experimental were conducted in static and dynamic modes operation with variation of parameters aspect ratio (height over diameter of the tank), flow rates, initial temperature difference and thickness of insulations. The static mode was performed on a certain portion of cool and warm volume occupying the tank. On the dynamic mode, experiment was performed through charging and discharging cycles. In this research, temperature distributions were used to evaluate percentage of recoverable cooling capacity and mixing effect.

Karim [43] investigated performance evaluation of a stratified chilled water tank using experimental study. The experiments were conducted on the charging of stratified TES tank. In this study, water temperature distribution was used to evaluate the performance of stratified TES tank with respect to various inlet diffuser configurations and charging flow rates.

Walmsley et al. [44] used siphoning method to manage thermocline thickness in experimental stratified TES tank. Water temperature distribution was used to evaluate the effect of re-established method on stratified TES tank operations.

2.3.2 Parameters Derived from Temperature Distribution

Temperature distribution are utilized to determine parameters in stratified TES tank such as thermocline thickness and half-cycle figure of merit [35]. Thermocline thickness is often used to measure the separation performance of the TES tank with different inlet diffuser configurations of stratified TES tank. Thinner thermocline is desired, since it expresses a small portion of mixing in tank [27]. The other performance parameter in stratified TES tank, half-cycle figure of merit was determined based on lost capacity due to mixing and conduction in the stratified TES tank. Conceptually, half-cycle figure of merit reflects the ratio of useful capacity over theoretical capacity within charging or discharging cycles.

Determination of performance parameters was based on the thickness of thermocline profile in the temperature distribution. The thickness of thermocline is defined as a region limited by upper and bottom limit points in the temperature distribution. Arbitrary values in determination of the edges of thermocline thickness has been defined based on different approaches [45].

Yoo, et al. [45] estimated thermocline thickness by extrapolating the thermocline edges from mid point of thermocline. Using interpolation, thermocline edges is determined as region fringed to linear gradient of thermocline profile. This approach has drawback in determination of thermocline edges not at the real upper and lower limit of thermocline profile.

Homan, et al. [46] implemented the lower edge of the thermocline at the point where temperature located at the highest usable temperature for the application. The upper edge is assumed to be located at the linear region from midpoint of thermocline thickness. The shortcoming of this approach is that temperature profile would have two different values of thermocline thickness.

Musser and Bahnfleth [47] used a flexible and more reliable method. A dimensionless cut-off temperature on each edge of the profile was chosen to bind the region in which most of the overall temperature change occurs. It was suggested that the amount of the temperature profile to discard should be large enough to eliminate the effects of small temperature fluctuation at the extremities of the thermocline, but small enough to capture most of temperature change. The dimensionless cut-off temperature (Θ) take forms as the following.

$$\Theta = (T-T_c)/(T_h-T_c) \tag{2.1}$$

With T is a determined water temperature, T_c and T_h are average cool and water warm water temperature, respectively.

Comparing the approaches that have been reviewed, dimensionless cut-off ratio temperature by Musser and Bahnfleth [47] offers advantage as it could cover wider implementation for determining thermocline thickness in stratified TES tank.

Method for determination of the thermocline thickness was carried out by estimation from continuous temperature distribution profile. In order to have accurate solution, continues profile was obtained using temperature distribution recorded in short time interval such as minute [34]. As it was determined based on estimation, the method has drawback from its accuracy. Another difficulty in determination of thermocline thickness arose if the temperature distribution are available as discrete data, such as hourly interval time, due to ambiguity in determining the thermocline edges [48].

Several literatures reported the current efforts for improving the method for determination parameters using temperature distribution function [48-50]. It has been initiated by formulating thermocline thickness based on functional relationship of temperature distribution. The improved approach offers beneficial in determination parameters exactly from formulation.

2.3.3 Degradation of Stratification Temperature Distribution

Identification of temperature distribution characteristics requires consideration of several factors affecting degradation of temperature stratification. There are four factors that mainly affect degradation of stratifications namely conduction across the thermocline, mixing during the initial stages of charging and discharging, heat loss to the surroundings and conduction through the walls [23]. Degradation of the stratification identifies changing in shape of the typical temperature distribution expressing as broadening of thermocline thickness and changing the inclination cool and warm water temperature.

i. Conduction across the thermocline

Conduction across the thermocline was found to be a minor factor in degradation of stratification. This is due to low thermal conductivity of water inside stratified TES tank. This factor is commonly available in the form of conductivity parameter in one-dimensional model [51]. Since the stratified TES tank store both cool and warm water, therefore this factor can not be avoided.

ii. Mixing effect on stratified TES tank

Mixing introduced by the inflow in the TES tank operations as a major contributor to the degradation of the stored energy [52]. The mixing affects the degradation of temperature distribution as well as cumulative cooling capacity in the stratified TES tank. This leads to turbulent flows that enhance mixing and broaden the thermocline. The mixing near the inlet nozzles has more significant effect on the temperature distribution in the tank and mainly affected by diffuser characteristics [26]. Hence, In the operation of stratified TES tank, it is recommended to install appropriate diffuser at nozzle connections [30].

Mixing can also affect water temperature difference between supplied and existing water in the stratified TES tank. In the case of charging cycle where cooler water is introduced into the cool water volume settled in the lower part of the tank, mixing effect has small influence in degrading of temperature distribution. On the other hand, at condition of initial discharging where warm water enters the cool water in the upper part of the tank, mixing has highest influence to the temperature water distribution degradation [45]. This is due to infringement of warm water into cool water volume that enhances mixing in the stratified TES tank.

iii. Conduction through the wall

The conduction along the wall affects cooling the warm water region close to the wall and heating the cool water region. This leads to buoyancy induced convective currents that broaden the thermocline. The conducting wall factor exist in the static condition in the tank as reported in the experimental researches by [53, 54].

However, in some dynamic cases such as in the charging mode, the heat conduction through the wall was found to have a negligible effect on stratification [55]. Small effect of conduction through the wall has also been shown on analytical studies of stratified TES tank [46]. In the temperature distribution analysis, the conduction through the wall was eliminated [34].

In the construction of stratified TES tank, there are some suggestions to reduce the conducting wall factors. The recommendation is that an insulation layer should be applied at the interior surface of the tank and the tank wall must be made of a material with has smaller conductivity [27] .

iv. Heat loss to surrounding

Together with other factors, heat loss to surrounding influence degradation of temperature distribution in enhancing the mixing and broadening thermocline. Experimental study shows that heat loss surrounding affecting stratification of water temperature distribution [42]. The occurrence of heat loss to surrounding can be reduced by installing sufficient external insulation of the tank [23].

2.4 Charging Cycle in Stratified TES Tank

The stratified TES tank is operated either at charging or discharging mode. The charging mode is performed when no cooling demand has to be served whereas discharging mode is performed for meeting cooling demand. Both modes are performed while the TES tank remains full of water. In the charging cool water is introduced from the lower nozzle while the warm water is withdrawn from the upper nozzle. Due to changing of cool-warm during the cycle, water temperature distribution in the TES tank change with respect to time [42]. During charging the temperature profile move upward to the upper tank [30, 47].

Temperature distribution profile in the charging cycle is mainly affected by the preceding discharging. The highest degradation temperature profile occurred at initial discharging. As temperature profile move away from the nozzle, mixing effect decrease and conduction across thermocline increases with respect to time [34].

The former temperature profile is brought over as the discharging progressing and the final state of discharging cycles will be initial state of charging. In the charging cycles, mixing effect has no significant influence to the degradation of temperature distribution. This is due to commencing of cool water into cool water region in the lower part of the TES tank. For this condition, some researches use a constant assumption of thermocline thickness during charging periods [56, 57].

2.4.1 Empty and Full Capacities

Monitoring of empty and full capacity of charging stratified TES tank is required on the TES tank system incorporated to the utility plant. For the case of stratified TES tank incorporated to district cooling plant, the cut-off water temperature has important role in determination limit capacity in the charging mode [29]. Empty capacity reflects the lowest capacity of the TES tank to serve cooling demand is identified at lower nozzle elevation has cut-off water temperature. Exceeding this temperature causes supplying higher temperature to meet cooling demand. Full capacity of stratified TES tank, on the other hand, is reached when upper nozzle elevation temperature equals to cut-off water temperature. If the charging is continued, the chillers operate in part load condition which indicates less additional cumulative cooling capacity on the charging. Limit capacity is defined as capacity difference between full and empty capacity in the charging. Temperature distributions at empty and full capacity of charging stratified TES tank are illustrated at the beginning and the end of charging in Figure 2.1.

At empty capacity condition, cool water depth is located above lower nozzle elevation. This condition is identified when the cumulative cooling capacity of TES tank has been discharged [58]. The full capacity of the stratified is determined at full charged condition. It is identified when outlet charging temperature equal to secondary limit temperature, that is normally determined approximately to cool water temperature [22].

For the purpose of measuring the performance of stratified TES tank, determination of empty and full test capacity is referred to charging temperature. For measuring half-cycle figure of merit [35], the empty capacity has uniform temperature at average warm temperature. Whereas full test capacity is determined at the outlet temperature is equal to the inlet temperature.

2.4.2 Inlet and Outlet Charging Temperature

Charging cycle is considered as a close charging system between TES tank and chillers equipment [22]. The charging inlet temperature is the water temperature entering the TES tank through lower nozzle after being cooled by the chillers. The outlet charging temperature is exit water temperature from the tank through upper nozzle. Figure 2.3 illustrates the inlet and outlet temperature during charging cycles.

Initially, the inlet temperature stays fairly constant and slightly decreases later as charging progress. Similarly, this trend occurs in charging outlet temperature, with steeper decrease. The outlet and inlet water temperature characteristic is influenced by temperature distribution in the stratified TES tank. The decreased temperature emerges after upper limit point of thermocline profile commencing the upper nozzle [30]. Decreasing trends of outlet temperature is also used as an indication of the occurrence of partial load in the chillers during charging [29].

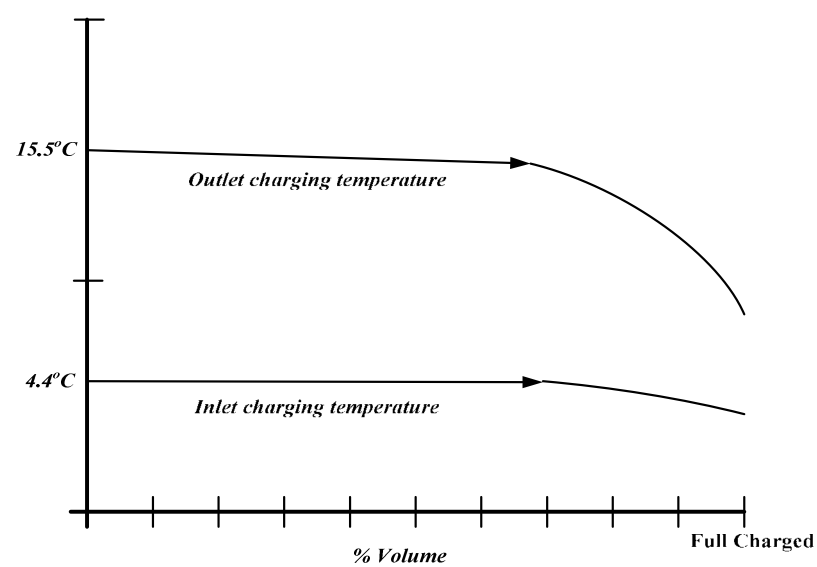

Figure 2.3 Inlet and outlet stratified TES tank temperature during charging [22]

The relationship between outlet and charging temperature depend on working cooling capacity of the chillers. The chillers parameters such as working evaporator temperature and flow rate affect the values of the inlet water in the charging of stratified TES tank [22].

2.4.3 Stratified TES Tank Operation

In the operation of stratified TES tank, the important parameter to be monitored is cumulative cooling capacity stored in the tank. The cumulative cooling capacity is determined by multiplication of water mass, specific heat and temperature difference in the storage to reference temperature [25]. This is calculated based on reference temperature criterion reflecting initial warm water temperature. The other parameter that has to be identified in the operation of stratified TES tank is the charging duration. This is conducted to estimate sufficient charging duration during off-peak demands [44].

2.5 Model of Stratified TES Tank

A number of studies of stratified TES tanks were conducted based on heat transfer aspect utilizing one-, two- and three- dimensional models [59]. Selection of the model depends upon the dimensional flow in the study. One-dimensional flow model is suitable for study in one flow direction; otherwise two- or three-dimensional models can be utilized. Comparing between the models, two- and three-dimensional model have specific requirement, which make them suitable for accounting hydrodynamic, thermal and geometric conditions only for specific configuration of stratified TES tank [23]. Because of specific requirements two- and three-dimensional models are generally avoided despite their potential for assessing stratified TES tank design concepts.

One dimensional that is highlighted here has an advantage that could be performed as general simulation model. It does not require detailed heat transfer aspect that makes it only suitable for specific configuration of stratified TES tank. The other consideration is that one-dimensional flow models lies in the fact that they are computationally more efficient than two- or three-dimensional models, which make them ideal to be utilized for simulation of charging model. Even though it is simple, more accurate result can be achieved [23].

2.5.1 One-Dimensional Model

One-dimensional model covers general heat transfer aspect in the storage tank. Conceptually, the one-dimensional model is established based on uniform temperature at horizontal layers with one-dimensional flow direction. The one-dimensional nature of the temperature distribution of a stratified TES tank was recognized from early experimental studies [54] and [60]. Jaluria and Gupta [54] investigated thermal decay of an initially stratified fluid in two insulated rectangular tanks. After initially stratified temperature distributions were established and the thermal decay was monitored in term of temperature distribution with respect to time. The measured temperature distribution in static tests exist uniform at horizontal direction. The experimental studies using cylindrical tank was carried out by Gross [60]. The result showed that the radial measurement of temperature distribution in the stratified tank also has horizontal uniformity temperature.

The one-dimensional model of stratified TES tank may be classified into two categories depending on inlet temperature conditions. The classification of the models is suitable for varied inlet temperature and relatively constant inlet temperature. In the case of varied inlet temperature, the model has two types namely fully mixed and non mixed TES tank [61]. These models characterize temperature distribution of the TES tank in term of mass flow rate, temperature difference and overall heat transfer coefficient. A number of literatures reported the usage of the model, however, most application are used for hot water storage tank and solar energy [62]. This is related to its capability of covering variation of inlet temperatures.

For the case of relatively constant inlet temperature as chilled water stratified TES tank, one accurate model has been developed based on one-dimensional conduction and convection equation [63]. The equation can be derived using an energy balance on the control volume of stratified TES tank. The control volume represents a fluid region of uniform temperature on horizontal direction. It is assumed that the flow is one-dimensional subject to convection occurrence of the charging flow rate and conduction between cool and warm water inside the tank.

The thermo-physical properties of the fluid are assumed at the constant average of cool and warm water temperature. Conduction from the wall is assumed to be negligible. Justification for the assumptions has been demonstrated by Gretarsson et al. [63], resulting in energy equation of laminar flow as shown in Equation 2.2.

$$\frac{\partial T}{\partial t} + v.\frac{\partial T}{\partial x} = \alpha \frac{\partial^2 T}{\partial x^2} + \frac{UP}{A.\rho.C_p}(T_a - T) \tag{2.2}$$

With A is the cross-sectional area of the tank, v is the vertical velocity in the tank, U is the overall heat transfer coefficient, P is the tank perimeter, α is thermal diffusivity, T_a ambient temperature and x is tank elevation.

The conduction and convection equation is capable of covering the factor degradation of temperature distribution. The conduction across the thermocline exhibit as thermal diffusivity (α) and heat loss to surrounding is expressed in the last right term of Equation 2.2. The conducting wall factor is not explicitly derived in the parameter, however can be accommodated through initial temperature condition. Factor of the mixing effects which cause turbulent flow is accounted for by introducing effective diffusivity factor [64] as defined as Equation 2.3.

$$\varepsilon_{eff} = (\alpha + \varepsilon_H)/\alpha \tag{2.3}$$

Hence, the Equation 2.4 can be described as a parabolic equation as follows.

$$\frac{\partial T}{\partial t} + v\frac{\partial T}{\partial x} = \alpha.\varepsilon_{eff} \frac{\partial^2 T}{\partial x^2} + \frac{UP}{A.\rho.C_p}(T_a - T) \tag{2.4}$$

Solution of the conduction and convection model can be carried out based on 2 methods namely analytical and numerical solution. Homan [65] used analytical solution on the conduction and convection equation model based on Laplace transform. The solution reveals characterization of temperature distribution and thermocline thickness as a function of Peclet and Froude number.

Jaluria [66] performed analytical solution with assumption of steady state in stratified TES tank. Using this solution, temperature distribution was obtained as a function of TES dimension and time. However, analytical solution is suitable for a few idealized circumstances. Numerical solutions are required for most realistic and practical conditions [67].

Numerical solution can be carried out to solve conduction and convection equation model either using finite element or finite difference. Finite element solution was conducted by Al Najem et al. [68] adopting Chapeau-Galarkin method to correlate mixing factor to Reynolds and Richardson numbers. However, the utilization of finite element was not expanded in the stratified TES tank application. This is due to difficulties in specifying related parameter of mixing in the stratified TES tank. On the other hand, finite difference was often used by many researchers. The advantage of finite difference are ready to be extended to solve various dimensional model [69] and capable of solving partial differential equations such as elliptic, hyperbolic and parabolic [70]. Extensive of finite difference literatures exist on the fluid dynamic and heat transfer aspects [67, 71, 72].

2.5.2 Finite Difference Solution

One scheme for solving all kinds of partial-differential equations is to replace derivatives by difference quotients and converting to difference equation. Solving these equations simultaneously give values for the function to approximate the true values [73]. The difference equations can be written corresponding to each point of grid that subdivides the region with unknown functions.

Using finite difference, the partial difference equation is discretized so that the values of the unknown variable are considered only a finite number of nodal points instead of continuous region. Hence, finite difference method used small segmental element of the tank (Δx) and is observed within time interval (Δt). The basic approaches of discretization is based on Taylor series expansion with backward, central or upward methods [74].

The finite difference solution is subjected to the appropriate initial and boundary conditions. Using ordinary solution, however, the equation generates numerical conduction as a pseudo mixing in the result [75]. Special procedure to eliminate the numerical conduction is by splitting the equation into two cases namely conduction and convection cases [76].

The conduction case is presented as Equation 2.5.

$$\frac{\partial T}{\partial t} = \alpha.\varepsilon_{eff}\frac{\partial^2 T}{\partial x^2} + \frac{UP}{A.\rho.C_p}(T_a - T) \tag{2.5}$$

And the convection case is expressed as Equation 2.6.

$$\frac{\partial T}{\partial t} + v\frac{\partial T}{\partial x} = 0 \tag{2.6}$$

The splitted equation of conduction-convection is performed using buffer-tank concept [76]. Conceptually, the buffer concept tank regulates combination of conduction-convection equations. Conduction is implemented continuously in the calculation, whereas convection is periodically applied at regular time. The buffer tank is used to solve pseudo-mixing in the numerical solution covering variation of flow rate, therefore it has been used for finite difference solution in stratified thermal energy storage cases [77].

The finite different solution can be chosen either implicit or explicit method [74]. The finite difference is unconditionally stable in implicit solution, whereas in explicit solution requires some conditions for stability requirement. The difference between the two solutions is that implicit need iterative method to solve simultaneous calculation, whereas an explicit method is solved using sequential calculation [67]. The accuracy of results between implicit and explicit methods are approximately similar [78].

A number of researches were conducted using finite different to solve one-dimensional flow conduction and convection equation model for various purposes [57], [24], [79] and [80].

Zurigat, et al. [57] utilized the one-dimensional conduction and convection model to compare parameters in six models based on varied inlet temperature models of stratified TES tank. The comparison was conducted using experimental data of TES tank model with insulated externally. The comparison showed that conduction and convection model is capable of quantifying the parameters on varied inlet temperature models.

Nelson et al. [24] utilized non-dimensional equation to perform parametric study on thermally stratified chilled water storage in charging, discharging and static mode. The solution used finite difference with crank nicholson implicit method.

Models of Wildin and Truman [79] used finite difference to solve one-dimensional model to evaluate mixing at the inlet region, thermal capacitance of the tank wall and heat exchange with the surroundings. Mixing in the inlet is quantified by averaging the temperatures of a specified number of liquid elements, *NM*, near inlet nozzle. Results show that the model capable to quantify the thermocline and mixing temperature at several of *NM* parameters.

Zurigat, et al. [80] used one-dimensional flow to predict thermocline development in stratified TES tank. A practical measure of quantifying the mixing was obtained by introducing effective diffusivity factor in one-dimensional model. The solution used finite difference method based on implicit method.

These literatures showed evidence that conduction and convection model are capable in expressing TES tank characteristic. In performing conduction and convective model, mixing effect factor requires to be specified by selecting effective diffusivity (ε_{eff}). The value of effective diffusivity depends on different inlets nozzle conditions and inflow mixing conditions [80]. In the charging of stratified TES tank, however, the effective diffusivity is assumed constant. Among the reason due to charging is conducted when cool water depth located above inlet nozzle elevation. Hence, the mixing does not have significant effect to the degradation of temperature distribution. With regard to this phenomenon, the selection of effective diffusivity parameter in conduction and convection model is performed by referring to initial condition in the charging of stratified TES tank [81, 82].

Votsis, et al. [81] also assumed a constant effective diffusivity factor in their study which involve an insulated tank. Truman and Wildin [82] used conduction and convection model to characterize inlet mixing factor using specified number of segments adjacent to the inlet flows. This model was validated with experimental measurements and reveals that constant effective diffusivity is suitable for charging mode in the TES tank.

2.6 Chillers

The literature reviews are related to vapor compression and absorption chillers. Models of the chiller are also reviewed both for compression and absorption chillers.

2.6.1 Vapor Compression Chillers

The vapor compression cycle is often used for air conditioning and refrigeration applications [83]. There are four main equipments in the vapor compression chillers namely evaporator, compressor, condenser and expansion valve [84]. In the four equipments, refrigerant is circulated as a close charging system. Condenser works at high pressure is used to condense the refrigerant vapor, whereas evaporator is used to vaporize the refrigerant in the low pressure stage. Compression and expansion of the refrigerant are carried out by compressor and expansion valve, respectively. In the condenser, the refrigerant vapor is condensed by rejecting the condenser heat (*Qcond*). Vaporization of the refrigerant in the evaporator is obtained from the load (*Qev*). In district cooling plant, the evaporator heat is used to generate cool chilled water. Schematic cycle of vapor compression chiller is presented in Figure 2.4.

The vapor compression chillers require electrical power to operate the compressor and circulate the refrigerant. The vapor compression chillers are categorized based on the type of compressor being used such as reciprocating, centrifugal and screw compressor [85].

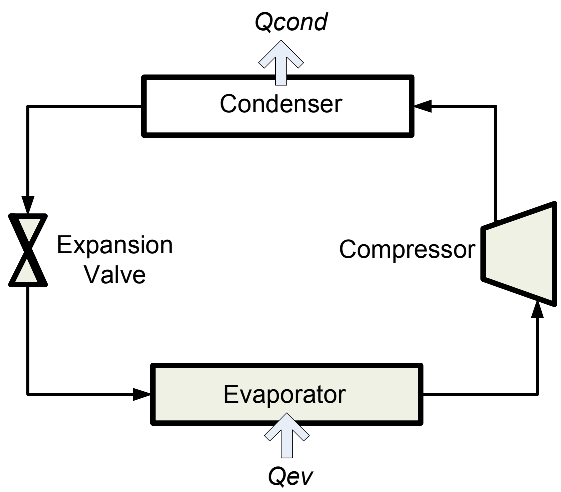

Figure 2.4 Schematic cycle of vapor compression chiller [84]

2.6.2 Absorption Chillers

Absorption chillers were also widely used in cooling and refrigerating purposes. The different working process of the absorption chiller compare to vapor compression chiller is that it replaces the electric driven compressor with a combination of generator-absorber equipments [29]. Absorption chillers require much less electricity than vapor compression chillers. Although electricity is required to drive the circulation pumps in the absorption chillers, the amount of electricity is very small compared to vapor compression chillers [86].

Absorption chillers are often incorporated to cogeneration plant. This take advantage from its capability working at low temperature operation served by waste heat from the turbines of cogeneration plant [87]. Utilization of waste heat by absorption chiller increase heat recovery of the cogeneration plant thereby increases the thermal efficiency of cogeneration plant.

The main equipments of absorption chiller are absorber, generator, condenser, evaporator and expansion valve [88, 89]. Absorption chillers use a liquid solution which is made of mixed adsorbent and refrigerant. Evaporator and absorber works at low pressure whereas condenser and generator at high pressure stage. Refrigerant from the evaporator enter the absorber at low pressure stage. Utilizing external cooling in the absorber (*Qabs*), the refrigerant is absorbed by adsorbent. Since the solution has much more refrigerant, it becomes a weak solution. The weak solution is pumped to the generator which has external supplied heat (*Qgen*). Having heated in the generator, the refrigerant is released from the solution that makes it as strong solution. The strong solution which has higher concentration of adsorbent is re-circulated into the absorber, whereas the refrigerant is circulated to condenser. After being cooled by the condenser heat (*Qcond*), the refrigerant condenses at high pressure. The condensed refrigerant pressure is reduced in expansion valve and circulated to the evaporator. Evaporator heat (*Qev*) for vaporizing the refrigerant is obtained from heat load. In district cooling plant, the evaporator is used to generate cool chilled water. The main heat to operate the absorption chiller is obtained utilizing waste heat to the generator. Schematic cycle of absorption chiller is presented in Figure 2.5.

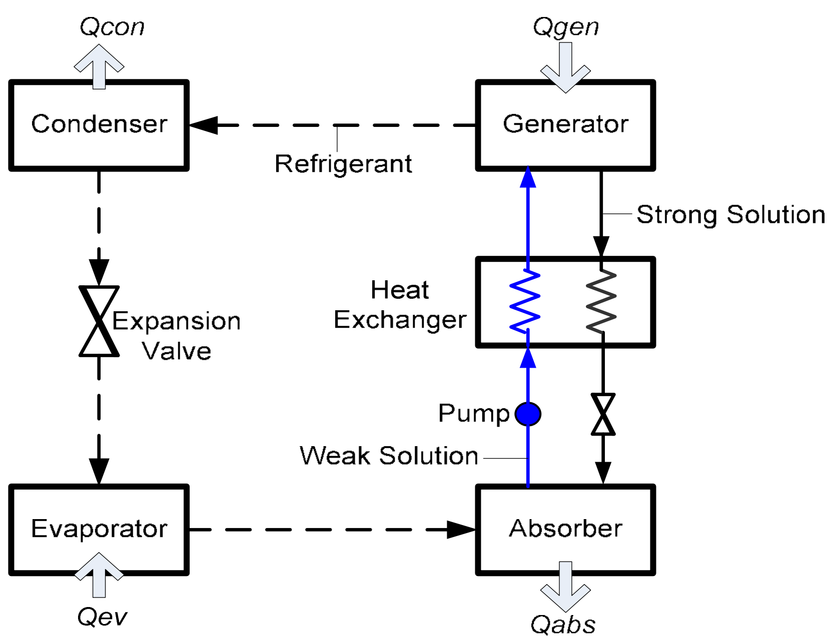

Figure 2.5 Schematic cycle of absorption chiller [90]

Absorption chillers are classified according to the type of heat used as the input, whether it has a single, two are more stages generator [89]. Chillers having one generator are called single-stage absorption chillers, and those with two generators are called two-stage absorption chillers. Absorption chillers operate using steam, hot water or hot gas as externally heat energy source for indirect fires chillers. While those which has its own flame source are categorized as direct-fired absorption chillers.

Several liquid solutions are commonly used in absorption chillers, such as water-lithium bromide, water-ammonia and water-ammonia-hydrogen. Among the most common absorbent-refrigerant is lithium bromide and water [90]. The advantage of using liquid of water-lithium bromide is trouble free and easy to operate. However, careful attention should be noted regarding to its operational limitation. The operational limitation are freezing refrigerant and crystallization [89].

i. Freezing refrigerant

The freezing refrigerant limitation in the absorption chiller is due to water work as refrigerant. Related to this limitation, leaving chilled water temperature in the evaporator has to be kept not too close to freezing temperature of $0^{o}C$ at atmospheric pressure. As a precaution to this limitation, the supply chilled water temperature and flow rate into the evaporator should be maintained within a limited range. At constant flow rate of absorption chillers, the supply chilled water entering the evaporator has to be maintained above limit temperature.

ii. Crystallization

The basic mechanism of crystallization is that lithium bromide solution becomes so concentrated that crystals of the lithium bromide are formed and plug the equipment connection. The location where crystallization most likely to occur is when the strong solution entering the absorber, that is the concentrated solution at the lowest temperature [91]. Several factors which causes crystallization of the absorption chillers are air leakage, excessive condenser cooling, excessive heat input to generator and electric power failures [92, 93]. The value of temperature limit of absorption chillers depends on the working pressure, temperature and concentration of the solution in each component.

2.6.3 Model of Chillers

The requirement for predicting chiller performance characteristic has led to the development of different simulation technique [94]. In a simple chillers, the simple model seems to be satisfactory solution to predict energy performance of the chillers, however, in a complex chillers system, the calculation are lengthy by utilizing complicated model. The main consideration for selecting the parameter in the simulation is strongly depending upon the intended purposes of the simulation. The other consideration is the relationship between the parameters used in the simulation [95].

According to the literatures of the chillers, two types of model can be implemented namely first principle and correlation-based models [96]. First principle model are based on thermodynamics equations related to chillers component, used solely or coupled integrally in the chillers. The usage of thermodynamic equation at the chillers component encourages development of general model. The second type, correlation based models relate the energy performance of the chillers to different operating parameters using regression analysis of the measured data.

In the vapor compression chillers, numerous models were developed both for first principle and correlation-based. First principle models are used for several purposes. Cecchini and Marshal [97] developed first principle model for simulating refrigerating and air conditioning. The models used assumption of steady state operation, pressure drop neglected, constant sub cooling at the condenser outlet and constant superheating at the evaporator outlet. Gordon and Ng [98] developed model to relate coefficient of performance and cooling energy of the chillers model using a simple thermodynamic model. The model was developed to relate condenser and evaporator internal losses, the chilled water leaving temperature and condenser water entering temperature.

The correlation based model for vapor compression chillers have been used for several purposes. Strand et al. [99] developed models for direct and indirect ice-storage simulation. The evaporator, compressor and condenser were linked into a simulation program. Figuera et al. [100] developed model for water-cooled centrifugal chillers by correlating data of condenser supply temperature in water cooled chillers. Jahing et al. [101] presented a semi-empirical method for representing domestic refrigerator/freezer compressor. McIntosh et al. [102] developed two models for vapor compression chillers using a simple refrigeration cycle as the framework for compressor and heat exchangers. The model was developed in the simulation for fault detection and diagnosis of vapor compression chillers.

Models of absorption chillers have also been developed for simulation in predicting the performance [103-108]. In the first principle model, the simulations model used mass balances and energy balances related to operation condition of pressure, temperature and concentration of solution at each component [109, 110]. This involved parameters of chilled water, cooling water, heat input and cooling capacity. With these parameters, a simulation is used to calculate the required heat supply temperature, cooling water flow rate, temperature, pressure and concentration at all state points [90].

First principle model was used for simulation as a whole or specified component of absorption chillers. For the whole absorption chiller, first principle model was developed to simulate various configurations with different working fluids Grossman et al. [103, 104]. Later this model was enhanced for predicting performance of single and double stages absorption chillers Gommed and Grossman [105], and three stages of absorption chillers, Grossman et al. [106]. For the case of specified component, the first principle model was developed for simulation in absorber, Seewald and Perz-Blanco [107]. The model was developed as a simple approach covers the effect of various parameters on the performance in the absorber.

Hellmann and Zieger [108] introduced a simple model for absorption chillers and heat pumps. The model simplified the complexity of thermodynamic equations to only two algebraic equations, one for coefficient of performance and the other for cooling capacity.

Determination of outlet temperature as a function of inlet temperature was performed based on two equations of energy balance in the evaporator component of the chillers [111]. The model can be used as general model both vapor compression and absorption chillers.

The energy balance in the chilled water side is obtained from the evaporator. Hence chillers cooling capacity (Q_C) is equal to evaporator heat (Qev), take form as Equation 2.7.

$$Q_C = \dot{m}_C . C_p . (T_{inC} - T_{out\,C}) \tag{2.7}$$

Energy balance from both chilled water and refrigerant sides in the evaporator part of the chillers is formed as Equation 2.8.

$$Q_C = UA \frac{(T_{inC} - T_{ev}) - (T_{outC} - T_{ev})}{\ln\left[(T_{inC} - T_{ev}) / (T_{outC} - T_{ev})\right]} \tag{2.8}$$

With $\dot{m}_C$ is mass flow rate, C_p is specific heat, UA is overall heat transfer coefficient times area, T_{inC} and T_{outC} are inlet and outlet chilled water temperatures, whereas T_{ev} is evaporator temperature.

Evaporator part of the chillers is assumed working at constant evaporator temperature [67, 111]. Determination of outlet chilled water temperature as a function of inlet chilled water temperature was obtained by equalizing both Equations 2.6 and 2.7. Using the model, cooling capacity can also be determined based on the size of the chillers involving of flow rate, inlet and outlet chilled water temperature and UA parameters.

Partial working load can be calculated as the actual capacity over design cooling capacity the chillers ($Q_{C,des}$), that is expressed as Equation 2.9.

$$PL = \frac{\dot{m}_C . C_p . (T_{inC} - T_{out\,C})}{Q_{C,des}} \tag{2.9}$$

2.7 Non Linear Regression Fitting

A method to represent a series of data into a mathematical model is curve fitting. The advantage of using curve fitting is it enables visualization of data characteristics, to obtain important parameters and to summarize the relationships among variables [112]. Conceptually, fitting a mathematical model on data set is to establish equation that defines the dependent variable as a function of an independent variable with one or more parameters.

2.7.1 Non Linear Regression Fitting Steps

The important steps in data fitting analysis are determination of the model, selection of fitting equations suitable to the model and interpreting the best fitting analysis [113].

i. Selection of the model

Models are categorized into two parts depend on how it was described namely empirically and mechanistically [114]. Empirical model simply describe the general shape of the data set. In contrast, mechanistic model are specifically formulated to provide insight into physical process that is thought to govern the phenomenon under study. Parameters derived from mechanistic models are in quantitative estimated of real system properties. In general, the mechanistic model is more useful in the implementation, because they represent quantitative formulation in the process.

ii. Selection of fitting equations

Fitting equations suitable to the model can be selected based on linear or non linear equations. Several fitting equations that could be categorized as non linear regression equations are polynomial, peak, hyperbola, logarithm, exponential decay, exponential rise, exponential growth, power, sigmoidal, rational, ligand binding and wave form [20], [115]. Fitting to the equations are performed by using non linear regression fitting that requires iterative method [116]. In the iterative method, fitting was performed by minimizing deviation between the observed and predicted values by successive small variations and reevaluation until a minimum deviation is reached. Non linear fitting always starts with an initial guess of parameter values [117].

iii. Interpreting the best-fitting parameters

Several evaluations have to be considered in ensuring the accuracy of fitting analysis result, such as close requirement to the data, suitability and precision the best fit parameter values [118]. For this purpose, interpreting the best fit parameter of non linear regression fitting utilizes some statistical approach for evaluating the goodness of fitting and important intervals [64].

In assessing modeling results, the important evaluation is whether the iteration converged to a set of values for the parameters. The possible error caused by choosing initial values or iterative procedure that could not find a minimum deviation [117]. There is a quantitative value that describes how well the model fits the data. An even better quantitative value is coefficient of determination, R^2. It is computed as the fraction of the total variation of the y values of data points that is attributable to the assumed model curve, and its values typically range from 0 to 1. Values close to 1 indicate a reliable best fitting [118].

2.7.2 Curve Fitting Software Package

Even though solution of non linear regression fitting has been established, the key factor in having satisfactorily results for the fitting is in selecting the mathematical function. The mathematical function are determined contain the related parameter suitable to data characteristics. The parameter values must also be evaluated to make sense from standpoint of the model. The solution of non linear regression in the fitting can be solved utilizing some commercial software. Many commercial software programs perform linear and nonlinear regression analysis and curve fitting, among them is SIGMAPLOT [119]. Selection of the appropriate fitting software considers its capability in conducting non linear regression fitting and performing best fitting of the data.

2.8 Summary of the Literature Reviews

Chapter two has presented a general review of the stratified TES tank. The reviews discussed previous works of the TES tank, the requirement criteria in the charging, temperature distribution and its degradation factors, simulation model of stratified TES tank and its solutions, reviews on absorption and electric chillers models and non linear regression fitting.

In the review of stratified TES tank, it is noted that temperature distribution holds important role for determination of the charging parameters. Not only cumulative cooling capacity, the other important parameters of the TES tank can be determined accordingly, such as thermocline thickness as well as half-cycle figure of merit. However, the methods to determine the parameters were based on estimation from the captured temperature distribution profile. The estimation method has drawback of its accuracy, therefore it requires to be enhanced. Some efforts in defining parameters based on temperature distribution function have been initiated. Implementation of the function in the charging simulation of stratified TES tank, however, has not been established yet.

In reviewing the charging of stratified TES tank, it is noted that the limit capacity criteria has significant effect in the charging cycle. However, the formula describing the limit capacity criteria was not performed. Further, simulation charging model covering these parameters has not been established yet.

Review simulation models of stratified TES tank shows that it has been a mature object for simulation. Subject to one-dimensional flow, the model were developed covering many aspect of charging variables, for various purposes and parametric analysis. However, those researches were conducted as solely TES tank system. The close charging system model integrating of the TES tank with the chillers equipments has not been developed yet.

This study is aimed to develop simulation models which incorporate absorption chillers in combination with electric chillers to charge stratified TES tank. This is performed by developing of single and two-stage charging models using two approaches, namely open and close charging systems. The open charging system utilizes formulation based on temperature distribution analysis. For close charging system, the charging model is developed by integrating of TES tank and chiller parameters utilizing one-dimensional model.

CHAPTER 3
METHODOLOGY

This chapter delivers an understanding of methodology implemented in this study. The methodology was adopted to meet the objective which covers development of charging models for stratified TES tank using open and close charging system.

3.1 Charging of Stratified TES Tank Models

The methodology in this research involved three main parts, namely development and simulation of charging models using open system, development and simulation of charging models using close charging system and comparison of the models. The charging models in open system models were developed based on temperature distribution analysis, while on the close charging system, charging models were established by integrating the TES tank and chillers. The charging models developed using open system were designated as models type (I) whereas the charging models on close system were designated as models type (II).

In the open system, the charging models were discussed in term of determination charging parameters, development and simulation of the models for single stage and enhancement for two-stage of charging stratified TES tank. The steps in the open charging system are as follows.

i. Determination of charging parameters based on temperature distribution analysis. It involved the following steps :

   a. Determination of temperature distribution parameters.
   b. Selection of temperature distribution function.
   c. Formulation of charging parameters in the simulation models type (I).

ii. Single stage charging model type (I).

   a. Development of single stage charging model type (I).
   b. Verification of single stage charging model type (I).
   c. Simulation of single stage charging model type (I).
   d. Validation of charging parameter values in the single stage charging model type (I).

iii. Two-stage charging models type (I) were obtained from enhancement of the single stage charging model type (I). The models were used for simulation of two-stage charging stratified TES tank utilizing absorption and electric chillers sequentially.

In the close system, the charging models type (II) was discussed in term of development of the single stage charging, verification and simulation for single stage charging and enhancement of the model for two-stage charging in the stratified TES tank.

i. Development of close charging system charging models.
   The charging model type (II) was developed by integrating physical models of the stratified TES tank and chillers.

   a. Physical model of stratified TES tank was based on one dimensional model with conduction and convection equation.
   b. Chillers model utilized energy balance in the evaporator.
   c. The solution approach for integrated stratified TES tank and chillers models adopted finite difference method.

ii. Single stage charging model type (II)
   Developing of single stage charging model (II) is as follows:

   a. Development of single stage charging model type (II).
   b. Verification of single stage charging model type (II).
   c. Simulation of single stage charging model type (II).

iii. Enhancement for two-stage charging model type (II).

The charging model type (II) was used for simulation two-stage charging of stratified TES tank utilizing absorption and electric chillers sequentially.

The last section discussed on the evaluation of the two models type (I) and (II). It was performed by comparing the simulation results in the single stage and two-stage charging of the stratified TES tank. The methodology used in this research is presented in Figure 3.1. The single stage charging models type (I) and (II) were verified and validated using historical operating data of the stratified TES system. The historical data was also used as a basis for selection of temperature distribution function.

3.2 Historical Data of Operating TES Tank

TES tank system of a district cooling plant was acquired for this study. The TES tank is a vertical cylindrical tank made from steel. The TES tank has a designed capacity of 10,000 RTh (35,161.7 kWh) and is equipped with two 1,250 RT (4,395.2 kW) of steam absorption chillers (SACs) and four 325 RT (1,142.8 kW) electric chillers (ECs). The district cooling plant is designed to serve cooling demand of academic facilities at Universiti Teknologi PETRONAS. Cooling demand is supplied by circulating chilled water from steam absorption chillers and discharging TES tank during on-peak demand hours. Charging of the TES tank is served by electric chillers (ECs) during off-peak hours. The schematic flow diagram of the charging is illustrated in Figure 3.2.

The TES tank has cylindrical vertical tank type with inside diameter and height of 22.3 m and 15 m, respectively. The tank has 5,400 m^3 water storage capacities. Lower nozzle is made from pipe with diameter of 0.508 m (20” Nominal Pipe Size) located at elevation of 1.824 m, while diameter of upper nozzle is 0.305 m (12” Nominal Pipe Size) at elevation of 12.3 m. Both nozzles are provided with diffusers on its end-connection in the storage tank. Overflow line is connected at elevation of 14.025 m. The entire tank is externally insulated with polystyrene of 300 mm thickness. The tank is internally coated with epoxy paint.

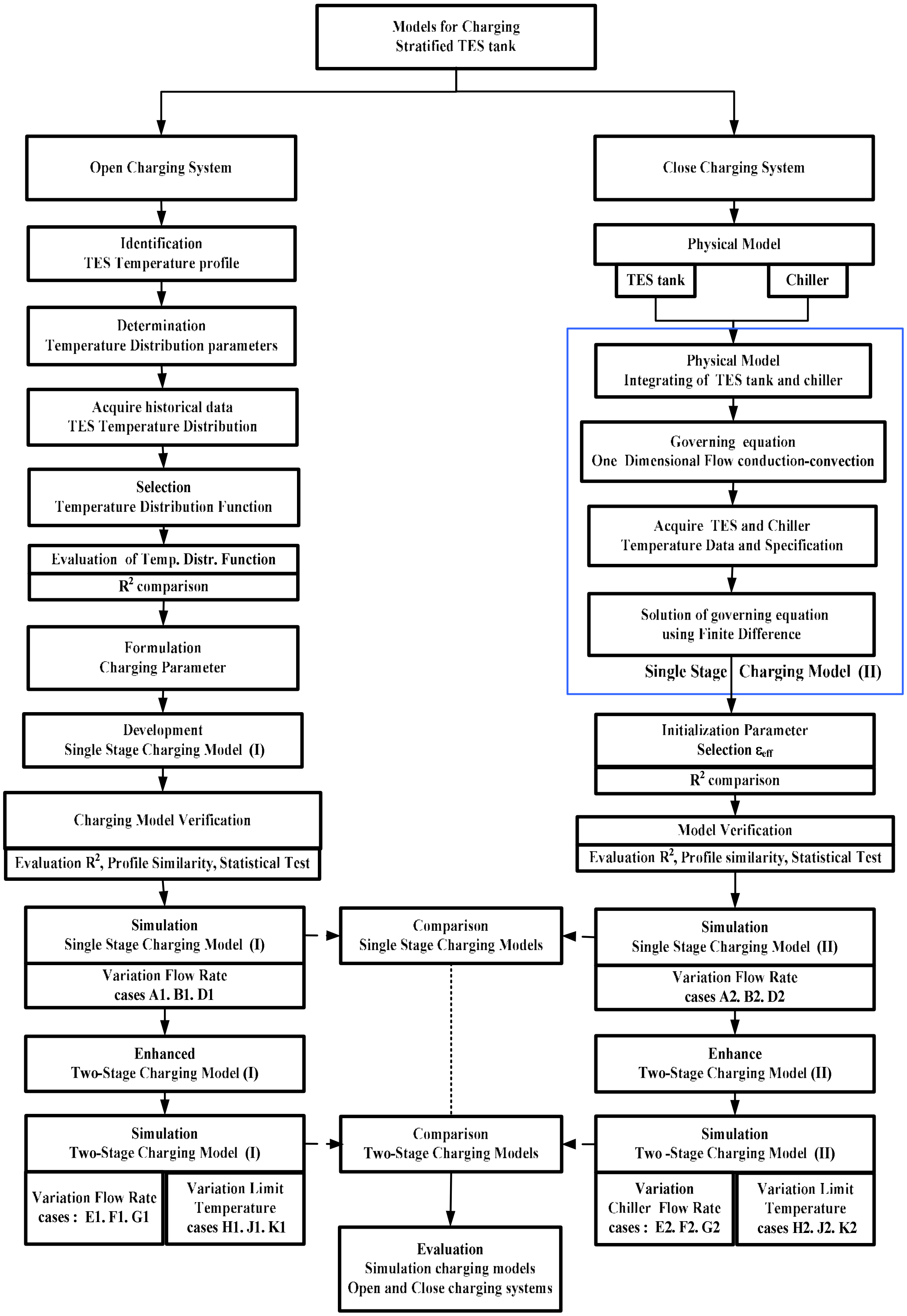

Figure 3.1 Methodology

SAC has specification of 504 m^3/hr flow rate while EC has designed flow rate of 131 m^3/hr. Both SACs and ECs have designed inlet and outlet temperature of 13.5^{o}C and 6^{o}C, respectively.

The tank is equipped with 14 temperature sensors, installed at approximately 1 m vertical interval for measuring the water temperatures inside of the tank. The lowest temperature sensor is located at 0.51 m elevation. All temperatures are hourly recorded with data acquisition system.

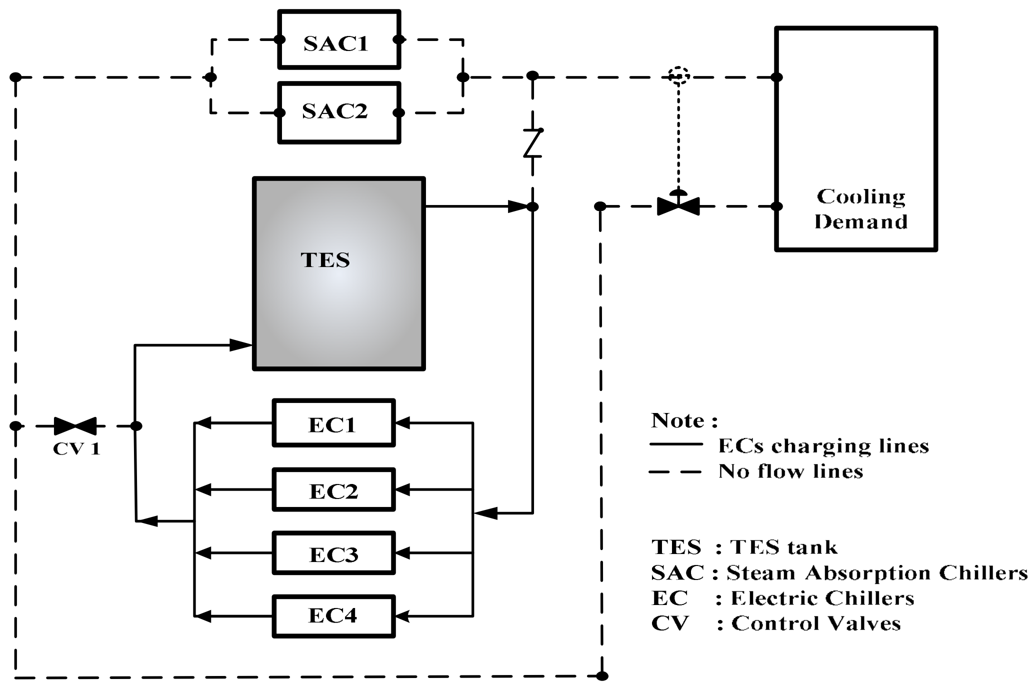

Figure 3.2 Schematic flow diagram of charging TES tank system

Water temperature TES data during the charging cycle were acquired and analyzed for this study. The data were selected for constant flow rate of 393 m^3/hr and 524 m^3/hr. The charging is usually served by three or four of ECs, during off-peak hours from 18.00 hours to 7.00 hours. Three data sets of 393m^3/hr were on September 9, 2008; September 11, 2008 and September 19, 2008, designated as data set IA, IB and IC, respectively. Three other hourly data sets of 524 m^3/hr were on May 8, 2009; June 22, 2009 and June 24, 2009, designated as data set IIA, IIB and IIC, respectively. The plots of temperature distribution data are attached in Appendix A.

3.3 Single and Two-Stage Charging

The objective of this study is to develop simulation models which incorporate absorption chillers in combination with electric chillers to charge stratified TES tank. This is to be achieved by developing single and two-stage charging models. The single stage model simulates charging of stratified TES tank with electric chiller (EC), whereas charging with combination of absorption and electric chillers is simulated in two-stage charging.

3.3.1 Single Stage Charging

In the single stage, the charging of stratified TES tank is performed by electric chiller (EC). The charging is began at empty capacity and ended at full capacity. Schematic diagram of single stage charging is presented in Figure 3.3.

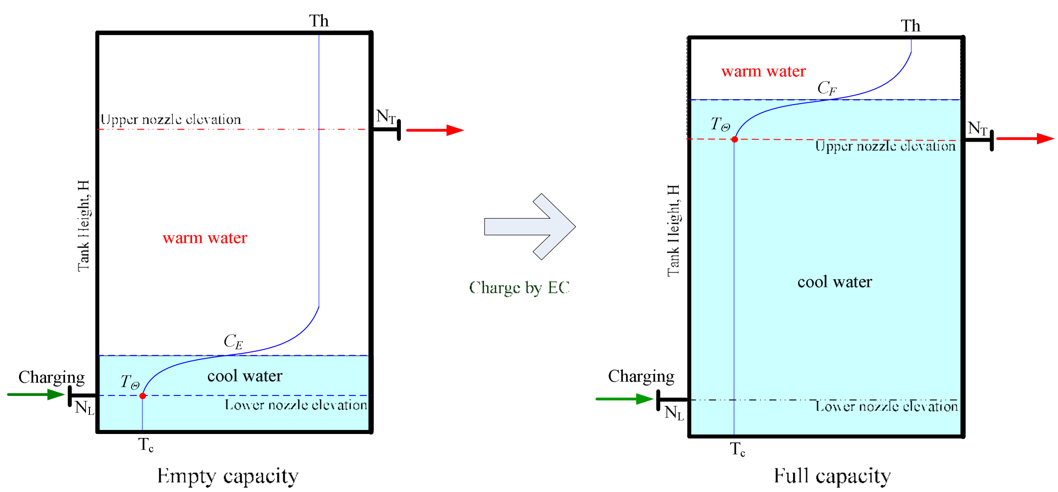

Figure 3.3 Schematic diagram of single stage charging

It can be seen in Figure 3.3, both empty and full capacity are described in term of water temperature at nozzle elevation. The empty capacity was identified when the water temperature at lower nozzle elevation equal to cut-off temperature (T_Θ) express a certain temperature approximate to average cool water temperature. In this empty capacity, cool water depth (C_E) is located at lower part of the tank. On the other hand, full capacity is identified when water temperature at upper nozzle elevation equal to cut-off temperature. The cool water depth at full capacity (C_F) is located at the upper part of the tank. During charging, temperature distribution has an S-curve profile which relates temperatures of cool, warm and thermocline regions. The cool and warm water temperatures are designated as T_c and T_h, respectively.

3.3.2 Two-Stage Charging

Two stage charging model is aimed to simulate charging of stratified TES tank involve absorption and electric chillers sequentially. The first stage charging is performed by using absorption chiller (SAC), while electric chiller (EC) is used on the second stage. Schematic diagram of the two-stage charging is presented in Figure 3.4.

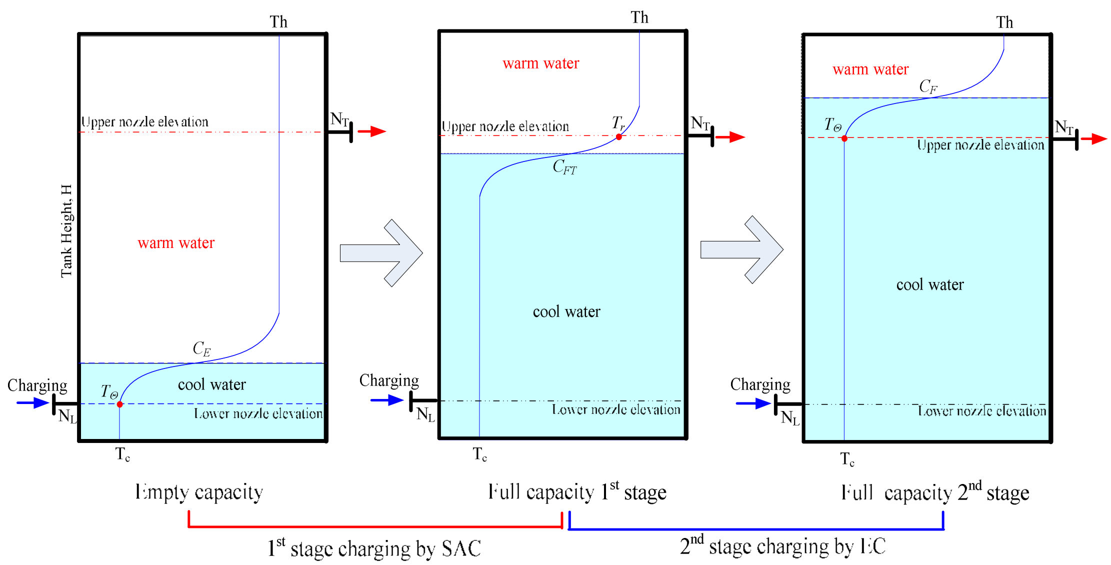

Figure 3.4 Schematic diagram of two-stage charging

In the first stage charging by absorption chiller, the charging is began at empty capacity and ended at full capacity. Condition of empty is similar with that on the single stage, whereas full capacity is identified when outlet charging temperature equal to limit temperature of the absorption chiller. Cool water depths in the single and two stage charging are (C_E) and (C_{FT}), respectively. This full capacity was determined by equalizing water temperature at upper nozzle to limit temperature (T_r). This condition was used as an initial state of the second stage charging. Determination of empty capacity at the first stage and full capacity at the second stage was performed based on cut-off temperature similar with that on the single stage charging.

In this study, both single and two-stage charging were developed using open and close charging systems. The single stage charging model is first developed and validated prior to enhancement for the two-stage charging.

3.4 Open Charging System Model

The open charging system model was developed based on temperature distribution analysis in stratified TES tank. The temperature distribution analysis commence with identification of temperature distribution profiles, determining the related parameters, selection of temperature distribution function as well as formulating of charging parameters. These steps were performed prior to establishing model type (I) both for single and two-stage charging stratified TES tank.

3.4.1 Temperature Distribution

As discussed in the section 2.4, the charging of stratified TES tank is performed under the condition that the TES tank is always full of water. The water comprises of three layers i.e. the cool water in the lower part, the warm water in the upper part and thermocline region in the middle part of the tank. Accordingly, water temperature distribution form a specific S-curve reflecting cool, warm and transition temperatures of the three layers. Along with additional cool water in the lower part of the TES tank, the S-curve move upward from initial to final condition of charging cycles. The typical S-curve temperature distribution is illustrated in Figure 2.1. The S-curve has a slight inclined line of cool and warm water temperatures. In the modelling, however, the cool and warm water temperatures were always generated at constant values [46]. Hence, the cool and warm water temperatures were exhibited as straight line of its average value. The following discussion is focused on the S-curve shape with constant values of cool and warm water temperatures.

3.4.1.1 Parameters of Temperature Distribution Profile

Determination of parameters affecting S-curve temperature distribution profile is referred to Figure 2.1. The temperature distribution profile is schematically drawn with respect to tank elevation as illustrated in Figure 3.5. The Figure 3.5 is used as a basis for determination of temperature distribution parameters.

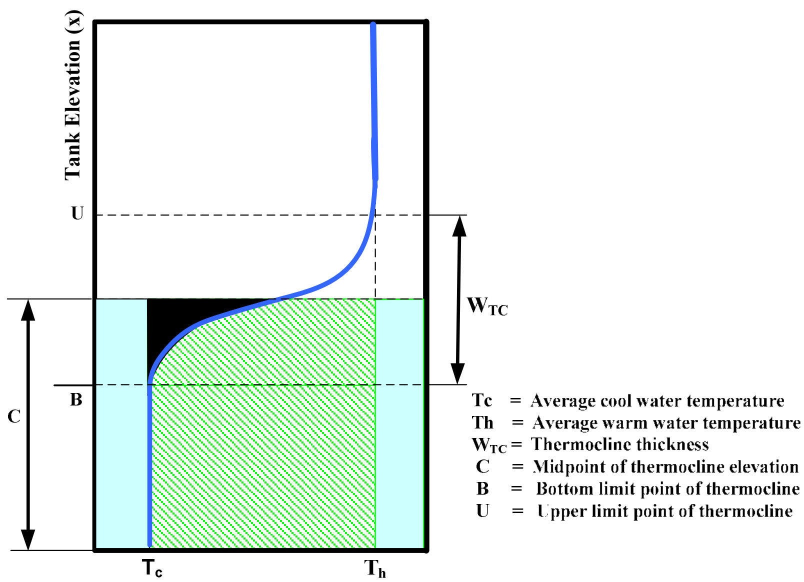

Figure 3.5 Temperature profile in stratified TES tank

The parameters for temperature distribution profile were determined as follows:

i. Average cool temperature was described as T_c.
ii. Average of warm temperature was defined as T_h.
iii. The thermocline profile was defined as
    a. Position of midpoint of thermocline (C).
    b. Slope gradient of thermocline profile (S).
iv. The thickness of thermocline (W_{TC}).
v. Bottom limit point of thermocline (B) was defined as a point where bottom edge of thermocline profiles located.
vi. Upper limit point of thermocline (U) was defined as position of upper edge of thermocline profiles.

From Figure 3.5, it is shown that the temperature profile parameters are T_c, T_h, C and S. Cool and warm water exist at the lower and upper parts of storage tank. The boundary line between cool and warm water was identified at C expressing the position of midpoint of thermocline thickness. The C also indicated the cool water depth in the TES tank. The thermocline thickness (W_{TC}) was defined as the region limited by bottom limit point (B) and upper limit point (U). Hence, the temperature distribution were established as a function of parameters T_c, T_h, C and S with variable height of tank (x), as given in Equation 3.1.

$$T(x) = f(T_c, T_h, C, S, x) \tag{3.1}$$

3.4.1.2 Selection of Temperature Distribution Function

Selection of the temperature distribution function was performed based on Equation 3.1. The function contained parameters in an independent equation. This was to simplify the extension in formulating charging parameters. The selection of the function was aimed to develop a mechanistic model representing the temperature distribution profile. The criteria for the selection was based on capability in forming the S-curve profile and contain parameters suitable to the requirement as illustrated in Figure 3.5.

Selection of the temperature distribution function was conducted using non linear regression fitting. A commercial software SIGMAPLOT was utilized as a tool to solve non linear regression in the fitting the function [119]. Evaluation of the goodness of fitting was evaluated using coefficient of determination (R^2). The R^2 value approximate to unity indicates that the functions are capable of representing the temperature distribution profile.

The function was selected based on historical data of temperature distribution. For this purpose, six operating data sets were acquired namely IA, IB, IC, IIA, IIB and IIC as described in section 3.2. The data sets were charging at 393 m^3/hr and 524 m^3/hr.

3.4.2 Formulation of Charging Parameters

This section is addressing on formulating the important charging parameters of the models in open charging system, namely limit capacity and temperature transition. Prior to define the charging parameters, determination of limits point of thermocline and the thickness of thermocline were undertaken.

3.4.2.1 Limit Points

Limit points were defined as points at the edge of temperature profile that bounds the thermocline thickness. Limit points were determined by utilizing cut-off water temperature as reference points on the thermocline profile. Some concepts of limit points have been reviewed in Section 2.3. Among them, dimensionless cut-off temperature concept proposed by Musser [47] was adopted. The dimensionless cut-off temperature takes the form of $\Theta = (T - T_c)/(T_h - T_c)$.

The limit points on the edges of thermocline profile namely bottom limit (*B*) and upper limit (*U*) were determined by incorporating dimensionless cut-off temperature to temperature distribution function as described in Equation 3.1. The *B* and *U* were referred at a certain distance from *C*, therefore it was expressed as a function of dimensionless cut-off temperature (Θ), position of midpoint of thermocline (*C*) and slope gradient (*S*) and takes form as Equation 3.2.

$$B, U = f(\Theta, C, S) \tag{3.2}$$

3.4.2.2 Thermocline Thickness

Thermocline thickness (W_{TC}) was defined as the width of mixing region between cool and warm water. The thermocline thickness (W_{TC}) was a region limited by bottom and upper limit points, (*B*) and (*U*), respectively. Thermocline thickness was established by inserting dimensionless cut-off temperature into Equation 3.1.

Thermocline thickness was functionally derived as a function of dimensionless cut-off temperature (*Θ*) and slope gradient (*S)* in Equation 3.3.

$$W_{TC} = f(\Theta, S) \tag{3.3}$$

3.4.2.3 Limit Capacity Criteria

Limit capacity criteria has significant role in developing charging model of stratified TES tank. The limit capacity criteria were used to determine empty and full capacity, where charging began or ended. The limit capacity were derived based on two criteria namely water level limit and temperature limit.

i. Water level limit criteria

Using water limit criteria, limit capacity of the charging was determined based on bottom limit point (*B*) elevation. It involves empty and full capacity in the charging of stratified TES tank. When the bottom limit is located at the lower nozzle elevation, the condition TES tank is at empty capacity. Full capacity, on the other hand, is achieved when the bottom limit point at the same level with upper nozzle elevation. The concept in defining empty and full capacity based on water level limit is illustrated in Figure 3.6.

Figure 3.6(a) shows empty capacity condition that was obtained by positioning bottom limit point (*B*) to lower nozzle elevation. Figure 3.6(b) illustrates the bottom limit point (*B*) at upper nozzle elevation which indicates the full capacity in the charging. Position of midpoint of thermocline which indicates cool water depth was determined by equalizing based on limit point (*B*) Equation 3.2 to nozzle elevation.

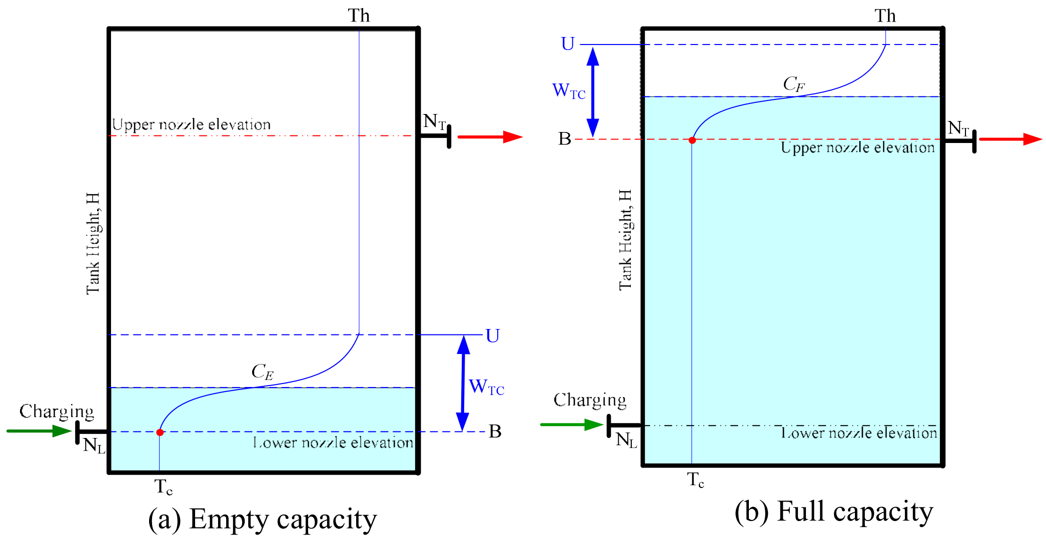

Figure 3.6 Empty-full capacity based on water level limit criteria

The cool water depth at empty capacity (C_E) was derived as Equations 3.4, and cool water depth at full capacity (C_F) was expressed in Equation 3.5.

$$\text{Empty capacity } (C_E), \quad B = f(\Theta, C, S) = N_L \tag{3.4}$$

$$\text{Full capacity } (C_F), \quad B = f(\Theta, C, S) = N_T \tag{3.5}$$

ii. Temperature limit criteria

In the case of charging using absorption chillers, the full capacity of the charging was considered based on temperature limitation. The outlet charging temperature has to be maintained above the limit temperature (T_r). Limit temperature is a value of a certain temperature between cool and warm water temperature. Solution of the problem was conducted using temperature limit criteria. Determination of empty and full capacities based on temperature limit criteria is presented in Figure 3.7.

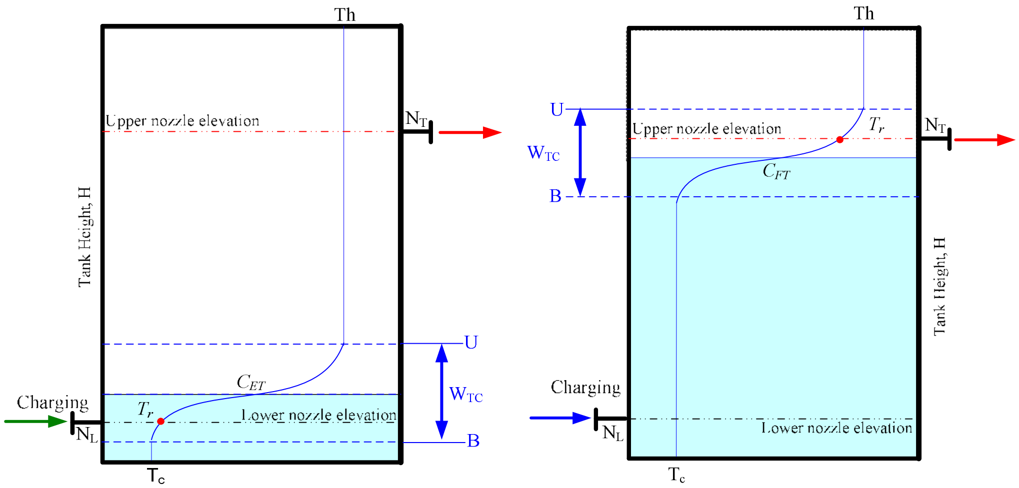

(a) Empty capacity (b) Full capacity

Figure 3.7 Empty-full capacity based on temperature limit criteria

Figure 3.7(a) shows empty capacity that was obtained on the condition of water temperature at lower nozzle equal to a limit temperature (T_r). Determination of full capacity was performed referring to Figure 3.7(b). From Figure 3.7(b), it can be seen that full capacity was achieved when the water temperature at upper nozzle elevation was equal to limit temperature (T_r). The cool water depth of these conditions was determined by equalizing of temperature distribution function (Equation 3.1) to limit temperature, while the x variable was referred to the nozzle elevations. Determination of cool water depth at empty capacity (C_{ET}) is described in Equations 3.6, whereas cool water depth at full capacity (C_{FT}) is determined based on Equation 3.7.

$$\text{Empty capacity,} \quad x{=}N_L \text{ and } T(x) = f(T_c, T_h, C, S, x) = T_r \tag{3.6}$$

$$\text{Full capacity,} \quad x{=}N_T \text{ and } T(x) = f(T_c, T_h, C, S, x) = T_r \tag{3.7}$$

iii. Temperature transition point

Temperature transition is a point of charging temperature decreases from fairly constant. It was achieved when the upper limit point of thermocline reach the upper nozzle elevation. The temperature transition point condition is schematically drawn in Figure 3.8.

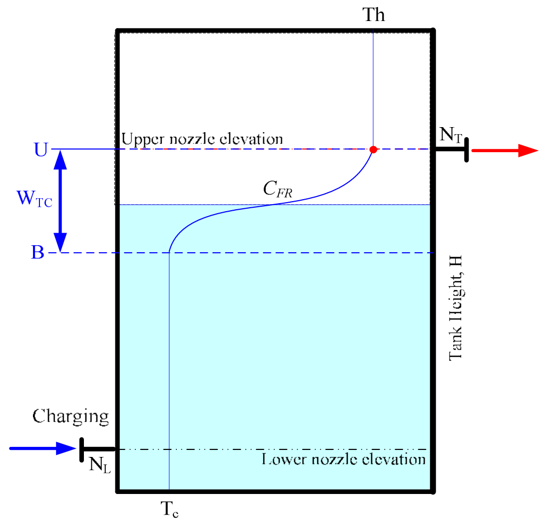

Figure 3.8 Temperature transition point

The cool water depth at temperature transition point (C_{FR}) was determined by equalizing upper limit points (Equation 3.2) to upper nozzle elevation. Determination of C_{FR} was performed by equalizing upper limit point to upper nozzle elevation as in Equation 3.8.

$$U = f(\Theta, C, S) = N_T \tag{3.8}$$

Formulation of the charging parameters based on temperature distribution analysis was used to develop models in open charging system. It was developed for single stage charging model type (I).

3.4.3 Single Stage Charging Model Type (I)

In the single stage charging model type (I), the discussion is divided into three parts namely development, verification and simulation of the model for single stage charging of stratified TES tank.

3.4.3.1 Developing Single Stage Charging Model Type (I)

Charging model type (I) was developed by introducing cool water at lower nozzle and withdrawing warm water from the upper nozzle. The outlet charging water was not re-circulated into the lower nozzle, hence the model was called as open charging system. The open charging system is schematically drawn in Figure 3.9.

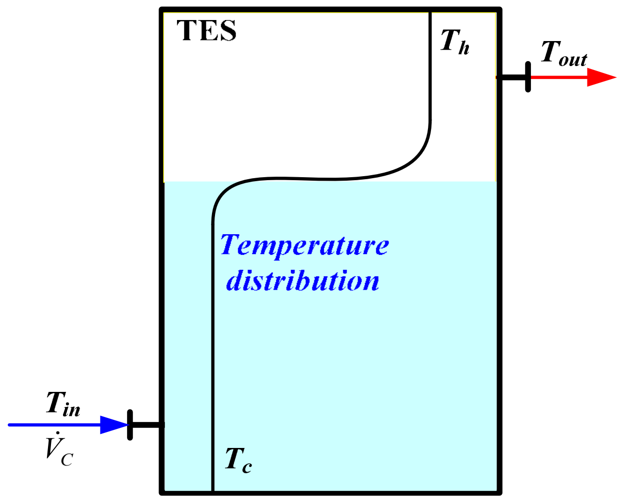

Figure 3.9 Schematic flow of open charging system

As shown in Figure 3.9, cool water that is introduced from the lower nozzle has inlet temperature of T_{in} and charging flow rate of $\dot{V}_C$. The cool water depth is indicated as hatch area in the lower part of the tank. The following sections explain assumptions and charging parameters that were used in the model.

i. Assumptions of the single stage charging model type (I)

The assumptions made in the single stage charging model type (I) are as follows:

a. Constant inlet charging temperature at average cool water temperature (T_c).

b. Charging has flow rate of $\dot{V}_C$.

c. Temperature distribution has similar profile during charging periods. Hence, parameters of average cool and warm water temperatures as well as slope gradient (T_c, T_h and S) are constant.

d. Cool water depth (C) increases with respect to time and is proportional to charging flow rate over cross sectional area of the tank. Hence, increasing of cool water depth during charging was determined as Equation 3.9.

$$\Delta C = \dot{V}_C / A \tag{3.9}$$

Based on the assumption, temperature distribution parameters could be determined for charging stratified TES tank simulation. It is capable of generating temperature distribution at observed time interval.

ii. Charging parameters of single stage charging model type (I)

Formulations as described in section 3.4.2 were used to determine charging parameters of the model. The charging parameters were cool water depth, charging duration as well as cumulative cooling capacity.

a. Cool water depth

Cool water depths were determined based on formulation from temperature distribution analysis. Cool water depths were used to indicate the conditions of empty capacity, temperature transition point as well as full capacity.

(i) Cool water depth at empty capacity (C_E) was determined using water level limit criteria in the solution of Equation 3.4. Optionally, it could also be determined based on temperature limit criteria from the solution of Equation 3.6.

(ii) Cool water depth at temperature transition point (C_{FR}) was determined based on solution of Equation 3.8.

(iii) Cool water at full capacity (C_F) was determined by referring to water level limit criteria in the solution of Equation 3.5. It could also be determined based on temperature limit criteria in the solution of Equation 3.7.

b. Charging duration

Charging duration was defined as time required for performing charging from initial to final state. It was determined based on cool water depth differences during the charging to achieve temperature transition point as well as for full capacity.

(i) Charging duration to achieve transition temperature (t_{CFR}) point was defined as follows.

$$t_{CFR} = \frac{C_{FR} - C_E}{\dot{V}_C}.A \tag{3.10}$$

(ii) Charging duration for full capacity (t_{CF}) during the charging wass determined as follows.

$$t_{CF} = \frac{C_F - C_E}{\dot{V}_C}.A \tag{3.11}$$

With C_E, C_{FR}, C_F are cool water depths at empty capacity, temperature transition point and full capacity, respectively. $\dot{V}_C$ is charging flow rate and A is cross sectional area of the tank.

c. Cumulative cooling capacity.

Cumulative cooling capacity was utilized to determine cooling energy stored in the observed time interval during the charging. It was determined based on temperature distribution consist of N slabs of the tank. The cumulative cooling capacity (Q_{cum}) is presented in Equation 3.12.

$$Q_{cum} = M_n.C_p.\sum_{n=1}^{N}(T_r - T_n) \tag{3.12}$$

M_n is mass of water at each slab, C_p is specific heat, T_r is reference temperature, T_n is water temperature at each slab and N is number of slabs in TES tank.

3.4.3.2 Verification of Single Stage Charging Model Type (I)

The temperature distribution of the model was verified before implementing in the simulation. The steps taken to verify the model are the follows.

i. Acquire observed data set which consists of hourly temperature distribution within a certain charging period. The data set of IA was used consist six hours of charging from 18.00 hours to 03.00 hours at flow rate of 393 m^3/hr.

ii. Determination of parameters T_c, T_h, C and S for the observed temperature distribution data set. It was performed by using SIGMAPLOT package for non linear regression fitting on the observed data.

iii. Generation of temperature distribution in the model. It was first carried out by determining parameter values T_c, T_h, C and S similar with that on initial condition of the observed data. Increasing of cool water depth (ΔC) was determined based on Equation 3.9. The temperature distributions of the model were generated from parameters of T_c, T_h, C and S.

iv. Evaluation of temperature distribution of the observed data and model. The evaluation used three criteria i.e temperature distribution similarity, temperature parameters similarity and *t*-statistical test. The evaluations are explained as follows:

    a. Similarity of temperature distribution.
    The evaluation was performed by determining the goodness relationship of the temperature distribution. It was performed using coefficients of determination (R^2) of temperature distribution between the observed data and the model.

    b. Similarity of temperature distribution parameters.
    It was conducted by comparing parameters T_c, T_h, C and S between the observed data and model.

    c. Statistical test.
    Evaluation of significant similarity between the observed data and model was performed using *t* statistical test [64]. The assessment was to see whether the

model can be accepted or not to represent temperature distribution on the observed data. The Null hypothesis of the test is that temperature distribution between observed data and model is similar. Therefore:

Null hypothesis H$_o$: $y_i^1 - y_i^2 = 0$

Alternative hypothesis H$_a$: $y_i^1 - y_i^2 \neq 0$

t computed in the hypothesis test is the ratio of the mean data value ($\bar{y}$) difference and its standard deviation (σ). It was determined between the observed data and model, designated as subscript 1 and 2, respectively. The t computed takes form as in Equation 3.13.

$$t_{comp} = \frac{\bar{y}^1 - \bar{y}^2}{\sqrt{\sigma_1^2 + \sigma_2^2}} \tag{3.13}$$

The standard deviation observed data and model were calculated using Equations 3.14 and 3.15, respectively

$$\sigma_1 = \sqrt{\frac{\Sigma(y_i^1 - \bar{y}^1)^2}{n-1}} \tag{3.14}$$

$$\sigma_2 = \sqrt{\frac{\Sigma(y_i^2 - \bar{y}^2)^2}{n-1}} \tag{3.15}$$

With $\bar{y}^1$ and $\bar{y}^2$ are mean values of the observed data and model, σ_1 and σ_2 are standard deviations of the observed data and model, whereas y_i^1 and y_i^2 are temperature distributions of the observed data and model.

The region for null hypothesis acceptance is t computed < t critical. The t critical value is equal to $t_{(f,\beta/2)}$ in the table t distribution with reference to significance level (β) and value of the number of degree of freedom (f). The significance level indicates the level of probability that the hypothesis would be rejected. The t distribution table is presented in Appendix E.

3.4.3.3 Simulation of Single Stage Charging Model Type (I)

The steps taken in conducting simulation of the single stage charging model type (I) is presented in Figure 3.10. The simulation of the single stage charging model type (I) involve with input parameters and determination values of the charging parameter.

i. Input parameters of the simulation

   a. Initial temperature distribution parameters.

      Initial temperature was determined based on empty capacity as described in the limit capacity criteria, hence require parameters of T_h, T_c, S and predetermined of dimensionless cut-off temperature (Θ). The parameter Θ was used to determine cut-off water temperature, as stated in section 2.3.2.

   b. TES tank configuration parameters.

      TES tank configuration parameters required lower and upper nozzles elevation, described as N_L and N_T, respectively. The other required parameters were diameter (D), effective water depth (H) and number of slabs in the TES tank.

   c. Charging flow rate.

   d. Observation time intervals

ii. Determining of charging parameter values in the simulation

   Parameters that were determined in the simulation are cool water depth and charging duration. All parameters were observed in term of empty capacity, temperature transition and full capacity. The cool water depth at temperature transition point (C_{FR}) and full capacity (C_F) were determined based on solution of Equation 3.8 and 3.5, respectively. The charging duration to achieve transition temperature (t_{CFR}) and full capacity (t_{CF}) were determined based on solution of Equation 3.10 and 3.11, respectively.

iii. Temperature distribution of the simulation was generated by parameter incorporated to temperature distribution function as described in Equation 3.1. Cumulative cooling capacity was determined based on Equation 3.12.

Simulation of single stage charging model type (I) was performed in three cases namely A1, B1 and D1. The cases of A1, B1 and D1 which involve variation of charging flow rates of 524 m^3/hr, 393 m^3/hr and 262 m^3/hr, were treated as having the same initial temperature in the TES tank configuration. Simulation was performed using TES tank configuration parameters as presented in Table 3.1, where chiller parameter shown in Table 3.2. Initial temperature referred to parameter values of *Tc*, T_h, *C* and *S*. The TES tank configuration parameter as tabulated in Table 3.1 was used for all simulation cases in this study.

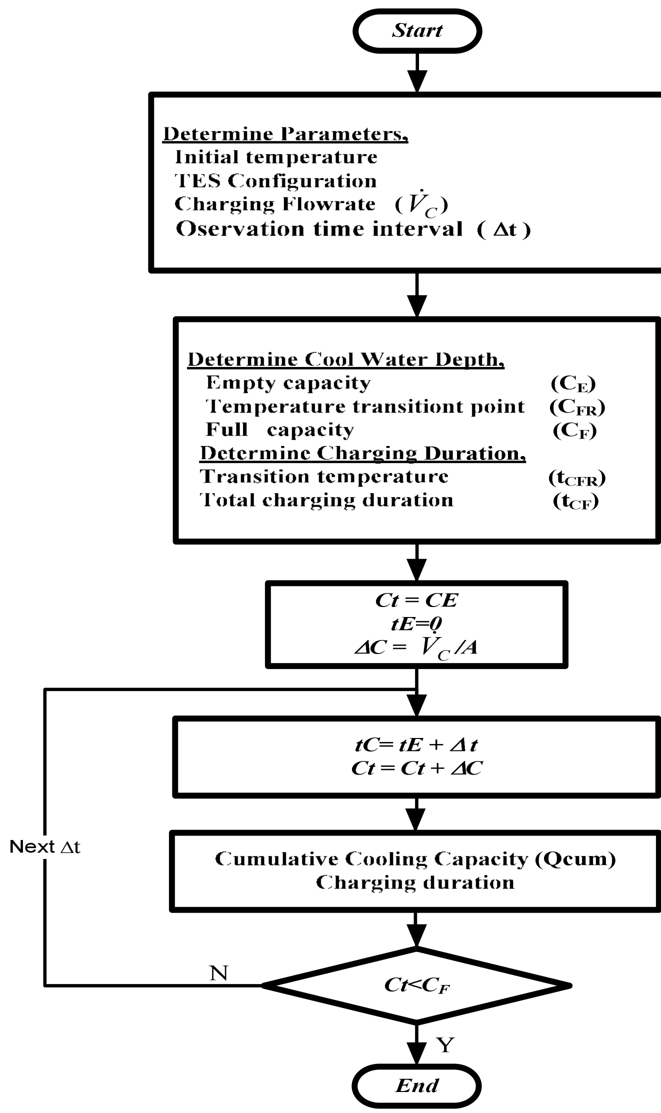

Figure 3.10 Simulation steps in single stage charging model type (I)

Table 3.1 TES tank configuration parameters

TES tank configuration	Notation	Value	Unit
Diameter	V	22.3	M
Effective water depth	H	14	M
Lower nozzle elevation	N_L	1.824	M
Upper nozzle elevation	N_T	12.3	M
Number of slabs	N	14	

Table 3.2 Chiller parameters value of simulation cases A1, B1 and D1

Variation charging flow rate cases	Flow Rates	
Case A1	524	m^3/hr
Case B1	393	m^3/hr
Case D1	262	m^3/hr

3.4.3.4 Validation of Single Stage Charging Model Type (I)

Validation of single stage charging model type (I) was performed in term of charging duration and cumulative cooling capacity. Validation of the model was conducted by taking temperature parameters from initial condition on the observed data, similar with that on the simulation. The steps of the simulation and validation are as follows:

i. Data set IB and IC were utilized as observed data.
ii. Determination of parameters Tc, T_h, C and S in the initial condition of the observed data.
iii. Determination of parameters Tc, T_h, C and S in the model and determination of incremental increasing of cool water depth (ΔC).
iv. Generation of temperature distribution in the model.
v. Determination of charging duration at full capacity (t_{CF}) of the observed data and model. For the observed data, interpolation was carried out on the upper nozzle elevation to obtain outlet charging temperature which is equal to cut-off temperature. In the model, charging duration was determined based on Equation 3.13.
vi. Determination of cumulative cooling capacity (Q_{cum}) both for observed data and model based on Equation 3.15.

vii. Comparison of charging duration and cumulative cooling capacity between the observed data and model.

3.4.4 Two-Stage Charging Model Type (I)

This section focuses on enhancing the single stage charging for two-stage charging model type (I). The enhancement and simulation involved charging of the TES tank by absorption and electric chillers sequentially.

3.4.4.1 Enhancement of Two-stage Charging Model Type (I)

The model was enhanced for implementation of two-stage charging stratified TES tank. Absorption chiller was used at the first stage, whereas electric chiller was used in the second stage of charging. The constraint in implementing absorption chillers in the first stage charging was the occurrence of limit temperature. The limit temperature in the absorption chillers was considered as a change state between the first and second stage of charging. Hence, the full capacity in the first stage charging was due to limitations on the outlet TES temperature.

Solution of temperature limitation was undertaken by utilizing limit capacity criteria, as described in 3.4.2.3. Empty and full capacities in the simulation were based on Equations 3.4 and 3.7, respectively. The steps taken for developing two-stage charging simulation is presented in Figure 3.11.

The steps taken in the simulation of two-stage charging model type (I) is almost similar with that on the single stage charging model, with additional charging flow rates and full capacity in the second charging. Parameters that were determined in the simulation namely cool water depth, charging duration as well as cumulative cooling capacity.

i. Cool water depth

Cool water depths at empty capacity (C_E) as well at temperature transition (C_{FR}) in the first charging were determined similar to that of the single stage simulation.

Cool water depths at empty capacity (C_E) as well at temperature transition (C_{FR}) were determined using solution of Equation 3.4 and 3.8, respectively. The cool water depth at full capacity at the first stage charging (C_{FT}) was determined using full capacity based on criteria temperature limit, using solution of Equation 3.7. For the second stage charging, cool water depth at full capacity (C_F) was determined using full capacity on water level limit criteria, which was based on solution of Equation 3.5.

ii. Charging duration

In the first stage, charging duration for temperature transition (t_{CFR}) was determined as follows.

$$t_{CFR} = \frac{C_{FR} - C_E}{\dot{V}_{C1}}.A \tag{3.16}$$

Charging duration for full capacity at the first stage (t_{CFT}) was determined as follows.

$$t_{CFT} = \frac{C_{FT} - C_E}{\dot{V}_{C1}}.A \tag{3.17}$$

In the second stage, charging duration for full capacity (t_{CF}) was determined as in Equation 3.18.

$$t_{CF} = \frac{C_F - C_{FT}}{\dot{V}_{C2}}.A \tag{3.18}$$

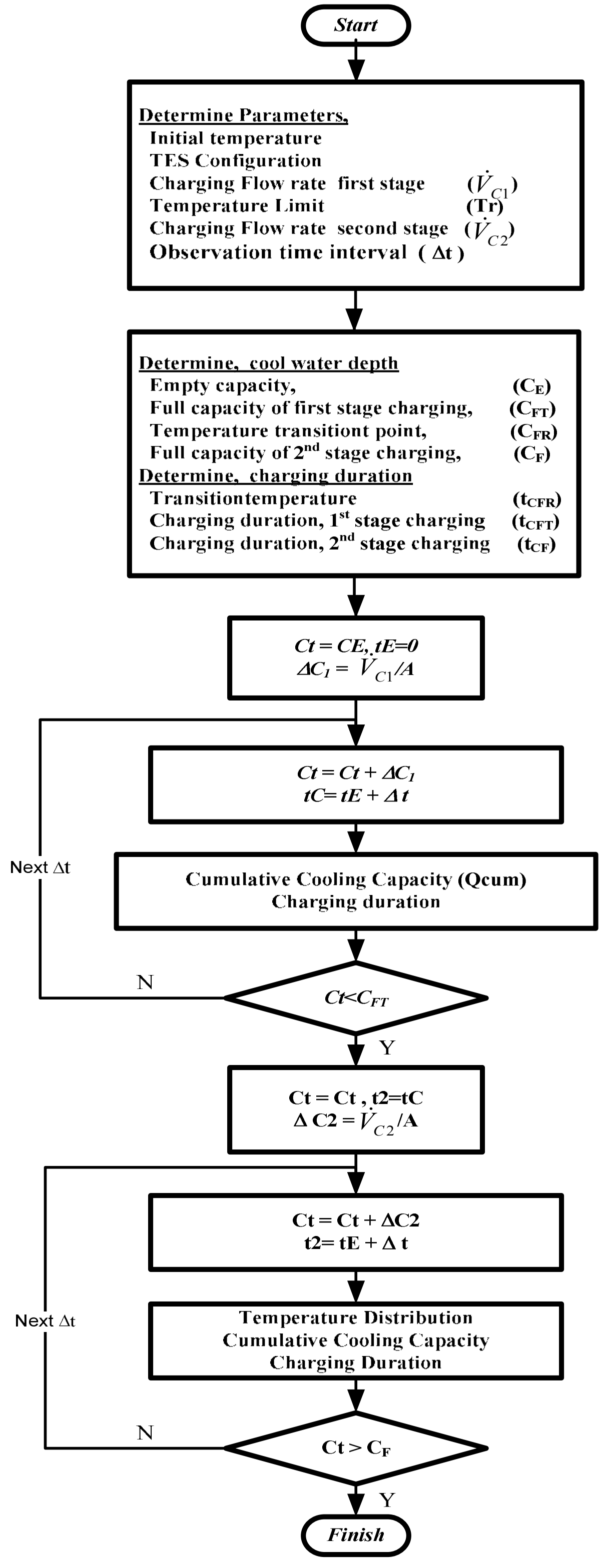

Figure 3.11 Simulation steps in two-stage charging model type (I)

3.4.4.2 Simulation of Two-stage Charging Model Type (I)

Simulation of two-stage charging model was performed in two cases. In the first case, charging flow rate variation of the second stage at 262 m^3/hr, 393 m^3/hr and 524 m^3/hr, as cases E1, F1 and G1, respectively. Whereas on the second case, charging simulation was carried out with variation of limit temperature at 7°C, 9°C and 11°C, as reflected in cases H1, J1 and K1. The flow rates at the first and second stage were using flow rates at 504 m^3/hr and 393 m^3/hr. Both cases were conducted at similar TES tank configurations as described in Table 3.1. Description of chiller parameters variation of the two-stage charging model type (I) cases are presented in Table 3.3 and 3.4 for flow rate and limit temperature, respectively.

Table 3.3 Chiller parameters for simulation cases E1, F1 and G1

Variation of charging flow rate (Cases E1, F1, G1)	**Notation**	**Value**	**Unit**
Absorption chillers (1st stage)			
Flow Rate	$\dot{V}_{C1}$	504	m^3/hr
Limit Temperature	T_r	9	°C
Electric chillers (2nd stage)			
Case E1	$\dot{V}_{C2}$	524	m^3/hr
Case F1	$\dot{V}_{C2}$	393	m^3/hr
Case G1	$\dot{V}_{C2}$	262	m^3/hr

Table 3.4 Chiller parameters for simulation cases H1, J1 and K1

Variation of limit temperature (Cases H1, J1, K1)	**Notation**	**Value**	**Unit**
Absorption chiller (1st stage) Flow Rate	$\dot{V}_{C1}$	504	m^3/hr
Electric chiller (2nd stage) Flow Rate	$\dot{V}_{C2}$	393	m^3/hr
Case H1	T_r	7	°C
Case J1	T_r	9	°C
Case K1	T_r	11	°C

The simulation charging models as discussed in Section 3.2 were developed considering temperature distribution profile analysis. In this model the charging was assumed to have constant temperature parameters during charging periods. The temperature profile movement was due to increasing of cool water volume in the lower part of the tank. In the real cycles, however, charging is performed in close system working at various operating conditions of TES tank and chillers. Related to this, development and simulation models based on close charging system were discussed in the next section.

3.5 Close Charging System

Selection of model in the simulation environment holds important role in achieving accurate representation of system characteristic. In this study, selection of one-dimensional flow model rather than two and a three-dimensional model is because of two reasons. First, the one-dimensional flow model has capability in covering factors that affect degradation of temperature distribution namely conduction through the wall, conduction between cool and warm water, mixing effect in initial flow of charging as well as heat loss to surroundings. The other main reason is that utilizing one-dimensional model enables modelling of general configuration of the TES tank system. Development and simulation of charging models using close system were undertaken by utilizing convection and conduction equation. The models were developed for single and two-stage charging in the stratified TES tank.

3.5.1 Single Stage Charging Model Type (II)

The models in close charging system were developed in a single stage charging model type (II). The developed model was aimed to cover the fact that charging cycles was operated as a close circulation system between the TES tank and chillers. Schematic flow diagram of close charging system is illustrated in Figure 3.10.

As illustrated in Figure 3.12, chilled water was circulated in the close charging system between TES tank and chillers. The chilled water was cooled in the chillers prior to be flown in the lower part of the tank through lower nozzle. Adding of cool chilled water increases the cool water volume in the tank and affected temperature profile moves upward to the upper part of the tank. In addition, supplying cooler chilled water also has an effect on the mixing temperature in the lower part of the TES tank.

Hence, several factors affecting the charging cycles such as temperature distribution, flow rate and working temperature of the chillers, mixing temperature and temperature losses in the piping lines (ΔT_1 and ΔT_2) have to be considered. These factors were accommodated in the physical model of TES tank and the chillers in the next section.

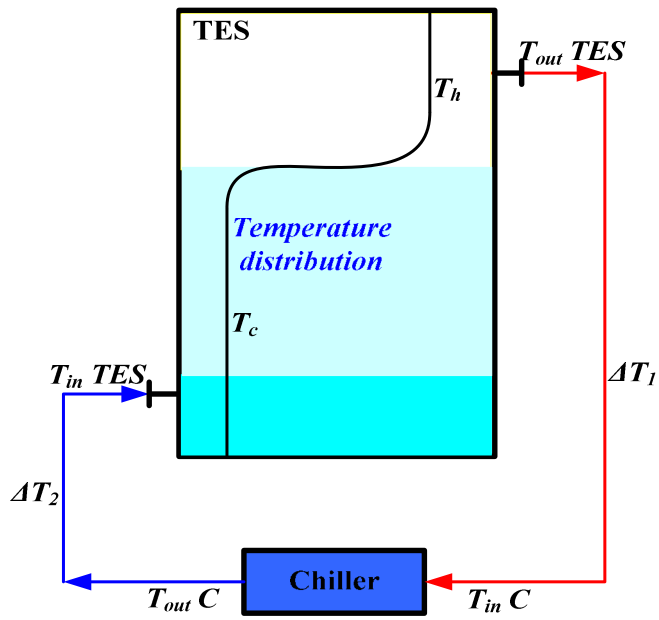

Figure 3.12 Schematic flow diagram of close charging system

3.5.1.1 Physical Model of Stratified TES Tank

Implementation of one-dimensional model was expressed in term of conduction and convection cases that occur in the TES tank. Occurrence of conduction was caused by cool and warm water temperature difference, whereas convection was due to flowing of chilled water in the TES tank. The physical model of the stratified TES tank is presented in Figure 3.13. Energy balance on elemental volume emerges in the form of transient conduction and convection one-dimensional flow.

As shown in Figure 3.13, the charging cycle iss illustrated in a cylindrical TES tank with diameter (D) and effective water depth (H). The cylindrical tank is assumed has N equal slabs in the longitudinal direction. The TES tank is well insulated. Among the factors affecting temperature distribution degradation, conduction between cool and warm water, and mixing effects were emphasized. Heat losses to surrounding and conduction through the tank wall were negligible. The heat loss to surrounding was ignored in the installation of sufficient external insulation of the tank. Whereas conducting wall effect was neglected due to internal coating of the tank.

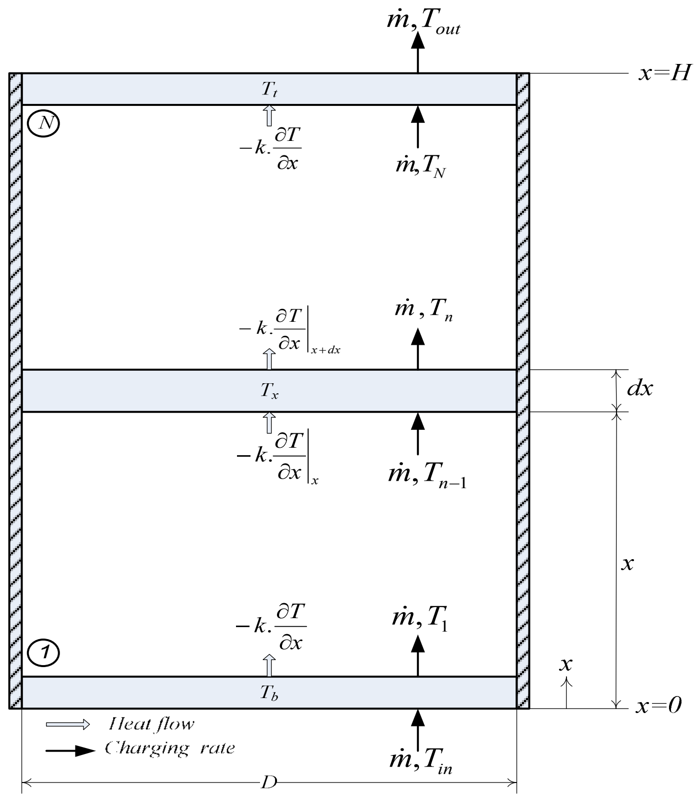

Figure 3.13 Physical model of stratified TES tank [4]

The energy balance of the water at a distance x from the bottom of the tank is identified as a parabolic partial differential equation which as in Equation 3.19.

$$\rho.A.c_p.\frac{\partial T}{\partial t} = k.A.\frac{\partial^2 T}{\partial x^2} - \dot{m}.c_p.\frac{\partial T}{\partial x} \tag{3.19}$$

Converting the mass flow rate, $\dot{m} = \rho.v.A$ and thermal diffusivity $\alpha = k/(\rho.c_p)$, reveal that Equation 3.19 was suitable to Equation 2.4, with the absence of last term that express the heat loss to surrounding.

The effect of conduction across the thermocline was accounted for in term of thermal diffusivity (α) that occurs due to conduction heat transfer between cool and warm water in the tank. The mixing effect factor was emphasized by pronouncing effective diffusivity factor [80]. The effective diffusivity factor form as $\varepsilon_{eff} = (\alpha + \varepsilon_H)/\alpha$, has value greater than unity in turbulent flow and for laminar flow the value of ε_{eff} is equal to 1.

Accommodating the two aforementioned factors affecting the degradation of stratification, Equation 3.19 became to Equation 3.20.

$$\frac{\partial T}{\partial t} + v\frac{\partial T}{\partial x} = \alpha.\varepsilon_{eff}\frac{\partial^2 T}{\partial x^2} \tag{3.20}$$

Equation 3.20 was divided into two cases, i.e conduction and convection equation. This was done to avoid any pseudo mixing in the numerical calculation as discussed in Section 2.4.

The conduction equation takes the form of Equation 3.21.

$$\frac{\partial T}{\partial t} = \alpha.\varepsilon_{eff}\frac{\partial^2 T}{\partial x^2} \tag{3.21}$$

The convection equation form is as follow.

$$\frac{\partial T}{\partial t} + v\frac{\partial T}{\partial x} = 0 \tag{3.22}$$

Since the assumption of a well insulated tank was used in this study, the temperature gradient across the top and bottom boundaries of the tank was assumed to be zero. It is expressed in Equation 3.23.

$$\frac{\partial T}{\partial x} = 0 \text{ at } x = 1 \text{ and } x = N \tag{3.23}$$

The solution was carried out numerically based on finite difference method. As a numerical solution, finite difference solves the equations as discrete solutions. This was performed by subdividing the region into a number of small slabs (Δx) in the height of TES tank and observed time interval (Δt). Each slab was assumed to represent constant temperature at horizontal layer [67].

In this study, the finite difference solution was solved using explicit method. The convergence stability of the explicit method was performed on the convection and conduction equation. Using differentiating technique, conduction equation in Equation 3.21 was described as Equation 3.24.

$$\frac{T_x^{t+1} - T_x^t}{\Delta t} = \alpha.\varepsilon_{eff}.\frac{T_{x-1}^t - 2.T_x^t + T_{x+1}^t}{\Delta x^2}$$

$$T_x^{t+1} = (1 - 2.\varepsilon_{eff}.\alpha.\frac{\Delta t}{\Delta x^2}).T_x^t + \alpha.\varepsilon_{eff}.\frac{\Delta t}{\Delta x^2}(T_{x-1}^t + T_{x+1}^t) \qquad (3.24)$$

The convergence stability of Equation 3.24 requires limitation of $\alpha.\varepsilon_{eff}.\ (\Delta t/\Delta x^2)$ value designated as AMIX value. The stability occurred in the condition as described in Equation 3.25 [74].

$$\text{AMIX} = \alpha.\varepsilon_{eff}\ (\Delta t/\Delta x^2) \leq 0.5 \qquad (3.25)$$

Convection equation solution takes the form of Equation 3.26.

$$\frac{T_x^{t+1} - T_x^t}{\Delta t} + v.\frac{(T_x^t - T_{x-1}^t)}{\Delta x} = 0$$

$$T_x^{t+1} = v.\frac{\Delta t}{\Delta x}.T_{x-1}^t + (1 - v.\frac{\Delta t}{\Delta x}.T_x^t) \qquad (3.26)$$

On the stability criteria, the Courant number designated as FLOW = $v.\Delta t/\Delta x$ must not be greater than unity. Therefore, the time interval (Δt) and segmental element (Δx) are chosen to fulfil the stability requirement as given by [74].

$$\text{FLOW} = v.\Delta t/\Delta x \leq 1 \qquad (3.27)$$

The solution of boundary condition as described in Equation 3.23 of the tank was calculated using Equation 3.28.

$$\frac{T_{x+1}^{t} - T_{x}^{t}}{\Delta x} = 0 \qquad (3.28)$$

Solution of the combined conduction and convection equations is effectively obtained using buffer tank concept [76]. The purpose of using buffer tank concept is to eliminate pseudo mixing in the solution. Using the buffer concept, one fictitious inlet buffer tank is placed at the bottom of the tank. The inlet buffer tank stores the incoming flow of water and is evaluated at regular time intervals. If accumulated water equals to one segment volume, the water is pulsed into the tank. Numerically this indicates that the convection equation is derived using FLOW = 1. Referring to Equation 3.26, condition of FLOW = 1 leads to Equation 3.29.

$$T_{x}^{t+1} = T_{x-1}^{t} \qquad (3.29)$$

Solution of boundary condition in Equation 3.28 reveal that T_{o}^{t} = T_{1}^{t} at the bottom of the tank and T_{N+1}^{t} = T_{N}^{t} at the top of the tank. T_{o}^{t} is the temperature at inlet buffer tank. The conduction equation was applied for each observed time interval, whereas the convection was implemented only at FLOW = 1 that indicate of one filled segment of the tank. The convection equation might be invoked occasionally, every third and forth time, depending on the flow rate. Thus, convection and conduction equation can be combined together without introducing pseudo-mixing through numerical procedures.

3.5.1.2 Model of Chillers

As illustrated in Figure 3.10 chilled water is circulated in a close charging system between TES tank and chillers. Outlet TES temperature, after accommodating temperature losses (ΔT_1), chilled water flows into the chillers at temperature T_{inC}. The chilled water is cooled in the chillers and exit at temperature T_{outC}. The chilled water is re-circulated into the TES tank, after accommodating temperature losses (ΔT_2) from its connection piping.

Cooling capacity in the chillers is calculated based on temperature difference between inlet and outlet temperature of chilled water as expressed in Equation 2.7. This cooling capacity is equal to cooling capacity given by evaporator component of the chillers, expressed as Equation 2.8 in Chapter 2.

The model of the chillers was developed as general equation to represent cooling capacity for both vapor compression and absorption chillers. The chiller model was also utilized to correlate inlet and outlet charging temperature. It was performed by equalizing both Equations 2.7 and 2.8. The relationship between outlet and inlet chilled water temperature takes form as Equation 3.30.

$$T_{out\ C} = T_{ev} + \frac{T_{in\ C} - T_{ev}}{e^{(UA/\dot{V}_C.\rho.C_p)}} \tag{3.30}$$

The outlet temperature of the chillers (T_{outEC}), after having temperature losses (ΔT_2) entering the TES tank at temperature at (T_{inTES}). The entered volumes mix with chilled water in the bottom part of TES tank and exist at mixing temperature (T_{mix}). The refrigerant temperature is designated as working evaporator temperature, T_{ev}. The assumption is the evaporator works at a constant temperature [11].

Mixing temperature occurs due to mix condition of entered volume and chilled water region at the lower part of TES tank. The chilled water influenced by mixing has volume of V_{LC} and temperature of T_{LC}, whereas the entered charging volume is multiplication of chillers flow rate ($\dot{V}_C$) with time interval Δt. Mixing temperature was calculated based on energy balance as described by Equation 3.31. The mixing temperature adopted concept of Wildin and Truman [79].

$$T_{mix} = \frac{V_{Lc}.T_{Lc} + \dot{V}_C.\Delta t.T_{inTES}}{V_{Lc} + \dot{V}_C.\Delta t} \tag{3.31}$$

3.5.1.3 Developing Single Stage Charging Model Type (II)

Developing single stage charging model type (II) was performed by integrating TES tank and chillers models. The solution was carried out using finite difference in explicit method, while buffer tank concept was involved in combining convection and conduction equations in the TES tank. The steps taken for the solution is presented in Figure 3.14.

The model was first carried out with initialization of the parameters, involving determination of initial temperature, thermo-physical property of water in the tank configuration parameter and chillers parameter. In addition, selecting ε_{eff} was also undertaken.

The initialization parameters of the charging model type (II) are described as follows.

i. Water temperature distribution in the initial charging condition.
   Initial temperature was used as starting state for charging. It was obtained from reading the temperature distribution or generated from empty capacity from the limit capacity criteria. Using limit criteria, initial temperature was generated using temperature distribution in Equation 3.1 with cool water depth at empty condition (C_E) as defined in Equation 3.4.

ii. Determination of average cool and warm water temperature.
   These temperatures were used to determine the value of thermal diffusivity (α). It was defined as average temperature of cool and warm water. The value of thermal diffusivity (α) was obtained from Appendix F.

iii. TES tank configuration parameters.
   TES tank configurations were used to determine parameters in the single charging model type (II). The TES tank configuration parameters consist of D, H, N_L, N_T and number of slabs (N).

   a. Number of observed slabs in TES tank (N) indicate the position of temperature sensors. Further, each slab was divided into small (L) numbers of Δx segments to cover parameter FLOW equal to 1 used in this method, hence observed interval time Δt was obtained accordingly using Equation 3.28.

b. TES tank configuration parameters were diameter (D), effective water depth (H), lower and upper nozzle elevations, N_L and N_T, respectively. These data were used to determine the mixing volume (V_{LC}), mixing temperature (T_{LC}), and outlet charging TES temperature (T_{outTES}).

iv. Chillers parameters were flow rate ($\dot{V}_C$), UA and evaporator temperature (T_{ev}). In addition, it was also required temperature losses at piping connection in the upstream and downstream of the chillers, (ΔT_1) and (ΔT_2), respectively. Those data were used to determine inlet and outlet chillers temperatures, T_{inC} and T_{outC}, respectively.

The other important parameter for identifying mixing effect was required prior to parameters initialization. It was performed by selection of effective diffusivity (ε_{eff}). The procedure in selection of ε_{eff} was discussed in section 3.5.1.4.

After initializing the parameters of the model, temperature distribution was performed to determine the outlet charging temperature (T_{outTES}), cool water volume influenced by mixing (V_{LC}) and temperature in the mixing region (T_{LC}). T_{outTES} was determined from temperature distribution considering upper nozzle elevation in the stratified TES tank. The volume V_{LC} was obtained based on cool water volume in the lower part of tank which was influenced by inlet flow. Temperature T_{LC} was determined as the average temperature of cool water volume in the V_{LC} region. Determination of these values was described in Section 3.5.3.

Next, the solution of the model followed the buffer concept based on finite difference method. Prior to define mixing temperature (T_{mix}), several temperature series have to be determined. Outlet charging temperature (T_{outTES}) was obtained based on temperature distribution at upper nozzle elevation. Water mixing volume temperature at (T_{LC}) was determined as average temperature in the mixing region. Inlet charging temperature (T_{inTES}) was determined from Outlet charging temperature (T_{outTES}) plus losses temperature (ΔT_1). Explanations of these formulae are described in Equations 3.32 to 3.36.

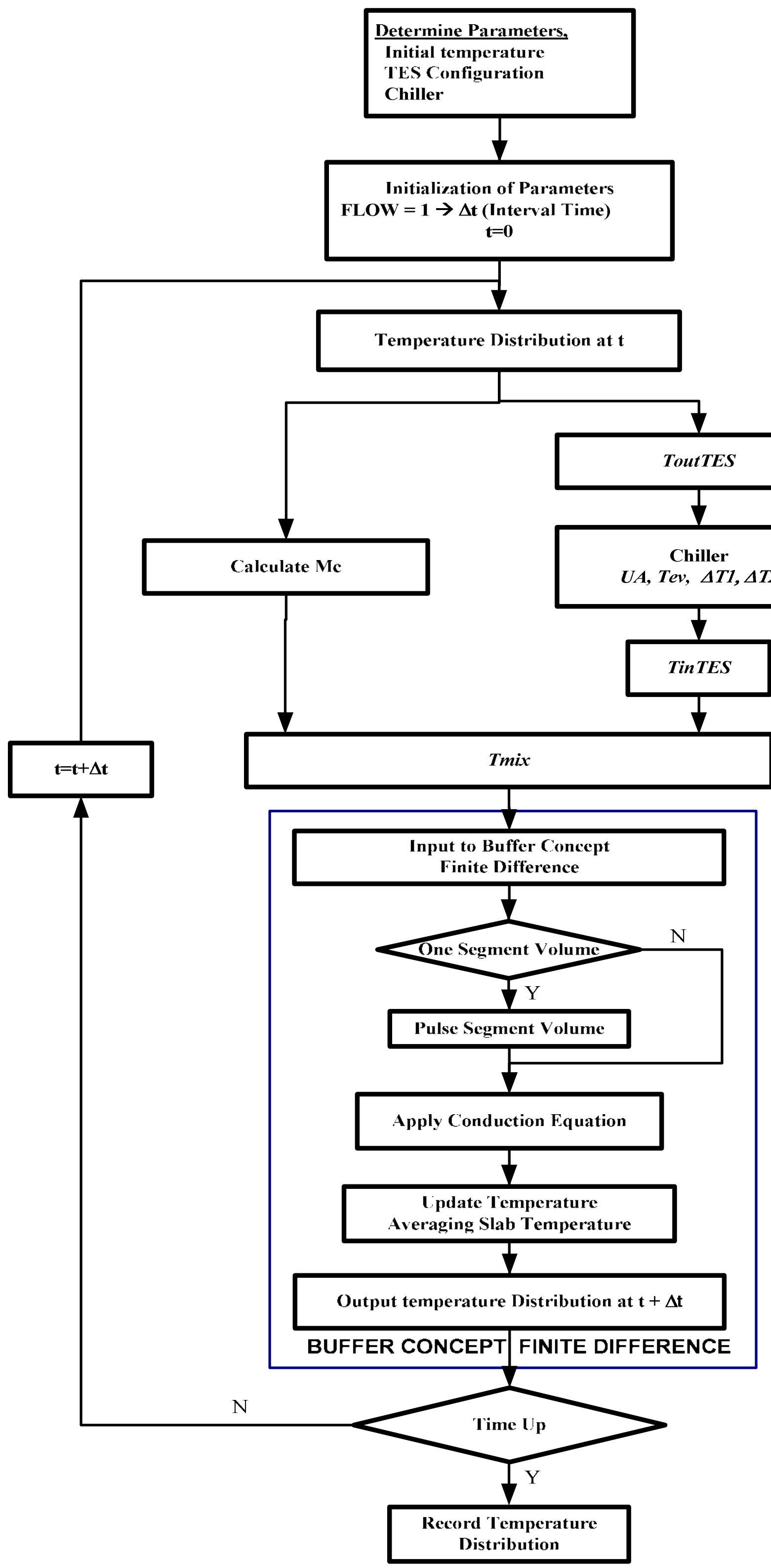

Figure 3.14 Solution steps in integrating of TES tank and chiller models.

3.5.1.4 Selection of Effective Diffusivity

Prior to parameters initialization, effective diffusivity (ε_{eff}) were selected properly. Selection of ε_{eff} was aimed to cover temperature distribution profile in the range of working flow rate. The appropriate ε_{eff} was selected from various observations. Higher value ε_{eff} indicates more slope gradient of thermocline profile. The other purpose of selecting ε_{eff} was to observe whether the convergence criteria in Equation 3.25 were reached or not. If the model requires AMIX value less than 0.5, it indicates that it can be solved using explicit method. On the other hand, if AMIX is observed exceeding 0.5 means that finite difference should be solved in implicit method.

The selection of ε_{eff} was performed using data set IA for charging flow rate of 393 m^3/hr. The mixing effect was selected from 0 to 250 in the range of AMIX lower than 0.5. The evaluation in the selection utilized coefficient of determination, R^2. The selection of ε_{eff} involved TES tank configuration parameter and chillers parameter, whereas initial temperature was taken from the observed data.

3.5.2 Verification of Single Stage Charging Model Type (II)

The single stage charging model type (II) developed in Section 3.5.1.3 has to be verified prior to conduct simulation. The verification was performed in two charging flow rate cases i.e 393 m^3/hr and 524 m^3/hr. For flow rate of 393 m^3/hr, the verification used data set of IB and IC. For the case of charging flow rate 524 m^3/hr, data sets of IIB and IIC were used.

Inputs of the model were initial water temperature distribution, TES tank configuration and chillers parameters (flow rate, UA, T_{ev}, ΔT_1 and ΔT_2) besides thermo-physical properties of chilled water. The initial temperature was obtained from the observed data and the parameters in TES tank configuration taken from Table 3.1. Determination of chillers parameters is explained in the following section.

3.5.2.1 Chillers Parameters

The chiller parameters consist of flow rate, *UA* and evaporator temperature (T_{ev}). Parameters *UA* and T_{ev} were determined based on Equations 2.7 and 2.8 incorporating to designed data of the chillers namely inlet and outlet temperature ($T_{inC,des}$, $T_{outC,des}$), flow rate ($\dot{V}_C$) and designed chiller cooling capacity ($Q_{C,des}$).

In this study, design inlet and outlet water temperature were 13.5°C and 6°C, respectively. Chillers were assumed to have constant evaporator temperature (T_{ev}) of 4°C. The obtained values of *UA* parameter are tabulated in Table 3.5.

Table 3.5 Values of *UA* parameter in the chillers

Flow rate ($\dot{V}_C$) (m^3/hr)	Cooling Capacity ($Q_{C,\ des}$)	*UA* (kW/°C)
131	*325 RT(1,142.75 kW)*	238.14
262	*650 RT (2,285.5 kW)*	476.28
393	*975 RT(3,428.25 kW)*	714.41
524	*1200 RT (4,571.0 kW)*	952.55
504	*1250 RT (4,395.2 kW)*	916.19

3.5.2.2 Evaluation in Model Verification

The verification of the model was carried out by evaluating the temperature distribution similarity and temperature profiles similarity. To endorse acceptance of the model, the statistical test was also adopted. The evaluation of temperature values, profile similarity as well as statistical test were similar to that of single charging model type (I), described in section 3.4.3.2.

Since the operating TES tank data were available as hourly recorded, it is required to divide each slabs of the TES tank to a numbers of small segment to get the appropriate time interval. Selection of the segment numbers is performed to achieve similar observed hourly interval. Hence, the multiplication of observed time interval (Δt) is approximating similar to hourly interval.

3.5.3 Simulation of Single Stage Charging Model Type (II)

Simulations single stage charging model type (II) was conducted in variation of chillers parameter. The simulation was treated using same initial temperature, TES tank configuration parameter and the limit temperature (T_r) = 9°C. The TES tank configuration parameter was similar on the charging model type (I) as in Table 3.1, whereas chillers parameter is tabulated in Table 3.6, with all ΔT_1 and ΔT_2 are equal to zero. The simulation was denoted as cases A2, B2 and D2.

Table 3.6 Chiller parameters value of simulation cases A2, B2 and D2.

Simulation cases	Notation	Value	Unit
Case A2	$\dot{V}_C$	524	m^3/hr
	UA	952.5	kW/°C
	T_{ev}	4	°C
Case B2	$\dot{V}_C$	393	m^3/hr
	UA	714.4	kW/°C
	T_{ev}	4	°C
Case D2	$\dot{V}_C$	262	m^3/hr
	UA	476.3	kW/°C
	T_{ev}	4	°C

Simulation was extended to observe charging characteristics in term of temperatures T_{inTES}, T_{outTES}, T_{mix} and cumulative cooling capacity (Q_{cum}). It was also extended to perform observation of chiller cooling capacity (Q_C) and partial working load of the chillers. Observation was carried out until reaching cumulative cooling capacity exceeds its nominal holding capacity of 49,226.44 kWh.

For this purpose, the calculation of the aforementioned parameters was formed based on temperature distribution in the TES tank, hence related to water slabs in the TES tank. In this study, the TES elevation was divided into 14 slabs, which were located serially as 1 to 14 from the bottom to the upper part. The slab temperature was identified in the middle of the slab. Since the simulation involved temperature were expressed accordingly. All equations were described in term of subscript t express observation time intervals.

Outlet charging TES temperature was determined as water temperature at the upper nozzle which is located at 12.3 m elevation. Determination of T_{outTES} was based on interpolation of temperature slabs 12 and 13, therefore was calculated as Equation 3.32.

$$T_{outTES,t} = T_{12,t} + 0.8(T_{12,t} - T_{11,t}) \tag{3.32}$$

Inlet water temperature entering the chillers was calculated as in Equation 3.33.

$$T_{inC,t}=T_{outTES,t}+\Delta T_1 \tag{3.33}$$

The outlet water temperature from the chillers was determined from Equation 3.31, and takes form as Equation 3.34.

$$T_{out\,C,t} = T_{ev} + \frac{T_{in\,C,t} - T_{ev}}{e^{(UA/\dot{V}_{C,t}.\rho.Cp)}} \tag{3.34}$$

Inlet water temperature entering the TES tank was identified as in Equation 3.35

$$T_{inTES,t}=T_{outC,t}+\Delta T_2 \tag{3.35}$$

Mixing temperature was calculated as a mixed temperature between the cool water volume and the entering volume water from the chillers, as described in Equation 3.36.

$$T_{mix,t+\Delta t} = \frac{V_{Lc,t}.T_{Lc,t} + \dot{V}_{C,t+\Delta t}.\Delta t.T_{inC,t+\Delta t}}{V_{Lc,t} + \dot{V}_{C,t+\Delta t}.\Delta t} \tag{3.36}$$

Determination of cool water volume influenced by mixing (V_{LC}) was based on assumption of two influenced slabs region. This considered lower nozzle elevation of 1.824 m. It was determined as the water volume at two slabs of TES tank, as Equation 3.37.

$$V_{Lc,t} = 2.\ A.\ \rho \tag{3.37}$$

The temperature in the mixing region (T_{LC}) was determined as average cool water temperature of slabs 1 and 2 at the lower part of the tank, as in Equation 3.38.

$$T_{LC,t} = (T_{1,t}+T_{2,t})/2 \quad (3.38)$$

On the other aspect, chillers working parameters were determined in term of cooling capacity (Q_C) and percentage of partial working load (PL).

Cooling capacity of the chillers was calculated as in Equation 3.39.

$$Q_{C,t} = \dot{V}_{C.t}.C_p.(T_{inC,t} - T_{outC,t}) \quad (3.39)$$

Partial working load of the chillers was calculated as working cooling capacity over the design cooling capacity of the chillers as Equation 3.40.

$$PL_t = Q_{C,t}/Q_{Cdes} \quad (3.40)$$

3.5.4 Two-Stage Charging Model Type (II)

The single stage charging model type (II) was enhanced for two-stage charging stratified TES tank. It was performed to cover charging with two types of chillers sequentially, namely absorption and electric chiller. The special issue in two-stage charging is the occurrence of limit temperature at outlet TES temperature, due to temperature limitation of the absorption chillers is explained in the following section.

3.5.4.1 Enhancement of Two-Stage Charging Model Type (II)

As previously discussed, the two-stage charging simulation used the absorption chillers in the first stage and electric chiller in the second stage. The first stage charging is performed from empty to full capacity. The empty capacity is identified from initial temperature distribution. The full capacity of the first stage charging is determined in the condition of outlet charging temperature equal to limit temperature. The simulation steps taken for the two-stage charging is presented in Figure 3.15.

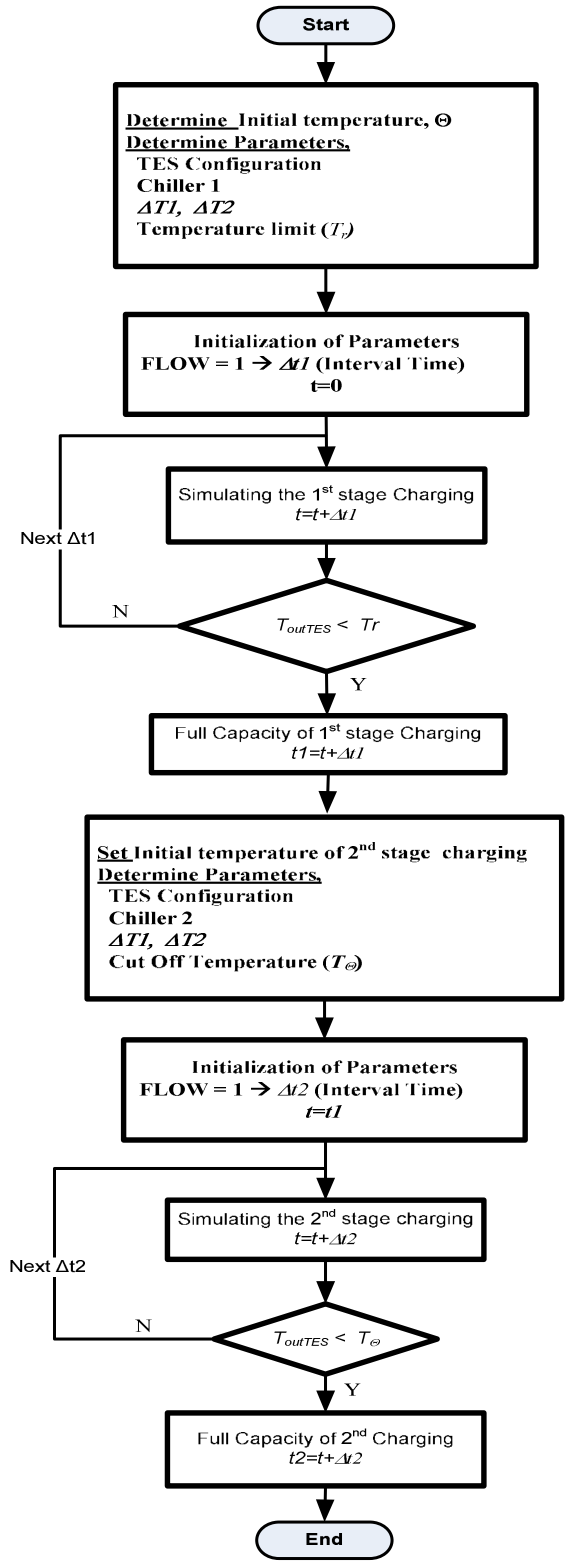

Figure 3.15 Simulation steps in two-stage charging model type (II)

Inputs of the two-stage charging simulation were initial temperature, TES tank configuration, chillers parameter and temperature losses in piping connection. In addition, limit temperature of absorption chillers at the first stage charging was also required. After parameter initialization, the simulation was performed in the first stage charging. The full capacity of the first charging was reached when outlet charging temperature equals to the limit temperature of the absorption chiller. The simulation was then continued for the second stage charging which is served by electric chillers. In the second stage charging, full capacity of the first charging was set as the initial condition. The second stage charging could work either as the same or different observed time interval as on the first stage charging. The full capacity of the second stage charging is a condition of outlet TES tank temperature equals to the designated cut-off temperature. Determinations of full capacities in the first and second stage of charging were carried out by interpolation between two observed time intervals.

3.5.4.2 Simulation of Two-Stage Charging Model Type (II)

Simulation of two-stage charging model type (II) was performed using absorption chillers in the first stage, whereas electric chiller was utilized in the second stage. The simulations of two-stage charging were performed in two cases i.e variation of chillers parameters and limit temperature.

i. Variation of chillers parameters

The input parameters of TES tank configuration are shown in Table 3.1. Temperature losses ΔT_1 and ΔT_2 were taken as zero. Variation of chillers parameters were carried out in the second stage charging, whereas the first stage charging used absorption chillers at the flow rate of 504 m^3/hr. The simulation was carried out for three cases i.e E2, F2 and G2. Values of the chillers parameters in the simulation are tabulated in Table 3.7.

Table 3.7 Chiller parameters value of simulation cases E2, F2 and G2

Chillers parameters	**Notation**	**Value**	**Units**
Absorption chiller (1st stage)	$\dot{V}_{C1}$	504	m^3/hr
	UA	952.5	kW/^{o}C
	T_{ev}	4	^{o}C
	T_r	9	^{o}C
Electric chiller (2nd stage)			
Case E2	$\dot{V}_{C2}$	524	m^3/hr
	UA	952.5	kW/^{o}C
	T_{ev}	4	^{o}C
Case F2	$\dot{V}_{C2}$	393	m^3/hr
	UA	714.4	kW/^{o}C
	T_{ev}	4	^{o}C
Case G2	$\dot{V}_{C2}$	262	m^3/hr
	UA	476.3	kW/^{o}C
	T_{ev}	4	^{o}C

ii. Variation of limit temperature

The other simulation of the two-stage charging model type (II) was performed with variation of limit temperature. The input parameters of initial temperature and TES tank configuration were similar with that of the variation chillers parameter in the two-stage charging model type (II). The simulation was carried out for three cases i.e H2, J2 and K2. Variations of the chillers parameter in the simulation of the model is tabulated in Table 3.8.

Table 3.8 Chiller parameters value of simulation cases H2, J2 and K2

Simulation cases H2, J2, K2	**Notation**	**Value**	**Unit**
Absorption chiller (1st stage)			
UA = 916.2 kW/^{o}C, T_{ev} = 4^{o}C	$\dot{V}_{C1}$	504	m^3/hr
Electric chiller (2nd stage)			
UA = 714.4 kW/^{o}C, T_{ev} = 4^{o}C	$\dot{V}_{C2}$	393	m^3/hr
Variation limit temperature (T_r)			
Case H2	T_r	7	^{o}C
Case J2	T_r	9	^{o}C
Case K2	T_r	11	^{o}C

3.6 Comparison of Charging Models

Two different approaches were utilized for developing the models namely open and close charging system. The simulation models were developed for single and two-stage charging. In the open charging system, the models were designated as type (I) whereas in the close charging system, the models were established as type (II). Comparisons of the two models are discussed in the following section.

3.6.1 Comparison of Single Stage Charging Models

Comparison was carried out in the charging simulation cases on flow rate variation. The comparisons were discussed in term of charging duration and cumulative cooling capacity. The comparison between single stage charging model types (I) and (II) were performed by comparing cases A1, B1, D1 and A2, B2, D2. The simulations were treated to have similar parameters of initial temperature and TES tank configuration parameters.

In addition, comparisons were also performed to observe additional cool water temperature and charging parameters obtained from the simulations. Temperature of additional cool water was carried out by comparing the average cool water temperature (T_c) in the simulation model type (I) and mixing temperature (T_{mix}) in the simulation model type (II). Comparisons were performed for the parameters values of charging duration and cumulative cooling capacity.

3.6.2 Comparison of Two-stage Charging Models

Comparison between the two-stage of charging models were carried out for two cases of flow rate and limit temperature variation. The simulation cases of E1, F1 and G1 were compared for flow rate variation. Limit temperature variation involves comparisons of cases H1, J1, K1 and cases H2, J2, K2.

CHAPTER 4
RESULTS AND DISCUSSION

The main aim of the analysis and simulation undertaken in this study is to enable the integration of absorption chillers to complement electric chillers for charging the stratified TES tank. This was done by developing simulation models that have capability in generating temperature distribution as well as determining charging parameters. Development of the simulation models were performed into two different approach namely open and close charging systems. Using open charging system, the charging model for single stage type (I) was developed and then enhanced for two-stage charging model type (I). Similarly for close system, the charging model for single stage type (II) was developed and enhanced for two-stage charging model (II). Both single stage charging model type (I) and type (II) were validated using historical data obtained from district cooling plant at Universiti Teknologi PETRONAS. The following section highlights the results of the development, validation and simulations of the models.

4.1 Open Charging System

The main component in developing the models for open charging system is determination of charging parameters based on temperature distribution function. The temperature distribution function used for determination the parameters was selected to represent temperature distribution profile.

4.1.1 Temperature Distribution

The temperature profile forms an S-curve shape containing parameters T_h, T_c, C and S. The important step that was undertaken to identify temperature profile was selecting a function that represents the profile and having related parameters. Identification of typical S-curve profile was performed utilizing operating temperature distribution data of stratified TES tank.

4.1.1.1 Selection of Temperature Distribution Function

One data set of temperature distribution IA was used for the selection. The data consist of serially temperature data recorded during the charging cycle from 18.00 hours to 03.00 hours in the following day with charging flow rate 393 m^3/hr. Plot of the temperature data is presented in Figure 4.1.

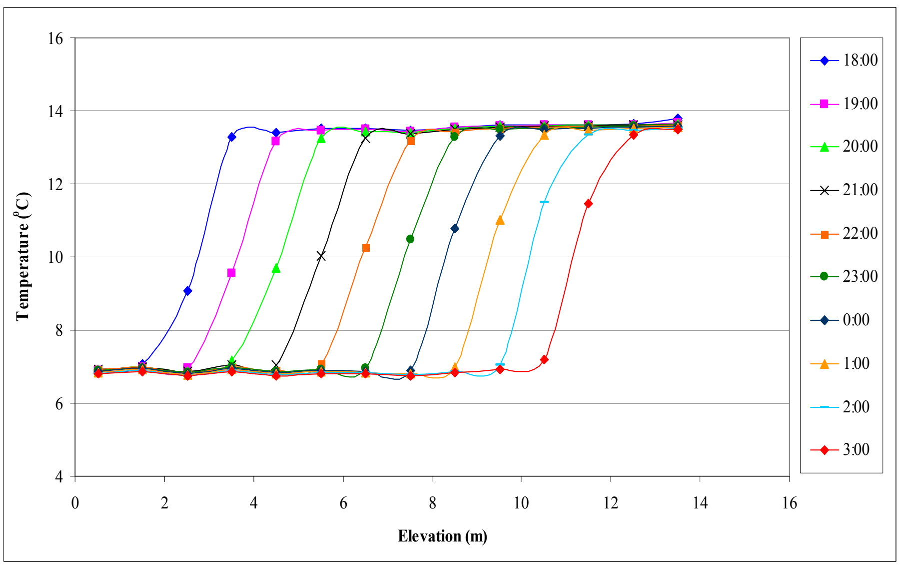

Figure 4.1 Temperature distribution of data set IA (September 9, 2008)

Data shown in Figure 4.1 were used for non linear curve fitting using commercial software SIGMAPLOT. Selection of temperature distribution function was performed on the fitting equation family which has S-curve profiles. The selection was performed in three steps as follows.

i. Capability to represent S-curve profile.
ii. Contain four parameters of T_c, T_h, C and S.
iii. Contain suitable parameters as described in Figure 3.3.

The selection of temperature distribution function is tabulated in Table 4.1. From Table 4.1, it can be seen that there are 16 equations that have capability in representing S-curve profile. The equations were obtained from sigmoidal and ligand binding equation groups [115]. In the second step, equations numbered 1, 3, 4, 6, 8, 10, 11, 13 and 15 as per Table 4.1 failed to fulfil the four parameters criteria. In the third step, one equation was found meeting the requirement namely sigmoid dose response (variable slope) equation.

To achieve the requirement as described in Figure 3.3, the sigmoid dose response (variable slope) equation was modified. The modification was performed by replacing the term of $\log_{EC50}$ with C, min with T_c, max with T_h and Hill Slope to S.

Table 4.1 Selection of temperature distribution function

Number	Equation Types	Results and Reasons
1	Three Parameter Sigmoid	Not applicable, 3 parameters
2	Four Parameter Sigmoid	Not suitable parameters
3	Five Parameter Sigmoid	Not applicable, 5 parameters
4	Three Parameter Logistic	Not applicable, 3 parameters
5	Four Parameter Logistic	Not suitable parameters
6	Five Parameter Logistic	Not applicable, 5 parameters
7	Four Parameter Weibull	Not suitable parameters
8	Five Parameter Weibull	Not applicable, 5 parameters
9	Four Parameter Gompertz Growth	Not suitable parameters
10	Five Parameter Gompertz Growth	Not applicable, 5 parameters
11	Three Parameter Chapman	Not applicable, 3 parameters
12	Four Parameter Chapman	Not suitable parameters
13	Three Parameter Hill	Not applicable, 3 parameters
14	Four Parameter Hill	Not suitable parameters
15	Sigmoid Dose Response	Not applicable, 3 parameters
16	Sigmoid Dose Response (Variable Slope)	Accepted, $Y = \min + \dfrac{\max - \min}{1 + 10^{(LogEC_{50} - X)HillSlope}}$

The modified equation is designated as sigmoid dose response (SDR) function which takes the following form.

$$T = T_c + \frac{T_h - T_c}{1 + 10^{(C-X)S}} \tag{4.1}$$

The SDR function relates temperature distribution to variable X and parameters T_c, T_h, C and S.

The parameters T_c and T_h were temperature in ^{o}C. Parameter C is the dimensionless mid point of thermocline thickness and S is related to slope gradient of the function.

The variable X expresses the dimensionless elevation, $X = x.N/H$. The x is elevation of mid point of the slab, H is water effective depth of the tank , N is number of slabs in the TES tank.

Evaluation of SDR function utilized temperature distribution data of charging flow rate 393 m^3/hr and 524 m^3/hr. This was performed by utilizing the whole operating data sets of IA, IB, IC, IIA, IIB and IIC which are included in Appendices A1 to A6.

One evaluation using temperature data set IA is discussed in this section. Fitting SDR function to the data is presented in Figure 4.2. In Figure 4.2, temperature data are shown as marked points, while curvature lines are the fitting function. It can be seen that the temperature distribution resulted to more clear demarcation of the temperature in the asymptotes curve region following the SDR function.

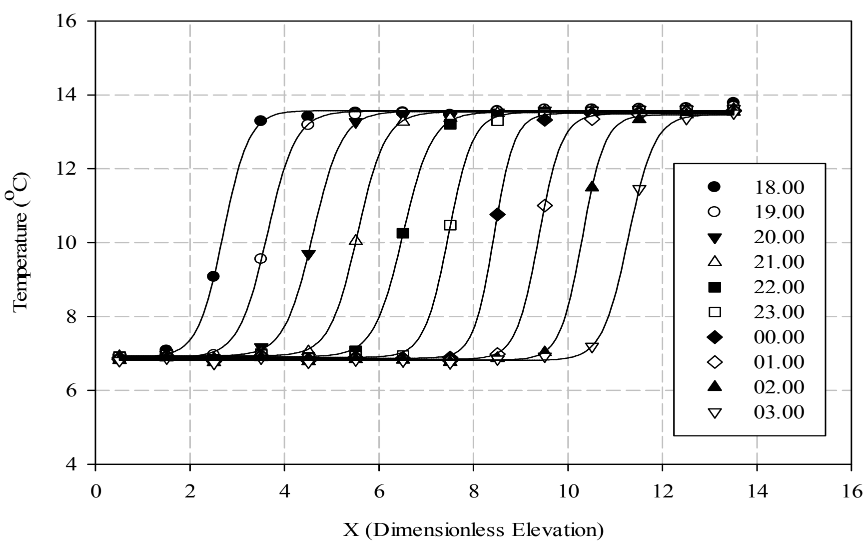

Figure 4.2 SDR fitting of temperature distribution data set IA

The fitting plot in Figure 4.2 was used to determine values of T_c, T_h, C and S by curve fitting method. The values of T_c, T_h, C and S are tabulated in Table 4.1. Coefficient determination (R^2) for evaluation the goodness of fitting are also presented in the table.

It is noted the R^2 values in Table 4.2 are greater than 0.99, which indicate that the temperature data fitted well to the SDR function. The function enabled to figure out S-curve profile of temperature distribution.

Table 4.2 Parameters of SDR fitting on data set IA

Chrg. Hrs.	T_c (°C)	T_h (°C)	C	S	R^2
18:00	6.9	13.6	2.7	1.6	0.999
19:00	6.9	13.6	3.6	1.4	0.999
20:00	6.9	13.6	4.6	1.4	1.000
21:00	6.9	13.5	5.5	1.5	1.000
22:00	6.9	13.5	6.5	1.4	1.000
23:00	6.9	13.5	7.5	1.7	1.000
0:00	6.9	13.5	8.4	2.0	1.000
1:00	6.8	13.5	9.4	1.8	1.000
2:00	6.8	13.5	10.3	1.8	1.000
3:00	6.8	13.5	11.3	1.6	1.000

SIGMAPLOT was also performed to fit data set of IA, IB, IC, IIA, IIB and IIC in the Appendices A1-A6. Results of the fitting are included in Appendices G1-G6, respectively. Summary of the curve fitting results is presented in Table 4.3.

Table 4.3 Summary results of SDR fitting

Data sets	Charging Hours	R^2	Observation Results	Remarks
IA	18.00 - 3.00	> 0.992	Passed	Appendix G1
IB	18.00 - 3.00	> 0.992	Passed	Appendix G2
	4.00 - 7.00	-	In-corvergence	
IC	18.00 - 3.00	> 0.997	Passed	Appendix G3
	4.00 - 7.00	-	In-corvergence	
IIA	18.00 - 0.00	> 0.994	Passed	Appendix G4
	1.00 - 7.00	-	In-corvergence	
IIB	19.00 - 3.00	> 0.993	Passed	Appendix G5
	4.00 - 6.00	-	In-corvergence	
IIC	19.00 - 3.00	> 0.992	Passed	Appendix G6
	4.00 - 6.00	-	In-corvergence	

From Table 4.3, it is shown that charging hours which has S-curve temperature distribution could be fitted well to SDR function. Otherwise, it could not be covered due to in-convergence fitting, since the SDR parameters values were not obtained in the non linear fitting iteration. It is noted that R^2 values for certain S-curve temperature profile are higher than 0.992 which indicate that SDR function could fit well to the temperature distribution.

This finding improved characterization of water temperature distribution in stratified TES tank. Using SDR function, temperature distribution could be determined based on T_c, T_h, C and S parameters, hence offers benefits in determination of temperature distribution based on functional relationship.

4.1.1.2 Characteristic of Sigmoid Dose Response Function

In order to identify changing effect of the parameters in SDR function, characterization is required. It was performed by variation of T_c, T_h, C and S.

i. Variation of average cool water temperature (T_c)

Characterization was carried out at constant $T_h = 13.5^{o}$C, $C = 7$ and $S = 1$, whereas T_c varies from 1^{o}C to 10^{o}C. The variation of T_c in SDR function is shown in Figure 4.3.

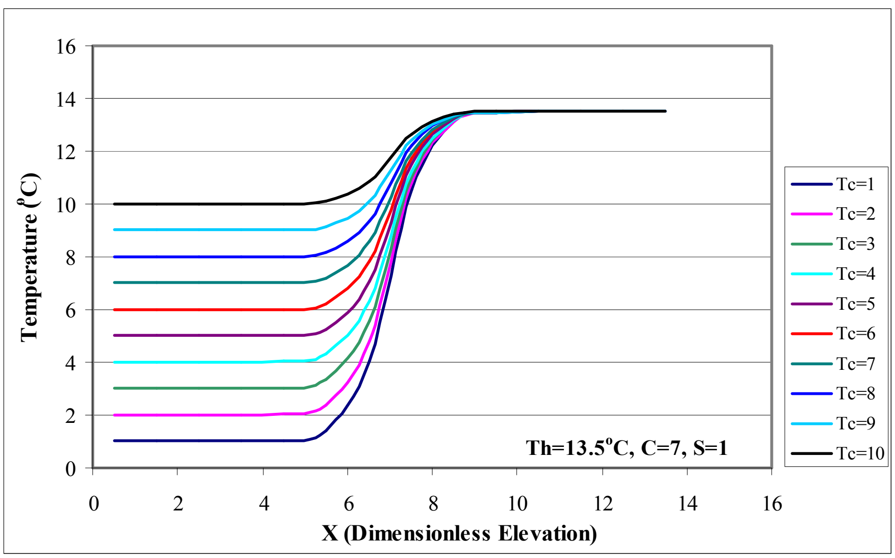

Figure 4.3 Variation of average cool water temperature (T_c) in SDR function

From Figure 4.3, it is noted that decreasing T_c affect changing of the asymptote line. However, the midpoints of thermocline is still located fix at X values equal to 7, this indicates that C values are not affected by changing of T_c. Slope gradient (S) emerges as a connecting line from asymptote T_c and T_h.

ii. Variation of average warm water temperature (T_h)

Analysis was conducted at T_c = 6°C, C = 7 and S = 1 with variation T_h at 7°C, 8°C, 9°C, 10°C, 11°C, 12°C, 13°C and 13.5°C. The variation of T_h in SDR function is presented in Figure 4.4.

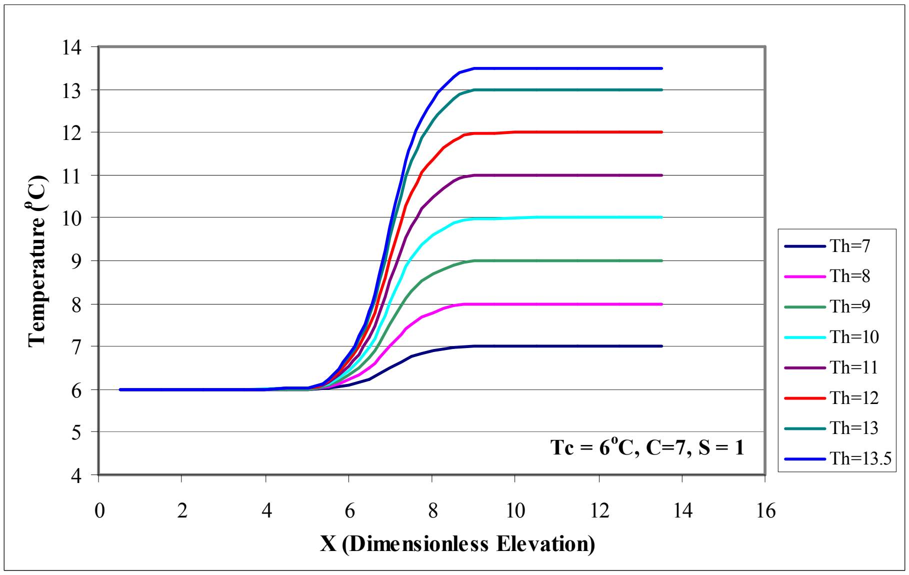

Figure 4.4 Variation of average warm water temperature (T_h) in SDR function

As seen in Figure 4.4, variation of T_h values affect changing of asymptote line. However, the values of T_c and C are not influenced by variation of T_h. The midpoints of thermocline fixed at X values equal to 7, which indicates that C values are constant. Slope gradient (S) emerges as a connecting line from asymptote T_c and T_h.

iii. Variation of midpoint of thermocline thickness (C)

Characterization was conducted at T_c = 6°C, T_h = 13.5°C, S = 1, with parameter C varied from 0, 2, 4, 6, 8, 10, 12 and 14. The variation of C in the SDR function is presented in Figure 4.5.

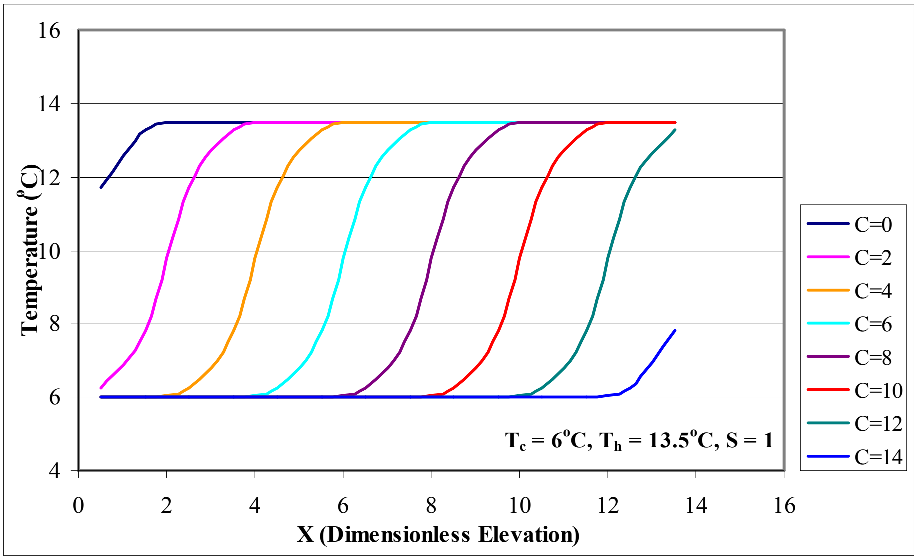

Figure 4.5 Variation of midpoint of thermocline (*C*) in SDR function

As shown in Figure 4.5, variation of *C* influences the temperature profile in SDR function. The temperature profile move upward with increasing of *C*. Parameter *C* reflects the midpoint of thermocline as the boundary limit between warm and cool water. This is also used as identification of cool water depth in the TES tank.

iv. Variation of slope gradient (*S*)

Variation of parameter *S* was performed at constant parameters of T_c = 6°C, T_h = 13.5°C and *C* = 7. The variation of *S* is illustrated in Figure 4.6. From Figure 4.6, it is noted that changing of *S* values affected the slope gradient temperature distribution. With *S* equal to 0, the temperature distribution profile is horizontal. Increasing in values of *S* caused steeper thermocline profile, as shown for the range values of *S* of $0<S<5$. At the *S* values equal to 5 and above, similar temperature profiles occurred at the steepest gradient.

Based on SDR function characteristics, it is shown that parameters T_c and T_h affect the asymptote value of the curve, *C* affect the midpoint of thermocline, whereas *S* involves with slope gradient of temperature profile. In the implementation of SDR function, $T_{c,}$ T_h and *C* values are selected to suit the water temperature condition in the stratified TES tank. Values of T_c and T_h reflect average cool and warm water temperatures, whereas C indicates the cool water depth. The value of slope gradient of thermocline profile (S) is recommended to be in the range of $0<S<5$.

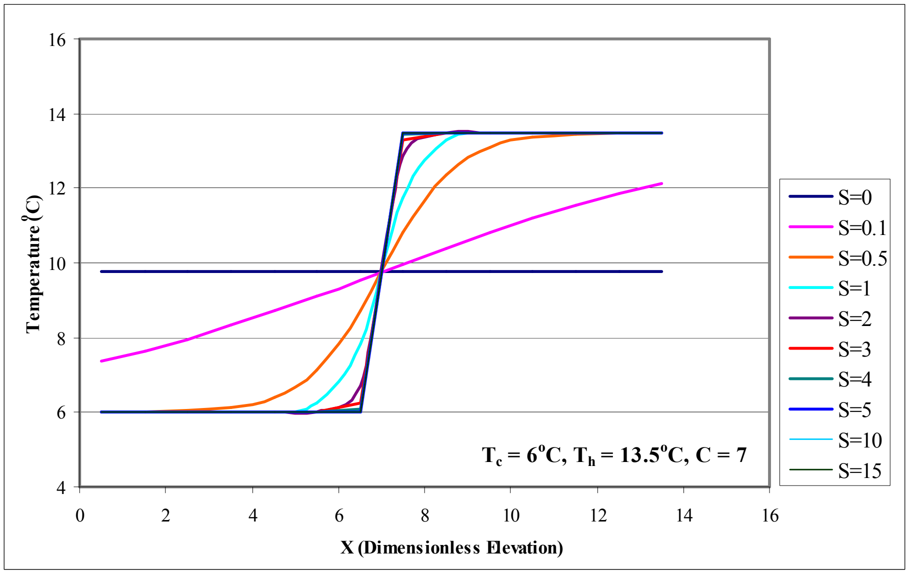

Figure 4.6 Variation of slope gradient (S) in SDR function

4.1.2 Formulation of Charging Parameters

Formulations of charging parameters namely limit points, thermocline thickness, limit capacity criteria and temperature transition points were performed utilizing SDR function. The formulation was based on solutions of equations in Section 3.3.2.

4.1.2.1 Limit Points and Thermocline Thickness

The determination concept of thermocline thickness based on S-curve temperature profile as illustrated in Figure 3.1. The formulation of limit points involves with upper and bottom limit points (U) and (B), referred to Equation 3.2.

For this purposes, dimensionless cut-off temperature $\Theta=(T-T_c)/(T_h-T_c)$, Musser [28], was utilized to indicate the edge of thermocline profile. Hence, SDR function is described as in Equation 4.2.

$$\frac{1}{\Theta} = 1 + 10^{(C - X)S} \tag{4.2}$$

Where the distance from C to X express the half-thickness of the thermocline.

$$C - X = \frac{\log(\frac{1}{\Theta} - 1)}{S} \tag{4.3}$$

By predetermining the value of Θ at a certain value, X identifies the position of bottom limit point (B) as described in Equation 3.2. Hence, bottom limit point (B) takes the form of Equation 4.4.

$$B = C - \frac{\log(\frac{1}{\Theta} - 1)}{S} \tag{4.4}$$

As described in Figure 3.1, upper limit point was obtained by adding half thickness of thermocline to midpoint of thermocline. Therefore upper limit point (U) of the thermocline can be expressed as in Equation 4.5.

$$U = C + \frac{\log(\frac{1}{\Theta} - 1)}{S} \tag{4.5}$$

Accordingly, thermocline thickness (W_{TC}) can be represented as twice the value of half-thickness of thermocline as in Equation 4.6.

$$W_{TC} = \frac{2.\log(\frac{1}{\Theta} - 1)}{S} \tag{4.6}$$

It is noted that SDR function is capable of formulating parameters of limit points and thermocline thickness. This would enable accurate determination of parameters rather than the estimation method [34], [36] and [40]. The improved method in the formulation of the parameter based on SDR function was also utilized to evaluate thermocline thickness [48, 49] and performance analysis [50] in stratified TES tank.

Parameters of the open charging system model were also developed based on SDR function. The parameters were limit capacity criteria and temperature transition point.

4.1.2.2 Limit Capacity Criteria

As described in the Section 3.3.2.3, limit capacity criteria can be defined based on water level limit and temperature limit criteria. Both these criteria were used to define empty and full capacities in the charging of stratified TES tank.

i. Water level limit criteria

Based on water level limit criteria, cool water depth at empty capacity was determined by equalizing bottom limit point in Equation 4.4 with lower nozzle elevation (N_L). As a result, cool water depth on empty capacity (C_E) was obtained as the following.

$$C_E = N_L + \frac{\log\left(\frac{1}{\Theta} - 1\right)}{S} \tag{4.7}$$

Full capacity, on the other hand, was defined by equalizing bottom limit point in Equation 4.4 with upper nozzle elevation (N_T). This was used to define cool water depth at full capacity criteria (C_F) as in Equation 4.8.

$$C_F = N_T + \frac{\log\left(\frac{1}{\Theta} - 1\right)}{S} \tag{4.8}$$

ii. Temperature limit criteria

Based on temperature limit criteria, cool water depth on empty capacity (C_{ET}) was formulated as in Equation 4.9.

$$C_{ET} = N_L + \frac{1}{S}.\log\left\{\left(\frac{T_h - T_c}{T_r - T_c}\right) - 1\right\} \tag{4.9}$$

Equation (4.9) was obtained by equalizing temperature in SDR function to the limit temperature (T_r), while variable X is equalized to the lower nozzle elevation (N_L). Full capacity based on temperature limit criteria was obtained by equalizing temperature in SDR function with limit temperature (T_r) and variable X is referred to upper nozzle elevation (N_T). Hence, cool water depth on full capacity (C_{FT}) was obtained as defined by Equation 4.10.

$$C_{FT} = N_T + \frac{1}{S}.\log\left\{\left(\frac{T_h - T_c}{T_r - T_c}\right) - 1\right\} \tag{4.10}$$

4.1.2.3 Temperature Transition Point

As described in Section 3.3.2.3, temperature transition point can be defined by utilizing upper limit point. The cool water depth at temperature transition point (C_{FR}) was obtained by equalizing upper limit point (U) in Equation 4.5 to the upper nozzle elevation (N_T). Hence, cool water depth at temperature transition point was obtained as in equation 4.11.

$$C_{FR} = N_T - \frac{\log\left(\frac{1}{\Theta} - 1\right)}{S} \tag{4.11}$$

From these results, it is noted that SDR function is capable of representing formulation the important parameters in the charging of stratified TES tank. The findings show that SDR function offer advantage of formulation parameters not only limit points and thermocline thickness, but also limit capacity criteria and temperature transition point in the charging of stratified TES tank.

4.1.2.4 Implementation of SDR Function

Prior to development of open charging model, the values of charging parameters were specified. It involved determination of initial temperature and selection of limit capacity criteria.

i. Determination of initial temperature distribution

Determination of initial condition during charging involves knowing how much cool water temperature in the lower nozzle. It can be performed by utilizing parameters in SDR function together with dimensionless cut-off temperature (Θ) and lower nozzle elevation.

The parameter of dimensionless cut-off ratio values can be selected in the range of 0 to 0.5 covering minimum and maximum thermocline thickness. For $\Theta = 0$ indicate that the thermocline limit points are located at T_c and T_h, therefore giving a maximum thickness. At this condition cut-off temperature is equal to T_c. With $\Theta = 0.5$, the value of cut-off temperature is equal to $(T_c + T_h)/2$ and the limit points are at midpoint of thermocline region. It has zero values of the thermocline thickness. However, calculation using SDR function at Θ equal to 0 and 0.5 revealed cool water depth at ∞ and 0 values, respectively. Therefore, the range of $0<\Theta<0.5$ can be chosen for its implementation, depending on the appropriateness of the requirements. The smaller Θ value indicates that the cut-off temperature is approximately at cool water temperature, T_c.

One case for determining initial temperature is explained in this section is when $T_c = 6^{o}C$, $T_h = 13.5^{o}C$, with lower nozzle elevation at 1.824 m. It was performed by determining cool water depth at empty condition (C_E) from selection of parameters S and Θ. The value of cool water depth was determined based on Equation 4.7 with various parameters of S and Θ is presented in Figure 4.7.

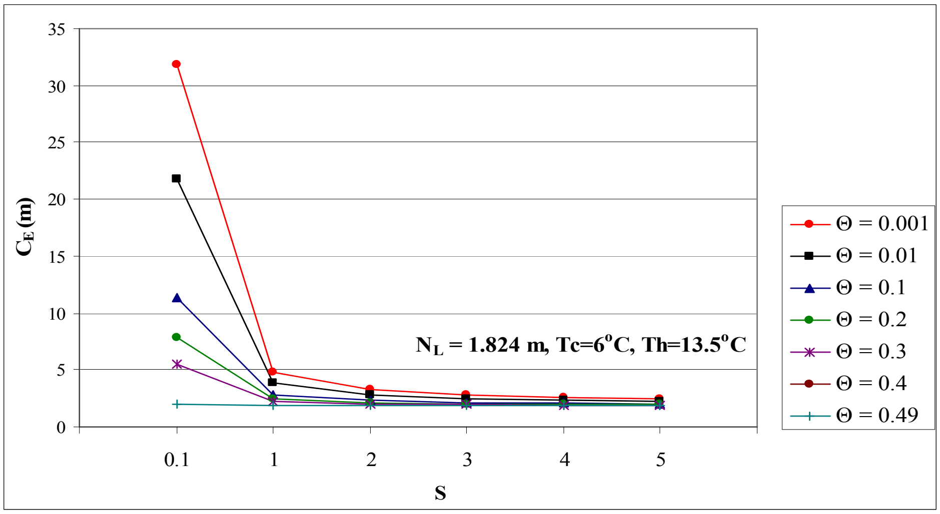

Figure 4.7 C_E in variation of S and Θ

From Figure 4.7, it can be seen that cool water depth at initial condition (C_E) depends on the parameters of S and Θ. Increasing value of S decreases the cool water depth, since higher S identifies steeper thermocline profile in temperature distribution. The values of C_E is also affected by Θ, which reflects the required cut-off cool water temperature in the lower nozzle. At value of $S = 1$ and $\Theta = 0.01$, the cool water depth was obtained at 3.84 m. Variation of cut-off water temperature in the lower nozzle with respect to Θ is shown in Figure 4.8.

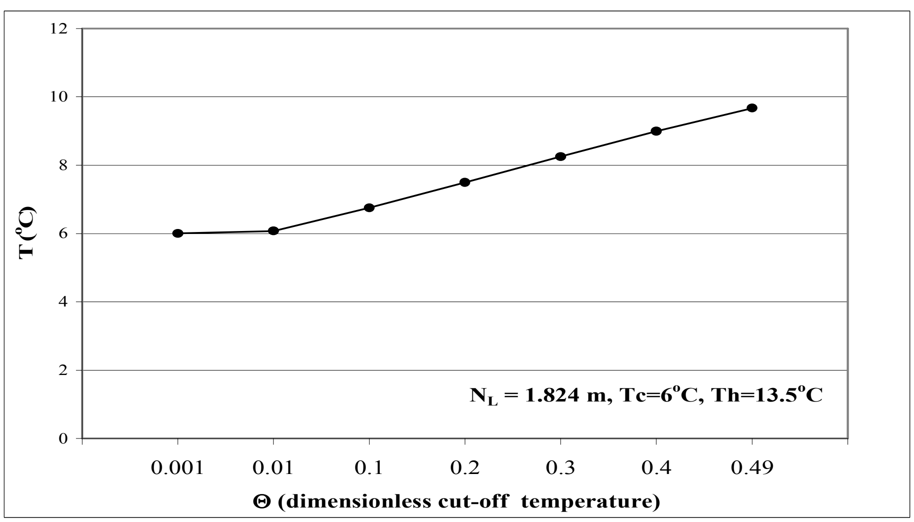

Figure 4.8 Cut-off water temperatures in variation of Θ

It can be seen from Figure 4.8, cut-off water temperature at lower nozzle increase with increasing value of Θ. At value $\Theta = 0.01$, the cut-off water temperature obtained equals to 6.075°C.

ii. Selection of limit capacity criteria

Limit capacity can be derived using two criteria namely water level and temperature limit. Using water level limit criteria, empty and full capacity was derived using Equations 4.7 and 4.8, whereas for temperature limit, were described in Equations 4.9 and 4.10.

Reviewing at the two criteria, it is noted that the related equations are similar. It is shown by comparing empty capacity in the Equations 4.7 and 4.9, for water level limit and temperature limit criteria, respectively. By transforming $(T_h-T_c)/(T-T_c)$ to the term of $1/\Theta$, the two equations are equal. This is also shown in the comparison of Equations 4.8 and 4.10 for full capacity as well. Hence, both criteria can be implemented in the charging stratified TES tank. If Θ value is available, it is recommended to use water limit criteria. On the other hand, if it is required to determine based on limit temperature, it should be solved using temperature limit criteria.

4.1.3 Single Stage Charging Model Type (I)

The open charging model was developed based on temperature distribution function. Generation of temperature distribution of the model adopted SDR function. The assumptions of the temperature distribution profile were constant for T_c, T_h and S, whereas cool water depth (C) increases proportionate in charging flow rate.

In the open model, charging parameters was determined from SDR function formulation. Full capacity based on water level limit criteria in Equation 4.8 was used. The duration of charging to achieve full capacity was calculated based on Equation 3.11, whereas charging duration to reach transition temperature was determined based on Equation 3.10. Evaluation of the open model was performed by verification on the temperature distribution and validation on the charging parameters.

4.1.3.1 Verification of Single Stage Charging Model Type (I)

To check the temperature distribution profile, the verification of the model was required. Verification of the model was performed using (i) temperature data similarity (ii) temperature parameters similarity and (iii) *t*-statistical test. Related to this purpose, data set IA was taken for verification of model single stage charging model type (I).

The observed data of temperature distribution is presented in Figure 4.1. The data shows charging duration from 18.00 hours to 03.00 hours of the following day with constant charging flow rate of 393 m^3/hr. Fitting of SDR function to the data is presented in Table 4.1. The model was developed with T_c, T_h, S and C values at initial temperature at 18.00 hours. The values of T_c, T_h and S are 6.9, 13.6 and 1.6, respectively, while the initial cool water depth (C_E) was obtained equal to 2.7. At observation interval time equal to 60 minutes, the increased cool water depth was calculated based on Equation 3.9 with value of 1 m. Temperature distribution of the model was generated using SDR function. The temperature distribution on the single stage charging model type (I) is presented in Figure 4.9. Temperature distribution profile as shown in Figure 4.9 was used to perform evaluation for single stage charging model type (I).

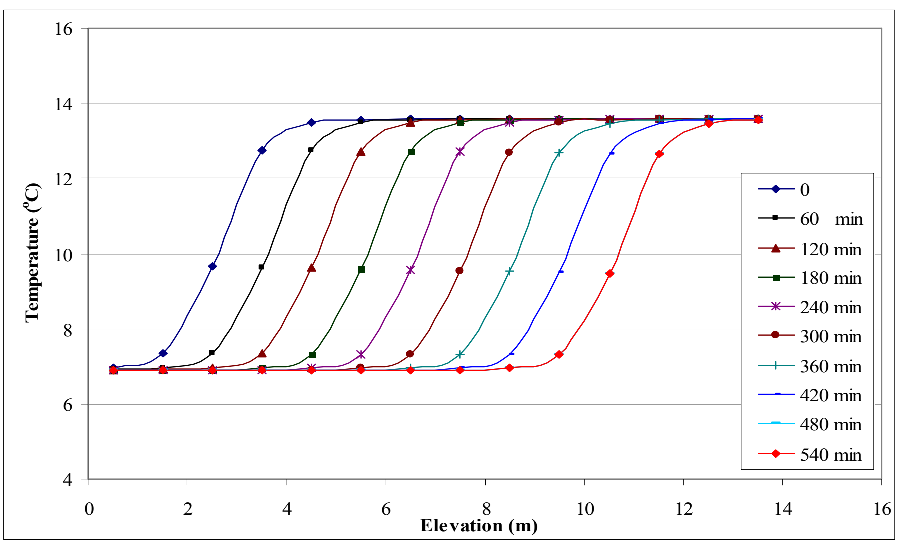

Figure 4.9 Temperature distribution of charging model type (I) on data set IA

i. Temperature distribution data similarity

The verification was evaluated by comparing R^2 value of temperature distribution in Figures 4.1 and 4.9. The results are tabulated in Table 4.4. It is shown that all R^2 values are higher than 0.95. This indicates that temperature distributions generated by the model are similar with that on the observed data.

Table 4.4 R^2 verification of charging model type (I)

Data	to	Model	R^2
Chrg. Hrs.		Chrg. time (min)	
18:00	-	0	0.998
19:00	-	60	0.997
20:00	-	120	0.997
21:00	-	180	0.996
22:00	-	240	0.995
23:00	-	300	0.991
0:00	-	360	0.986
1:00	-	420	0.979
2:00	-	480	0.963
3:00	-	540	0.958

ii. Temperature distribution parameters similarity

The second evaluation was carried out by comparing temperature SDR parameters of the observed data and model. Comparison of parameters T_c and T_h are presented in Figure 4.10, while parameters C and S are shown in Figure 4.11. Temperature parameters deviation between the data and model is presented in Figure 4.12.

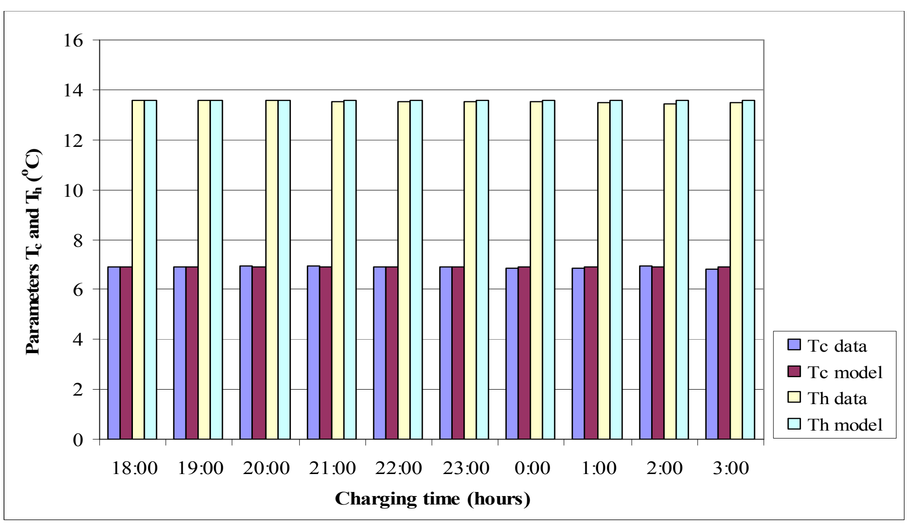

Figure 4.10 Comparison of SDR parameters T_c and T_h in verification of charging model type (I)

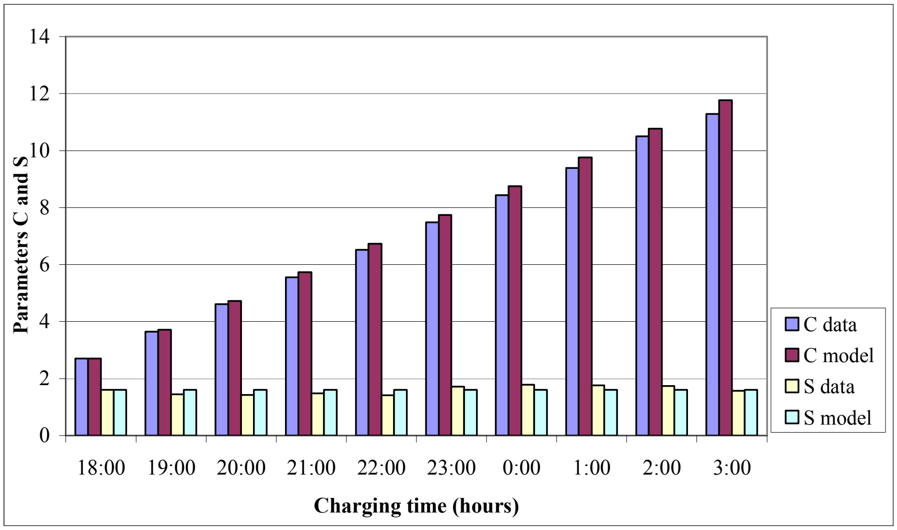

Figure 4.11 Comparison of SDR parameters *C* and *S* in verification of charging model type (I)

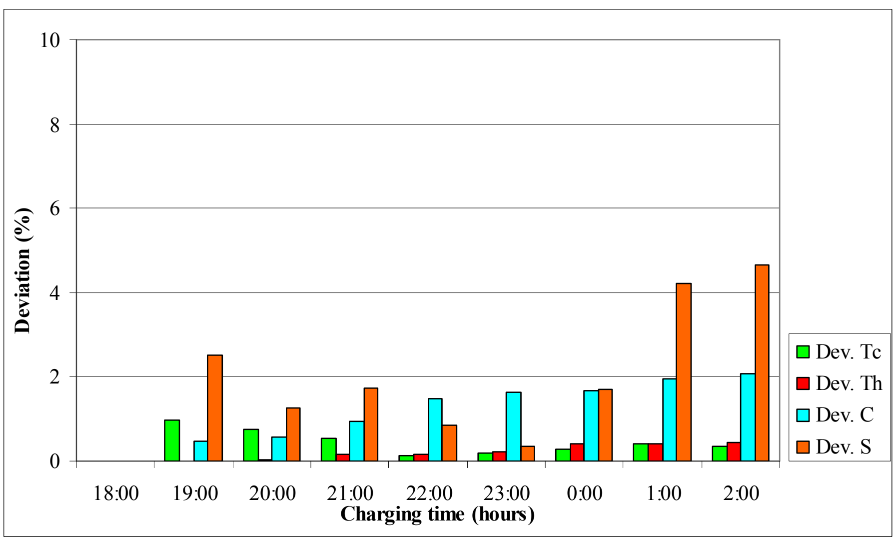

Figure 4.12 Percentage deviations of SDR parameters in verification of charging model type (I)

From Figures 4.10, it can be seen that parameters of T_c and T_h have constant trend within the charging periods. Both observed data and model have constant trend of parameters T_c and T_h. As shown in Figure 4.11, parameter *C* increases linearly while *S* has constant trend during the charging. These trends are also indicated on both obser data and model. Figure 4.12 shows smaller percentage deviation of T_c and T_h, and relatively higher deviations of C and S. The deviation of parameter S fluctuates and parameter C increases as the charging progressing. Combination of these parameters influences temperature distribution in the observed data and model. This influences to decreasing of R^2 temperature distribution with respect to charging duration as shown in Table 4.4. It is noted that deviation of all the parameters are found to be below 5%.

Based on the results, it is highlighted that the assumption of constant T_c, T_h and S parameters in the single stage changing model type (I) is suitable for charging stratified TES tank. This finding infers that thermocline profile of temperature distribution during charging periods is relatively constant. This finding is consistent with that of other research [56, 57]. In addition, it is also shown that SDR function can be utilized as a means to evaluate temperature distribution in stratified TES tank.

iii. Statistical test

Statistical test was used to justify the acceptance similarity between the observed data and the model. It was determined based on t statistical approaches that were described in Section 3.3.51. The values of t computed are presented with respect to charging time in Figure 4.13.

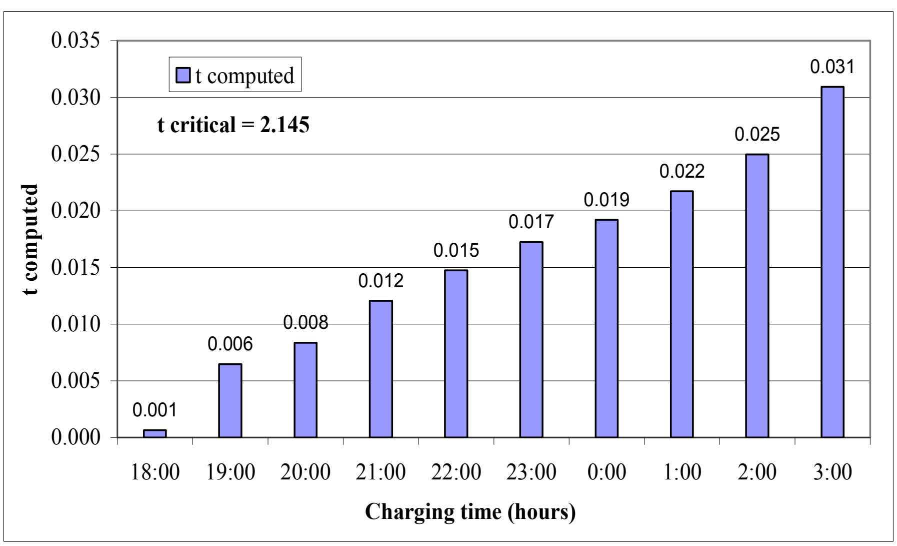

Figure 4.13 t computed values in verification of charging model type (I)

It can bee seen from Figure 4.13 that *t* computed values are relatively small compared to *t* critical (=2.145) that was obtained with confidence level of 95 % and 14 number of data. Determination *t* critical value was based on *t* distribution table in Appendix E. It is shown that all *t* computed values are less than *t* critical, which indicates that null hypothesis was accepted. It is noted that the two temperature distribution data are similar, thus single stage charging model type (I) was statistically accepted.

Based on the three evaluations result, it is shown that temperature distribution in single stage charging model type (I) is capable of representing of charging characteristic in the stratified TES tank. It is noted that the temperature distribution has relatively constant parameters during charging periods, while cool water depth increase proportionate to the charging flow rate.

4.1.3.2 Simulation of Single Stage Charging Model Type (I)

Simulation of single stage charging model type (I) was performed to determine the charging parameters. It was carried out with flow rate variation of 524 m^3/hr, 393 m^3/hr and 262 m^3/hr, for cases A1, B1 and D1, respectively. Simulation was performed using input parameters of initial temperature, TES tank configuration and chillers parameter. The values of initial temperature parameter are tabulated in Table 4.5 and TES tank configuration is presented in Table 3.1.

Table 4.5 Initial temperature parameters of simulation charging model type (I)

Parameter Initial Temperature:	Notation	Value	Units
Average cool water temperature	T_c	6	^oC
Average warm water temperature	T_h	13.5	^oC
Slope gradient	S	1	
Dimensionless cut-off temperature	Θ	0.01	
Cut-off temperature		6.075	^oC

The simulations were carried out using 60 minutes observation time. Temperature distribution profile of the simulations with respect to charging duration are presented in Figures 4.14, 4.15 and 4.16, for cases A1, B1 and D1, respectively. The observation of charging parameters is carried out in term of cool water depth and charging duration. The temperature distribution are presented with respect to tank elevation and referred to 60 minute observation time interval. Cool water depths of initial condition (C_E), temperature transition point (C_{FR}) and full capacity (C_{FT}) are determined based on equation 4.7, 4.11 and 4.10, respectively. Determination of charging duration to reach temperature transition point and full capacity are based on equation 3.10 and 3.11, respectively. The charging durations for temperature transition points and full capacity are written in the legend of the figures.

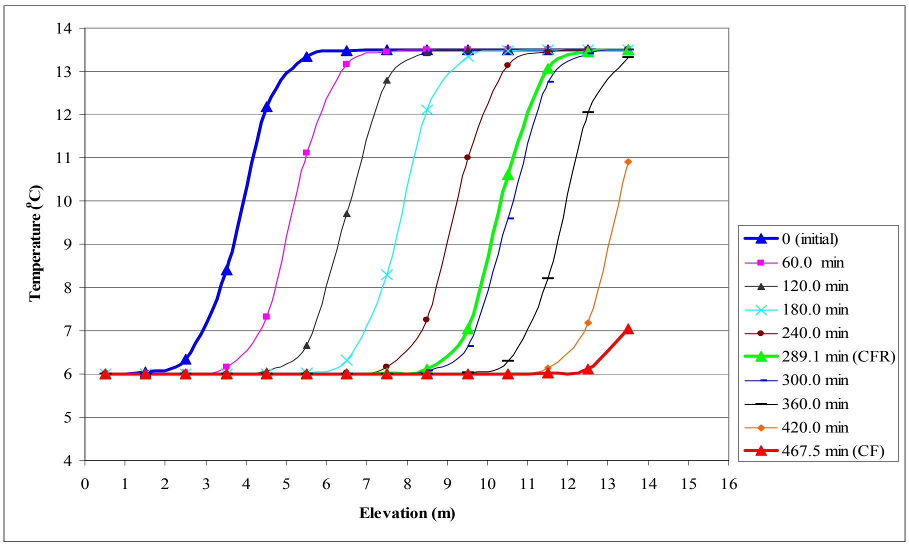

Figure 4.14 Temperature distribution of simulation case A1 in single stage charging model type (I) with flow rate 524 m^3/hr.

From Figure 4.14, 4.15 and 4.16, it can be seen that each simulation case has different span of temperature distribution profiles. Wider temperature profile span is occurred for the higher charging flow rate. It indicates that increasing of cool water depth is significantly affected by charging flow rate. It is also shown on that figures, each simulation cases has different values of charging duration for temperature transition point (*CFR*) and full capacity (*CF*). Comparing of the three figures, it is noted that higher charging flow leads to reduce charging duration.

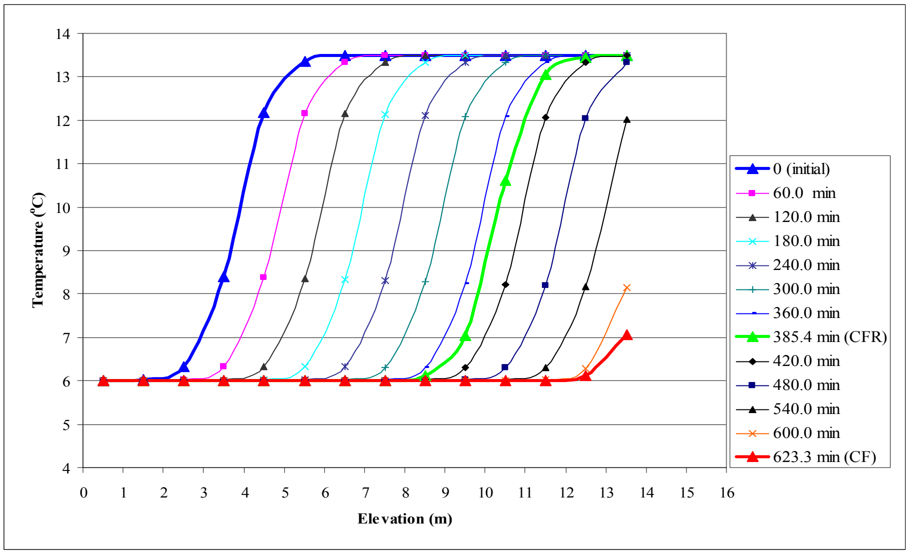

Figure 4.15 Temperature distribution of simulation case B1 in single stage charging model type (I) with flow rate 393 m^3/hr.

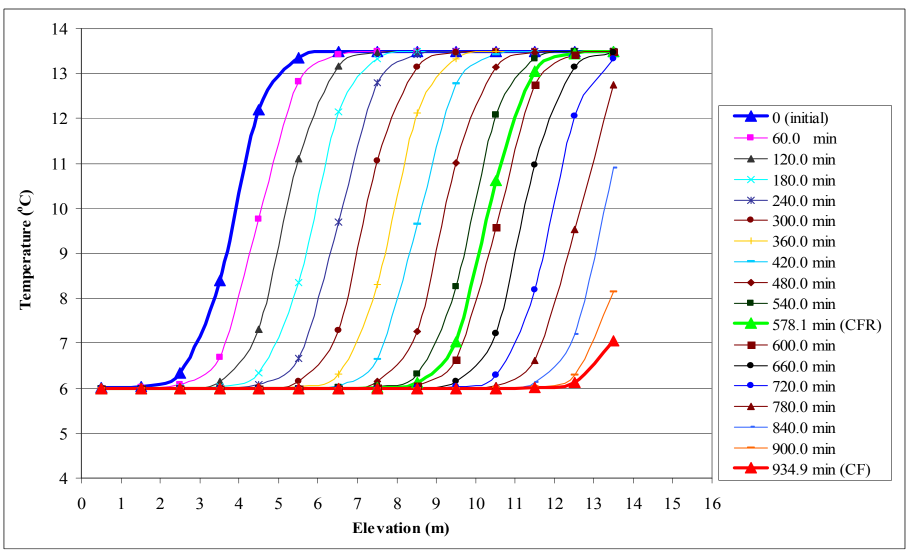

Figure 4.16 Temperature distribution of simulation case D1 in single stage charging model type (I) with flow rate 262 m^3/hr.

Cumulative cooling capacity (Q_{cum}) is also determined based on Equation 3.12 which considers water mass (M_n) of each slab, diameter (D) and slab numbers of the TES tank. Specific heat is calculated based on average of cool and warm water temperature, whereas reference temperature (T_{ref}) is taken to be equal to warm water temperature (T_h).

Hence, the cumulative cooling capacity is obtained as the following.

$$Q_{cum} = 453.91\sum_{n=1}^{14}(T_h - T_n) \text{ kWh} \tag{4.12}$$

Cumulative cooling capacity comparison result in the simulation cases A1, B1 and D1 is also presented in Figure 4.17.

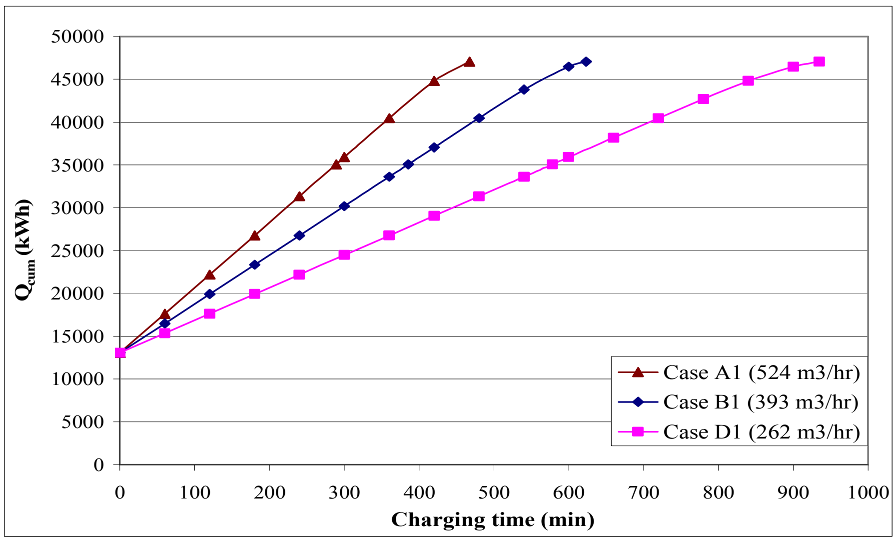

Figure 4.17 Cumulative cooling capacity of simulation cases A1, B1 and D1 in single stage charging model type (I).

Based on Figure 4.17, it is shown that initial and full capacity of each simulation has the same cumulative cooling capacity values. During the charging, increasing of charging flow rates increases the cumulative cooling capacity values. These are indicated at steeper cumulative cooling patterns in higher the charging flow rate.

The summary of the result for the single stage charging model type (I) simulation is tabulated in Table 4.6. It contain of cool water depth, charging duration and cumulative cooling capacity. All the observations are presented in term of initial condition, temperature transition point and full capacity. From Table 4.6, it is shown that charging duration to reach temperature transition has different values for each simulation case. However, all cool water depths at temperature transition point (C_{FR}) are similar at 10.3 m. In term of charging duration to achieve full capacity, it was found that increasing the values of flow rate also reduces the charging duration. Cool water depths at full capacity (C_F) for all cases are similar at 14.30 m.

Table 4.6 Parameter values of simulation cases A1, B1 and D1 in single stage charging model type (I).

Initial Condition, $T_c = 6^oC$, $T_h = 13.5^oC$, $S = 1$, $\Theta = 0.01$					
Variation Flow Rate	**C (m)**		**Q_{cum} (kWh)**	**Charging Time (min)**	**Remark**
Case A1, 524 m^3/hr	C_E	3.84	13,033.70	0.00	Empty Capacity
	C_{FR}	10.30	35,041.48	289.06	Temperature Transition
	C_F	14.30	47,119.93	467.46	Full Capacity
Case B1, 393 m^3/hr	C_E	3.84	13,033.70	0.00	Empty Capacity
	C_{FR}	10.30	35,041.48	385.41	Temperature Transition
	C_F	14.30	47,119.93	623.29	Full Capacity
Case D1, 262 m^3/hr	C_E	3.84	13,033.70	0.00	Empty Capacity
	C_{FR}	10.30	35,041.48	578.11	Temperature Transition
	C_F	14.30	47,119.93	934.93	Full Capacity

From Table 4.6, it is noted that cool water depth, charging duration as well as cumulative cooling capacity could be determined exactly for the single stage charging model type (I). Single stage charging model type (I) offers benefit in term of capability to determine charging parameter values based on formulation from SDR function.

4.1.3.3 Validation of Charging Duration in Single Stage Charging Model Type (I)

In order to ensure that the obtained values of charging parameter in the single stage charging model type (I) simulation are relevant, validation of the charging duration values was performed. It was carried out using data sets of IB and IC.

Initial condition of the two data sets IB and IC were fitted using SDR function. The parameter values were obtained from SIGMAPLOT analysis report included in Appendices G2 and G3. In data sets IB, the parameter values of T_c, T_h, C and S are 7.32°C, 13.63°C, 3.92 and 1.47, respectively. Data IC has parameter values of 7.73°C, 13.54°C, 3.19 and 1.11 for T_c, T_h, C and S, respectively. The data were obtained at R^2

of 0.998 and 0.997. It was shown that S value of data set IB is higher than that of data set IC. It indicates that data set IB has less inclined profile than data set IC.

In term of C values, it is inferred that both data has initial cool water depth above lower nozzle elevation, since it has value greater than 1.824 m. Data IB has more cool water depth than that for data IC.

The model was developed using the parameter values of T_c, T_h, C and S with hourly increased cool water depth (ΔC). Based on these values, generation of temperature distribution were performed using Equation 4.1. Plot of generated temperatures are shown in Figures 4.18 and 4.19, for data set IA and IB, respectively.

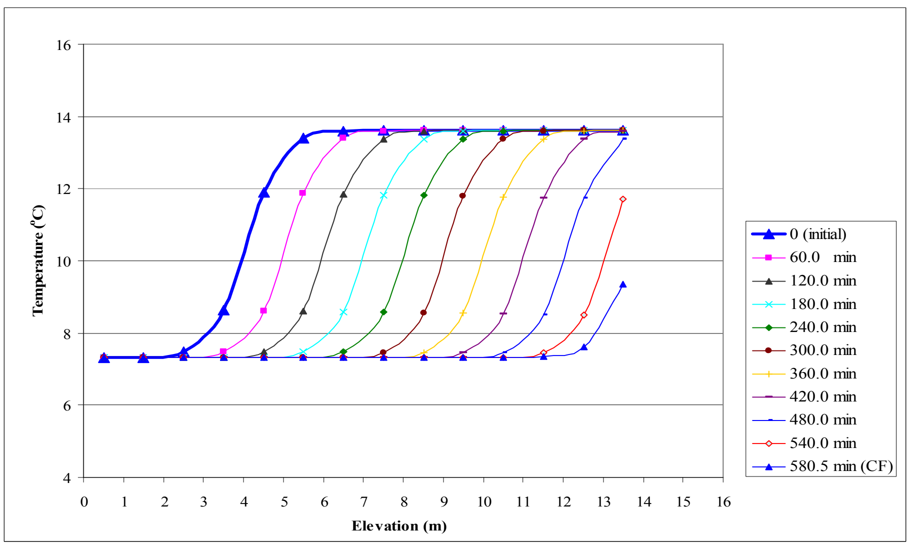

Figure 4.18 Temperature distribution of model validation data set IB for single stage charging model type (I).

Full capacity of the model was calculated based on Equation 4.8, and charging duration using Equation 3.11. On the other hand, determination of full capacity of the observed data was based on outlet charging temperature equal to cut-off temperature. It was carried out by interpolation of temperature distribution of the TES tank at elevation 12.3 m. Using Θ equals to 0.01, cut-off temperatures were obtained to be equal to 7.36°C and 7.75°C for data set IB and IC, respectively.

Validation results of the two data sets are tabulated in Tables 4.6 and 4.7 for data sets IB and IC, respectively. Evaluation was performed in term of cumulative cooling capacity and charging duration.

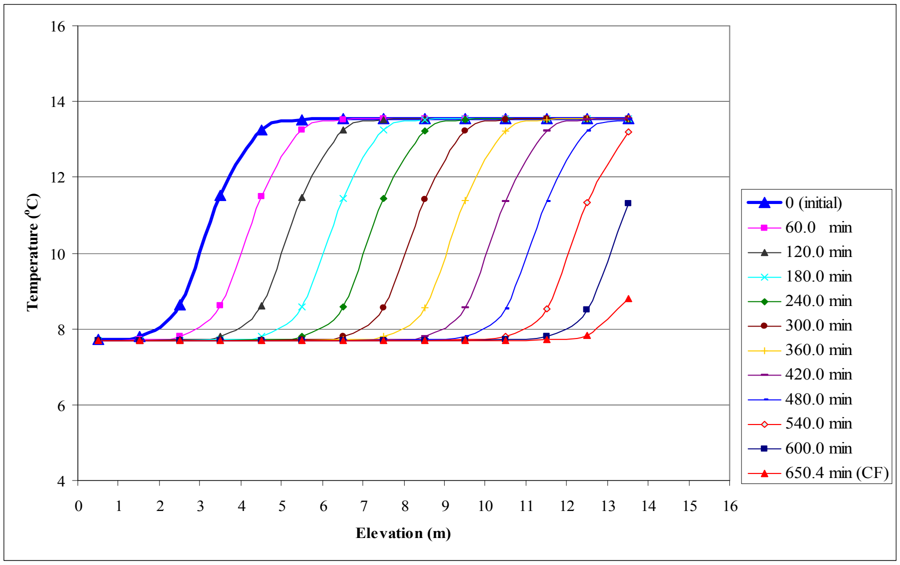

Figure 4.19 Temperature distribution of model validation data set IC for single stage charging model type (I).

Table 4.7 Validation result on data set IB

Data		**Simulation**			**Qcum Deviation**
Charging Hours	**Qcum**	**Tc=7.3°C, Th=13.6°C, S=1.5**			
		Charging Time	**Cool Water Depth**	**Qcum**	
	(kWh)	**(minutes)**	**(m)**	**(kWh)**	**(%)**
18:00	11432.3	0	3.9	11675.21	2.1
19:00	14092.0	60	4.9	14557.53	3.2
20:00	16938.5	120	5.9	17439.93	2.9
21:00	19704.8	180	6.9	20322.34	3.0
22:00	22564.5	240	7.9	23204.75	2.8
23:00	25477.3	300	9.0	26087.16	2.3
0:00	28361.1	360	10.0	28969.46	2.1
1:00	31126.7	420	11.0	31850.67	2.3
2:00	34080.1	480	12.0	34720.86	1.8
3:00	37061.9	540	13.0	37483.68	1.1
4:00	40001.0	600	14.0	39486.54	1.3
Full Condition		Full Condition (t_{CF})			
T_{outlet}=7.36°C		Θ=0.01, $T_{Θ}$=7.36°C		38212.02	**t_{CF} Deviation (%)**
587.27		580.46	13.66		**1.16**

It is shown in Tables 4.7 and 4.8; the values of parameters in the observed data can only be exposed in term of cumulative cooling capacity and charging duration. The charging duration was obtained using interpolation to obtain outlet temperature at the upper nozzle elevation. Using the model, on the other hand, parameters of charging duration as well cool water depth can be exactly determined based on formulation.

From Tables 4.7 and 4.8, it is noted that all cumulative cooling capacity value deviations are less than 6%. The difference was mainly due to sensitiveness of the cumulative cooling capacity equation with respect to summation of temperature distribution. Any small temperature difference leads to changes in the cumulative cooling capacity. In the comparison, it was shown that cumulative cooling capacity of the observed data is higher than that in the model. It was due to averaging of non linear regression fitting as a part of model processing. The other reason, since inlet temperatures were assumed constant in the model, the fluctuating temperature data was ignored. Comparison of charging duration between the data and model are also presented in Table 4.7 and 4.8. It was highlighted that charging duration values has relatively similar deviation which is lower than 2%.

Table 4.8 Validation result on data set IC

Data		**Simulation**			**Qcum Deviation**
Charging Hours	**Qcum**	**Tc=7.7°C, Th=13.5°C, S=1.1**			
		Charging Time	**Cool Water Depth**	**Qcum**	
	(kWh)	**(minutes)**	**(m)**	**(kWh)**	**(%)**
18:00	8645.4	0	3.2	8554.60	1.1
19:00	11311.1	60	4.2	11224.75	0.8
20:00	14131.7	120	5.2	13895.35	1.7
21:00	16996.1	180	6.2	16566.01	2.6
22:00	19821.4	240	7.2	19236.67	3.0
23:00	22623.6	300	8.2	21907.34	3.3
0:00	25514.5	360	9.2	24578.00	3.8
1:00	28428.0	420	10.2	27248.52	4.3
2:00	31161.6	480	11.2	29917.61	4.2
3:00	33971.1	540	12.3	32572.16	4.3
4:00	36936.3	600	13.3	35087.55	5.3
5:00	38850.3	660	14.3	36730.03	5.8
Full Condition		Full Condition (t_{CF})			
T_{outlet}=7.75°C		Θ=0.01, T_{Θ}=7.75°C		36577.80	**t_{CF} Deviation (%)**
657.07		650.44	14.11		**1.01**

Based on the validation results, it is noted that the single stage charging model type (I) is capable of determining charging duration in the stratified TES tank.

4.1.4 Two-Stage Charging Model Type (I)

Two-stage charging model was developed based on single stage charging model type (I). The model development was explained in Section 3.3.6. The difference between the two-stage to the single stage is the occurrence of limit temperature. Simulation of the two-stage charging model type (I) was carried out into two main cases namely variation of charging flow rate and limit temperature.

4.1.4.1 Simulation of Charging Flow Rate Variation

Simulation of two-stage charging model type (I) was carried out to cover charging with absorption and electric chillers sequentially. The simulation used initial temperature, TES tank configuration and variation of chillers parameter. The values of initial temperature parameters are tabulated in Table 4.5, TES tank configuration parameters were described in Table 3.1 and chiller parameter in Table 3.3.

Variation of charging flow rate for the first stage was performed using absorption chiller at 504 m^3/hr with limit temperature T_r = 9^{o}C. The second stage charging were carried out using electric chiller with flow rate of 524 m^3/hr, 393 m^3/hr and 262 m^3/hr, for cases E1, F1 and G1, respectively. The simulations were performed based on 60 minutes time interval observation. Temperature distribution for two-stage charging model type (I) are presented in Figures 4.20, 4.21 and 4.22 for cases E1, F1 and G1, respectively. Cumulative cooling capacity in the three simulation cases is presented in Figure 4.23.

The simulation was carried out to determine charging parameters in term of cool water depth, charging duration and cumulative cooling capacity. Cool water depths were determined for initial condition, transition temperature point and full capacity at the first and second stage of charging. Cool water depth of initial condition (C_E) and temperature transition point (C_{FR}) were referred to Equation 4.7 and 4.11. Cool water depths at full capacity of the first and second stage, (C_{FT}) and (C_F) , were based on Equations 4.10 and 4.8, respectively. Charging durations were determined in term of temperature transition point, full capacity of the first and second stage which designated as (t_{CFR}), (t_{CFT}) and (t_{CF}) were referred to Equations 3.16. 3.17 and 3.18, respectively. Cumulative cooling capacity (Q_{cum}) was determined based on Equation 3.12. The results summary of the two-stage charging model type (I) simulation is tabulated in Table 4.9.

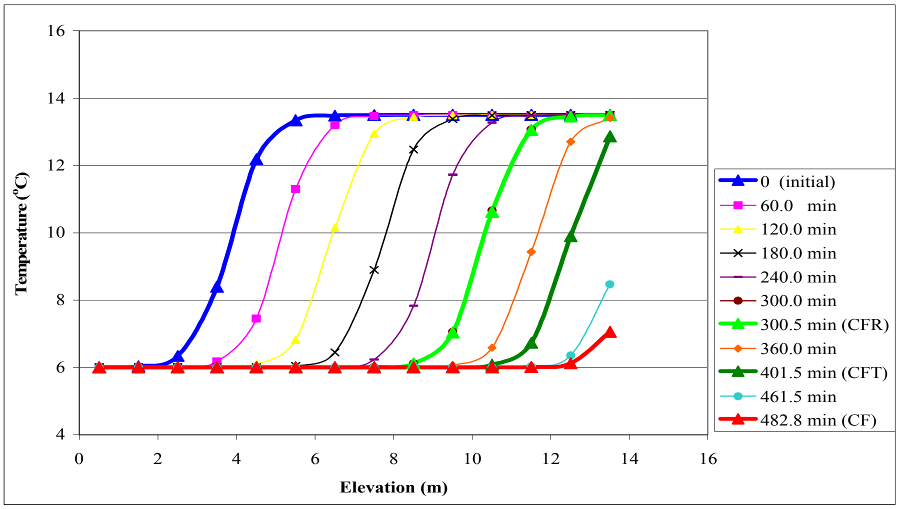

Figure 4.20 Temperature distribution of simulation case E1 in two-stage charging model type (I) with flow rate 504-524 m^3/hr and limit temp. (T_r) = 9°C.

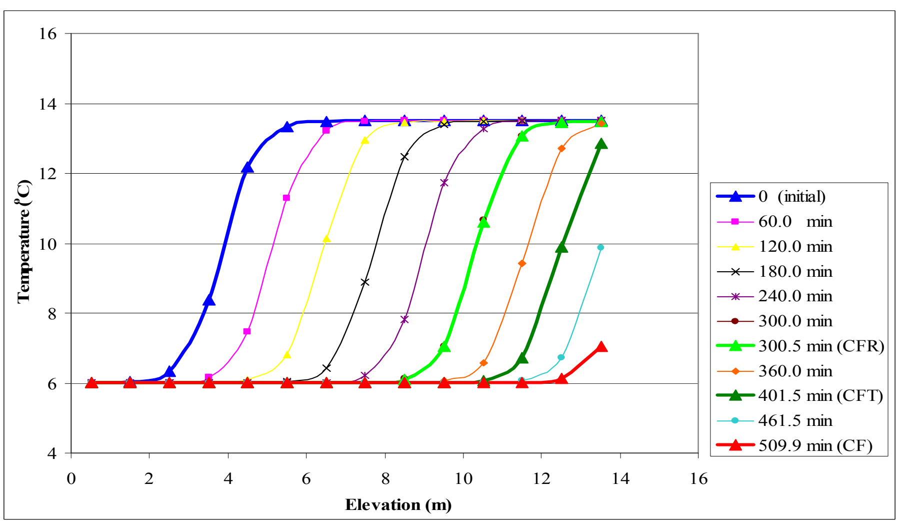

Figure 4.21 Temperature distribution of simulation case F1 in two-stage charging model type (I)with flow rate 504-393 m^3/hr and limit temp. (T_r) = 9°C.

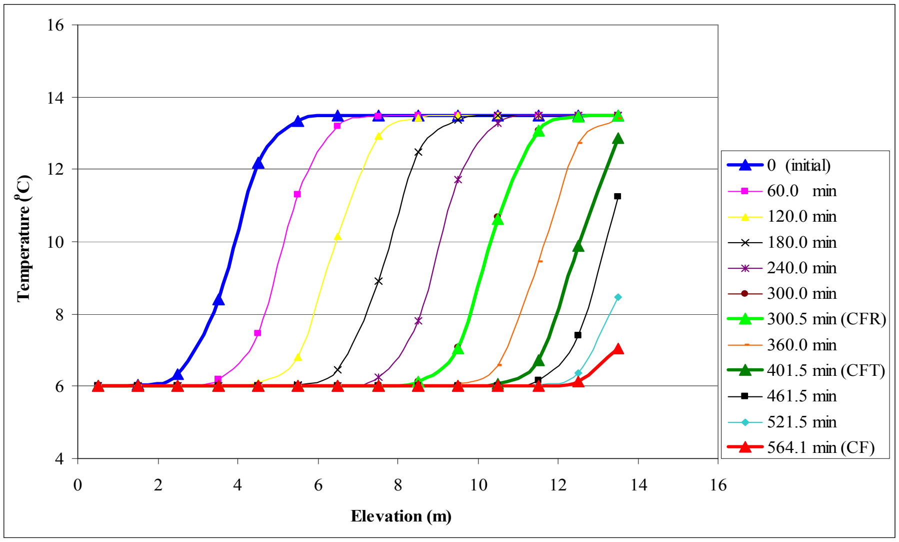

Figure 4.22 Temperature distribution of simulation case G1 in two-stage charging model type (I)with flow rate 504-262 m^3/hr and limit temp. (T_r) = 9°C.

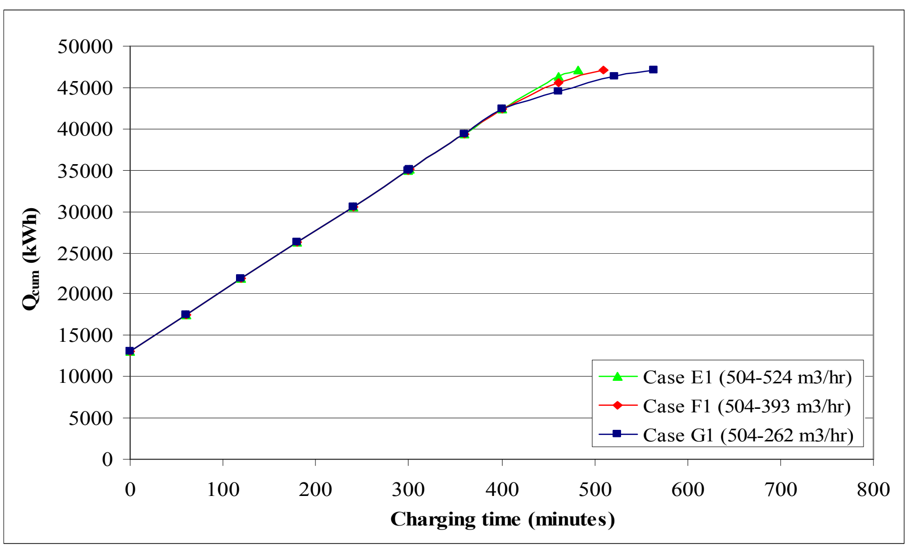

Figure 4.23 Cumulative cooling capacity of simulation cases E1, F1 and G1 of two-stage charging model type (I) in flow rate variation.

Table 4.9 Parameter values of simulation cases E1, F1 and G1

Initial Condition, $T_c = 6^oC$, $T_h = 13.5^oC$, S = 1, Θ = 0.01 and $T_r = 9^oC$					
Variation Flow Rate	**C (m)**		**Q_{cum} (kWh)**	**Charging Time (min)**	**Remark**
Case E1, 504-524 m^3/hr	C_E	3.84	13,033.70	0.00	Empty Capacity
	C_{FR}	10.30	35,041.48	300.53	Temperature Transition
	C_{FT}	12.48	42,402.86	401.45	Full capacity, 1st stage
	CF	14.30	47,119.93	482.79	Full capacity, 2nd stage
Case F1, 504-393 m^3/hr	C_E	3.84	13,033.70	0.00	Empty Capacity
	C_{FR}	10.30	35,041.48	300.53	Temperature Transition
	C_{FT}	12.48	42,402.86	401.45	Full capacity, 1st stage
	CF	14.30	47,119.93	509.90	Full capacity, 2nd stage
Case G1, 504-262 m^3/hr	C_E	3.84	13,033.70	0.00	Empty Capacity
	C_{FR}	10.30	35,041.48	300.53	Temperature Transition
	C_{FT}	12.48	42,402.86	401.45	Full capacity, 1st stage
	CF	14.30	47,119.93	564.12	Full capacity, 2nd stage

It can be seen from Figures 4.20 to 4.22 and Table 4.9 that having limit temperature of 9^{o}C the full capacity of the first stage was obtained for charging duration of t_{CFT} = 401.45 minutes. In all cases, temperature transition temperatures of the first stage was t_{CFR} = 300.53 minutes, which indicates the condition of upper limit points reaching the upper nozzle. It is also indicated that increasing charging flow rate in the second stage of charging reduce the charging duration. Cumulative cooling capacity at the initial condition and full capacity in the first stage was reached at 13,033.7 kWh and 35,041.48 kWh for cases E1, F1 and G1, respectively. Since all cases were performed at same condition of total full capacity, therefore cumulative cooling capacity of the second stage was similar at 47,119.93 kWh.

4.1.4.2 Simulation of Limit Temperature Variation

Simulation of two-stage charging model type (I) was carried out using absorption chiller and electric chiller at the first and second stage of charging. The charging flow rate of absorption chiller was 504 m^3/hr, whereas electric chiller has flow rate of 393 m^3/hr. The simulation was performed with variation of limit temperature (T_r) of 7^{o}C, 9^{o}C and 11^{o}C, designated as cases H1, J1 and K1 in Table 3.4.

Temperature distribution of three simulation cases in the two-stage charging model type (I) with variation of limit temperature are presented in Figures 4.24, 4.25

and 4.26 for cases H1, J1 and K1, respectively. Cumulative cooling capacity in the three cases of simulation is presented in Figure 4.27. Simulation of limit temperature variation was carried out for cool water depth, charging duration time as well as cumulative cooling capacity. Summary of the results charging parameters values is tabulated in Table 4.10.

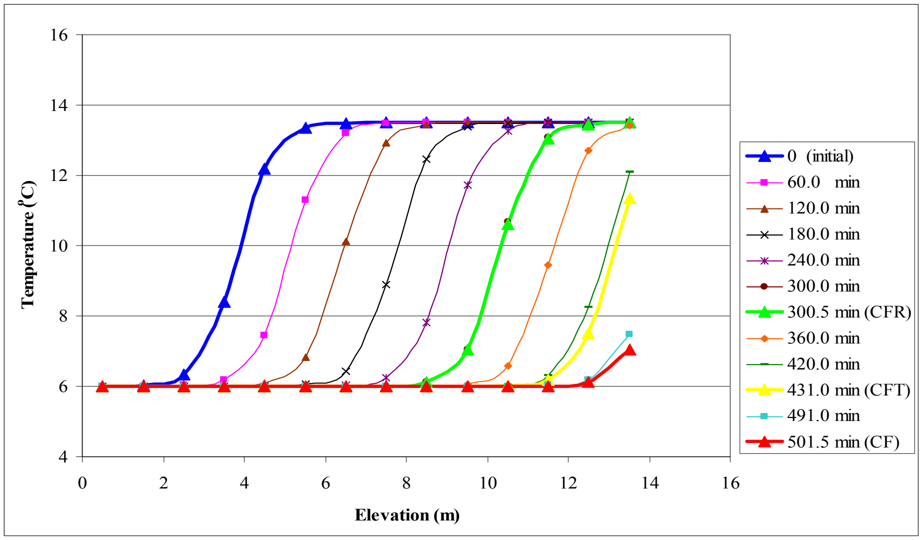

Figure 4.24 Temperature distribution of simulation case H1 of two-stage charging model type (I) with flow rate 504-393 m^3/hr and limit temp. (Tr)=7°C

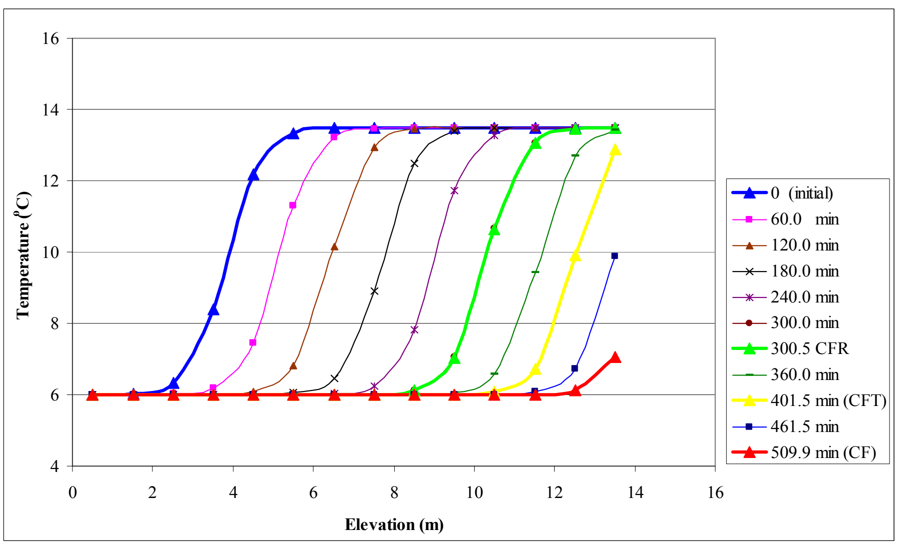

Figure 4.25 Temperature distribution of simulation case J1 of two-stage charging model type (I) with flow rate 504-393 m^3/hr and limit temp. (Tr)=9°C

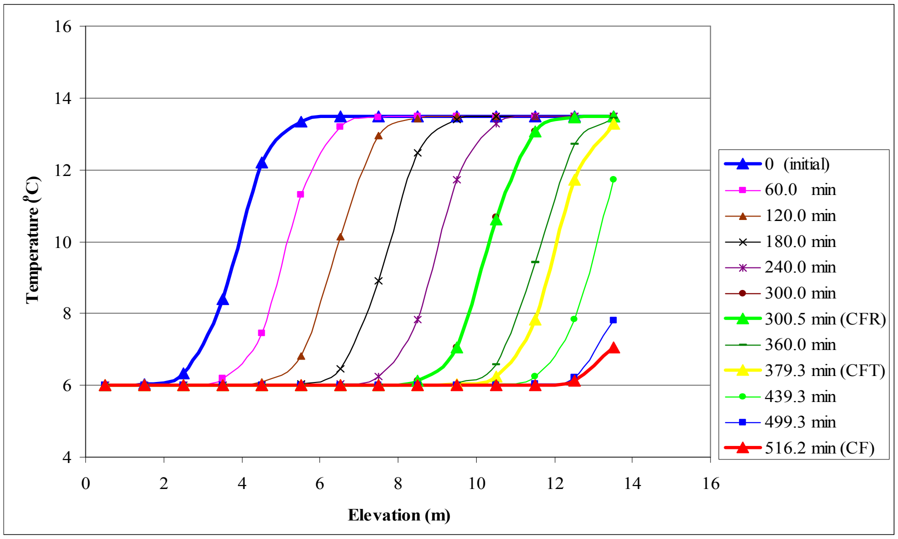

Figure 4.26 Temperature distribution of simulation case K1 of two-stage charging model type (I) with flow rate 504-393 m^3/hr and limit temp. (Tr)=11^oC

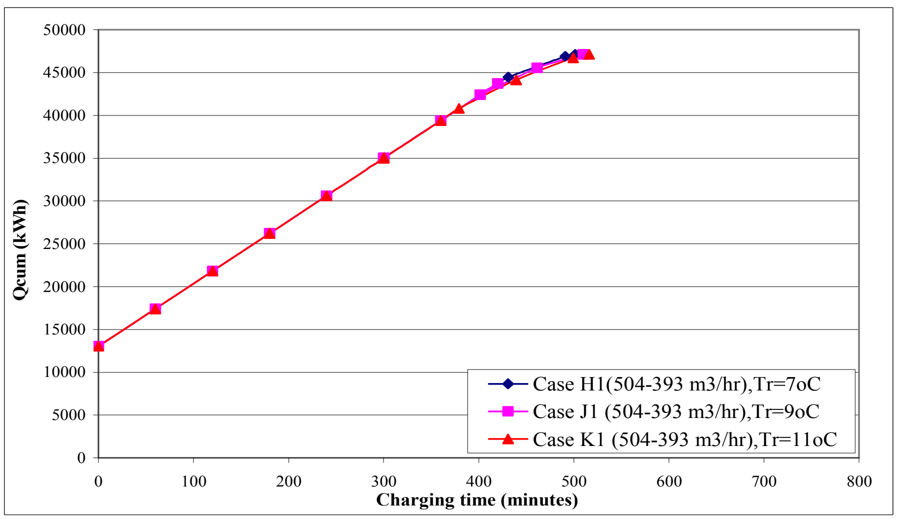

Figure 4.27 Cumulative cooling capacity of simulation cases H1, J1 and K1 of two-stage charging model type (I) in limit temperature variation.

As shown in Figures 4.24, 4.25 and 4.26, it is noted that increasing the limit temperature shown in cases H1, J1 and K1 reduces the cool water depth (C_{FT}) at the first stage of charging, hence reduces the charging duration as well as cumulative cooling capacity. The full capacities of the second stage charging were obtained at the same values of cool water depth as well as cumulative cooling capacity. It is also highlighted that decreasing full capacity in the first stage reduces the change state between the first and second stages. The consequence is that it takes longer charging duration of the second stage.

The discussion shows the result of the two-stage charging model type (I) simulation. These findings show that by utilizing SDR function has beneficial in determining exact values of the parameter from the formulation.

The model type (I) were developed based on open charging system with assumption of constant inlet water charging temperature. Using the assumptions, the models could not cover variation of inlet charging temperature. Therefore, it is required to develop another charging model enable covers variation of inlet charging temperature. The next section involve with simulation charging models type (II) which was developed based on a close charging system.

Table 4.10 Parameter values of simulation cases H1, J1 and K1

Initial Condition, Tc = 6°C, Th = 13.5°C, S = 1, Θ = 0.01 and Flow Rate 504-393 m^3/hr					
Variation Temperature Limit, T_r	**C (m)**		**Q_{cum} (kWh)**	**Charging Time (min)**	
Case H1, T_r = 7°C	C_E	3.84	13,033.70	0	Empty Capacity
	C_{FR}	10.30	35,041.48	300.53	Temperature Transition
	C_{FT}	13.11	44,457.82	431.05	Full capacity, 1st stage
	CF	14.30	47,119.93	501.54	Full capacity, 2nd stage
Case J1, T_r= 9°C	C_E	3.84	13,033.70	0	Empty Capacity
	C_{FR}	10.30	35,041.48	300.53	Temperature Transition
	C_{FT}	12.48	42,402.86	401.45	Full capacity, 1st stage
	CF	14.30	47,119.93	509.90	Full capacity, 2nd stage
Case K1, T_r = 11°C	C_E	3.84	13,033.70	0	Empty Capacity
	C_{FR}	10.30	35,041.48	300.53	Temperature Transition
	C_{FT}	12.00	40,802.65	379.28	Full capacity, 1st stage
	CF	14.30	47,119.93	516.16	Full capacity, 2nd stage

4.2 Close Charging System

As highlighted in the methodology section, the second type of charging models were developed using close charging system. In the model, TES tank was integrated to chillers equipment. The TES tank model adopted finite difference in explicit method, whereas inlet and outlet charging temperature were correlated using energy balance in the evaporator of the chillers. This method was aimed to generate temperature distribution in the charging of stratified TES tank. The following section was addressed on the simulation result of charging model type (II) for single and two-stage charging of stratified TES tank. The single stage model was performed with charging flow rate variation, whereas the two-stage was performed with variation of flow rate and limit temperature.

4.2.1 Single Stage Charging Model Type (II)

Single stage charging model (II) was developed based on one-dimensional conduction and convection equation. The model requires input of initial temperature, TES tank configuration and chillers parameters. Development of the model was explained in Section 3.4. This section discussed the result of verification and simulation of single stage charging model type (II).

4.2.1.1 Verification of Single Stage Charging Model Type (II)

Prior to conduct verification, it requires initialization of parameters involved with selection of effective diffusivity of the model. Using the selected effective diffusivity, the temperature distribution of charging model type (II) was verified.

i. Selection of effective diffusivity

Selection of the effective diffusivity (ε_{eff}) was performed using temperature data at charging flow rate of 393 m^3/hr. For this purpose, data set IA was used. The selection was performed using T_c = 6^{o}C and T_h = 13.5^{o}C, hence revealed an average temperature of 9.75^{o}C. Physical properties of water was obtained at average water temperature involving thermal conductivity (k) = 0.568 W/m.^{o}C, density (ρ) = 1,000 kg/m^3 and specific heat (C_p) = 4,198 J/kg.K. These were obtained from table of thermo-physical properties of water as in Appendix F. Accordingly, water thermal diffusivity, $\alpha = k/\rho.C_p$, was obtained at 0.000499 m^2/hr.

Parameters of TES tank configuration based on Table 3.3 were used in the selection. The dimension of the TES tank is diameter (*D*) of 22.3 m and effective water depth (*H*) of 14 m. The observation numbers of slabs are 14. In this study, four segments (Δx) were selected in each slab of the TES tank, resulting of Δx equal to 0.25 m. Courant number, FLOW, in the models was equal to 1, hence observed time interval (Δt) for charging flow rate at 393 m^3/hr was obtained equal to 14.93 minutes.

Convergence stability of the conduction equation was observed by defining AMIX not greater than 0.5. Utilizing Equation 3.25, the maximum of effective diffusivity for 393 m^3/hr was 251.67. In order to have suitable ε_{eff} representing flow rate variations, selection of ε_{eff} values was performed in various values of 1; 10; 50; 100; 200 and 250.

The temperature distribution in the selection was evaluated using coefficient of determination (R^2). Plots of temperature distribution in the selection are attached in Appendix B. Result summary of R^2 value in the selection is presented in Figure 4.28.

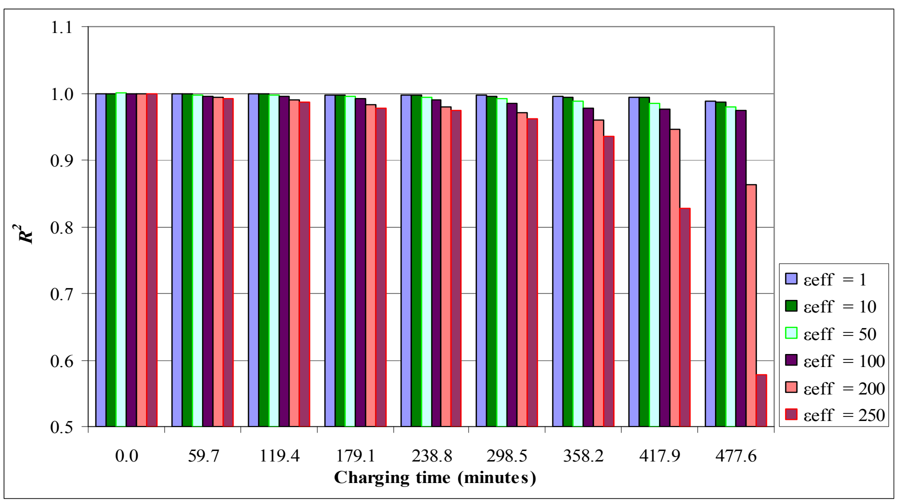

Figure 4.28 R^2 in variation effective diffusivity

In Figures 4.28, the R^2 of the temperature data is presented with respect to charging time. Selection was performed at various ε_{eff} in the range of stabilities of AMIX<0.5 identifies at ε_{eff} lower than 251.67. Referring to the figure, it can be seen that R^2 in the earlier charging time has values approximately equal to 1 which indicate the temperature distribution data are almost similar. At lower ε_{eff}, the R^2 closer to 1 is occurred at all charging time. Along with increasing of ε_{eff}, the R^2 value decrease gradually with respect to charging time. This is due to the fact that increasing of ε_{eff} revealed more inclined profile in the temperature distribution as shown in Appendix B. It indicates that the stability is reached at the low of ε_{eff} and gradually decreases in increasing value of effective diffusivity.

Thus, the model was suitable at low ε_{eff} values. It inferred that mixing factors does not dominate degradations of temperature distribution, since it is not influenced by mixing flow at its initial condition of the charging. Therefore, working ε_{eff} at 10 is used in the charging model type (II).

The other indication from the results obtained is that the model single stage charging model type (II) valid to be performed with explicit method. This is because of effective diffusivity (ε_{eff}) stable at AMIX lower than 0.5.

ii. Verification of single stage charging model type (II)

Verification of the model was performed to ensure the similarity of temperature distribution during charging. The verification of single stage charging model type (II) was performed with three evaluation types, namely R^2 between the observed and simulated data, temperature parameter similarity and *t*-statistical test.

Verification of charging single stage type (II) was carried out with 4 operating data sets of IB, IC, IIB and IIC. One of verification result at charging flow rate of 393 m^3/hr using data IB is discussed in this section. Plot of temperature distribution data set IB is shown in Appendix A2. Fitting SDR function of the data set IB is presented in Figure 4.29, whereas the verification is presented in Figure 4.30.

The verification utilized TES tank configuration that has diameter (*D*) of 22.3 m and effective water depth (*H*) of 14 m. It has 14 slabs which is provided with temperature sensor in the mid point of the slab. The four segments (Δx) were selected for each slab of the tank, resulting Δx equal to 0.25 m. Courant number, FLOW, in the model were selected equal to 1, hence reveals different observed time interval (Δt) for various charging flow rate. In the case of charging flow rate at 393 m^3/hr, resulting at

Δt = 14.93 minutes. The initial condition was taken at a similar value with of that in observed data. The values of UA, T_{ev}, ΔT_1 and ΔT_2 were equal to 714.4 W/^{o}C; 4^{o}C; 0.2^{o}C and 0.4^{o}C, respectively. Effective diffusivity ε_{eff} was taken equal to 10, considering the result in its selection.

In Figures 4.29 and 4.30, both fitting temperature data are presented with respect to dimensionless elevation of TES tank. Visually, both fitted temperature distributions are similar. Some intensive evaluations, however, were conducted to ensure its similarity. It was carried out by evaluating data distribution similarity, temperature parameter similarity and statistical test.

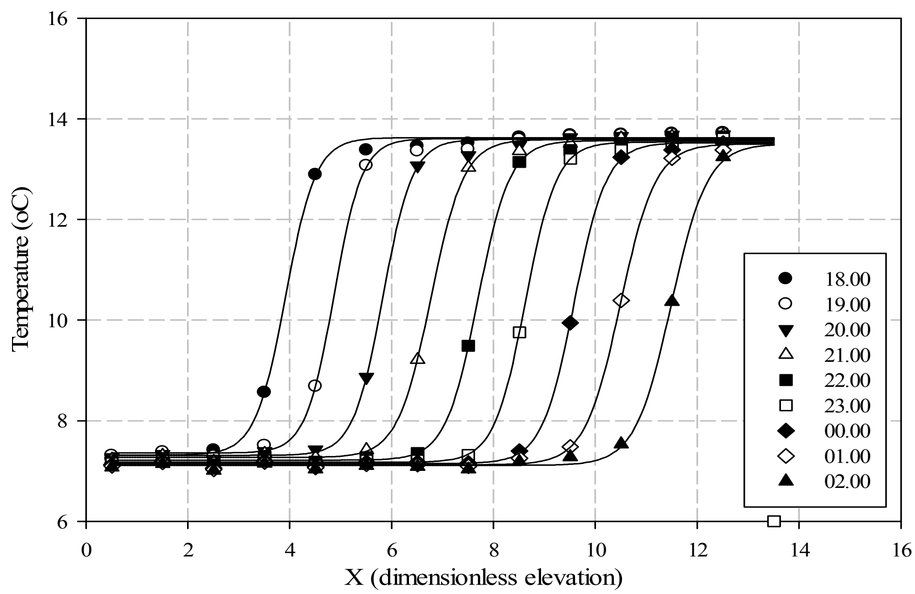

Figure 4.29 SDR fitting on data set IB

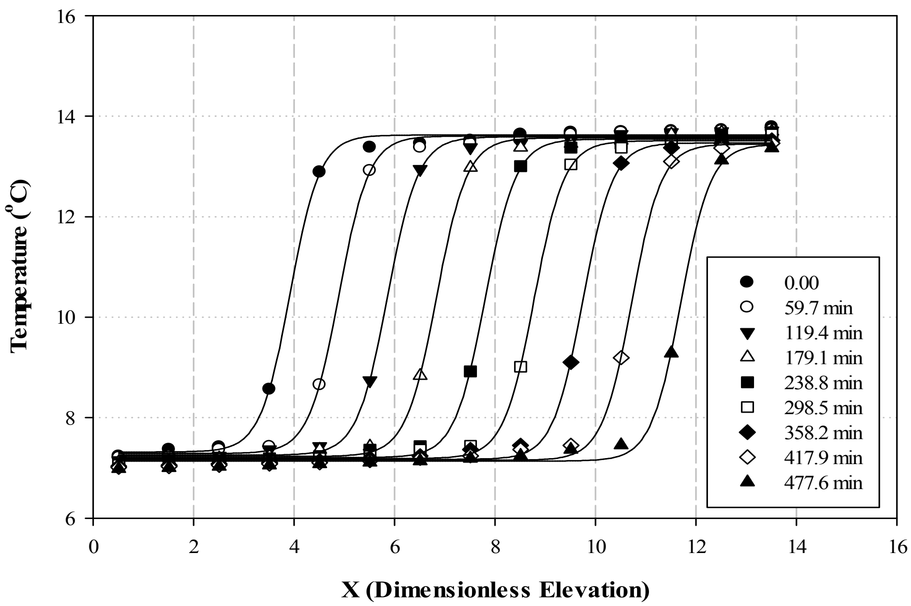

Figure 4.30 SDR fitting from charging model type (II) on data set IB

i. Temperature distribution similarity

The temperature data similarity was evaluated using R^2 value. It was performed by determining R^2 of temperature distribution of data set 1B and charging model type (II).

Table 4.11 R^2 verification of charging model type (II)

Data	to	Model	R^2
Chrg. Hrs.		Chrg. Time (min)	
18:00	-	0.0	1.000
19:00	-	59.7	0.999
20:00	-	119.4	0.999
21:00	-	179.1	0.999
22:00	-	238.8	0.997
23:00	-	298.5	0.995
0:00	-	358.2	0.993
1:00	-	417.9	0.985
2:00	-	477.6	0.984

From Table 4.11, it can be seen that R^2 between the two data approximately equal to unity, indicating both data are similar. It was shown at all charging hours.

ii. Temperature parameters similarity

Temperature parameters similarity was carried out by comparing parameters obtained from SDR function. It was performed by fitting of the observed and verified data using SIGMAPLOT. The parameters of the observed data from SIGMAPLOT are included in Appendix G2, and the verified data is presented in Appendix H1. Verification of data set 1B is discussed in this section. Comparison SDR parameters of T_c and T_h is presented in Figure 4.31, while comparison of parameters C and S is in Figure 4.32. Percentage parameter deviations of the two data sets are presented in Figure 4.33.

From Figure 4.31 and 4.32, it can be seen that both observed and model has same pattern of relatively constant at T_c and T_h. Figure 4.32 shows that the parameter S is constant during charging, while C has a linear increase with respect to charging hours. From Figure 4.33, it is shown that fluctuated deviation occurred on the parameters T_c, T_h. and S. The parameters deviation of C increases during the charging hours. It can be seen from Figure 4.32 that all parameters deviations are below than 5 %. The highest deviation occurred for S parameter.

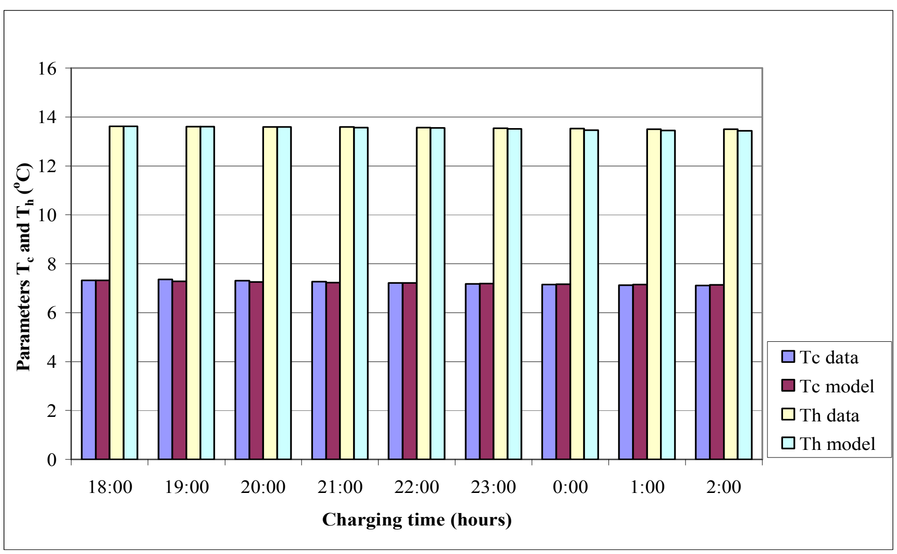

Figure 4.31 Comparison of SDR parameters T_c and T_h in verification of charging model type (II)

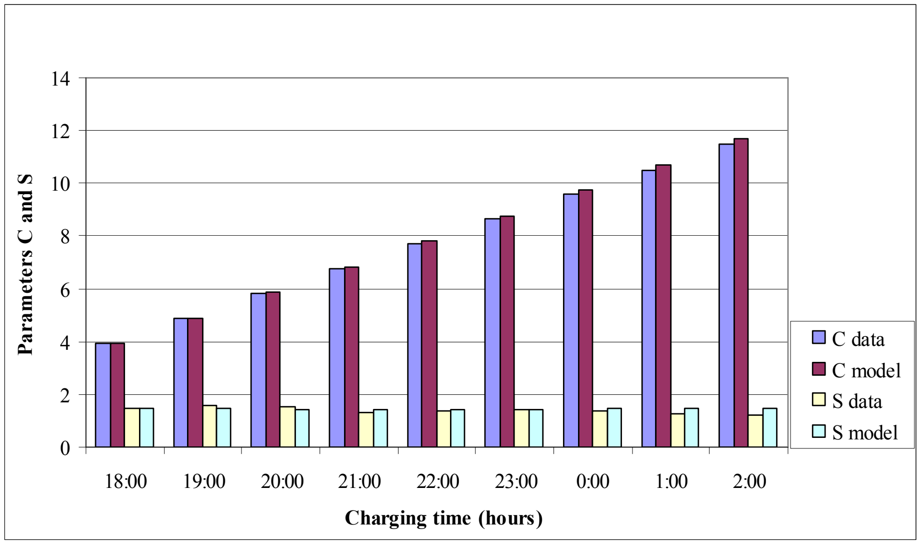

Figure 4.32 Comparison of SDR parameters C and S in verification of charging model type (II)

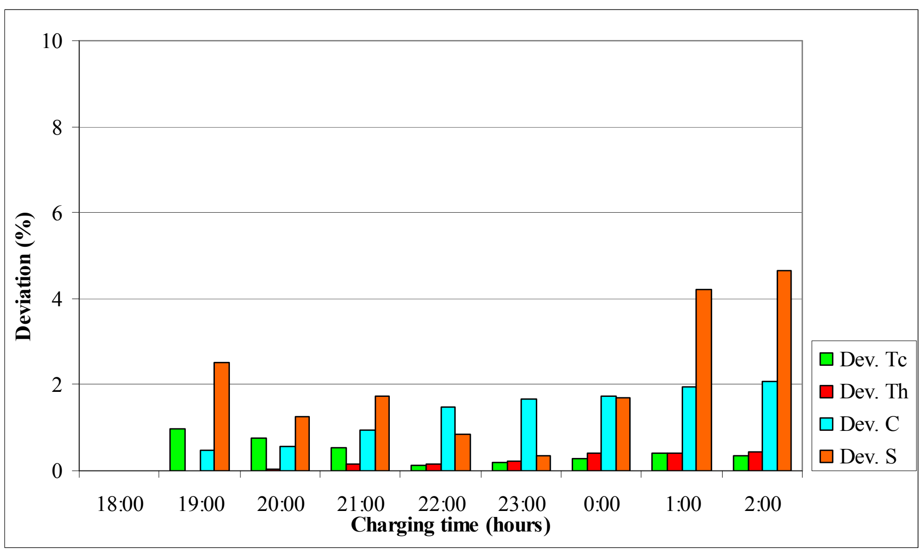

Figure 4.33 Percentage deviations of SDR parameters in verification of charging model type (II)

iii. Statistical test

Statistical analysis was performed to check the similarity acceptance of the model. It was carried out using t statistic test. The t computed values of the verification are presented in Figure 4.34. The t computed value was obtained from Equation 3.10, whereas t critical was obtained from Appendix E, with 14 numbers of data at 95% confidence level.

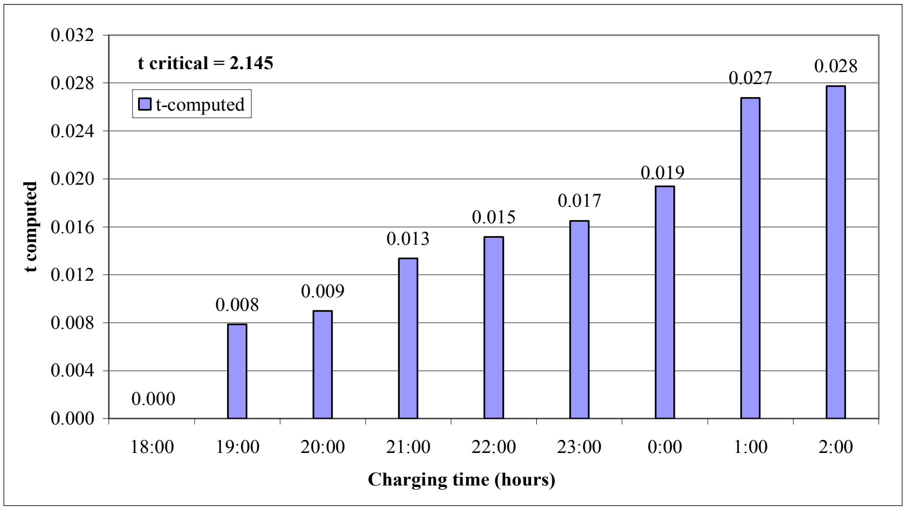

Figure 4.34 t computed values in verification of charging model type (II)

From Figure 4.34, it is shown that t computed value is very small compared to t critical which indicates that the temperature distribution both verified and observed data are similar. This finding shows that the null hypothesis was fulfilled, hence the model of single stage charging model type (II) was statistically accepted.

Verification of single stage charging model type (II) were also performed with other observed data for charging flow rate of 393 m^3/hr and 524 m^3/hr. The other verification for charging flow rate of 393 m^3/hr was performed using data set IC, whereas for charging flow rate 524 m^3/hr was carried out using data set IIB and IIC. Fitting SDR function of the verified data is attached in Appendix H. The three type of evaluation results on the verification model are attached in Appendices C1, C2 and C3, for data set IC, IIB and IIC, respectively. The results of the three evaluations are summarized in Table 4.12, 4.13 and 4.14, for R^2, parameter deviations and t-statistical test, respectively.

Table 4.12 Summary of R^2 in verification charging model type (II)

Data	Charging Hours	R^2	Remarks
IB	18.00-2.00	> 0.984	Table 4.11
IC	18.00-2.00	> 0.993	Appendix C.1.3
IIB	18.00-2.00	> 0.989	Appendix C.2.3
IIC	18.00-2.00	> 0.935	Appendix C.3.3

Table 4.13 Summary of parameters deviation in verification charging model type (II)

Data	Charging Hours	Parameter Deviations (%)				Remarks
		T_c	T_h	C	S	
IB	18.00-2.00	< 1.0	< 0.4	< 2.2	< 4.7	Figure 4.33
IC	18.00-2.00	< 1.5	< 0.2	< 1.5	< 5.0	Appendix C.1.6
IIB	18.00-2.00	< 1.7	< 0.2	< 1.6	< 5.2	Appendix C.2.6
IIC	18.00-2.00	< 2.7	< 0.9	< 2.5	< 5.1	Appendix C.3.6

From Table 4.12, it is shown that all R^2 of the verification are higher than 0.936 which indicate that the temperature distribution between data and model are also similar. Based on Table 4.13, it is noted that all parameters deviation for T_c, T_h and C are lower than 2% and deviation in the parameter C is less than 6%.

Table 4.14 Summary of t computed values in verification model type (II)

Data	Charging Hours	t-computed values	Remarks
IB	18.00-2.00	< 0.028	Figure 4.34
IC	18.00-2.00	< 0.019	Appendix C.1.7
IIB	18.00-2.00	< 0.030	Appendix C.2.7
IIC	18.00-2.00	< 0.033	Appendix C.3.7

As shown in Table 4.14, all t-computed values are smaller than t-critical of 2.145. Based on the results, it is noted that the simulation model single stage charging model type (II) capable of generating temperature distribution as similar as the historical data. The temperature distribution was statistically accepted.

4.2.1.2 Simulation of Single Stage Charging Model Type (II)

After being developed and verified, the single stage charging model type (II) was utilized for simulation. The simulation was performed with variation of chillers parameters in cases A2, B2 and D2. Inputs of the simulation are initial temperature, TES tank configuration and chillers parameters. The TES tank configuration parameters are described in Table 3.1, while chillers parameters are presented in Table 3.6.

Initial temperature of the simulation was obtained from generation parameters of T_h = 13.5°C, T_c = 6°C, C = 3.84, S = 1, and Θ = 0.01 using SDR function in Equation 4.1. The other parameters of effective diffusivity was taken at ε_{eff} = 10, whereas the losses temperature uses ΔT_1 = 0°C and ΔT_2 = 0°C.

For partial working load observation, simulation was performed exceeding that full capacity which is approximately at 9,226.4 kWh. Temperature distribution in single stage charging model type (II) of simulation cases A2, B2 and D2 are presented in Figures 4.35, 3.36 and 3.37. All simulation in cases A2, B2 and D2 were carried out with the same number of segments per slab and TES tank configuration. Four segments in each slab were chosen in the simulation resulting in Δx equals to 0.25 m. Using FLOW = 1 described in Equation 3.25, the observed time interval obtained were at 11.19 minutes, 14.93 minutes and 22.39 minutes, for cases A2, B2 and D2, respectively. Simulation was carried out at approximately one hour observation time, hence revealed at 56 minutes, 59.7 minutes and 111.9 minutes for cases A2, B2 and D2, respectively. Determination of charging duration time as well as cumulative cooling capacity was carried out by interpolation between the observed times interval.

Temperature distribution generated from simulation is presented in Figures 4.35, 4.36 and 4.37 for cases A2, B2 and D2, respectively. Cumulative cooling capacity calculated using Equation 3.16 with reference temperature equal to T_h = 13.5°C for the three cases is presented in Figure 4.38.

As shown in Figures 4.35 to 4.37, decreasing in values of charging flow rate as shown in cases A2, B2 and C2 reduce the span between temperature distributions. It indicates that smaller flow rate decreases the additional cool water depth. It is also shown that uniform temperatures of approximately 6°C at the whole elevation of the tank were obtained at observation time of 503.8 minutes, 656.8 minutes and 985.1 minutes for cases A2, B2 and C2, respectively. It indicates that uniform temperature at the whole elevation of the TES required shorter charging periods with higher charging flow rate.

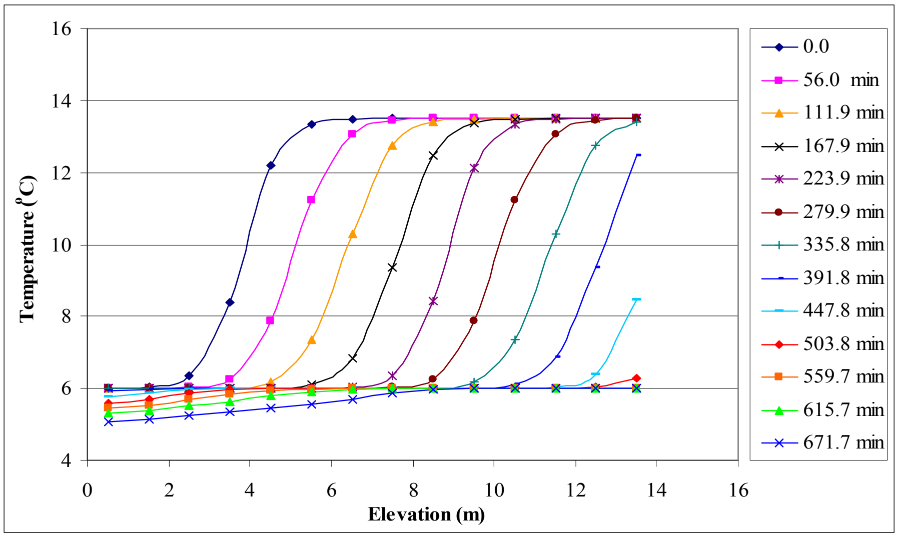

Figure 4.35 Temperature distribution of simulation case A2 in single stage charging model type (I) with flow rate 524 m^3/hr.

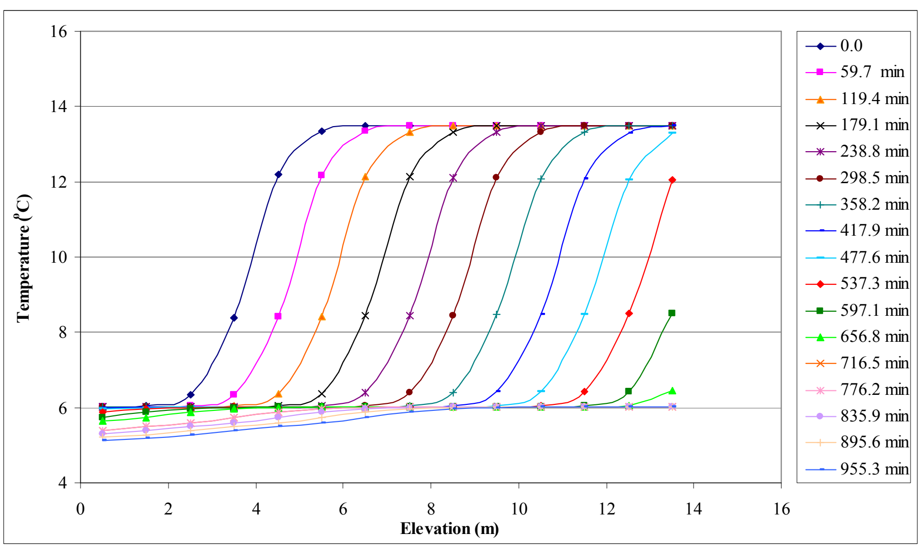

Figure 4.36 Temperature distribution of simulation case B2 in single stage charging model type (I) with flow rate 393 m^3/hr.

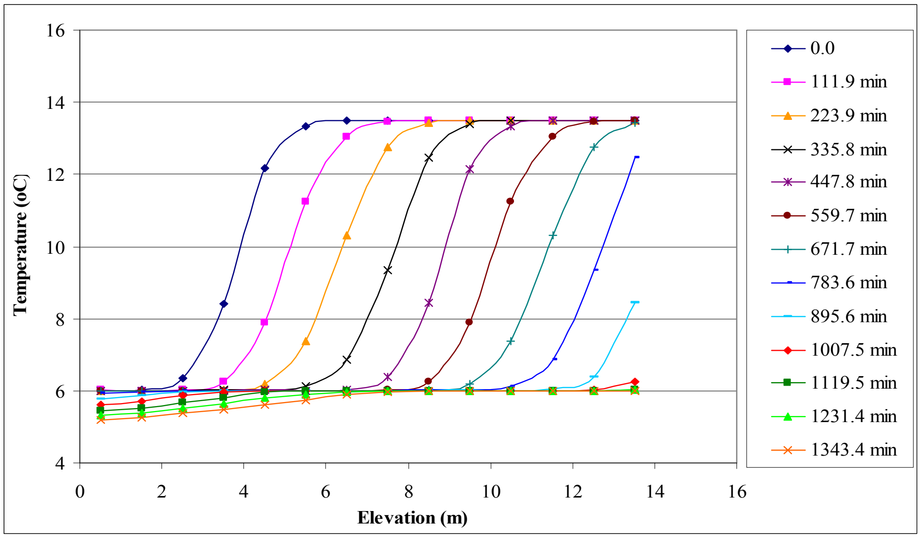

Figure 4.37 Temperature distribution of simulation case D2 in single stage charging model type (I) with flow rate 262 m^3/hr.

From the uniform temperature condition, charging still can be continued to have more cooling capacity. However, due to decreased in cool water temperature entering the chillers, the extended charging in stratified TES tank were carried out at partial working load of the chillers. The partial working load yields smaller additional cooling capacity in the tank.

Figure 4.38 shows a comparison of cumulative cooling capacity of the three cases of A2, B2 and D2. It is shown that steeper cumulative cooling capacity curves occurred at smaller charging flow rate. The smallest is in case D2. It shows that smaller charging flow rate requires longer charging duration to achieve full capacity. Initially, cumulative cooling capacity increase linearly and flattened after reaching the full capacity. If the charging is continued, it generates less additional cooling capacity. This is due to decreased outlet temperature in the charging.

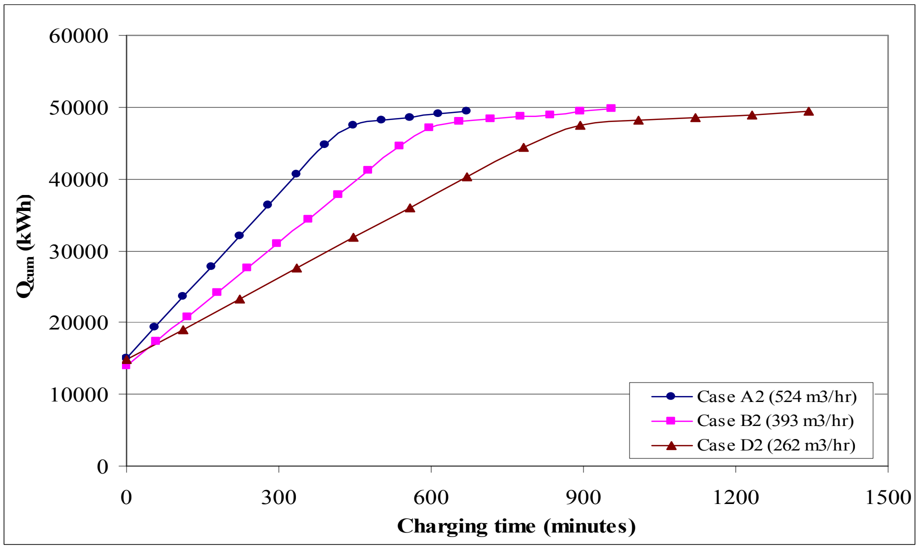

Figure 4.38 Cumulative cooling capacity of simulation cases A2, B2 and D2 of single stage charging model type (II).

Determination the values of charging duration and cumulative cooling capacity were also done in the simulation. Those values were determined based on initial condition, temperature transition point and full capacity charging of the stratified TES tank. Since the finite difference solution can only be performed using interval observation time, therefore determination of the two parameters was carried out by interpolation. Temperature transition was determined at time interval when the upper nozzle has outlet temperature which equals to 13.425^{o}C. Full capacity were recognized when the outlet charging temperature at the upper nozzle equals to 6.075^{o}C. The values of the charging duration as well as cumulative cooling capacity are summarized in Table 4. 15.

From Table 4.15, it is shown that higher charging flow rate leads to shorter charging duration in achieving temperature transition point as well as full capacity. Hence, cumulative cooling capacity at temperature transition decrease with reduced charging flow rate. This findings show that the close charging system capable of determining charging duration and cumulative cooling capacity of the stratified TES tank. It was performed by interpolation from temperature distribution generated by simulation charging model type (II). In addition, simulation charging models type (II) is capable of representing chillers partial working load characteristics. This is due its capability in covering fluctuated inlet at outlet charging temperature. The following section explains the results of partial working load analysis.

Table 4.15 Parameter values of simulation cases A2, B2 and D2

Initial Condition, $T_c = 6^oC$, $T_h = 13.5^oC$, S = 1, Θ = 0.01			
Variation Flow rate	**Q_{cum} (kWh)**	**Charging Time (min)**	**Remark**
Case A2, 524 m^3/hr	13,033.7	0	Empty Capacity
	35,294.1	293.1	Temperature Transition
	47,564.9	479.3	Full Capacity
Case B2, 393 m^3/hr	13,033.7	0	Empty Capacity
	35,142.7	390.0	Temperature Transition
	47,600.0	636.5	Full Capacity
Case D2, 262 m^3/hr	13,033.7	0	Empty Capacity
	35,332.9	587.2	Temperature Transition
	47,697.6	951.0	Full Capacity

i. Partial working load of the chillers

Partial working load of the chillers during charging was carried out by observing cooling capacity supplied by the chillers. Inlet, outlet and mixing charging temperature were first discussed. Determination of these temperatures was discussed in Section 3.4.4. The comparison of inlet, outlet and mixing temperature of cases A2, B2 and D2 in the simulation are presented in Figures 4.39 to 4.41, respectively. Chillers cooling capacity and percentage of partial load are presented in Figures 4.42 and 4.43.

Comparison of inlet and outlet charging temperatures in the simulation is presented in Figures 4.39 and 4.40. It can be seen that initially charging temperature is constant at a certain elevation, reduced incisively and finally stays constant at the lower temperature. The inlet charging temperature also shows similar trends. Starting time in reducing the temperature was due to commencing upper limit of thermocline into the upper nozzle. The temperature decreases incisively when upper limit point thermocline reaching the upper nozzle. The temperature finally stays constant at lower limit temperature after the bottom limit point thermocline reaching the upper nozzle. The high and low inlet temperatures are approximately at 6^{o}C and 5^{o}C for all cases, whereas high and low outlet temperatures are at 13.5^{o}C and 6^{o}C for all cases. Those inlet and outlet temperature are available in the range of two temperatures. This is due to proportional cooling capacity of the chillers given as by Equation 3.31.

Mixing temperature of the three simulation cases is presented in Figure 4.41. From Figure 4.41, it can be seen that initial mixing temperature stays fairly constant, and then start to decrease gradually. The mixing temperature decrease after thermocline profile commencing the upper nozzle. Thus mixing temperature affect the charging characteristic in single stage charging model type (II) stratified TES tank. The mixing temperature indicates additional cool water temperature in the lower part of the TES tank. This makes it different from single charging model type (I).

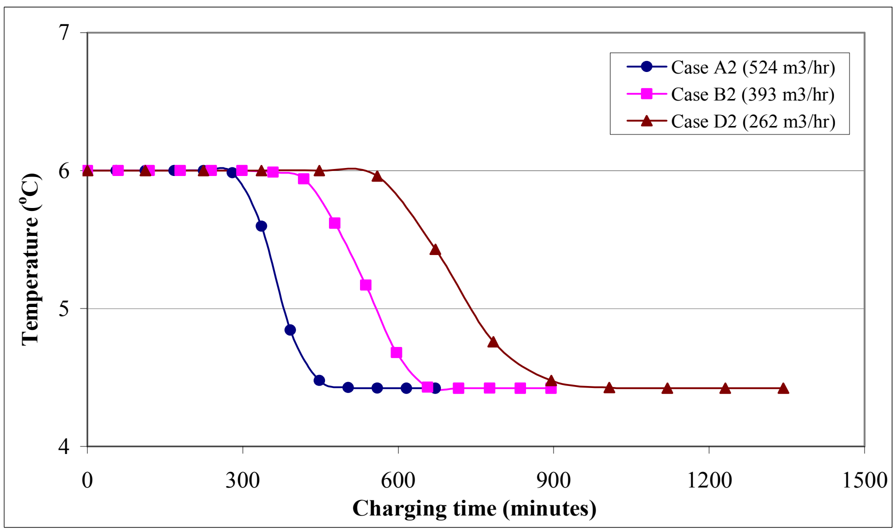

Figure 4.39 Inlet charging temperature of simulation cases A2, B2 and D2 in single stage charging model type (II)

Accordingly, the trend also occurs in the cooling capacity supplied by chillers as indicated in Figures 4.42. The high and low cooling capacities of cases A2, B2 and D2 have different values. This is due to different charging flow rate that influence the cooling capacity as described in Equation 2.7.

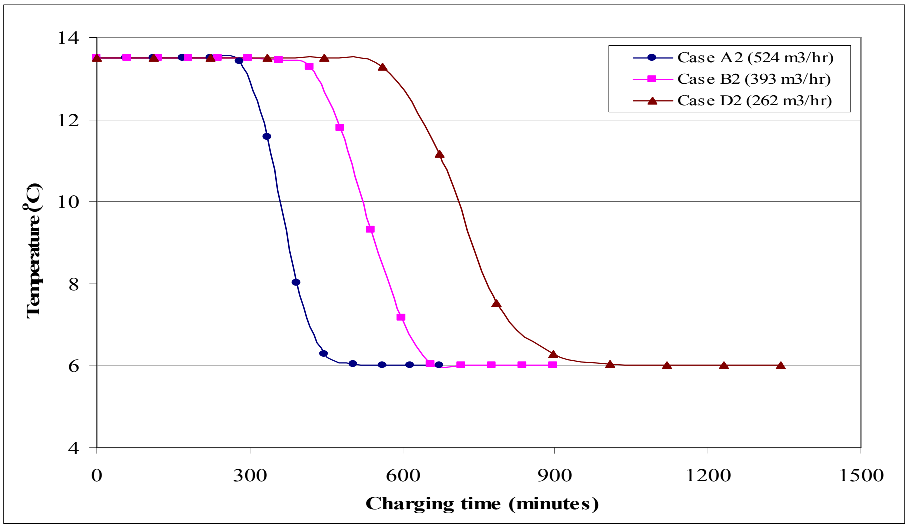

Figure 4.40 Outlet charging temperature of simulation cases A2, B2 and D2 in single stage charging model type (II)

Chillers partial working load of the simulation cases is shown in Figure 4.42. It can be seen that the trend of percentage partial load is similar with that on the inlet and outlet charging temperatures. Initially, chillers work at full load and later at lower partial load. In summarizing the charging characteristic, it is noted that the trend of inlet and outlet temperatures significantly affect the cooling capacity supplied by chillers.

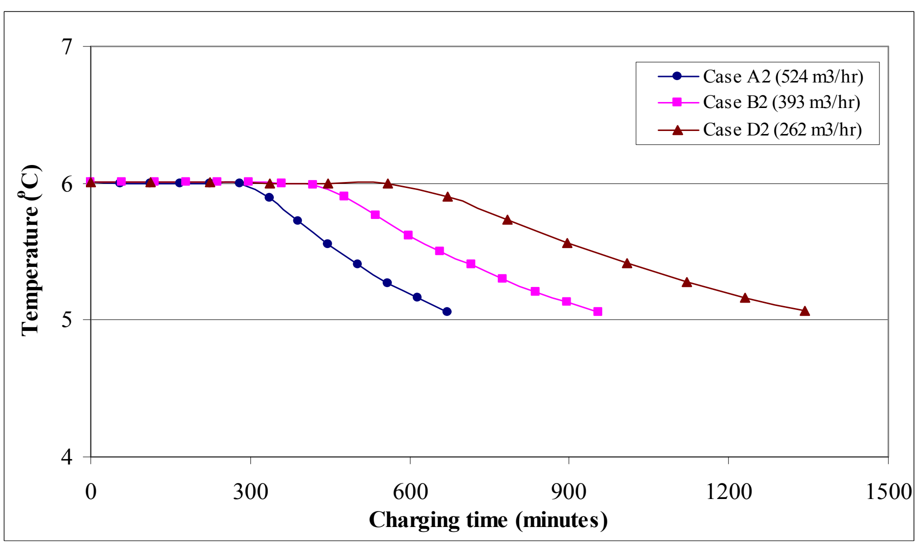

Figure 4.41 Mixing temperatures of simulation cases A2, B2 and D2 in single stage charging model type (II)

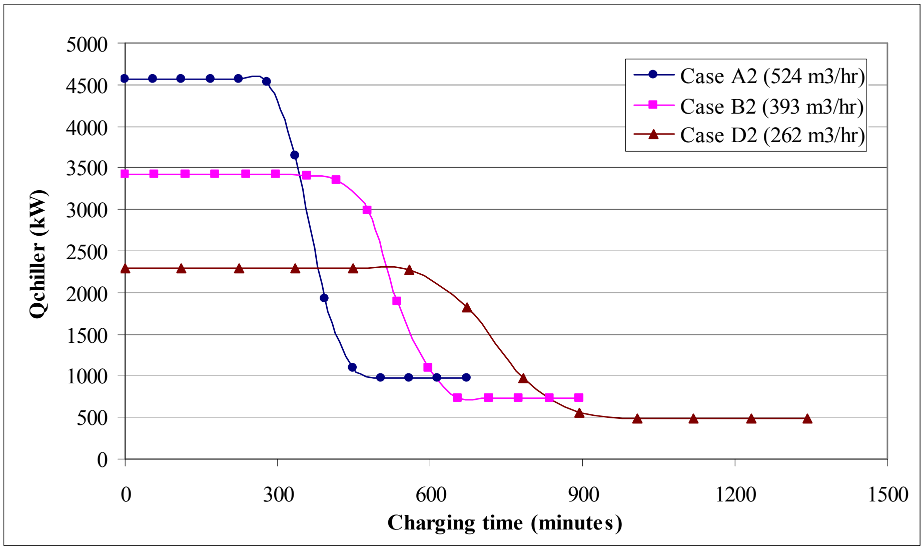

Figure 4.42 Chillers cooling capacity of simulation cases A2, B2 and D2 of single stage charging model type (II)

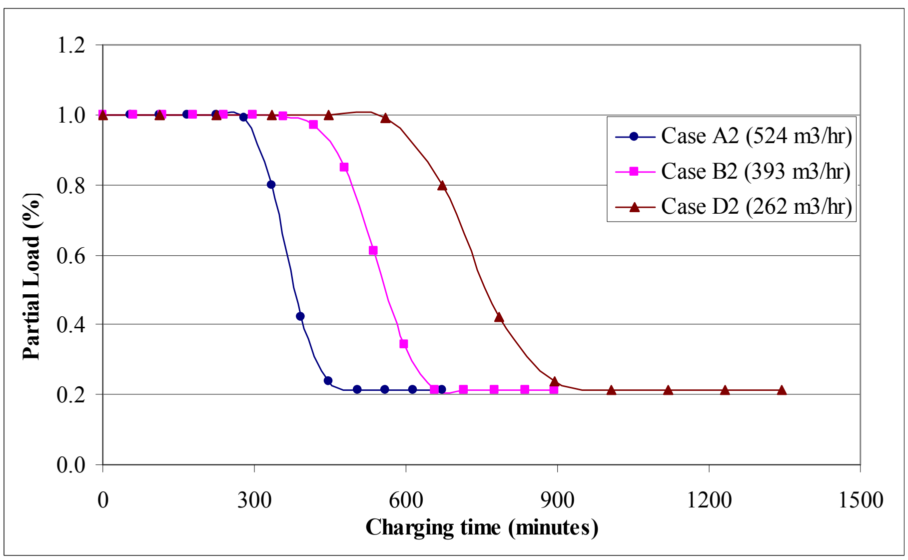

Figure 4.43 Chillers partial working load of simulation cases A2, B2 and D2 of single stage charging model type (II)

From the discussion, it is noted that the model is capable covering of partial working analysis in the charging stratified TES tank. This takes advantage of its capability to cover fluctuation of inlet charging temperature. The following conclusions are drawn from partial working load analysis.

i. Two important charging parameters that affect the partial load charging characteristic are temperature transition point and full capacity as predicted in Figure 3.6 and 3.4 (b), respectively.

   a. The temperatures transition point was obtained when the condition of outlet temperature equal to warm cut-off water temperature.

   b. Full capacity occurred at outlet temperature equal to cool cut-off water temperature.

ii. The charging duration values both for temperature transition point and full capacity is reduced by increasing of charging flow rate.

iii. The temperature transition and full capacity significantly affect the partial working load characteristics during charging. This involves inlet, outlet and mixing temperature as well as cooling capacity of the chillers.

4.2.2 Two-Stage Charging Model Type (II)

Two-stage of charging of stratified TES tank was enhanced from single stage charging model type (II) as explained in Section 3.4.4. The two-stage charging model type (II) was used to simulate absorption and electric chillers sequentially. The full capacity of the first stage charging was bounded by limit temperature of the absorption chillers that work at the first stage. The simulations were carried out with variations of chillers parameters and limit temperature.

4.2.2.1 Simulation of Chiller Parameter Variation

Variation of the chillers parameter was performed similar to that of the model type (I). The simulation involves several cases namely E2, F2 and G2. The first stage of charging was absorption chiller at flow rate of 504 m^3/hr and limit temperature was 9^{o}C. Whereas electric chiller at the second was at flow rate 524 m^3/hr, 393 m^3/hr and 262 m^3/hr, for cases E2, F2 and G2, respectively. The simulation used same initial temperature and TES tank configuration parameters with that on the simulation single stage, whereas chillers parameters are presented in Table 3.7.

All simulation in cases E2, F2 and G2 were carried out with four segments in each slab, resulting in Δx equals to 0.25 m. In the first stage, absorption chillers which work at flow rate 504 m^3/hr reveals time interval of 11.64 minutes. For the second stage, the time interval was obtained at 11.19 minutes, 14.93 minutes and 22.39 minutes for chillers in the second stage of these cases. The observation time of the simulation was approximately at hourly charging duration.

Temperature distribution generated from simulation in the first stage is presented in Figures 4.44, whereas Figures 4.45, 4.46 and 4.47 presents temperature distribution of the second stage of simulation for cases E2, F2 and G2, respectively. Cumulative cooling capacity was calculated using Equation 3.12 with reference temperature at T_h = 13.5°C. Comparison of cumulative cooling capacity values is presented in Figure 4.48. Whereas simulation result in term of inlet and outlet charging temperatures, mixing temperature, chillers cooling capacity, partial load of the chillers are attached in Appendix D.

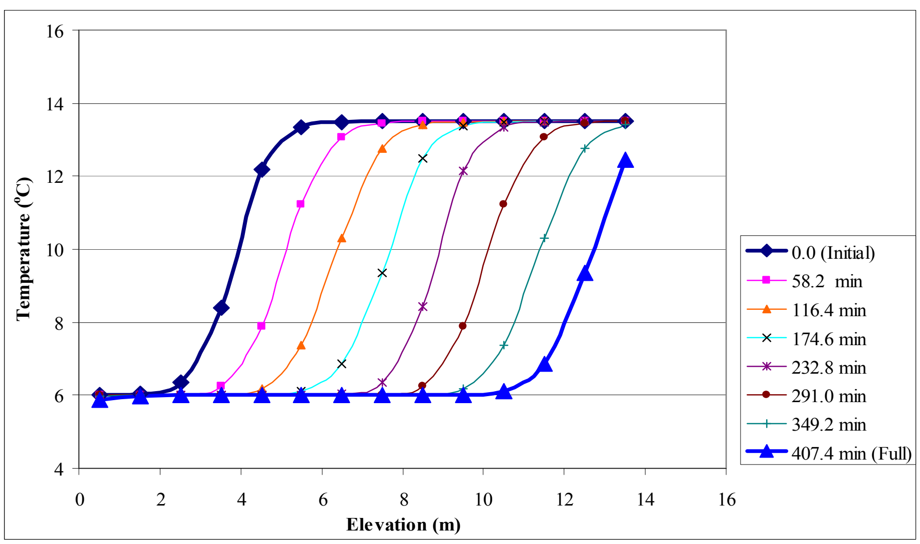

Figure 4.44 Temperature distribution of first stage charging simulation cases E2, F2 and G2 in two-stage charging model type (II) with flow rate 504 m^3/hr and limit temp. (Tr)=9°C

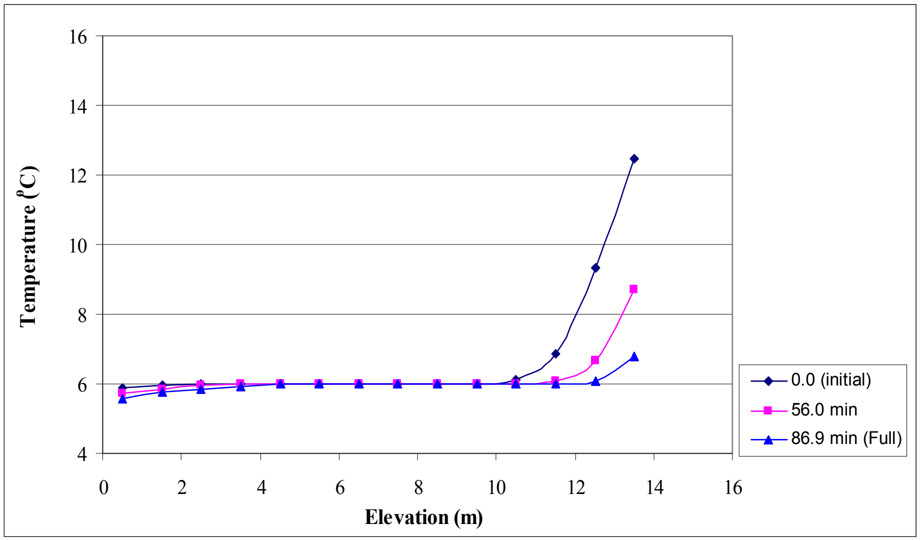

Figure 4.45 Temperature distribution of second stage charging simulation case E2 in two-stage charging model type (II) with flow rate 524 m^3/hr

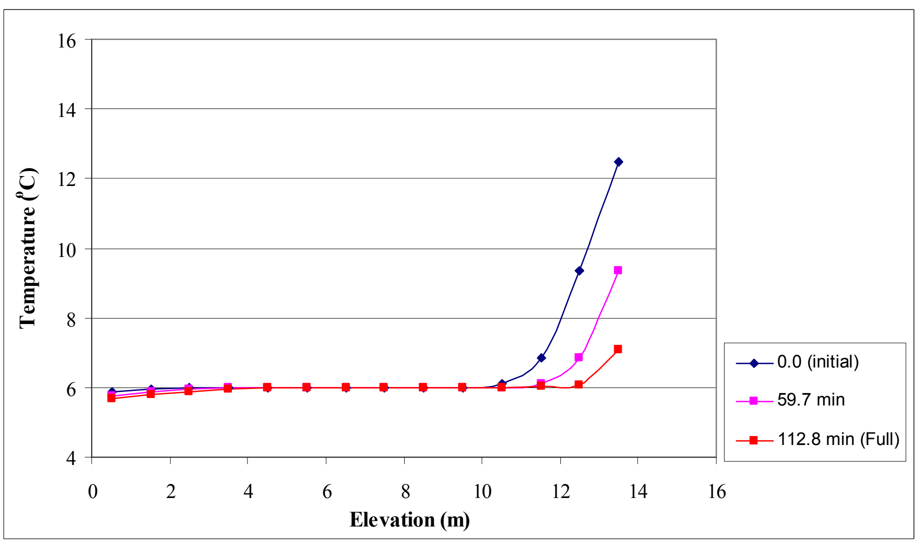

Figure 4.46 Temperature distribution of second stage charging simulation case F2 in two-stage charging model type (II) with flow rate 393 m^3/hr

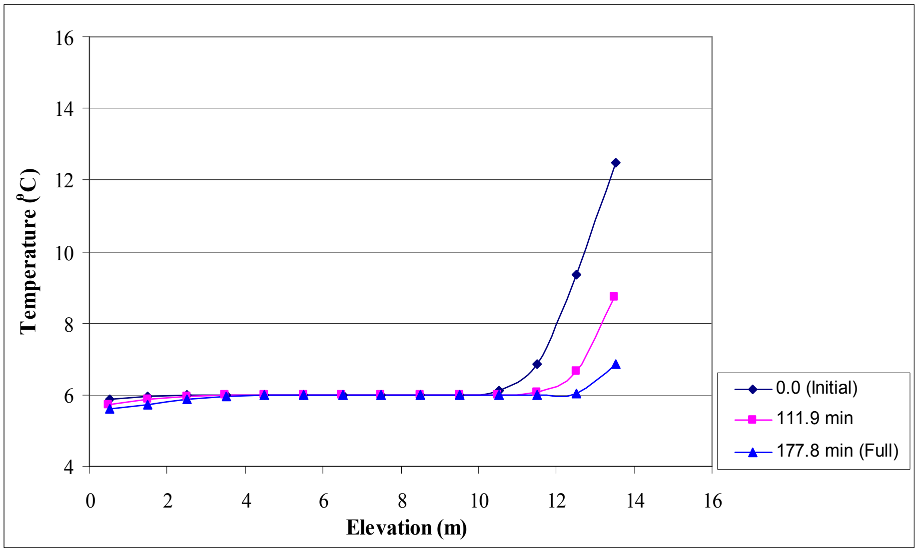

Figure 4.47 Temperature distribution of second stage charging simulation case G2 in two-stage charging model type (II) with flow rate 262 m^3/hr

Full capacity of the first stage in the simulation was determined by interpolation between two interval times at limit temperature of 9°C as outlet charging temperature. Temperature distribution at full capacity of the first stage charging was then set as initial temperature in the second stage. The charging was continued for chillers parameters at the second stage for cases E2, F2 and G2, respectively.

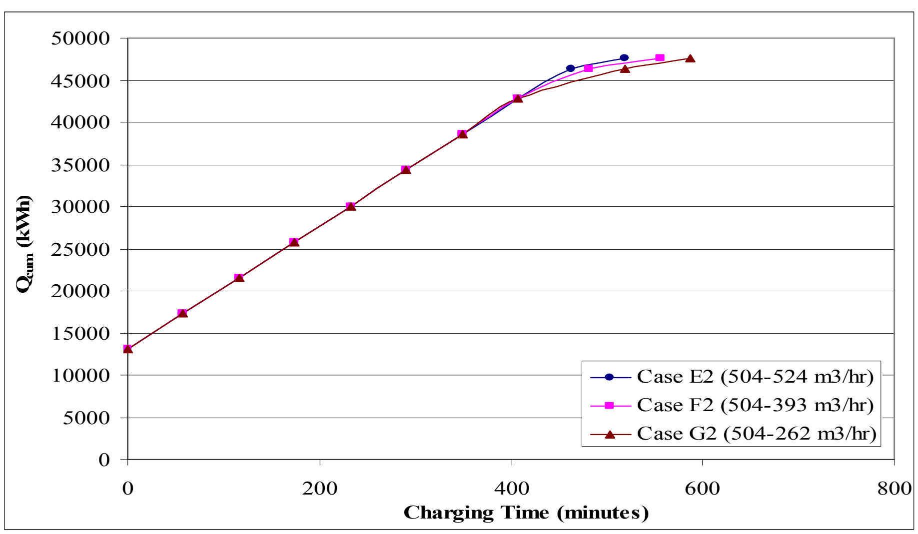

Figure 4.48 Cumulative cooling capacity of simulation cases E2, F2 and G2 in two-stage charging model type (II) with chillers variation.

In the second stage of charging simulation, full capacity was determined by interpolation to achieve outlet charging temperature equals to cut-off temperature at 6.075^{o}C. It indicates that decreased charging duration occurred at higher charging flow. Cumulative cooling capacity of the simulation is in Figure 4.48. It presents the cumulative cooling capacity of the three cases with respect to charging time. It can be seen that lower charging flow rate also lead to longer charging time.

Determination of the values of charging duration and cumulative cooling capacity was also performed in the simulation. These values were determined based on initial condition, temperature transition point and full capacity of charging the stratified TES tank. Temperature transition was determined at time interval when the upper nozzle has outlet temperatures equal to 13.425^{o}C. Full capacity was recognized when the outlet charging temperature at the upper nozzle is equal to 6.075^{o}C. The result is summarized in Table 4.16.

It is shown in Table 4.16, full capacity of the first charging for all simulation cases were obtained at similar charging duration of 407.4 minutes, while temperature transition was achieved at charging 305.2 minutes. At the second stage of charging, it is shown that higher charging flow rate leads shorter charging duration. This finding has similar pattern with that in the simulation charging models type (I).

Table 4.16 Parameters values of simulation cases E2, F2 and G2

Initial Condition, $T_c = 6^oC$, $T_h = 13.5^oC$, $S = 1$, $\Theta = 0.01$, $T_r = 9^oC$			
Variation Flow rate	**Q_{cum} (kWh)**	**Charging Time (min)**	**Remark**
Case E2, 504-524 m^3/hr	13,033.7	0.0	Empty Capacity
	35,194.0	305.2	Temperature Transition
	42,817.1	407.4	Full capacity, 1st stage
	47,582.2	494.2	Full capacity, 2nd stage
Case F2, 504-393 m^3/hr	13,033.7	0.0	Empty Capacity
	35,194.0	305.2	Temperature Transition
	42,817.1	407.4	Full capacity, 1st stage
	47,715.7	520.1	Full capacity, 2nd stage
Case G2, 504-262 m^3/hr	13,033.7	0.0	Empty Capacity
	35,194.0	305.2	Temperature Transition
	42,817.1	407.4	Full capacity, 1st stage
	47,698.1	585.1	Full capacity, 2nd stage

Partial working load analysis of the simulation is attached in Appendix D. Related to partial working load analysis, it is shown that outlet transition point occurred at smaller charging time than that at full capacity of the first stage of charging. This shows that the outlet transition point was achieved before reaching full capacity for both first and second charging. It indicates that full capacity in the first stage charging occurred at partial working of the chillers.

4.2.2.2 Simulation of Limit Temperature Variation

Simulation on two-stage charging model type (II) was enhanced to observe variation of limit temperature in the first stage charging. The first stage charging was with absorption chillers, whereas the second stage utilizes electric chillers. The limit temperature in the absorption chillers was varied at 7^oC, 9^oC and 11^oC express as cases H2, J2 and K2, respectively. The simulation used initial temperature as described in Table 4.7 and TES tank configuration parameters as shown in Table 3.1. The first stage charging flow rate was 504 m^3/hr and for the second stage was 393 m^3/hr, as presented in Table 3.7.

All simulation in cases H2, J2 and K2 were carried out with four segments in each slab resulting in Δx equals to 0.25 m. In the first stage, absorption chillers which work at flow rate 504 m^3/hr has time interval of 11.64 minutes whereas for the second stage was 14.93 minutes for flow rate 393 m^3/hr. The observation time of the simulation was taken approximately at hourly charging duration.

Temperature distribution of the simulations are presented in Figures 4.49, 4,50 and 4.51, for first charging of cases H2, J2 and K2, respectively. Temperature distributions in the second stage are presented in Figures 4.52, 4.53 and 4.54. Comparison of cumulative cooling capacity of these cases is presented in Figure 4.55.

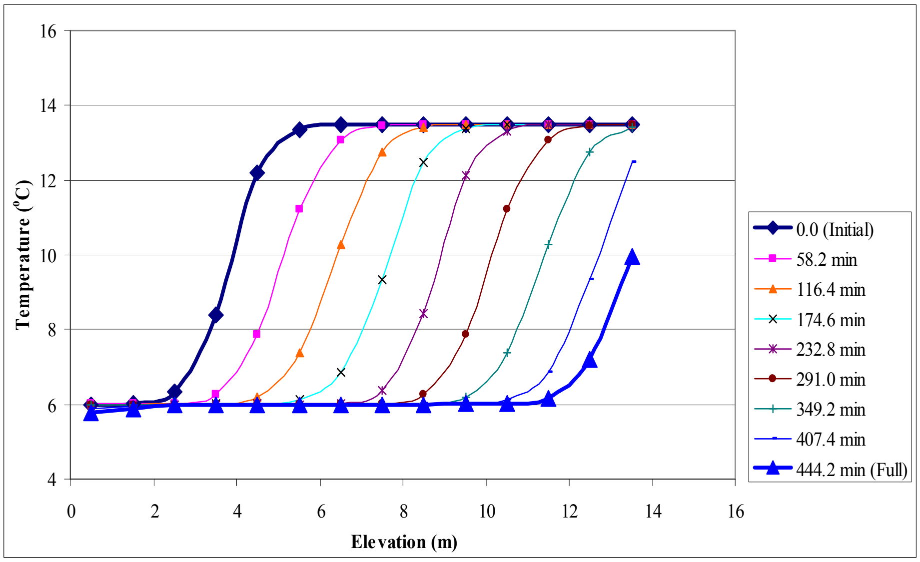

Figure 4.49 Temperature distribution of first stage charging simulation case H2 in two-stage charging model type (II) with flow rate 504 m^3/hr and limit temperature 7°C

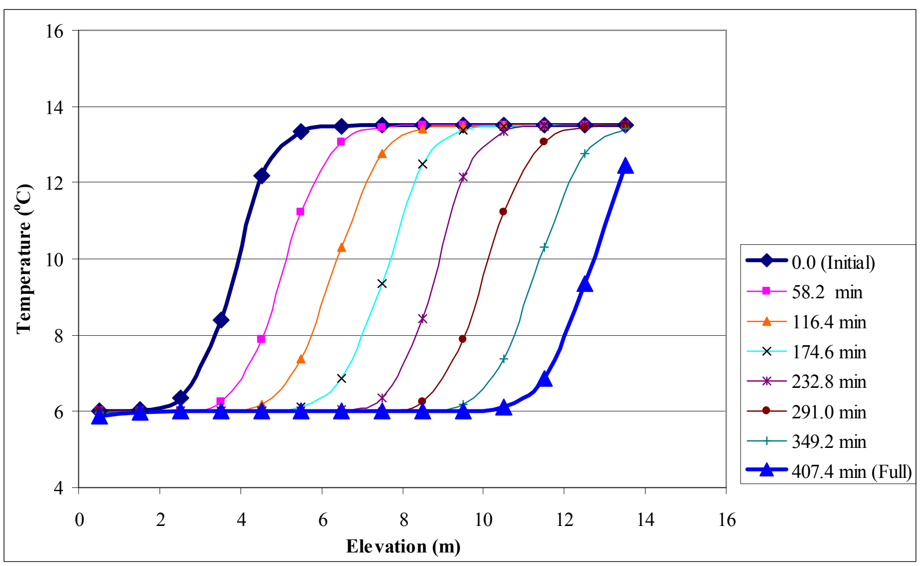

Figure 4.50 Temperature distribution of first stage charging simulation case J2 in two-stage charging model type (II) with flow rate 504 m^3/hr and limit temperature 9°C

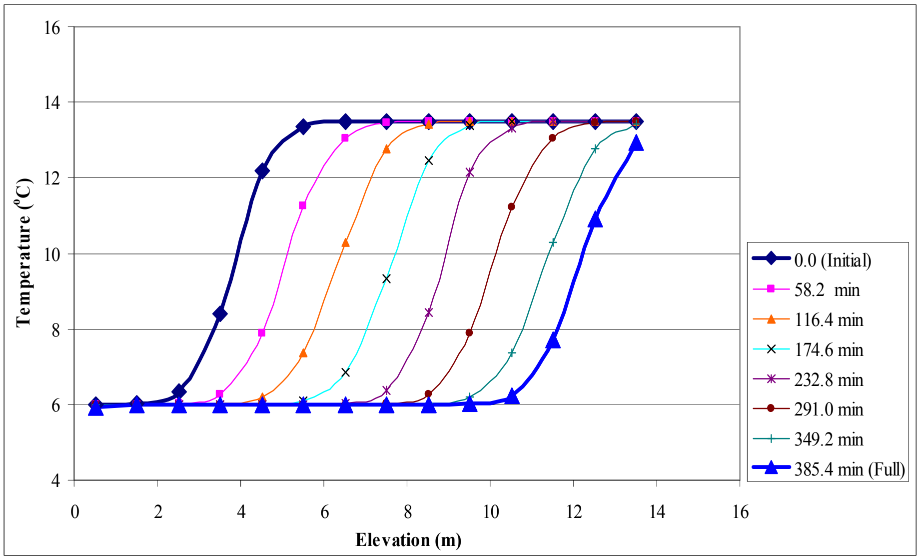

Figure 4.51 Temperature distribution of first stage charging simulation case K2 in two-stage charging model type (II) with flow rate 504 m^3/hr and limit temperature 11^{o}C

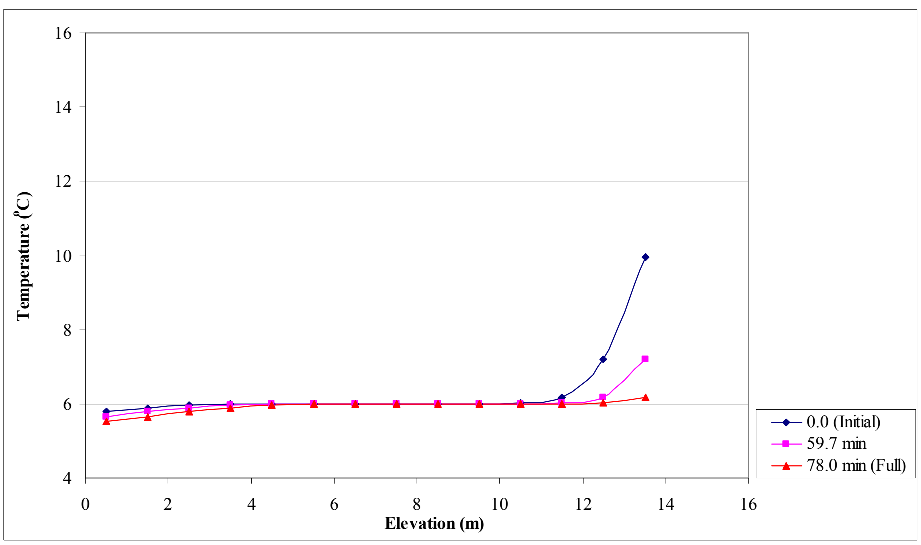

Figure 4.52 Temperature distribution of second stage charging simulation case H2 in two-stage charging model type (II) with flow rate 393 m^3/hr and limit temperature 7^{o}C

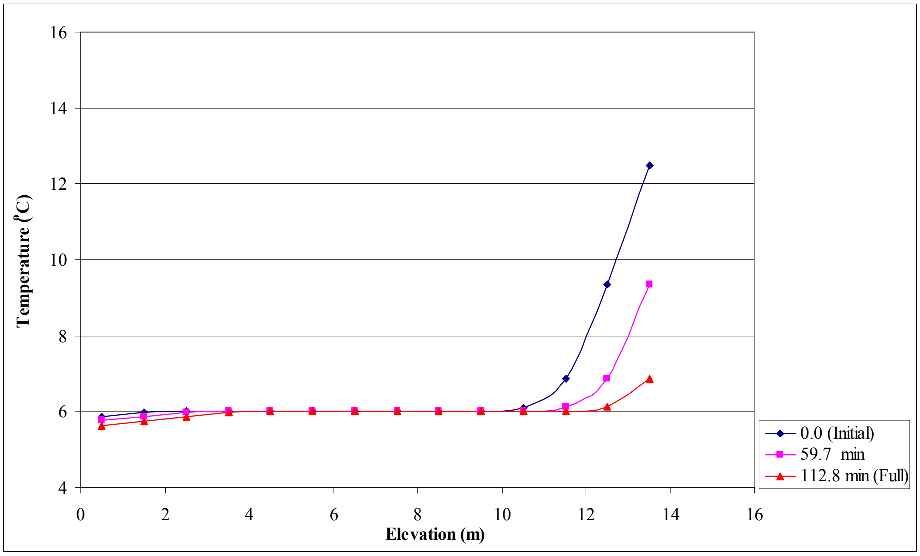

Figure 4.53 Temperature distribution of second stage charging simulation case J2 in two-stage charging model type (II) with flow rate 393 m^3/hr and limit temperature 9°C

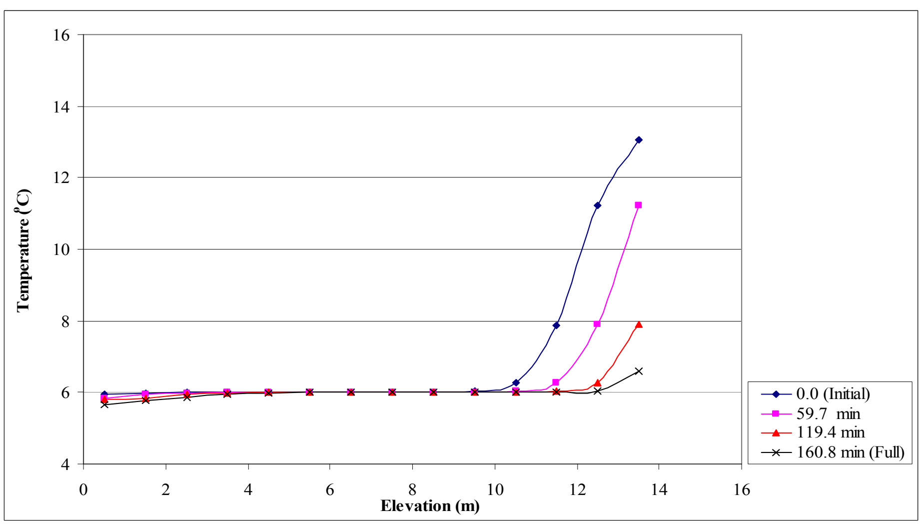

Figure 4.54 Temperature distribution of second stage charging simulation case K2 in two-stage charging model type (II) with flow rate 393 m^3/hr and limit temperature 11°C

Determination the values of charging duration and cumulative cooling capacity was also performed based on initial condition, temperature transition point and full capacity of charging the stratified TES tank. Temperature transition was determined at time interval when the upper nozzle has outlet temperatures equal to 13.425°C. Full capacities were calculated at outlet charging temperature at the upper nozzle equal to 6.075°C. The results are summarized in Table 4.17.

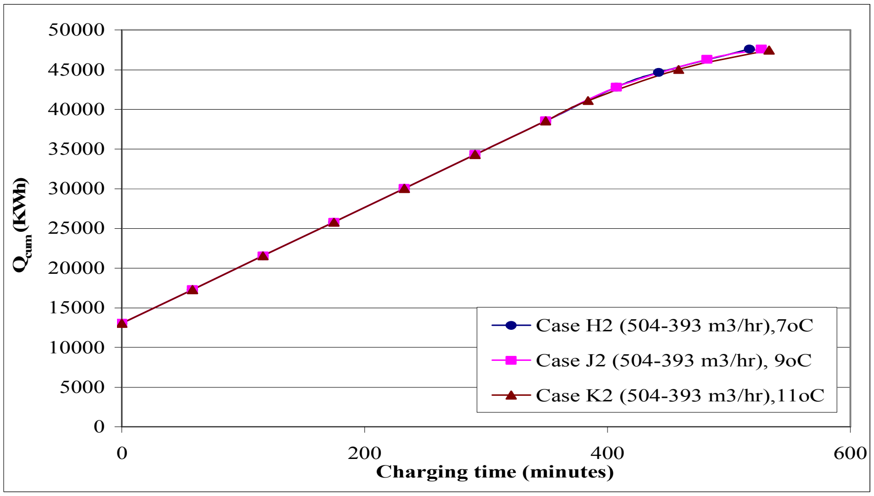

Figure 4.55 Cumulative cooling capacity of simulation cases H2, J2 and K2 of two-stage charging model type (II) in limit temperature variation

Table 4.17 Parameters values of simulation cases H2, J2 and K2

Initial Condition, Tc = 6°C, Th = 13.5°C, S = 1, Θ = 0.01, Flow Rate 504-393 m^3/hr, Variation Limit Temperature			
Variation Temperature Limit, T_r	**Q_{cum} (kWh)**	**Charging time (min)**	**Remarks**
Case H2, T_r = 7°C	13,033.7	0	Empty Capacity
	35,194.0	305.2	Temperature Transition
	45,326.5	444.2	Full capacity, 1st stage
	47,582.8	522.3	Full capacity, 2nd stage
Case J2, T_r = 9°C	13,033.7	0	Empty Capacity
	35,194.0	305.2	Temperature Transition
	42,817.1	407.4	Full capacity, 1st stage
	47,307.1	520.1	Full capacity, 2nd stage
Case K2, T_r = 11°C	13,033.7	0	Empty Capacity
	35,194.0	305.2	Temperature Transition
	41,485.0	385.1	Full capacity, 1st stage
	47,691.3	545.9	Full capacity, 2nd stage

As shown in Table 4.17, increased limit temperature lead to reducing of charging duration as well as full capacity in the first stage. However, charging durations as well as cumulative cooling capacity at temperature transition are constant, which indicates that it was not influenced by variation in limit temperature during charging. In the second stage charging, it is indicated that decreasing of limit temperature leads to increasing charging duration in the second stage.

4.3 Comparison of Charging Models Type (I) and (II)

The simulation results of the charging models type (I) and (II) showed that both are capable of simulation for single and two-stage charging stratified TES tank. As the two models were developed based on different approach, comparison of the two models was performed by equalizing input parameters. It was performed by simulating at the same initial temperature, TES tank configuration as well as flow rate parameters. Losses temperature in piping connection is assumed to be negligible.

The comparison was used to evaluate the values of charging duration as well as cumulative cooling capacity. In the model type (I), the parameters were calculated based on formulation. For model type (II), since utilizing finite difference in the calculation, the parameter was obtained based on interpolation between interval time observations. In the comparison, additional cool water temperature was considered. It involved average cool water temperature (T_c) in model type (I) and mixing temperature (T_{mix}) in model type (II). Comparison between the models was performed for single and two-stage charging stratified TES tank.

4.3.1 Comparison of Single Stage Charging Models

In single stage charging model, the comparison was performed with cases of A1, B1, D1 and A2, B2, D2 for model types (I) and (II), respectively.

i. Temperature of additional cool water

In the model type (I), additional cool water temperature presents as average cool water temperature (T_c), whereas in model type (II) present as mixing temperature (T_{mix}). Comparison of additional cool water temperature is presented in Figure 4.56.

From figure 4.56, it is shown that temperatures of additional temperature in model type (I) are constant within charging time observation. In the model type (II), initially temperature stays fairly constant until reaching temperature transition point and decrease gradually. Decreasing temperature is less than $1^{o}C$. This trend difference was due to open and close cycle considerations in the two models.

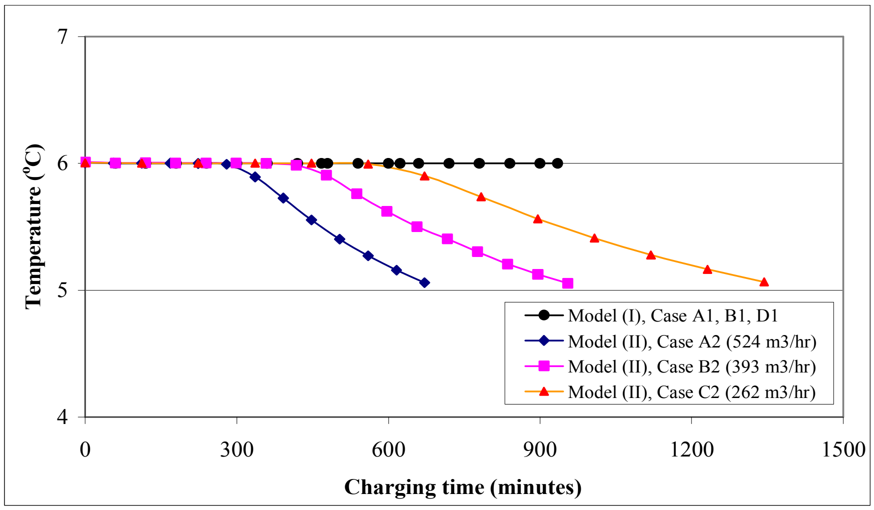

Figure 4.56 Comparison of additional cool water temperature of single stage charging model type (I) and (II).

ii. Values of Charging Parameters

Charging parameters values obtained from simulation model type (I) and (II) are compared in this section. Deviations of the parameter value in the single stage charging models are tabulated in Table 4.18.

From the parameters value deviation as tabulated in Table 4.18, it is shown that any slightly deviation occurs between the parameters. In term of charging durations, the deviation in temperature transition point is smaller than that in full capacity. The higher deviation in full capacity is due to effect of mixing temperature after reaching transition temperature. Charging duration in all simulation cases is lower than 3%. In comparing cumulative cooling capacity, the deviation occurs less than that on the charging duration. Deviation at cumulative cooling capacity at all simulation cases are below than 2%. Based on these results, it is noted that the charging parameter values both for models type (I) and (II) are approximately similar.

Table 4.18 Deviation parameter values of single stage charging models

Simulation Cases	Deviation		Remark
	Q_{cum} (%)	Charging Time (%)	
A1-A2, 524 m^3/hr	0	0	Empty Capacity
	0.7	1.4	Temperature Transition
	0.9	2.5	Full Capacity
B1-B2, 393 m^3/hr	0	0	Empty Capacity
	0.3	1.2	Temperature Transition
	1.0	2.1	Full Capacity
D1-D2, 262 m^3/hr	0	0	Empty Capacity
	0.8	1.6	Temperature Transition
	1.2	1.7	Full Capacity

4.3.2 Comparison of Two-Stage Charging Models

Comparisons of two-stage charging cycle was performed in the variation charging flow rate and limit temperature. In the charging flow rate variation, cases E1, F1 and G1 were compared to cases E2, F2 and G2, whereas in the limit temperature variation involves in comparisons between cases H1, J1, K1 and cases H2, J2, K2.

i. Flow rate variation

Comparison of the two models was carried out in term temperature of additional cool water and charging parameters. Temperature of additional cool water comparison was conducted by analysing mixing temperature of model type (II). This is due to constant temperature of additional cool water of the model type (I). The mixing temperature of model type (II) is presented in Figure 4.57.

From Figure 4.57, initially temperature stays fairly constant until reaching temperature transition point, and decrease gradually to the full capacity of the first charging. The mixing temperatures continue to decrease in the second stage of charging. Decreasing temperature is approximately less than 1^{o}C, which indicates that the mixing temperature fluctuate slightly.

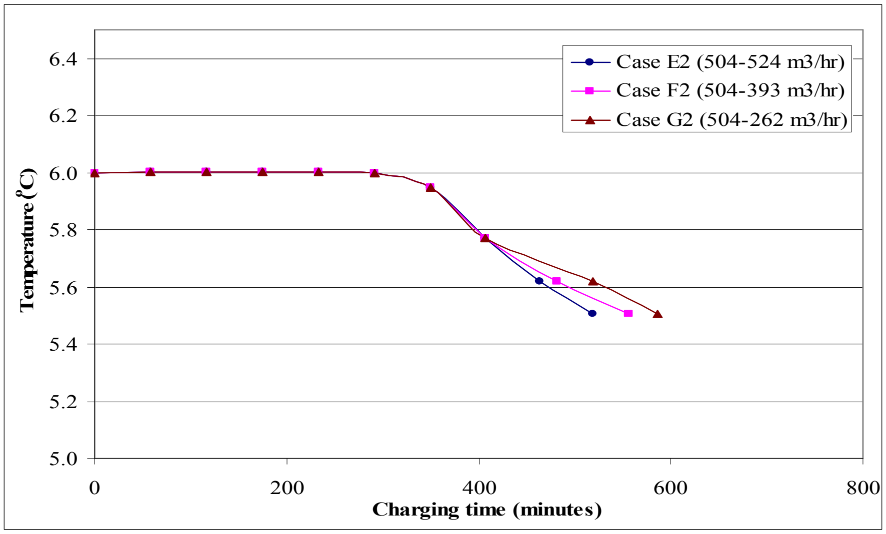

Figure 4.57 Mixing temperatures of two-stage charging model type (II) with flow rate variation

Deviation of the parameter values in the single stage charging models is tabulated in Table 4.19. From Table 4.19, it can be seen that charging duration deviation increases from temperature transition to full capacity. This is due to decreasing of additional cool water after thermocline profile reaching temperature transitional point. In all simulation cases charging duration deviation are smaller than 3% whereas cumulative cooling capacities are below than 2%.

Table 4.19 Deviation parameters values of two-stage models with flow rate variation

Variation Flow rate	Deviation		Remarks
	Qcum (%)	Charging Time (%)	
E1-E2, (504-524 m^3/hr)	0	0	Empty Capacity
	0.4	1.6	Temperature Transition
	1.0	1.5	Full capacity, 1st stage
	0.6	2.4	Full capacity, 2nd stage
F1-F2, (504-393 m^3/hr)	0	0	Empty Capacity
	0.4	1.6	Temperature Transition
	1.0	1.5	Full capacity, 1st stage
	0.4	2.0	Full capacity, 2nd stage
G1-G2,(504-262 m^3/hr)	0	0	Empty Capacity
	0.4	1.6	Temperature Transition
	1.0	1.5	Full capacity, 1st stage
	0.2	1.7	Full capacity, 2nd stage

ii. Limit temperature variation

Comparison of the two models was carried out in term temperature of additional cool water and charging parameters. It was first carried out in reviewing the mixing temperature of cases H2, J2 and K2 as presented in Figure 4.58.

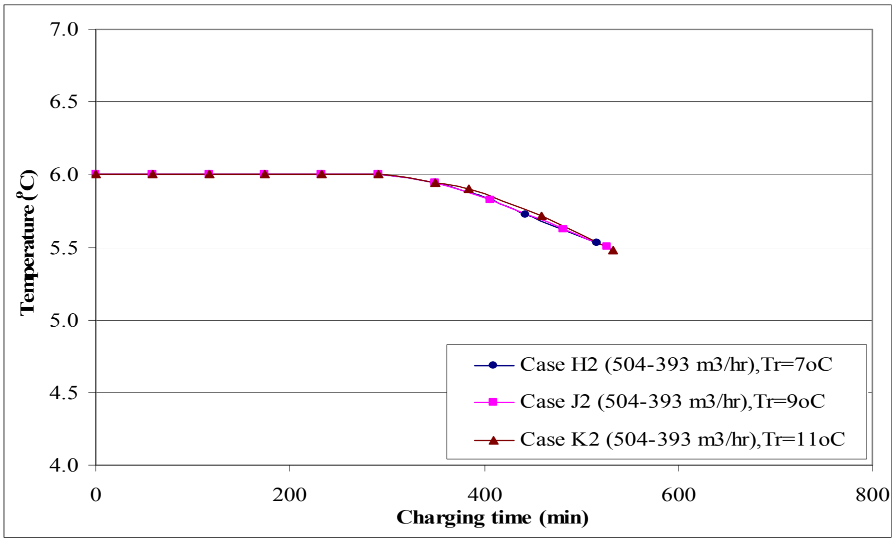

Figure 4.58 Mixing temperatures of two-stage charging model type (II) with limit temperature variation

It can be seen in Figure 4.58, initial mixing temperature was found constant and decrease after reaching temperature transition. In the second stage, the mixing temperature also decreases as continuation from the first stage of charging.

Deviation of the parameters values between the two models is shown in Table 4.20. From Table 4.20, it can be seen that the charging duration deviation are smaller than 4% whereas cumulative cooling capacity are below than 2%. Based on the comparison results, it can be concluded that both simulation charging models (I) and (II) are capable of determination parameters in the charging stratified TES tank. Deviation in charging duration between the two models is below 4%, whereas cumulative cooling capacity deviation is less than 2%.

Table 4.20 Deviation parameters values of two-stage models with limit temperature variation

Variation limit temperature	Deviation		Remark
	Qcum (%)	Charging time (%)	
H1-H2, (T_r=7°C)	0	0	Empty Capacity
	0.4	1.6	Temperature Transition
	2.0	3.1	Full capacity, 1st stage
	1.0	3.1	Full capacity, 2nd stage
J1-J2, (T_r=9°C)	0	0	Empty Capacity
	0.4	1.6	Temperature Transition
	1.0	1.5	Full capacity, 1st stage
	0.4	2.0	Full capacity, 2nd stage
K1-K2, (T_r=11°C)	0	0	Empty Capacity
	0.4	1.6	Temperature Transition
	1.7	1.5	Full capacity, 1st stage
	1.2	3.8	Full capacity, 2nd stage

4.3.2 Evaluation of open and close charging system

In this study, two types of simulation charging models have been developed with different approach. The simulation charging model type (I) was developed as an open charging system incorporated to water temperature distribution analysis. The simulation charging model type (II) was developed using close charging system by integrating TES tank and chillers. Summary evaluation between the two approaches that were used to develop the simulation models is presented in Table 4.21. The evaluation was performed in term of basic concept, solution method, inputs parameters, charging parameters and its capability in solving charging of stratified TES tank.

Table 4.21 Evaluation summary of open and close charging system

No.	Description	Open Charging System	Close Charging System
1.	Basic Concept	based on temperature distribution analysis	integrating TES tank and chillers Models
2.	Solution Equations	SDR function	conduction & convection Eq.
3.	Temperature Distribution generation	SDR function constant T_c, T_h, and S C increase ~ flow rate	finite difference method
4.	**Input Parameters**		
4a.	Initial Temperature	SDR function parameters (T_c, T_h, C , S) *and* Θ	temperature distribution water property (α), ε_{eff}
4b.	Tank Configuration	D,H,N,N_T,N_L	$D,H,N,N_T,N_L,\Delta T_1, \Delta T_2$
4c.	Chillers parameter	flow rate	flow rate, UA, T_{ev}
5.	**Charging parameter**		
5a.	Cool water depth	formulate using SDR function $C_E,C_F,C_{FR},C_{ET},C_{FT}$	not capable
5b.	Charging duration	t_{CF}, t_{CFR}	interpolation of temperature values at nozzle elevation
5c.	Cumulative Cooling Capacity	capable	capable
6.	Inlet charging temperature	constant temperature	covers fluctuating temperature
7.	Partial Load Analysis	not capable	capable
8.	Simulation Single Stage charging	capable simulation single stage charging model type (I)	capable simulation single stage charging model type (II)
9.	Simulation Two-Stage charging	capable simulation two- stage charging model type (I)	capable simulation two-stage charging model type (II)

Notation :

- C : Midpoint of thermocline
- C_E : Cool water depth of empty capacity (m)
- C_F : Cool water depth of full capacity (m)
- C_{ET} : Cool water depth of empty capacity (m)
- C_{FT} : Cool water depth of full capacity (m)
- C_{FR} : Cool water depth temp. transition (m)
- D : Tank diameter (m)
- H : Effective water depth (m)
- N : Number of slabs
- N : Upper nozzle elevation (m)
- N_L : Lower nozzle elevation (m)
- S : Slope gradient parameter
- T_r : Evaporator temperature (^{o}C)
- T_c : Average cool temperature (^{o}C)
- T_h : Average warm temperature (^{o}C)
- t_{CF} : Charging duration of full capacity (min)
- t_{CET} : Charging duration of temp. transition (min)
- UA : Overall heat transfer times area (kW/^{o}C)
- ΔT_1: Upstream piping losses temperature (^{o}C)
- ΔT_2: Downstream piping losses temperature(^{o}C)
- ε_{eff} : Effective diffusivity factor
- α : Thermal diffusivity (m^2/sec)
- Θ : Dimensionless cut-off temperature

From Table 4.21, it is noted that the open and close charging system are capable of solving charging stratified TES tank with different basic concept and solution methods. The input parameters in the two system models have some differences of TES tank configuration and chillers parameters. They have also different approach to determine charging parameters.

Sensitivity analysis of the charging models were performed on the single and two-stage charging models for both open and close charging system. It was used to determine how different values of charging parameters impact the charging duration and cumulative cooling capacity on the charging of stratified TES tank. On the single stage charging model, it was described in the simulation cases with variation of charging flow rate. On the two-stage charging models, it was carried out by simulating at variation of charging flow rate and limit temperature cases. The other charging parameter were kept constant namely initial temperature and TES tank configuration. The simulation result showed that charging duration and cumulative cooling for both systems were found similar. In addition, both systems were capable of solving temperature limitation in the absorption chillers.

The closing remarks from the evaluation of developing models in open and close charging system are as follow.

i. Single stage and two-stage charging model type (I) that were developed using open charging system has capability in determining charging parameters exactly based on formulation.

ii. Single stage and two-stage charging model type (II) that were developed using close charging system has capability of covering TES tank and chillers parameters in the charging of stratified TES tank. These charging models are capable covering of partial working load analysis.

4.4 Summary

Developing simulation models to overcome temperature limitation of charging stratified TES tank using absorption chillers have been accomplished through several comprehensive steps. It was developed for single stage and two-stage charging of stratified TES tank which involved electric chiller solely and combination with absorption chiller. The charging models were developed using open and close charging systems.

In the open charging system, the charging models were developed based on temperature distribution analysis. These models were designated as charging models type (I). Development of the charging model type (I) involved selection of temperature distribution function, formulation of charging parameters and simulation of single stage charging model. Verification of temperature distribution in the charging model type (I) was evaluated using three criteria namely temperature distribution similarity, temperature parameters similarity and statistical test. In addition, validation was performed in term of charging duration and cumulative cooling capacity. On the model verification it was found that the temperature was accepted to represent charging of stratified TES tank. It was described at R^2 higher than 0.95; parameters deviation less than 5% and accepted null hypothesis, for the first, second and third criteria respectively. On the validation, it was found that the deviation were less than 2% and 4%, for charging duration and cumulative cooling capacity, respectively. Development of two-stage charging model type (I) was performed by enhancing the single stage model. Simulation of two-stage charging was performed through some cases involving absorption chiller and electric chiller in sequence to charge the TES tank. Simulation results showed that the enhanced model was capable of solving temperature limitation on the absorption chiller.

In the close charging system, the model was developed by integrating TES tank and chillers parameters. Charging models solved using finite difference in explicit method was designated as charging model type (II). The model was also developed and simulated for single stage charging of stratified TES tank. Verification of temperature distribution was also performed with similar criteria with that on the open charging models. The model 8; parameters deviation less than 5% and accepted null hypothesis, for the first, second and third criteria respectively. The developed model was then enhanced for two-stage charging of stratified TES tank. The two-stage charging model was used for simulation. The simulation results showed that the model was also capable of solving temperature limitation in the absorption chiller.

Comparison between the open and close charging system were performed on the single and two-stage charging simulation cases. It was found that the charging duration and cumulative cooling capacity differences were less than 4% and 2%, respectively.

It is noted that charging models both for open and close charging were capable of simulation of charging of stratified TES tank using combination absorption and electric chillers. The models in open charging system offer beneficial of solving charging parameters based on formulation. The models in close charging system were capable of covering fluctuated temperature for partial working load analysis.

CHAPTER 5

CONCLUSIONS AND RECOMMENDATIONS

The dissertation focused on the study of charging stratified TES tank utilizing absorption chillers to complement electric chillers. This addresses the issue of absorption chillers not being used for charging the TES tank due to temperature limitation. The study was carried out by developing single and two-stage charging models using open and close charging systems. Based on the simulations results of the models, the following conclusions are arrived.

5.1 Conclusions

The conclusions in relation to the developed single and two-stage charging models using open and close charging systems are:

i. The case for the single and two-stage charging models were developed based on temperature distribution analysis in open charging system.

   a. The water temperature distribution analysis shows significant findings. Redefining parameters of an S-curve temperature distribution in term of average cool temperature (T_c), average warm temperature (T_h), cool water depth (C) and slope gradient of thermocline profile (S). Based on these parameters, the analysis reveals a function that could represent the temperature distribution namely sigmoid dose response (SDR) function.

   b. Charging parameters on the single and two-stage charging models in the open charging system were developed based on formulation of SDR function. The parameters are thermocline limit points, thermocline thickness and temperature transition as well as limit capacity. The parameters of limit capacity criteria enable determination of empty and full capacities in the charging stratified TES tank.

c. The single stage charging models has been developed in open charging system. Verification and validation was performed to the model using historical data of the operating TES tank. Results reveal that the single stage charging model is capable in determination of charging parameters in stratified TES tank based on formulation.

d. The enhancement of the single stage model for two-stage charging with absorption and electric chillers to charge the stratified TES tank sequentially was performed in open charging system. Results show that the model is capable of solving temperature limitation in the absorption chillers. The two-stage charging model is able to determine charging parameters based on formulation namely cool water depth, charging duration, limit capacities as well as temperature transition.

ii. The case for the single and two-stage charging models using close system model were developed by integrating TES tank and chillers.

a. The single stage charging models in close system was developed by adopting finite difference method in solving conduction-convection equation. The model was developed and verified using historical data of operating stratified TES tank. Results show that the model capable of covering fluctuated inlet charging temperature. In addition, the close charging system model enable prediction of partial working load of the chillers in the charging stratified TES tank.

b. The enhancement for the two-stage charging model was performed with absorption chillers and electric chillers to charge stratified TES tank in sequence. The simulations showed that the models also capable of solving temperature limitation in the absorption chillers. Thus, the model can be implemented for two-stage charging stratified TES tank using absorption and electric chillers.

iii. Comparison between the single and two-stage charging models in open and closes system was performed for evaluation of charging parameters, namely charging duration, empty and full capacities and temperature transition. Even though they have different features in the solution methods, the comparison results reveal similar parameters. This indicated that single and two-stage charging models for both systems could be implemented in the charging cycle of stratified TES tank.

5.2 Contribution of Thesis

The contribution of the thesis is summarized as follows:

i. The implementation of the single and two-stage charging models either using absorption chillers or combination with electric chillers could assist in shifting of energy usage from off-peak to on-peak demand.

ii. The implementation of two-stage charging models that used absorption chillers to complement electric chillers for charging of stratified TES tank could lead to higher energy utilization in district cooling plant. Waste heat from gas turbine can be effectively utilized by absorption chillers to charge the stratified TES tank.

iii. The single and two-stage charging models for both open and close systems can be used for assessing operation strategy in the charging of stratified TES tank.

iv. Development of single and two-stage charging models in close system that integrates the TES tank and chillers parameters, enable covering charging stratified TES tank under various operating condition. The models capable of prediction charging of stratified TES tank in partial working load of the chillers.

v. Developing of simulation charging models in open charging system by utilizing temperature distribution analysis, enabling determination of charging parameters exactly based on formulation. These findings reveal an improved method in characterization of temperature distribution for implementation in charging stratified TES tank.

5.3 Recommendations for Future Works

Future works related to this study could be undertaken on the SDR function as well as the charging models. Among the related works are as follows:

i. Temperature distribution parameters in stratified TES can be quantitatively characterized using SDR function. This function could be expanded for optimization of operation planning TES tank incorporated to district cooling plant.

ii. The single and two-stage charging models using open charging system capable of determination charging parameters exactly from formulation. Whereas in close charging system, the two models capable of covering parameters of the TES tank and the chillers. The models could be expanded for parametric analysis on various stratified TES tank configurations.

iii. The single and two-stage charging models have been developed using open and close system for charging of stratified TES tank. The two models could be implemented for discharging of the stratified TES tank.

iv. The charging models in close charging system have been developed based on one dimensional model. The models could be enhanced using two dimensional models.

REFERENCES

[1] ASHRAE, *HVAC Applications Handbook*, 1999.

[2] K. Thirakomen, "Co-generation and the New Era of Absorption Chiller," *[online]* www.ashraethailand.org, *21st* August 2010.

[3] N. L. Minh, "Modeling and Analysis of Cogeneration-based District Energy System," Mechanical Engineering, MSc Thesis: University of Western Ontario, 1996.

[4] D.P. Fiorino, "Case Study of a Large, Naturally Stratified Chilled-Water Thermal Storage Systems," *ASHRAE Transaction,* vol. 2, pp. 1161-1169, 1991.

[5] D.P. Gatley, "Successful Thermal Storage," *ASHRAE Transaction,* vol. IB, pp. 843-855, 1985.

[6] J.H. Horlock, *Cogeneration-combined Heat and Power (CHP): Thermodynamics and Economics*, Pergamon, Oxford, England, 1987.

[7] B.F. Kolanovski, *Small-scale Cogeneration Handbook*, 3rd ed., Fairmont Press Inc, 2008.

[8] S. Collin, "The Perfect Match: Combined Cycles and District Heating/Cooling," *Power*, vol. 135, pp. 117-120, 1991.

[9] Solar Energy Research Institute, "Economic Aspect of District Heating and Cooling," *Heating/Piping/Air Conditioning,* vol. 59, no. 9, pp. 47-56, 1987.

[10] C. Gochenour, "District Energy Trend: Opportunities and Issues," *World Bank Technical Paper no. 493,* 2001.

[11] M. Fallek, "Absorption Chillers for Cogeneration Applications," *ASHRAE Transactions SF 1B,* vol. 92 (2), pp. 321-327, 1986.

[12] P. Kumar and S. Devotta, "Study of an Absorption Refrigeration System for Simultaneous," *ASHRAE Transactions,* vol. 96, part 2, pp. 291-298, 1990.

[13] R.M. Tozer, "Absorption Refrigeration (Principles, Cycles and Applications to Cogeneration)," *Conference Cogeneration 92, Madrid 28-30,* pp. 170-175, 1992.

[14] R.M. Tozer and R.W. James, "Absorption Chillers Applied to CHP Systems," *Building Services Engineering Research and Technology,* vol. 16 (4), pp. 175–188, 1995.

[15] P.E. Hufford, "Absorption Chillers Maximize Cogeneration Value," *ASHRAE Transactions,* vol. 2(3), pp. 428-433, 1991.

[16] P.E. Hufford, "Absorption Chillers Improve Cogeneration Energy Efficiency," *ASHRAE Journals,* vol. 34, no. 3, pp. 46-53, 1992.

[17] Ainul Abedin, "Cogeneration: Balancing Heat Power Ratio," *ASHRAE Journals,* pp. 23-37, 2003.

[18] O.E. Ataer, *Storage of Thermal Energy, in Energy Storage Systems*: Encyclopedia of Life Support System (EOLSS), EOLSS Publishers, Oxford, UK, 2006.

[19] I. Dincer and M.A. Rosen, "Energetic, Environmental and Economic Aspects of Thermal Energy Storage System for Cooling Capacity," *Applied Thermal Engineering,* vol. 21, pp. 1105-1107, 2001.

[20] The Kaleida Graph Guide to Curve Fitting, *[Online]. Available:* http://www.synergy.com/Tools/curvefitting.pdf, 14th July 2010.

[21] ASHRAE, *Handbooks HVAC Applications*, 2003.

[22] E. Macki and G. Reeves , "Stratified Chilled Water Storage Design Guide," Electric Power Research Institute, 1988.

[23] Y.H. Zurigat and A.J. Ghajar, *Heat Transfer and Stratification in Sensible Heat Storage System, in Thermal energy Storage System and Applications,* 1st ed.: *Dincer and M Rosen*: John Willey and Sons, 2002.

[24] N. Tran and J.F. Kreider, "Field Measurement of Chilled Water Storage Thermal Performance," *ASHRAE,* vol. 95 (1), pp. 1106-1112, 1989.

[25] Electric Power Research Institute, *Commercial Cool Storage Design Guide* Springer-Verlag, 1987.

[26] M.W. Wildin, "Diffuser Design for Naturally Startified Thermal Storage," *ASHRAE Transaction,* vol. I, pp. 1094-1101, 1990.

[27] I. Dincer and M.A. Rosen, *Thermal Energy Storage Systems and Applications*, John Wiley and Sons Ltd., 2001.

[28] A. Musser, "Field Measured and Modelled Performance of Full Scale Cylindrical Stratified Chilled Water Storage Tanks," in *Graduate School* PhD Thesis: The Pennsylvania State University, 1998.

[29] S.K. Wang, *Handbook of Air Conditioning and Refrigeration*, 2nd ed. Mc. Graw Hill Company, 2000.

[30] Dorgan, E. Charles, Elleson and S. James, *Design Guide for Cool Thermal Storage*, Atlanta, GA, 1994.

[31] ASHRAE, *HVAC Applications Handbook*, 2007.

[32] M.W. Wildin and C.R. Truman, "Performance of Stratified Vertical Cylindrical Thermal Storage Tanks-Part 1: Scale Model Tank," *ASHRAE Transactions* vol. 95 (1), pp. 1086-1095, 1989.

[33] M.W. Wildin, E.I. Mackie and W.E. Harrison, "Thermal Storage Forum - Stratified Thermal Storage: A New/Old Technology," *ASHRAE Journal* vol. 32(4), pp. 29 - 39, 1990.

[34] A. Musser and W.P. Bahnfleth, "Evolution of Temperature Distributions in a Full-Scale Stratified Chilled-Water Storage Tank with Radial Diffusers," *ASHRAE Transaction,* vol. 104 (1), pp. 55-67, 1998.

[35] A. Musser and W.P. Bahnfleth, "Field-Measured Performance of Four Full-Scale Cylindrical Stratified Chilled-Water Thermal Storage Tanks," *ASHRAE Transaction* vol. 105 (2), pp. 218-230, 1998.

[36] W.P. Bahnfleth, Jing Song and J.M. Cimbala, "Measured and Modeled Charging of Stratified Chilled Water Thermal Storage Tank with Slotted Pipe Diffusers," *HVAC&R Research,* vol. 9, no. 4, pp. 467-491, 2003.

[37] A. Musser and W.P. Bahnfleth, "Parametric Study of Charging Inlet Diffuser Performance in Stratified Chilled Water Storage Tanks with Radial Diffusers: Part 2-Dimensional Analysis, Parametric Simulations and simplified Model Development," *HVAC&R Research,* vol. 7, no. 2, pp. 205-221, 2001.

[38] A. Musser and W.P. Bahnfleth, "Parametric Study of Charging Inlet Diffuser Performance in Stratified Chilled Water Storage Tanks with Radial Diffusers: Part 1-Model Development and Validation," *HVAC&R Research* vol. 7, no.1, pp. 31-49, 2001.

[39] Jing Song and WP Bahnfleth, "Parametric Study of Single-Pipe Diffusers in Stratified Chilled Water Storage Tanks," *HVAC&R Research,* vol. 10, no. 3, pp. 345-364, 2004.

[40] Jing Song and W.P. Bahnfleth, "Constant Flowrate Charging Characteristics of a Full-Scale Stratified Chilled Water Storage Tank with Double-Ring Slotted Pipe Diffusers," *Applied Thermal Engineering*, pp. 3067-3082, 2005.

[41] J.S. Caldwell and W.P. Bahnfleth, "Identification of Mixing Effects in Stratified Chilled-Water Storage Tanks by Analysis of Time Series Temperature Data," *ASHRAE Transaction,* vol. 104 (2), pp. 366-376, 1998.

[42] J.E.B. Nelson, A.R. Balakhrishnan and S. Srinivasa Murthy, "Experiments on Stratified Chilled-Water Tanks," *International Journal of Refrigeration,* vol. 22, pp. 216-234, 1999.

[43] M. Karim, "Performance Evaluation of A Stratified Chilled-Water Thermal Storage System," *World Academy of Science Engineering and Technology,* vol. 53, pp. 328-334, 2009.

[44] M.R.W Walmsley, M.J. Atkins and J. Riley, "Thermocline Management of Stratified Tanks for Thermal Storage," *Proceedings of 12th International Conference on Process Integration, Modelling and Optimisation for Energy Saving and Pollution Reduction. AIDIC, Rome, Italy; 10-13 May,* pp. 231-236, 2009.

[45] J. Yoo, M.W. Wildin and C.R. Truman, "Initial Formation of Thermocline in Stratified Thermal Storage Tanks," *ASHRAE Transaction,* vol. 92(2A), pp. 280-292, 1986.

[46] K. Homan, Sohn and Soo, "Thermal Performance of Stratified Chilled Water Storage Tanks," *HVAC&R Research,* vol. 2(2), pp. 158-170, 1996.

[47] W.P. Bahnfleth and A. Musser, "Thermal Performance of a Full Scale Stratified Chilled Water Storage Tank," *ASHRAE Transaction*, vol. 104(2), pp. 377-388, 1998.

[48] Joko Waluyo and M. Amin A. Majid, "Temperature Profile and Thermocline Thickness Evaluation of a Stratified Thermal Energy Storage Tank," *International Journal of Mechanical & Mechatronics Engineering IJMME-IJENS,* vol. 10, no. 1, pp. 7-12, 2010.

[49] M.A.A. Amin and Waluyo Joko, "Thermocline Thickness Evaluation on Stratified Thermal Energy Storage Tank of Co-generated District Cooling Plant," *Journal of Energy and Power Engineering,* vol. 4, no. 2, pp. 28-33, 2010.

[50] Joko Waluyo and M. Amin A. Majid, "Performance Evaluation of Stratified TES using Sigmoid Dose Response Function," *International Conference on Plant Equipment and Reliability, 15-17 June 2010, Kuala Lumpur, Malaysia,* 2010.

[51] J.E.B. Nelson, A.R Balakhrishnan and S. Srinivasa Murthy, "Parametric Studies on Thermally Startified Chilled Water Storage Systems," *Applied Thermal Engineering,* vol. 19, pp. 89-115, 1999.

[52] M.W. Wildin, "Flow Near the Inlet and Design Parameter for Stratified Chilled Water Storage," *ASME 91-HT-27,* 1991.

[53] C.F. Hess and C.W. Miller, "An Experimental and Numerical Study on the Effect of the Wall in a Cylindrical Exposure," *Solar Energy,* vol. 28, pp. 145-152, 1982.

[54] Jaluria Y and Gupta SK, "Decay of of Thermal Stratification in water Body for Solar Energy Storage," *Solar energy,* vol. 28, pp. 137-143, 1982.

[55] M.F. Lighstone, G.D. Raithby and K.G.T. Hollands, "Numerical Simulation of the Charging of Liquid Storage Tanks; Comparison with Experiment," *Journal of Solar Energy Engineering,* vol. 111, pp. 225-231, 1989.

[56] K. Homan, Sohn and Soo, "Thermal Performance of Stratified Chilled Water Storage Tanks " *HVAC&R Research,* vol. 2, pp. 158-170, 1996.

[57] Y.H. Zurigat, A.J Ghajar and P.M. Moretti, "A Comparison Study of One-Dimensional Models for Stratified Thermal Storage Tanks," *Transaction of ASME,* vol. 111, pp. 204-210, 1989.

[58] M. Wildin and C. Truman, "A Summary of Experience with Stratified Chilled Water Tanks " *ASHRAE Transactions* vol. 91 (1b), pp. 956-976, 1985.

[59] Y. Jaluria and K.E. Torrance, *Computational Heat Transfer*, 2nd ed., Taylor and Francis, 2003.

[60] R.J. Gross, "An Experimental Study of Single Medium Thermocline Thermal Energy Storage," *ASME Paper 82-HT-53,* 1982.

[61] E.M. Kleinback, W.A. Beckman and S.A. Klein, "Performance Study of One-Dimensional Moels for Stratified Thermal Storage Tanks," *Solar Energy,* vol. 50, pp. 155-166, 1993.

[62] V. Badescu, "Optimal Operation of Thermal Energy Storage Units Based on Stratified and Fully Mixed Water Tanks," *Applied Thermal Engineering 24,* pp. 2101-2116, 2004.

[63] S.P. Gretarsson, C.O. Pedersen and R.K. Strand, "Development of Fundamentally Based Stratified Thermal Storage Tank Model for Energy Calculations," *ASHRAE Transaction,* vol. 100, pp. 1213-1220, 1994.

[64] J. Devore and N. Farnum, *Applied Statistics for Engineers and Scientist*, 2nd ed., Thomson Learning Inc, 2005.

[65] Y. Ji and K.O. Homan, "On Simplified Models for the Rate and Time Dependent Performance of Stratified Thermal Storage," *Transaction of ASME,* vol. 129, pp. 214-222, 2007.

[66] Y. Jaluria, *Design and Optimization of Thermal Systems*: CRC Press, 2008.

[67] F.P. Incropera and D.P. Dewitt, *Introduction to Heat Transfer*: John Wiley and Sons, 2002.

[68] N.M. Al-Najem N.M. El-Refaee, "A Numerical Study for the Prediction of Turbulent Mixing Factor in Thermal Storage Tank," *Applied Thermal Engineering,* vol. 17, no. 12, pp. 1173-1181, 1997.

[69] M.N. Ozisick, *Heat Conduction*, 2nd ed., John Wiley and Sons, Inc., 1993.

[70] S.C. Chapra and R.P. Canale, *Numerical Methods for Engineers*, 6th ed., Mc Graw Hill International Edition, 2009.

[71] J.P Holman, *Heat Transfer*, 10th ed., Mc Graw Hill Higher Education, 2009.

[72] J.C. Tannehill, D.A. Anderson and R.H. Pletcher, *Computational Fluid Mechanics and Heat Transfer*, 2nd ed., Taylor and Francis, 2003.

[73] C.F. Gerald and P.O. Wheatly, *Applied Numerical Analysis,* 7th ed., Addison-Wesley Publishing Company, 2004.

[74] M.N. Ozisik, *Finite Difference Methods in Heat Transfer*, CRC Press Inc, 1994.

[75] J. Waluyo, M. Amin A. Majid and C. Rangkuti, "Analysis of Temperature Distribution of Chilled-Water Thermal Storage Tank," *National Postgraduate*

Conference, Universiti Teknologi PETRONAS, 25-26 March 2009, pp. 1-5, 2009.

[76] F.J.Oppel, A.J. Ghajjar and P.M. Moretti, "Computer Simulation of Stratified Heat Storage," *Applied Energy,* vol. 23, pp. 293-, 1986.

[77] F.J. Oppel, A.J. Ghajjar and P.M. Moretti, "A Numerical and Experiment Study of Stratified Thermal Storage," *ASHRAE Transaction,* vol. 92, no. 2, pp. 293-309, 1986.

[78] Clint N. Dawson and Todd F. Dupont, "Explicit/implicit Conservative Domain Decomposition Procedures for Parabolic Problems Based on Block-Centered Finite Differences," *SIAM Journal on Numerical Analysis,* vol. 31. no. 4, pp. 1045-1061, 1994.

[79] M.W. Wildin and C.R. Truman, "Evaluation of Stratified Chilled Water Storage Technique," Electric Power Research Institute Report, 1985.

[80] Y.H. Zurigat, A.J. Ghajar and P.M. Moretti, "Stratified Thermal Storage Inlet Mixing Characterization," *Applied Energy,* vol. 30, pp. 99-111, 1988.

[81] P.P. Votsis, S.A. Tasson, D.R. Wilson and C.J. Marquand, "Experimental and Theoretical of Mixed and Stratified Water Storage Tanks," *Proceedings of the Institution of Mechanical Engineers, Part-C Journal of Mechanical Engineering Science*, vol. 202, pp. 187-193, 1988.

[82] M.W. Wildin, "Performance of Stratified Vertical Cylindrical Thermal Storage tank, Part 2; Prototype Tank," *ASHRAE Transaction 95(1)*, pp. 1096-1105, 1989.

[83] W.C. Whitman, W.M. Johnson and J. Tomczyk, *Refrigeration and Air Conditioning Technology,* 5th ed.,Thompson Delmar Learning 2005.

[84] A.D. Althouse, C.H. Turnquist and A.F. Bracciano, *Modern Refrigeration and Air Conditioning*, Goodheart-Willcox, 2004.

[85] I. Dincer, *Refrigeration Systems and Applications*: John Wiley and Sons, 2003.

[86] H.R. Colen, *HVAC System Evaluation*. New York: RS Means, 1990.

[87] J.F. Kreider, *Handbook of Heating, Ventilating and Air Conditioning*: CRC Press, 2001.

[88] E.A. Koeppel, "The Modeling, Performance and Optimal Control of Commercial Absorption Chillers," Mechanical Engineering Department, MSc thesis: University of Wisconsin, 1994.

[89] ASHRAE, *ASHRAE Refrigeration Handbook*, 2002.

[90] K.E. Herold, R. Radermacher and S.A. Klein, *Absorption Chillers and Heat Pumps*, CRC Press Inc., 1996.

[91] M. Izquierdo, M. Venegas, P. Rodriquez and A. Leucona, "Crystallization as a Limit to Develop Solar Air-Cooled LiBr-H_2O Absorption System using Low-Grade Heat," *Solar Energy Materials and Solar Cells,* vol. 81, pp. 205-216, 2004.

[92] G.A. Florides, S.A. Kalogirou, S.A. Tassou and L.C. Wrobel, "Design and Construction of a LiBr-Water Absorption Machine," *Energy Conversion and Management,* vol. 44, pp. 483-2508, 2003.

[93] Xiaohong Liao and R. Radermacher, "Absorption chiller crystallization control strategies for integrated cooling heating and power systems," *International Journal of Refrigeration*, vol. 30, pp. 904-911, 2007.

[94] S.C. Sugarman, *HVAC Fundamentals*,Fairmont Press Inc, 2005.

[95] A.A. Bell, *HVAC Equations, Data and Rule of Thumbs*, 2nd ed., Mc Graw Hill, 2008.

[96] F. Kreith, *Handbook of Thermal Engineering*: Springer, 2000.

[97] C. Cecchini and F. Marshal, "Simulation of Refrigerating and Air Conditioning Equipment Based on Experiment Data," *ASHRAE Transaction,* vol. 97, pp. 388-393, 1991.

[98] J.M. Gordon and K.C. Ng, "Thermodynamic Modeling for Reciprocating Chillers," *Journal of Applied Physics,* vol. 75 (6), pp. 2769-2774, 1994.

[99] R.K. Strand, C.O. Pederson and G.N. Coleman, "Development of Direct and Indirect Ice-Storage for Energy Calculations," *ASHRAE Transaction,* vol. 100, part. 1, pp. 1230-1244, 1994.

[100] L.E. Figuera, M.A. Madina, M. Cathey and D.W. Nutre, "Modification and Validation of a Universal Thermodynamic Chiller Model Used to Evaluate the Performance of Water Cooled Centrifugal Chillers," in *The 11th Symposium on Improving Building Systems in Hot and Humid Climates, Texas*, pp. 57-65,1998.

[101] D.I. Jahing, D.T. Reindl and S.A. Klein, "A Semi Empirical Method for Representing Domestic Refrigerator/Freezer Compressor Calorimeter Test Data," *ASHRAE Transaction,* vol. 106 (2), pp. 122-130, 2000.

[102] B.D. McIntosh, J.W. Mirchell and A. Beckman, "Fault Detection and Diagnosis Part (I), Model Development and Application," *ASHRAE Transaction,* vol. 106 (2), pp. 268-282, 2000.

[103] G. Grossman and Michelson, "A Modular Computer Simulation of Absorption Systems," *ASHRAE Transaction,* vol. 91 (2B), pp. 1808-1827, 1985.

[104] G. Grossman, K. Gommed and D. Gadoth, "Computer Model for Simulation of Absorption Systems in Flexible and Modular Form," *ASHRAE Transaction*, vol. 93 (2), pp. 1590-1598, 1987.

[105] K. Gommed and G. Grossman, "Performance of Staged Absorption Heat Pumps: Water-Lithium Bromide Systems," *ASHRAE Transaction,* vol. 96 (1), pp. 1590-1598, 1990.

[106] G. Grossman, M. Wilk and R.C. DeVault, "Simulation and Performance Analysis of Triple-Effect Absorption Chiller Cycles," *ASHRAE Transaction*, vol. 100, part.1, pp. 452-462, 1994.

[107] J.S. Seewald and H. Perez-Blanco, "Simple Model for Calculating Performance of Lithium Bromide/Water Coil Absorber," *ASHRAE Transaction,* vol. 100, part. 2, pp. 318-328, 1999.

[108] H.M. Hellman and F.F. Ziegler, "Simple Absorption Heat Pump Modules for System Simulation Program," *ASHRAE Transaction,* vol. 105, part. 1, pp. 780-787, 1999.

[109] Joko Waluyo, M Amin A Majid and C. Rangkuti, "Simulation of Generated Chilled Water of a Cogeneration Plant," *International Conference on Plant Equipment and Reliability, 27-28 March 2008, Selangor, Malaysia,* 2008.

[110] ASHRAE, *ASHRAE Fundamental Handbooks*, 2005.

[111] N.V. Suryanarayana and O Arici, *Design and Simulation of Thermal Systems*, Mc. Graw Hill, 2002.

[112] S.L. Arlinghaus, *Practical Handbook of Curve Fitting*: CRC Press, 1994.

[113] J.R. Hauser, *Numerical Methods for Nonlinear Engineering Models*: Springer, 2009.

[114] E.N. Virtanen, *Applied Mathematical Modeling*, Nova Publishers, 2008.

[115] Systat Software Inc., "Regression Equation Library," in *SIGMAPLOT User's Guide*, Systat Software Inc., 2008.

[116] G.A.F. Seber and C.J. Wild, *Non Linear Regression,* John Wiley and Sons, 2003.

[117] D.M. Bates and D.G. Watts, *Non Linear Regression Analysis and Its Applications*, 2nd ed., John Wiley and Sons Inc., 2007.

[118] D. Erdman and M. Little, *Nonlinear Regression Analysis and Nonlinear Simulation Models*, *SAS Institute Inc.,* 2004

[119] Systat Software, *SigmaPlot 11 User's Guide*, Systat Software Inc.2008.

PUBLICATIONS

Conference Papers:

1. M. Amin A Majid, C. Rangkuti, J. Waluyo, "Operating Modes of a Thermal Energy Storage System of a Gas District Cooling Plant," Conference on Applications and Design in Mechanical Engineering, 25-26 October 2007, Kangar, Perlis, Malaysia.
2. J. Waluyo, M. Amin A Majid and C. Rangkuti, "Simulation of Generated Chilled Water of Cogeneration Plant," International Conference on Plant Equipment and Reliability, 27-28 March 2008, Selangor, Malaysia.
3. J. Waluyo, M. Amin A Majid and C. Rangkuti, "Analysis of Temperature Distribution of Chilled-Water Thermal Storage Tank," National Postgraduate Conference, 25-26 March 2009, Universiti Teknologi PETRONAS, Malaysia.
4. J. Waluyo and M. Amin A Majid, "Performance Evaluation of Stratified TES using Sigmoid Dose Response Function," International Conference on Plant Equipment and Reliability, 15-17 June 2010, Kuala Lumpur, Malaysia.

International Journals:

1. M Amin A Majid and J. Waluyo, "Thermocline Thickness Evaluation on Stratified Thermal Energy Storage Tank of Co-generated District Cooling Plant," *Journal of Energy and Power Engineering*, vol. 4, no. 2, Serial no: 27, ISSN 1934-8975, 2010.
2. Joko Waluyo and M Amin A Majid, "Temperature and Thermocline Thickness Evaluation of a Stratified Thermal Energy Storage," *International Journal of Mechanical & Mechatronics Engineering*, vol. 10, no: 01, ISSN 2077-1207, 2010.
3. Joko Waluyo and M Amin A Majid, "Performance Evaluation of Stratified TES using Sigmoid Dose Response Function," *Journal of Applied Science,* ISSN 1812-5654/DOI: 10.392/jas.2011, 2011.

4. J. Waluyo, M Amin A Majid and S. Anwar, "Development of Simulation Model for Charging Stratified TES Tank utilizing Temperature Distribution Analysis," *submitted to Journal of Energy Conversion and Management, Elsevier,* 2010.
5. J. Waluyo, M Amin A Majid and S. Anwar, "Two-stage Simulation Model for Charging Stratified TES Tank, " *submitted to Journal of Energy Conversion and Management, Elsevier,* 2010.

APPENDICES

APPENDIX A

Operating Temperature Data of TES District Cooling
Universiti Teknologi PETRONAS

A1. Data set IA
September 9, 2008 ; flow rate 393 m^3/hr.

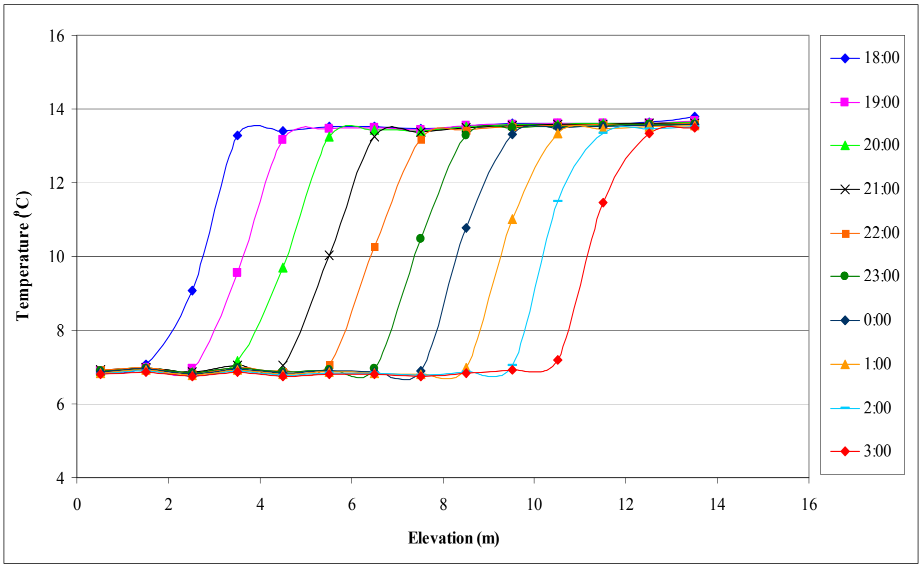

A2. Data set IB
September 11, 2008 ; flow rate 393 m^3/hr.

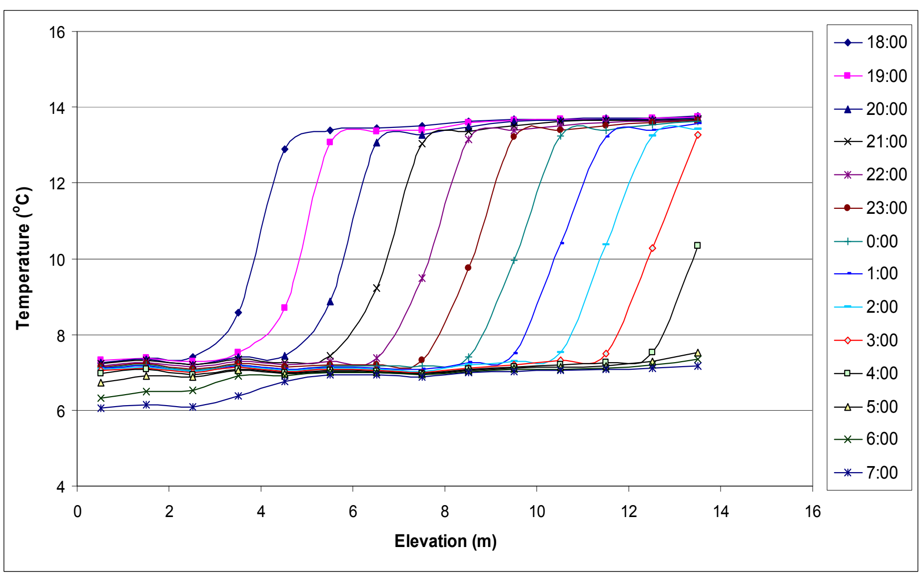

A3. Data set IC
September 19, 2008 ; flow rate 393 m^3/hr.

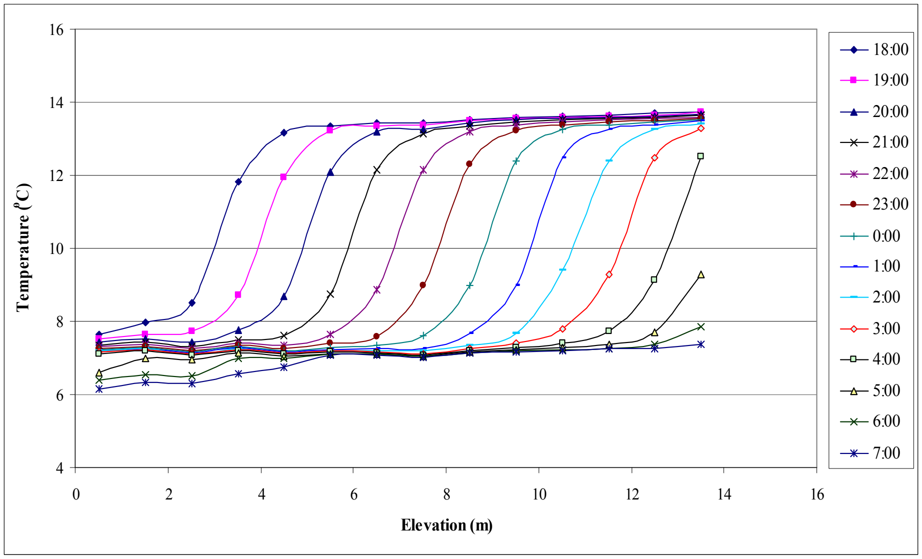

A4. Data set IIA
May 8, 2009 ; flow rate 524 m^3/hr.

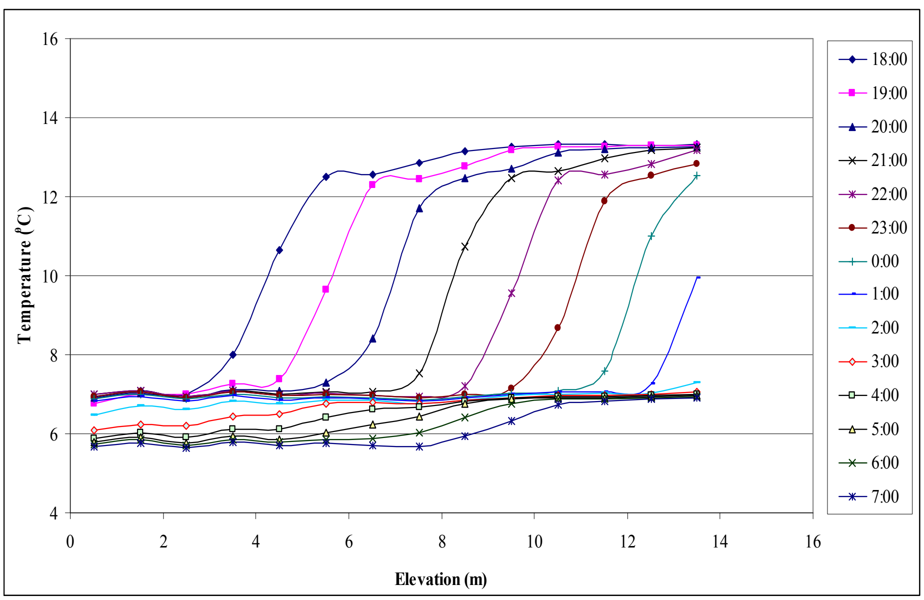

A5. Data set IIB

June 22, 2009 ; flow rate 524 m^3/hr.

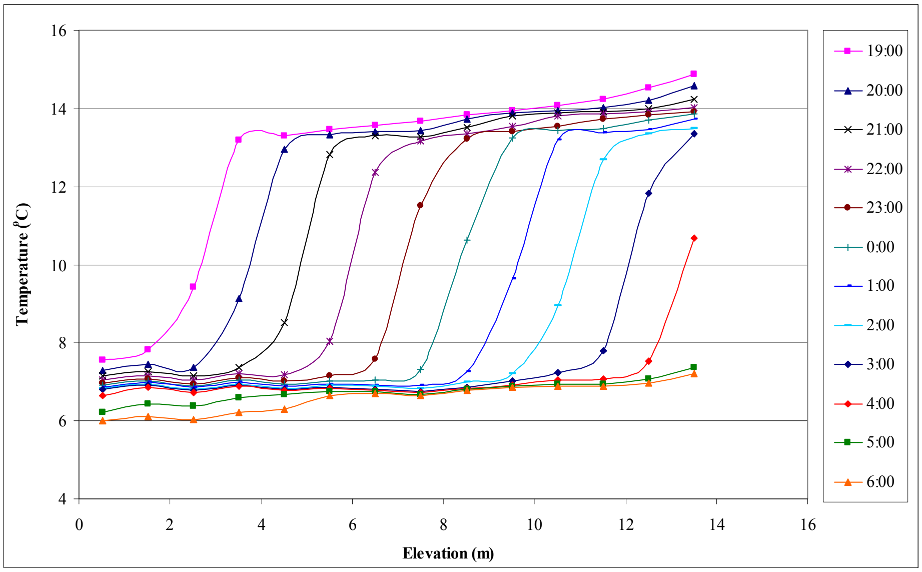

A6. Data set IIC

June 24, 2009 ; flow rate 524 m^3/hr.

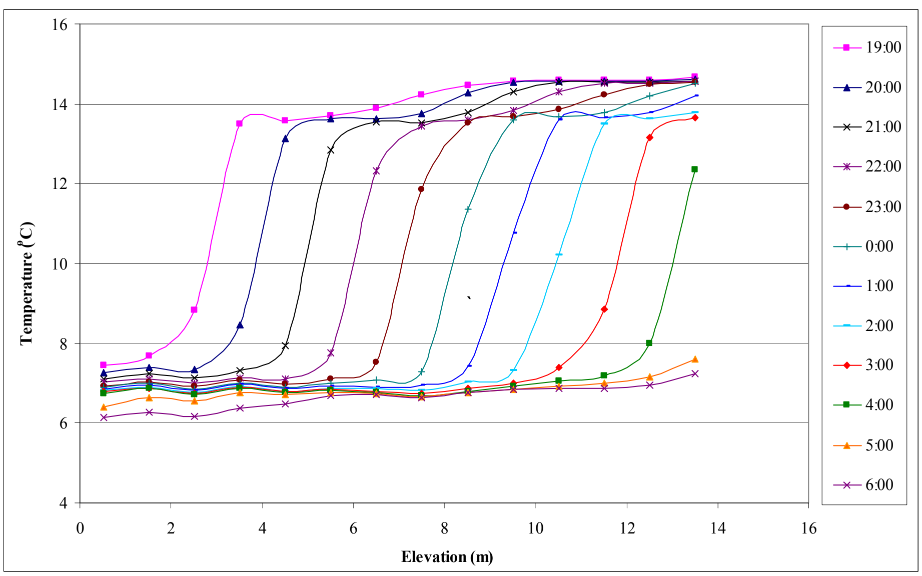

APPENDIX B
Selection of Effective Diffussivity (ε_{eff}) for Single Stage Charging Model Type (II)

B1. Effective Diffussivity = 1
Data set IA, flow rate 393 m^3/hr.

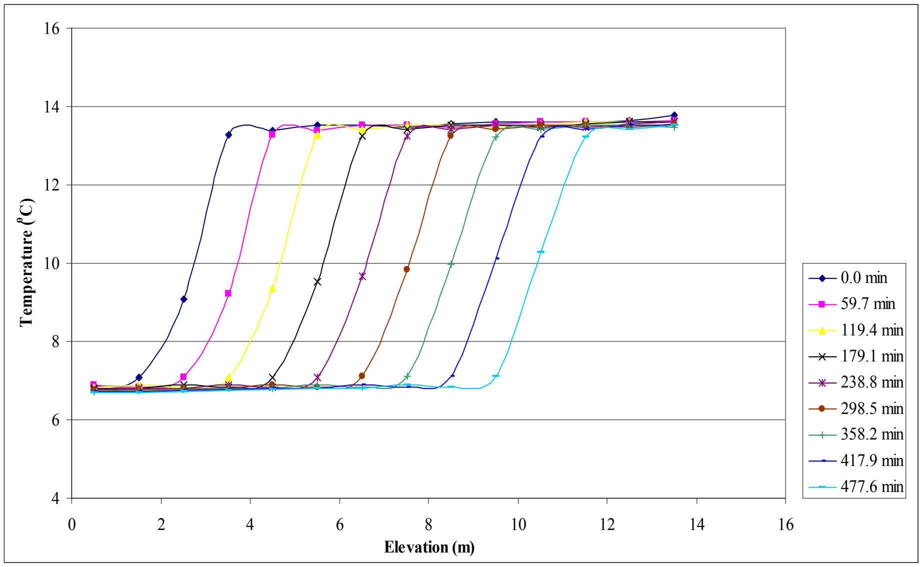

B2. Effective Diffussivity = 10
Data set IA, flow rate 393 m^3/hr.

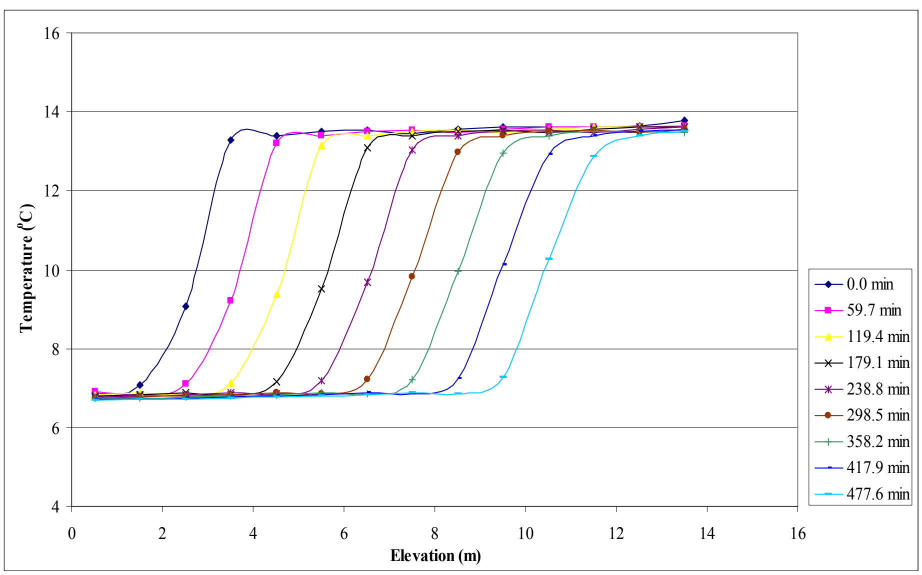

B3. Effective Diffussivity = 50
Data set IA, flow rate 393 m^3/hr.

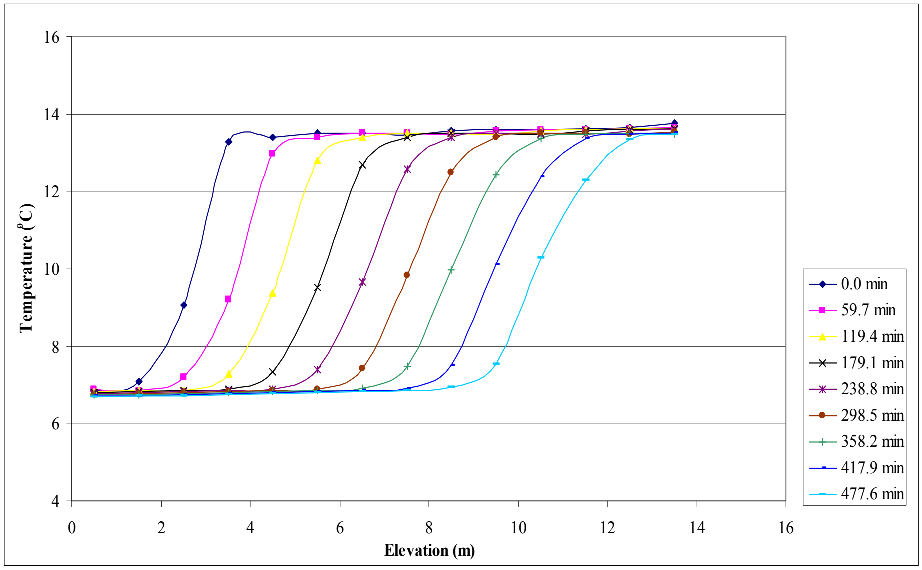

B4. Effective Diffussivity = 100
Data set IA, flow rate 393 m^3/hr.

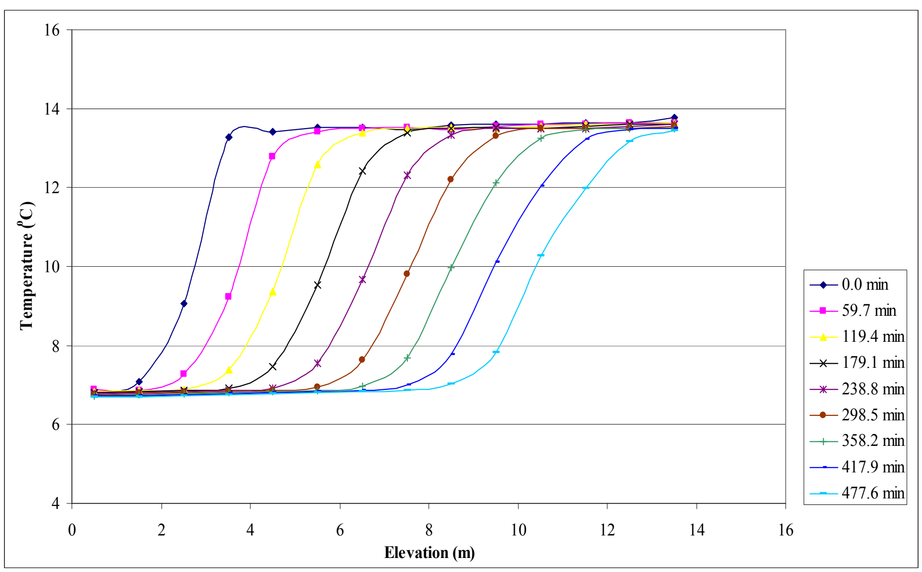

B5. Effective Diffussivity = 200
Data set IA, flow rate 393 m^3/hr.

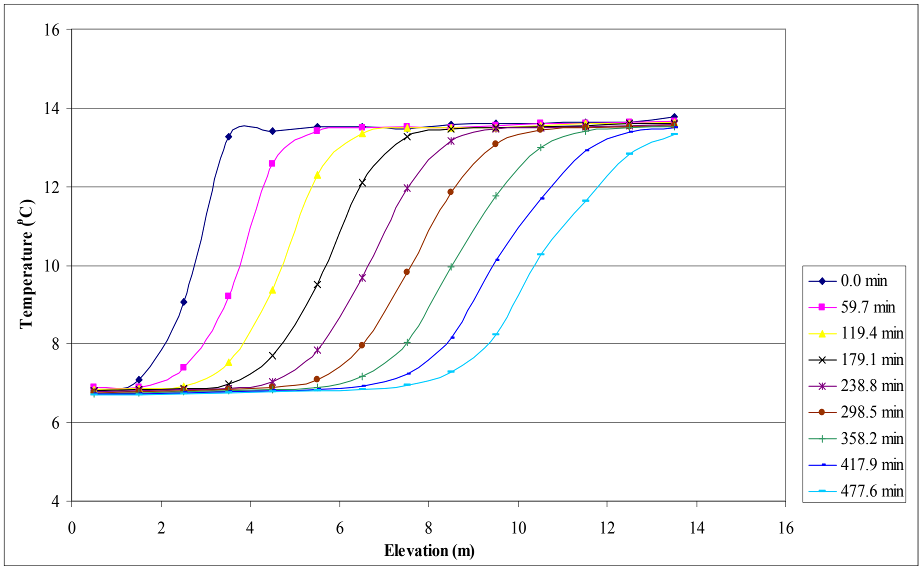

B6. Effective Diffussivity = 250
Data set IA, flow rate 393 m^3/hr.

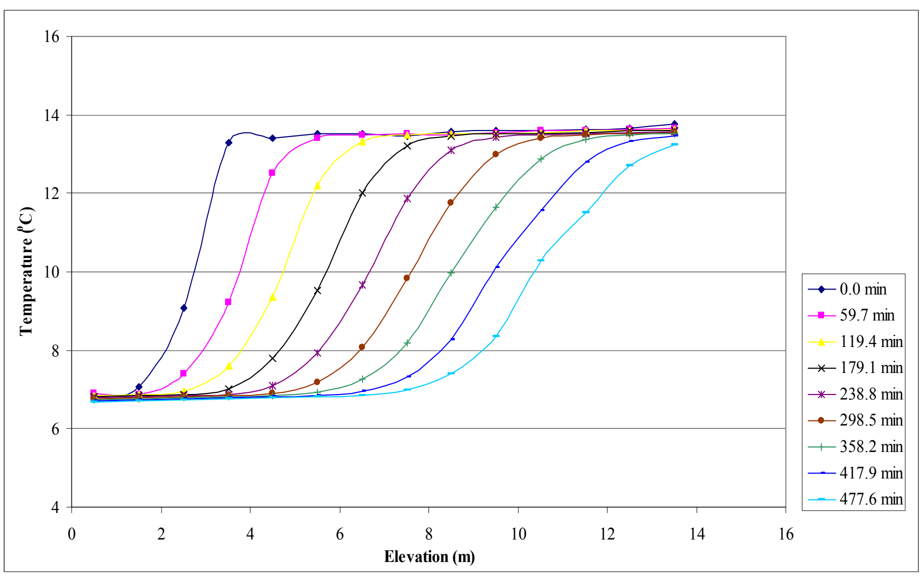

APPENDIX C

Temperature Distribution Verification in Single Stage Charging Model Type (II)

C.1 Verification (Data set IC)

C1.1 SDR fitting Data set IC

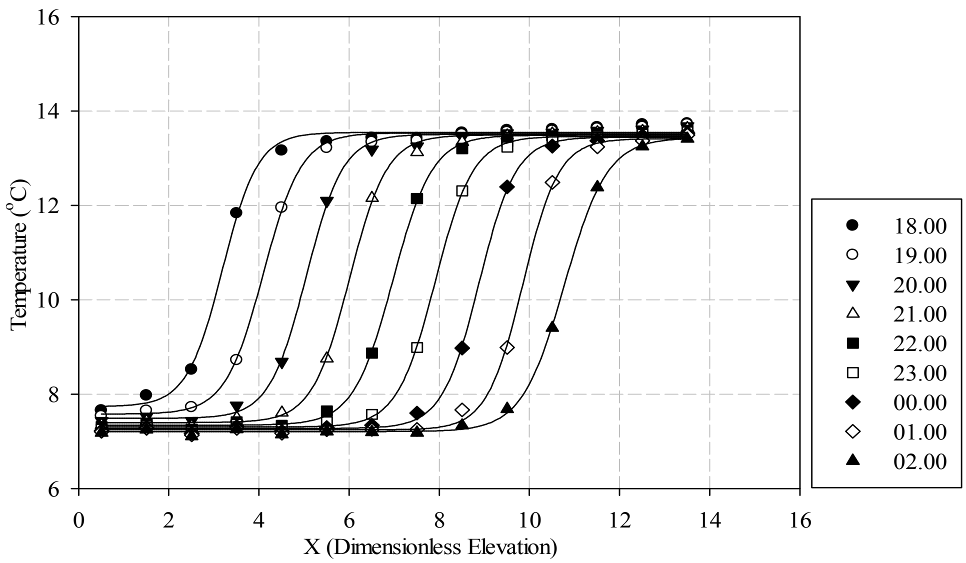

C.1.2 SDR Fitting Verification Data set IC

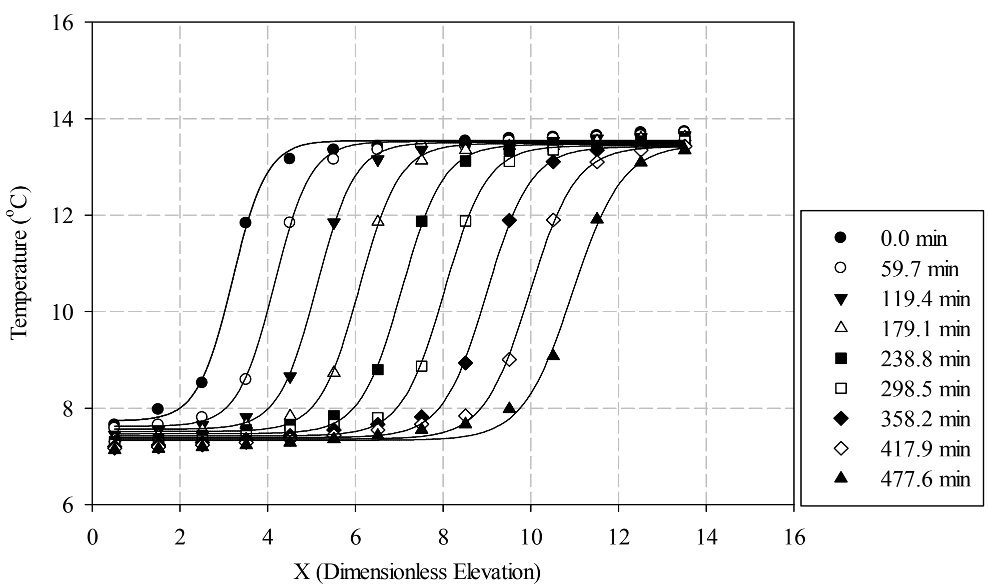

C.1.3 Evaluation criteria 1

R^2 verification (Data set IC)

Data	to	Model	R^2
Chrg. Hrs.		Chrg. time (min)	
18:00	-	0.0	1.000
19:00	-	59.7	0.999
20:00	-	119.4	0.999
21:00	-	179.1	0.999
22:00	-	238.8	0.998
23:00	-	298.5	0.997
0:00	-	358.2	0.997
1:00	-	417.9	0.995
2:00	-	477.6	0.993

C1.4 Evaluation criteria 2

C1.4.1 Comparison of parameters T_c and T_h (Data set IC)

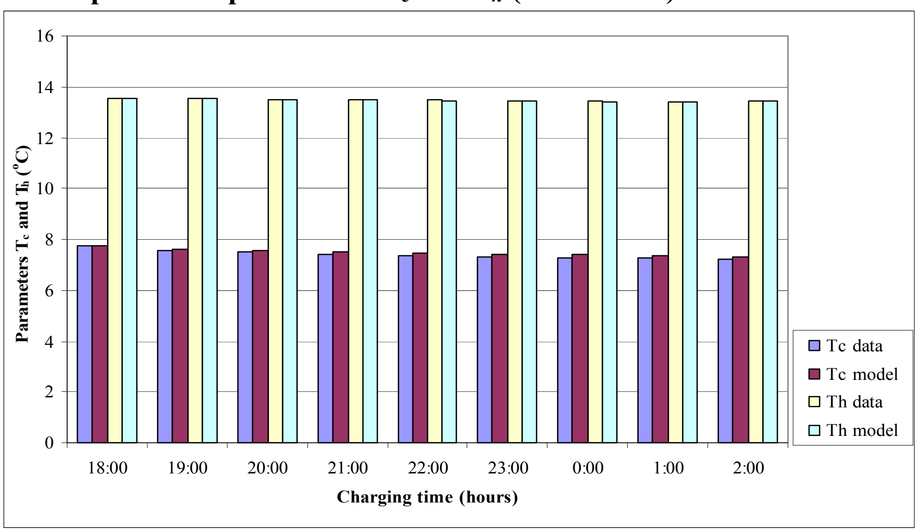

C.1.4.2 Comparison of parameters *C* and *S* (Data set IC)

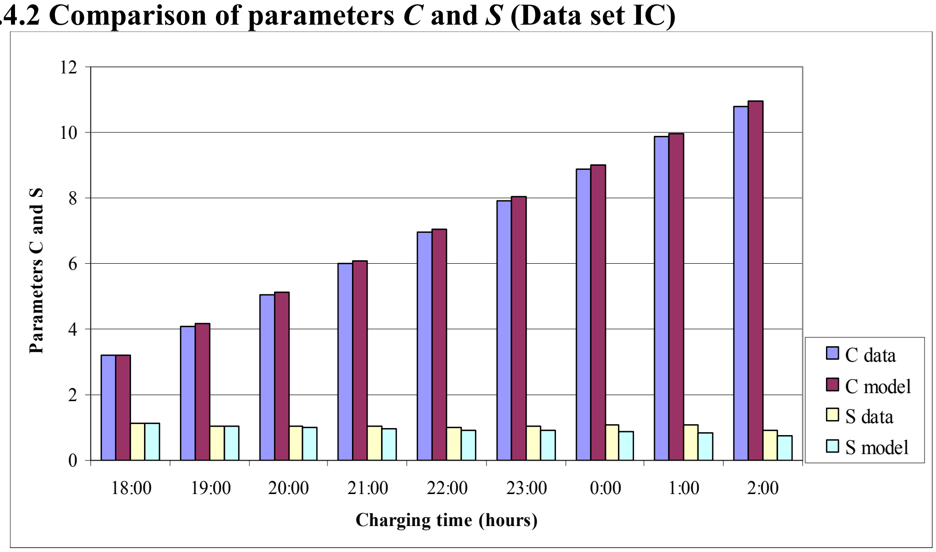

C.1.4.3 Percentage Deviation of SDR Parameters (Data set IC)

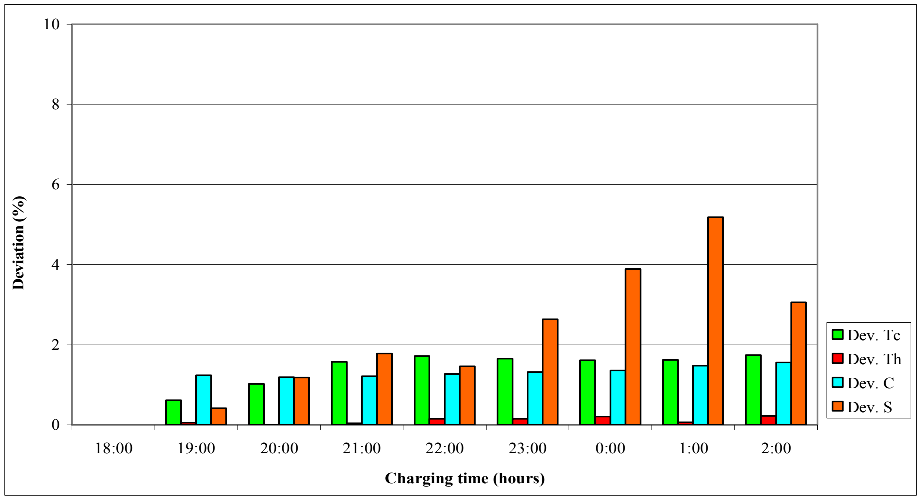

C.1.5 Evaluation criteria 3
Statistical Test (Data set IC)

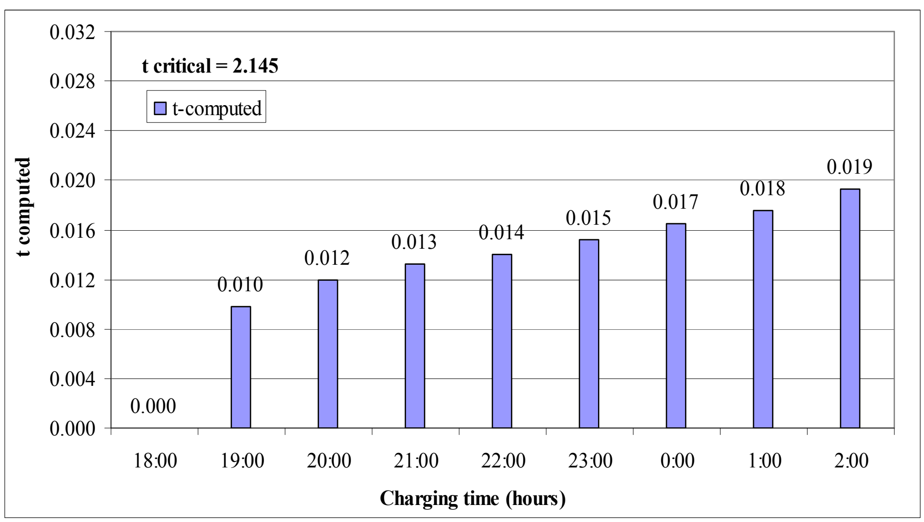

C.2 Verification: Data set IIB

C.2.1 SDR Fitting Data set IIB

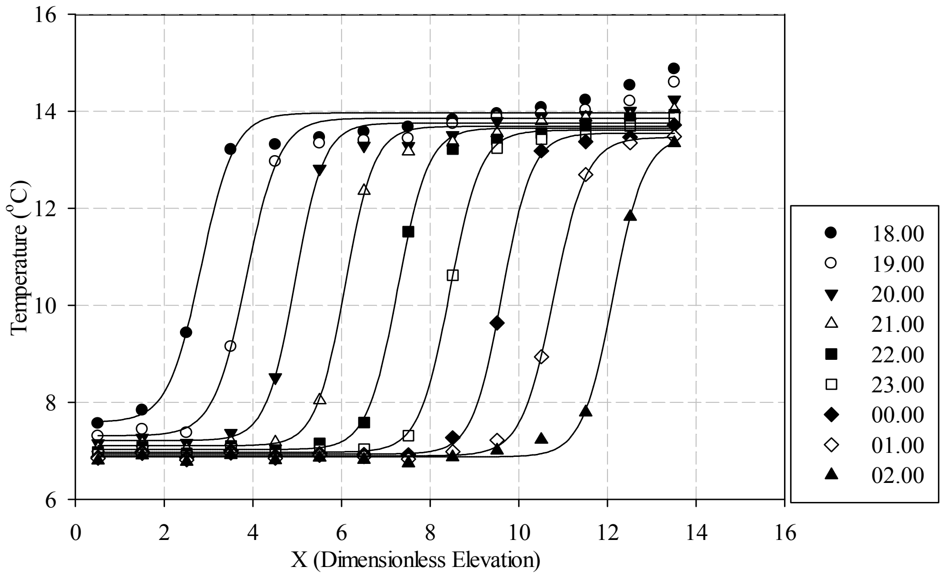

C.2.2 SDR Fitting Verification (Data set IIB)

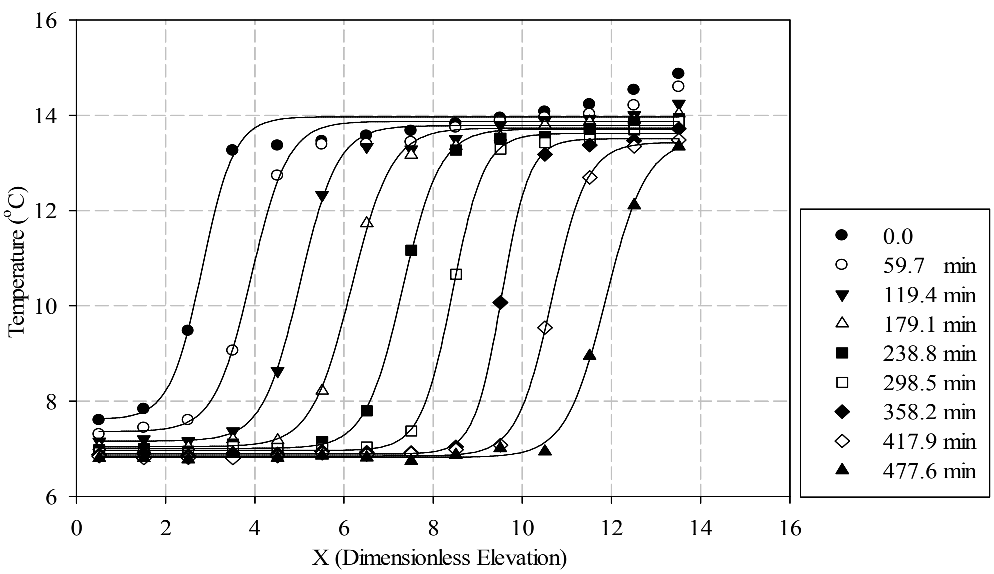

C.2.3 Evaluation criteria 1

R^2 verification (Data set IIB)

Data Chrg. Hrs.	to	Model Chrg. time (min)	R^2
18:00	-	0.0	1.000
19:00	-	59.7	0.999
20:00	-	119.4	0.996
21:00	-	179.1	0.996
22:00	-	238.8	0.995
23:00	-	298.5	0.994
0:00	-	358.2	0.992
1:00	-	417.9	0.992
2:00	-	477.6	0.989

C2.4 Evaluation criteria 2

C2.4.1 Comparison of parameters T_c and T_h (Data set IIB)

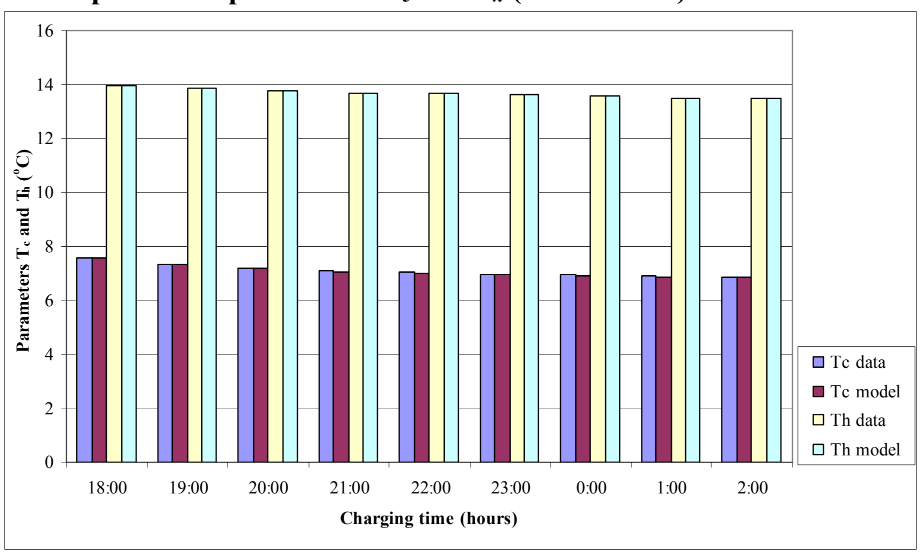

C.2.4.2 Comparison of parameters *C* and *S* (Data set IIB)

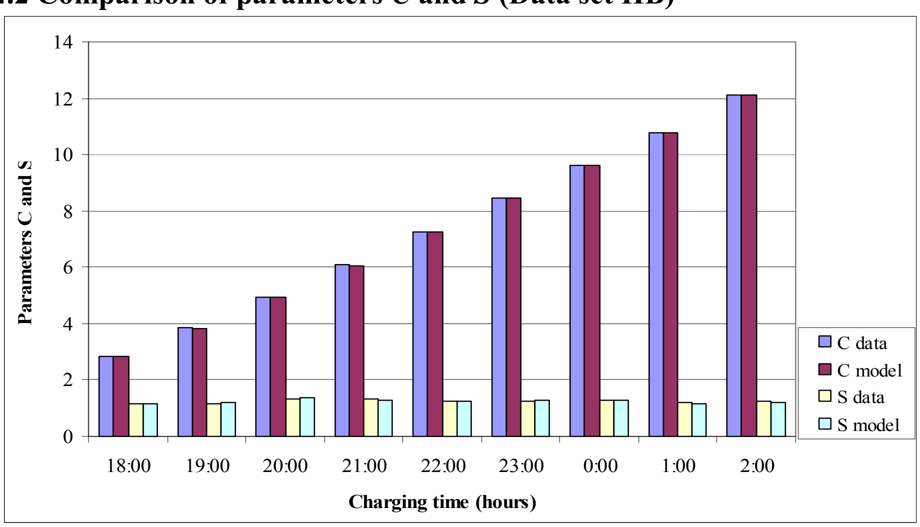

C.2.4.3 Percentage Deviation of SDR Parameters (Data IIB)

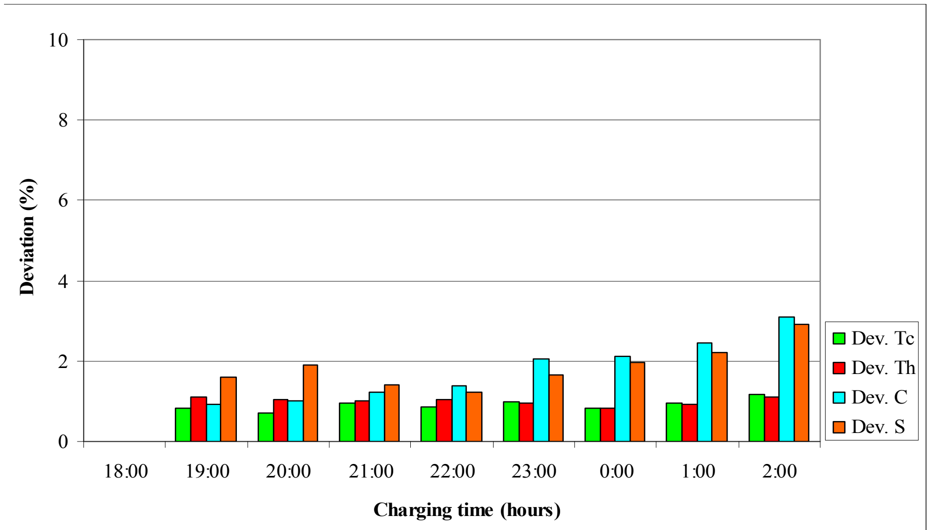

C.2.5 Evaluation criteria 3
Statistical Test (Data set IIB)

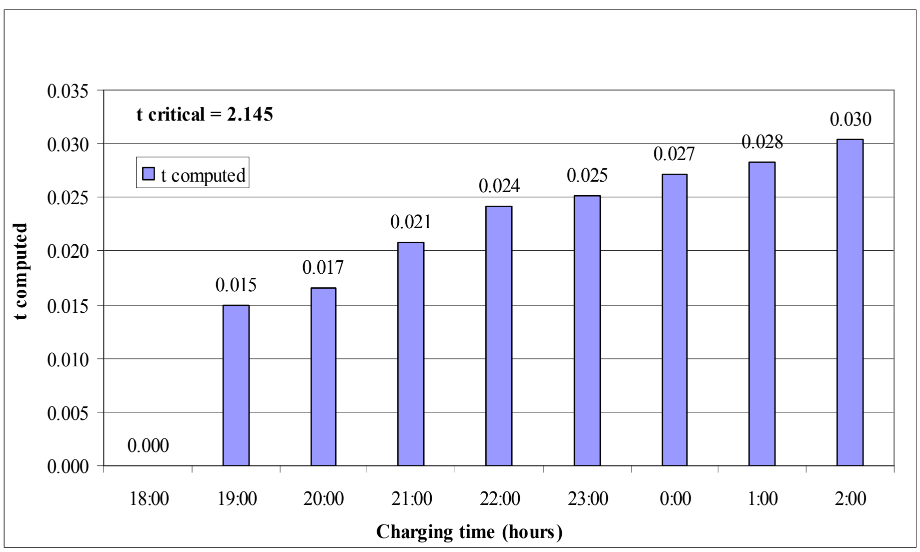

C.3 Verification: Data set IIC

C.3.1 SDR Fitting Data set IIC

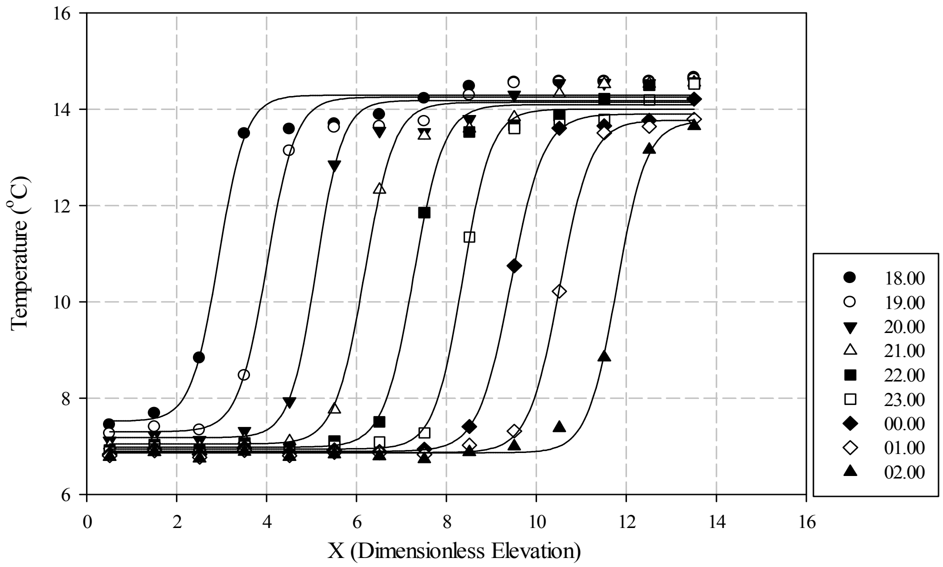

C.3.2 SDR Fitting Verification (Data set IIC)

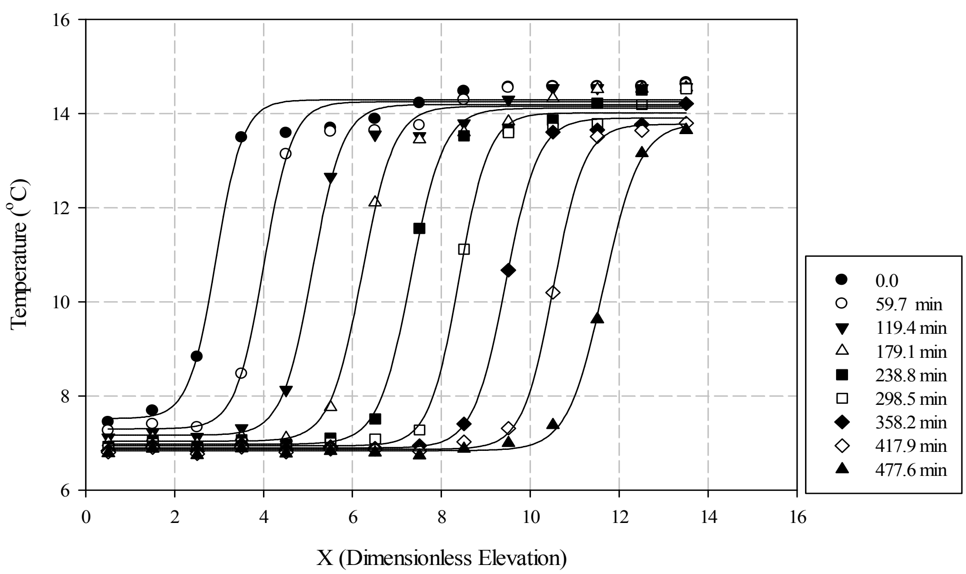

C.3.3 Evaluation criteria 1

R^2 verification (Data set II C)

Data	to	Model	R^2
Chrg. Hrs.		Chrg. time (min)	
18:00	-	0.0	1.000
19:00	-	59.7	0.998
20:00	-	119.4	0.983
21:00	-	179.1	0.961
22:00	-	238.8	0.960
23:00	-	298.5	0.950
0:00	-	358.2	0.940
0:01	-	417.9	0.936
0:02	-	477.6	0.932

C3.4 Evaluation criteria 2

C3.4.1 Comparison of parameters T_c and T_h (Data set II C)

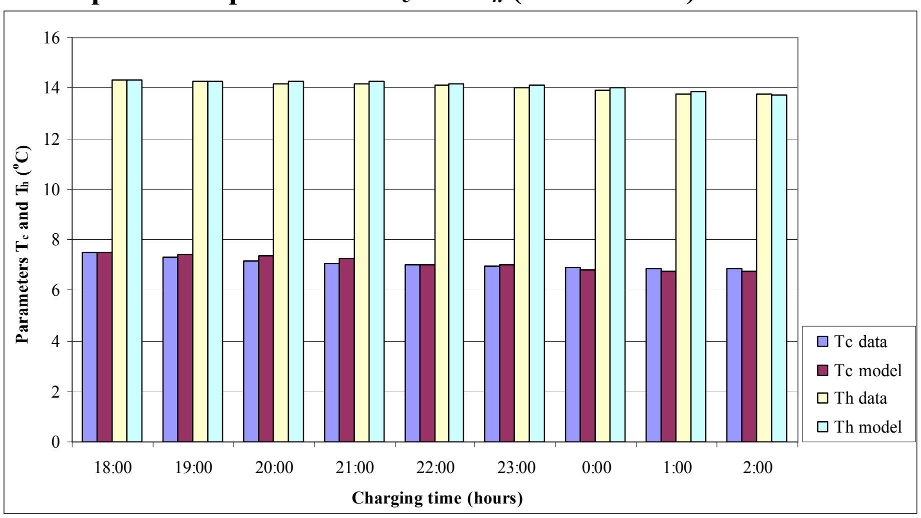

C.3.4.2 Comparison of parameters *C* and *S* (Data set IIC)

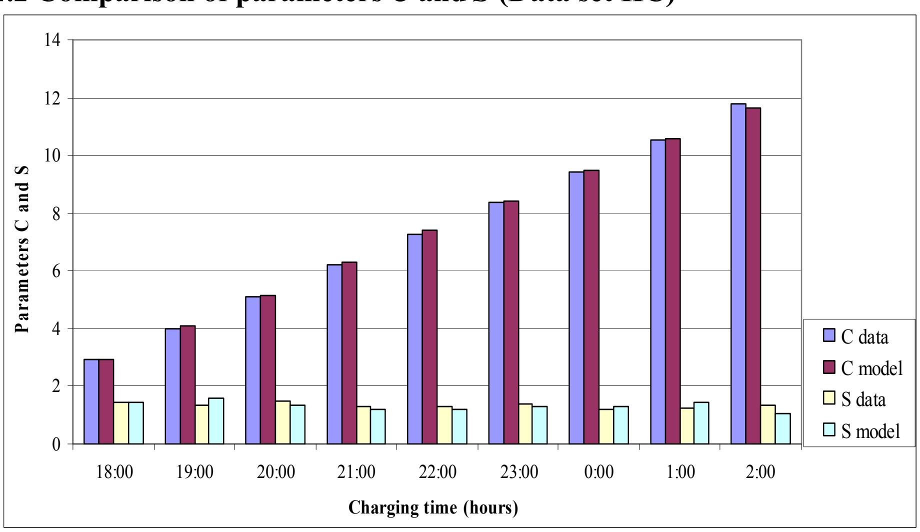

C.3.4.3 Percentage Deviation of SDR Parameters (Data IIC)

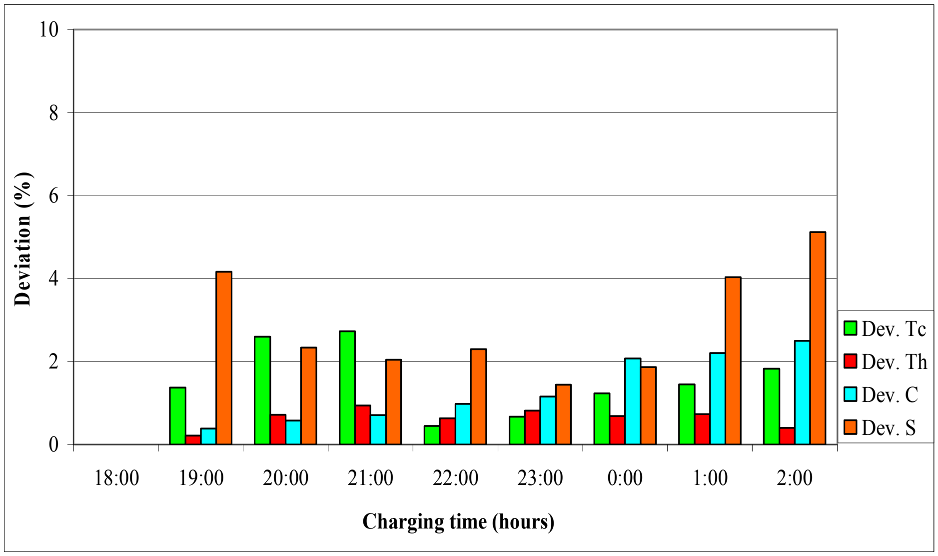

C.3.5 Evaluation criteria 3
Statistical Test (Data set IIC)

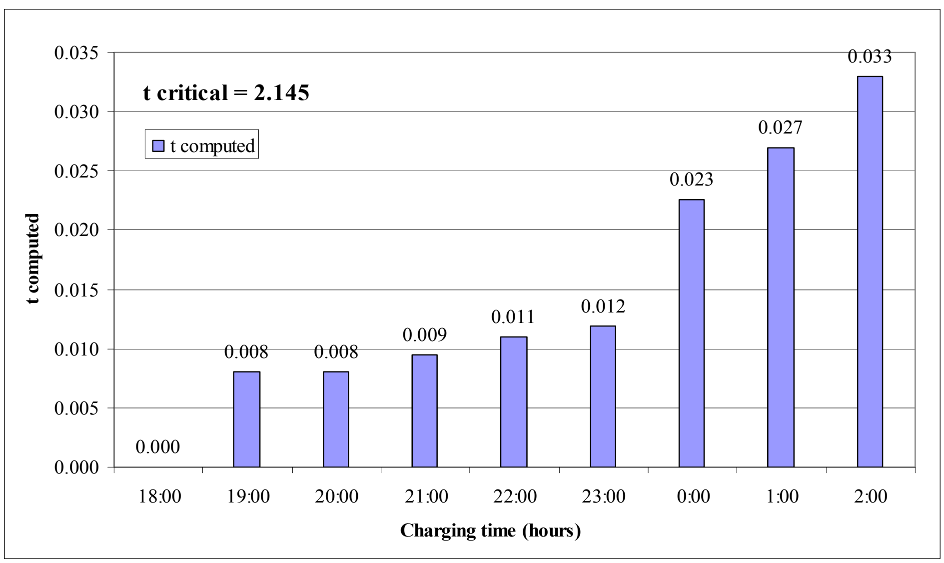

APPENDIX D
Partial Working Load Analysis of Two Stages Charging Model Type (II)
Simulation Cases E2, F2 and G2

D.1 Inlet charging temperature of simulation cases E2, F2 and G2:

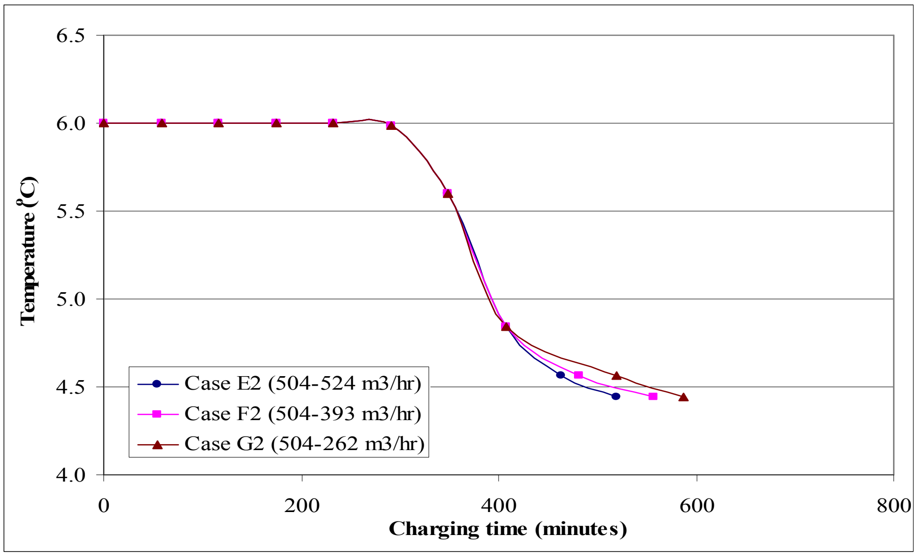

D.2 Outlet Temperature of Simulation Cases E2, F2 and G2:

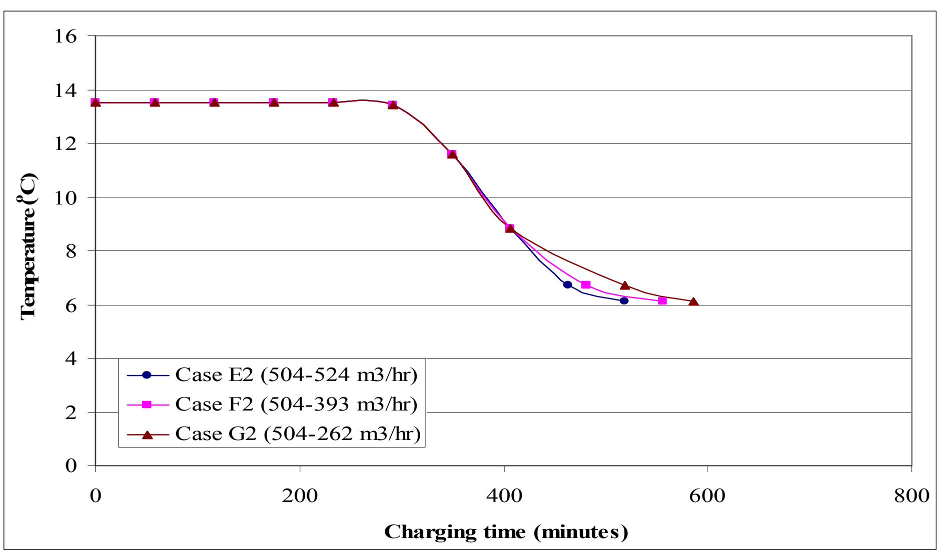

D.3. Mixing Temperature of Simulation Cases E2, F2 and G2:

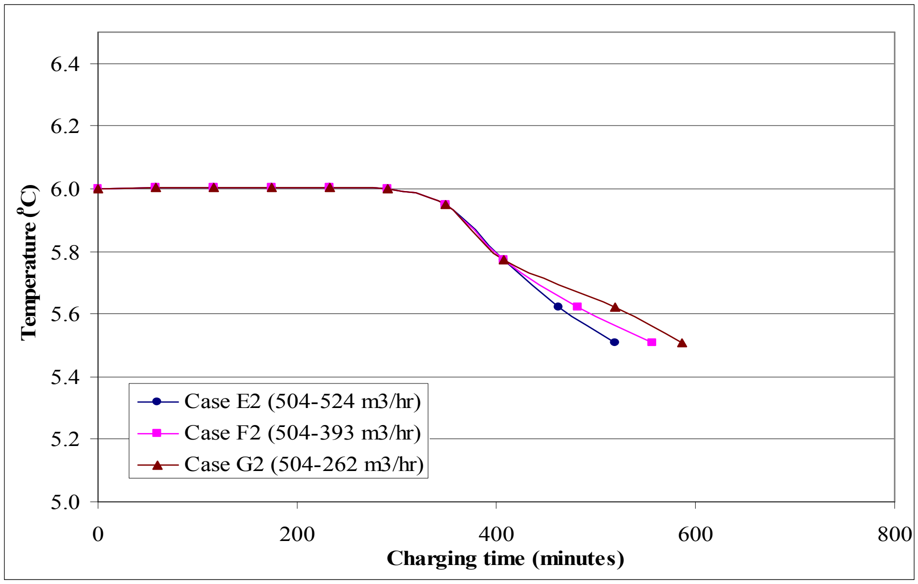

D.4 Chiller Cooling Capacity of Simulation Cases E2, F2 and G2:

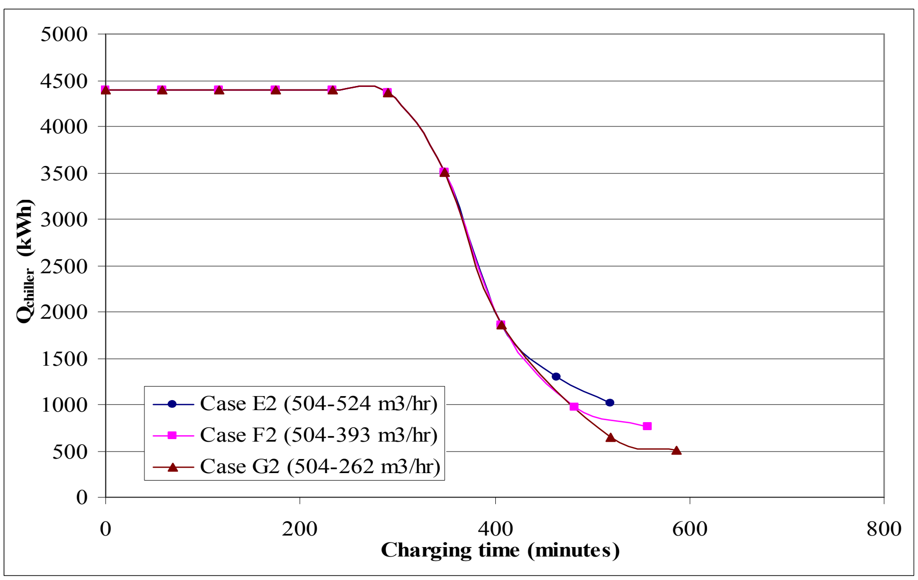

D.5. Percentage Partial Load of Simulation Cases E2, F2 and G2:

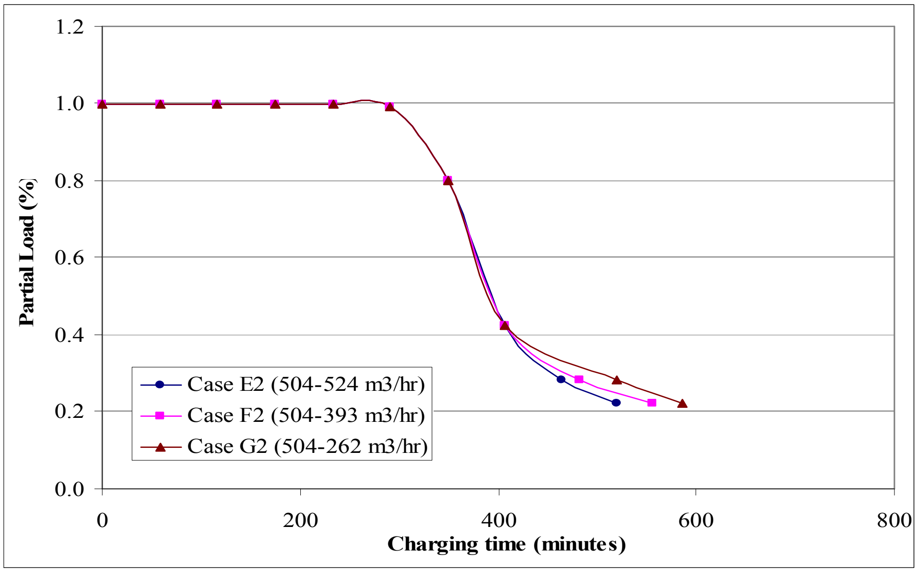

APPENDIX E
Table *t*-Distribution Critical Value
Source: http://www.im.pwr.wroc.pl/~wilczyn/tablice/ips6e_table-d.pdf

Table entry for p and C is the critical value t^* with probability p lying to its right and probability C lying between $-t^*$ and t^*.

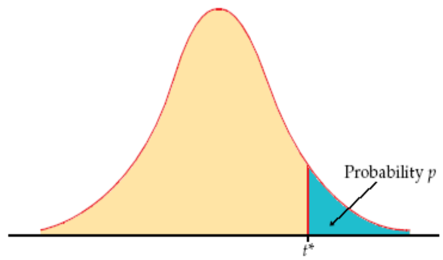

t distribution critical values

df = n	Upper-tail probability $p = \beta/2$											
	.25	.20	.15	.10	.05	.025	.02	.01	.005	.0025	.001	.0005
1	1.000	1.376	1.963	3.078	6.314	12.71	15.89	31.82	63.66	127.3	318.3	636.6
2	0.816	1.061	1.386	1.886	2.920	4.303	4.849	6.965	9.925	14.09	22.33	31.60
3	0.765	0.978	1.250	1.638	2.353	3.182	3.482	4.541	5.841	7.453	10.21	12.92
4	0.741	0.941	1.190	1.533	2.132	2.776	2.999	3.747	4.604	5.598	7.173	8.610
5	0.727	0.920	1.156	1.476	2.015	2.571	2.757	3.365	4.032	4.773	5.893	6.869
6	0.718	0.906	1.134	1.440	1.943	2.447	2.612	3.143	3.707	4.317	5.208	5.959
7	0.711	0.896	1.119	1.415	1.895	2.365	2.517	2.998	3.499	4.029	4.785	5.408
8	0.706	0.889	1.108	1.397	1.860	2.306	2.449	2.896	3.355	3.833	4.501	5.041
9	0.703	0.883	1.100	1.383	1.833	2.262	2.398	2.821	3.250	3.690	4.297	4.781
10	0.700	0.879	1.093	1.372	1.812	2.228	2.359	2.764	3.169	3.581	4.144	4.587
11	0.697	0.876	1.088	1.363	1.796	2.201	2.328	2.718	3.106	3.497	4.025	4.437
12	0.695	0.873	1.083	1.356	1.782	2.179	2.303	2.681	3.055	3.428	3.930	4.318
13	0.694	0.870	1.079	1.350	1.771	2.160	2.282	2.650	3.012	3.372	3.852	4.221
14	0.692	0.868	1.076	1.345	1.761	2.145	2.264	2.624	2.977	3.326	3.787	4.140
15	0.691	0.866	1.074	1.341	1.753	2.131	2.249	2.602	2.947	3.286	3.733	4.073
16	0.690	0.865	1.071	1.337	1.746	2.120	2.235	2.583	2.921	3.252	3.686	4.015
17	0.689	0.863	1.069	1.333	1.740	2.110	2.224	2.567	2.898	3.222	3.646	3.965
18	0.688	0.862	1.067	1.330	1.734	2.101	2.214	2.552	2.878	3.197	3.611	3.922
19	0.688	0.861	1.066	1.328	1.729	2.093	2.205	2.539	2.861	3.174	3.579	3.883
20	0.687	0.860	1.064	1.325	1.725	2.086	2.197	2.528	2.845	3.153	3.552	3.850
21	0.686	0.859	1.063	1.323	1.721	2.080	2.189	2.518	2.831	3.135	3.527	3.819
22	0.686	0.858	1.061	1.321	1.717	2.074	2.183	2.508	2.819	3.119	3.505	3.792
23	0.685	0.858	1.060	1.319	1.714	2.069	2.177	2.500	2.807	3.104	3.485	3.768
24	0.685	0.857	1.059	1.318	1.711	2.064	2.172	2.492	2.797	3.091	3.467	3.745
25	0.684	0.856	1.058	1.316	1.708	2.060	2.167	2.485	2.787	3.078	3.450	3.725
26	0.684	0.856	1.058	1.315	1.706	2.056	2.162	2.479	2.779	3.067	3.435	3.707
27	0.684	0.855	1.057	1.314	1.703	2.052	2.158	2.473	2.771	3.057	3.421	3.690
28	0.683	0.855	1.056	1.313	1.701	2.048	2.154	2.467	2.763	3.047	3.408	3.674
29	0.683	0.854	1.055	1.311	1.699	2.045	2.150	2.462	2.756	3.038	3.396	3.659
30	0.683	0.854	1.055	1.310	1.697	2.042	2.147	2.457	2.750	3.030	3.385	3.646
40	0.681	0.851	1.050	1.303	1.684	2.021	2.123	2.423	2.704	2.971	3.307	3.551
50	0.679	0.849	1.047	1.299	1.676	2.009	2.109	2.403	2.678	2.937	3.261	3.496
60	0.679	0.848	1.045	1.296	1.671	2.000	2.099	2.390	2.660	2.915	3.232	3.460
80	0.678	0.846	1.043	1.292	1.664	1.990	2.088	2.374	2.639	2.887	3.195	3.416
100	0.677	0.845	1.042	1.290	1.660	1.984	2.081	2.364	2.626	2.871	3.174	3.390
1000	0.675	0.842	1.037	1.282	1.646	1.962	2.056	2.330	2.581	2.813	3.098	3.300
z^*	0.674	0.841	1.036	1.282	1.645	1.960	2.054	2.326	2.576	2.807	3.091	3.291
	50%	60%	70%	80%	90%	95%	96%	98%	99%	99.5%	99.8%	99.9%
	Confidence level C											

APPENDIX F
Thermophysical Properties of Water

Temperature, T (K)	Pressure, P (bars)[b]	Specific Volume (m³/kg) $v_f \cdot 10^3$	Specific Volume (m³/kg) v_g	Heat of Vaporization, h_{fg} (kJ/kg)	Specific Heat (kJ/kg · K) $c_{p,f}$	Specific Heat (kJ/kg · K) $c_{p,g}$	Viscosity (N · s/m²) $\mu_f \cdot 10^6$	Viscosity (N · s/m²) $\mu_g \cdot 10^6$	Thermal Conductivity (W/m · K) $k_f \cdot 10^3$	Thermal Conductivity (W/m · K) $k_g \cdot 10^3$	Prandtl Number Pr_f	Prandtl Number Pr_g	Surface Tension, $\sigma_f \cdot 10^3$ (N/m)	Expansion Coefficient, $\beta_f \cdot 10^6$ (K⁻¹)	Temperature, T (K)
273.15	0.00611	1.000	206.3	2502	4.217	1.854	1750	8.02	569	18.2	12.99	0.815	75.5	−68.05	273.15
275	0.00697	1.000	181.7	2497	4.211	1.855	1652	8.09	574	18.3	12.22	0.817	75.3	−32.74	275
280	0.00990	1.000	130.4	2485	4.198	1.858	1422	8.29	582	18.6	10.26	0.825	74.8	46.04	280
285	0.01387	1.000	99.4	2473	4.189	1.861	1225	8.49	590	18.9	8.81	0.833	74.3	114.1	285
290	0.01917	1.001	69.7	2461	4.184	1.864	1080	8.69	598	19.3	7.56	0.841	73.7	174.0	290
295	0.02617	1.002	51.94	2449	4.181	1.868	959	8.89	606	19.5	6.62	0.849	72.7	227.5	295
300	0.03531	1.003	39.13	2438	4.179	1.872	855	9.09	613	19.6	5.83	0.857	71.7	276.1	300
305	0.04712	1.005	29.74	2426	4.178	1.877	769	9.29	620	20.1	5.20	0.865	70.9	320.6	305
310	0.06221	1.007	22.93	2414	4.178	1.882	695	9.49	628	20.4	4.62	0.873	70.0	361.9	310
315	0.08132	1.009	17.82	2402	4.179	1.888	631	9.69	634	20.7	4.16	0.883	69.2	400.4	315
320	0.1053	1.011	13.98	2390	4.180	1.895	577	9.89	640	21.0	3.77	0.894	68.3	436.7	320
325	0.1351	1.013	11.06	2378	4.182	1.903	528	10.09	645	21.3	3.42	0.901	67.5	471.2	325
330	0.1719	1.016	8.82	2366	4.184	1.911	489	10.29	650	21.7	3.15	0.908	66.6	504.0	330
335	0.2167	1.018	7.09	2354	4.186	1.920	453	10.49	656	22.0	2.88	0.916	65.8	535.5	335
340	0.2713	1.021	5.74	2342	4.188	1.930	420	10.69	660	22.3	2.66	0.925	64.9	566.0	340
345	0.3372	1.024	4.683	2329	4.191	1.941	389	10.89	668	22.6	2.45	0.933	64.1	595.4	345
350	0.4163	1.027	3.846	2317	4.195	1.954	365	11.09	668	23.0	2.29	0.942	63.2	624.2	350
355	0.5100	1.030	3.180	2304	4.199	1.968	343	11.29	671	23.3	2.14	0.951	62.3	652.3	355
360	0.6209	1.034	2.645	2291	4.203	1.983	324	11.49	674	23.7	2.02	0.960	61.4	697.9	360
365	0.7514	1.038	2.212	2278	4.209	1.999	306	11.69	677	24.1	1.91	0.969	60.5	707.1	365
370	0.9040	1.041	1.861	2265	4.214	2.017	289	11.89	679	24.5	1.80	0.978	59.5	728.7	370
373.15	1.0133	1.044	1.679	2257	4.217	2.029	279	12.02	680	24.8	1.76	0.984	58.9	750.1	373.15
375	1.0815	1.045	1.574	2252	4.220	2.036	274	12.09	681	24.9	1.70	0.987	58.6	761	375
380	1.2869	1.049	1.337	2239	4.226	2.057	260	12.29	683	25.4	1.61	0.999	57.6	788	380
385	1.5233	1.053	1.142	2225	4.232	2.080	248	12.49	685	25.8	1.53	1.004	56.6	814	385

390	1.794	1.058	0.980	2212	4.239	2.104	237	12.69	686	26.3	1.47	1.013	55.6	841	390
400	2.455	1.067	0.731	2183	4.256	2.158	217	13.05	688	27.2	1.34	1.033	53.6	896	400
410	3.302	1.077	0.553	2153	4.278	2.221	200	13.42	688	28.2	1.24	1.054	51.5	952	410
420	4.370	1.088	0.425	2123	4.302	2.291	185	13.79	688	29.8	1.16	1.075	49.4	1010	420
430	5.699	1.099	0.331	2091	4.331	2.369	173	14.14	685	30.4	1.09	1.10	47.2		430
440	7.333	1.110	0.261	2059	4.36	2.46	162	14.50	682	31.7	1.04	1.12	45.1		440
450	9.319	1.123	0.208	2024	4.40	2.56	152	14.85	678	33.1	0.99	1.14	42.9		450
460	11.71	1.137	0.167	1989	4.44	2.68	143	15.19	673	34.6	0.95	1.17	40.7		460
470	14.55	1.152	0.136	1951	4.48	2.79	136	15.54	667	36.3	0.92	1.20	38.5		470
480	17.90	1.167	0.111	1912	4.53	2.94	129	15.88	660	38.1	0.89	1.23	36.2		480
490	21.83	1.184	0.0922	1870	4.59	3.10	124	16.23	651	40.1	0.87	1.25	33.9	—	490
500	26.40	1.203	0.0766	1825	4.66	3.27	118	16.59	642	42.3	0.86	1.28	31.6	—	500
510	31.66	1.222	0.0631	1779	4.74	3.47	113	16.95	631	44.7	0.85	1.31	29.3	—	510
520	37,70	1.244	0.0525	1730	4.84	3.70	108	17.33	621	47.5	0.84	1.35	26.9	—	520
530	44.58	1.268	0.0445	1679	4.95	3.96	104	17.72	608	50.6	0.85	1.39	24.5	—	530
540	52.38	1.294	0.0375	1622	5.08	4.27	101	18.1	594	54.0	0.86	1.43	22.1	—	540
550	61.19	1.323	0.0317	1564	5.24	4.64	97	18.6	580	58.3	0.87	1.47	19.7	—	550
560	71.08	1.355	0.0269	1499	5.43	5.09	94	19.1	563	63.7	0.90	1.52	17.3	—	560
570	82.16	1.392	0.0228	1429	5.68	5.67	91	19.7	548	76.7	0.94	1.59	15.0	—	570
580	94.51	1.433	0.0193	1353	6.00	6.40	88	20.4	528	76.7	0.99	1.68	12.8	—	580
590	108.3	1.482	0.0163	1274	6.41	7.35	84	21.5	513	84.1	1.05	1.84	10.5	—	590
600	123.5	1.541	0.0137	1176	7.00	8.75	81	22.7	497	92.9	1.14	2.15	8.4	—	600
610	137.3	1.612	0.0115	1068	7.85	11.1	77	24.1	467	103	1.30	2.60	6.3	—	610
620	159.1	1.705	0.0094	941	9.35	15.4	72	25.9	444	114	1.52	3.46	4.5	—	620
625	169.1	1.778	0.0085	858	10.6	18.3	70	27.0	430	121	1.65	4.20	3.5	—	625
630	179.7	1.856	0.0075	781	12.6	22.1	67	28.0	412	130	2.0	4.8	2.6	—	630
635	190.9	1.935	0.0066	683	16.4	27.6	64	30.0	392	141	2.7	6.0	1.5	—	635
640	202.7	2.075	0.0057	560	26	42	59	32.0	367	155	4.2	9.6	0.8	—	640
645	215.2	2.351	0.0045	361	90	—	54	37.0	331	178	12	26	0.1	—	645
647.3[c]	221.2	3.170	0.0032	0	∞	∞	45	45.0	238	238	∞	∞	0.0	—	647.3[c]

[a]Adapted from Reference 19.
[b]1 bar = 10^5 N/m^2.
[c]Critical temperature.

APPENDIX G
Report of SIGMAPLOT Analysis (Data)

G.1 Data September 9, 2008

Result Summary of SIGMAPLOT Analysis Data (IA):

Charging Hour	T_c (°C)	T_h (°C)	C	S	R^2	Remarks
18:00	6.91	13.58	2.71	1.60	0.9987	Passed
19:00	6.90	13.56	3.64	1.44	0.9994	Passed
20:00	6.93	13.55	4.61	1.42	0.9995	Passed
21:00	6.94	13.54	5.55	1.48	0.9995	Passed
22:00	6.91	13.54	6.51	1.41	0.9997	Passed
23:00	6.89	13.53	7.47	1.71	0.9996	Passed
0:00	6.87	13.51	8.44	2.01	0.9996	Passed
1:00	6.85	13.49	9.39	1.80	0.9997	Passed
2:00	6.83	13.46	10.31	1.83	0.9997	Passed
3:00	6.82	13.47	11.28	1.57	0.9996	Passed

Result of SIGMAPLOT processing: September 9, 2008 (Data IA)

<u>Data set: 18.00 hours, data IA</u>

Nonlinear Regression - Dynamic Fitting **Thursday, July 22, 2010, 6:51:28 PM**

Data Source: Data 1 in Notebook2
Equation: Ligand Binding, sigmoidal dose-response (variable slope)
f=Tc + (Th-Tc)/(1+10^((C-x)*S))

Dynamic Fit Options:

Total Number of Fits	200
Maximum Number of Iterations	500

Parameter Ranges for Initial Estimates:

	Minimum	Maximum
Tc	-6.8210	20.4631
Th	-13.7781	41.3343
C	-2.8020	8.4059
S	-1.0000	3.0000

Summary of Fit Results:

Converged	100.0%
Singular Solutions	55.5%

Results for the Overall Best-Fit Solution:

R	Rsqr	Adj Rsqr	Standard Error of Estimate
0.9993	0.9987	0.9983	0.1068

	Coefficient	Std. Error	t	P
Tc	6.9070	0.0800	86.3819	<0.0001
Th	13.5758	0.0339	400.1587	<0.0001
C	2.7068	0.0259	104.5318	<0.0001
S	1.6024	0.1579	10.1492	<0.0001

Analysis of Variance: **(Appendix G.1 cont.)**

Analysis of Variance:

	DF	SS	MS
Regression	4	2197.3200	549.3300
Residual	10	0.1141	0.0114
Total	14	2197.4341	156.9596

Corrected for the mean of the observations:

	DF	SS	MS	F	P
Regression	3	84.8045	28.2682	2476.6469	<0.0001
Residual	10	0.1141	0.0114		
Total	13	84.9186	6.5322		

Statistical Tests:

Normality Test (Shapiro-Wilk) Passed (P = 0.9624)

W Statistic= 0.9781 Significance Level = 0.0500

Constant Variance Test Passed (P = 0.9637)

Data set: 19.00 hours, data IA (Appendix G.1 cont.)

Nonlinear Regression - Dynamic Fitting **Thursday, July 22, 2010, 6:51:51 PM**

Data Source: Data 1 in Notebook2
Equation: Ligand Binding, sigmoidal dose-response (variable slope)
f=Tc + (Th-Tc)/(1+10^((C-x)*S))

Dynamic Fit Options:

Total Number of Fits	200
Maximum Number of Iterations	500

Parameter Ranges for Initial Estimates:

	Minimum	Maximum
Tc	-6.8936	20.6807
Th	-13.6709	41.0127
C	-3.7123	11.1368
S	-1.0000	3.0000

Summary of Fit Results:

Converged	100.0%
Singular Solutions	56.5%

Results for the Overall Best-Fit Solution:

R	Rsqr	Adj Rsqr	Standard Error of Estimate
0.9997	0.9994	0.9992	0.0795

	Coefficient	Std. Error	t	P
Tc	6.8987	0.0494	139.5154	<0.0001
Th	13.5601	0.0266	510.1241	<0.0001
C	3.6380	0.0171	212.4881	<0.0001
S	1.4428	0.1045	13.8040	<0.0001

Analysis of Variance:
Analysis of Variance:

	DF	SS	MS
Regression	4	2064.9120	516.2280
Residual	10	0.0632	0.0063
Total	14	2064.9752	147.4982

Corrected for the mean of the observations:

	DF	SS	MS	F	P
Regression	3	105.4881	35.1627	5565.8055	<0.0001
Residual	10	0.0632	0.0063		
Total	13	105.5513	8.1193		

Statistical Tests:

Normality Test (Shapiro-Wilk)	Passed (P = 0.8736)
W Statistic= 0.9698	Significance Level = 0.0500
Constant Variance Test	Passed (P = 0.4532)

Data set: 20.00 hours, data IA (Appendix G.1 cont.)

Nonlinear Regression - Dynamic Fitting **Thursday, July 22, 2010, 6:52:08 PM**

Data Source: Data 1 in Notebook2
Equation: Ligand Binding, sigmoidal dose-response (variable slope)
f=Tc + (Th-Tc)/(1+10^((C-x)*S))

Dynamic Fit Options:

Total Number of Fits	200
Maximum Number of Iterations	500

Parameter Ranges for Initial Estimates:

	Minimum	Maximum
Tc	-6.8720	20.6160
Th	-13.6297	40.8890
C	-4.6641	13.9924
S	-1.0000	3.0000

Summary of Fit Results:

Converged	100.0%
Singular Solutions	59.5%

Results for the Overall Best-Fit Solution:

R	Rsqr	Adj Rsqr	Standard Error of Estimate
0.9998	0.9995	0.9994	0.0740

	Coefficient	Std. Error	t	P
Tc	6.9329	0.0396	175.2703	<0.0001
Th	13.5536	0.0262	517.4668	<0.0001
C	4.6084	0.0154	298.3218	<0.0001
S	1.4204	0.0981	14.4774	<0.0001

Analysis of Variance:
Analysis of Variance:

	DF	SS	MS
Regression	4	1933.3496	483.3374
Residual	10	0.0548	0.0055
Total	14	1933.4044	138.1003

Corrected for the mean of the observations:

	DF	SS	MS	F	P
Regression	3	121.4061	40.4687	7384.7919	<0.0001
Residual	10	0.0548	0.0055		
Total	13	121.4609	9.3431		

Statistical Tests:
Normality Test (Shapiro-Wilk) Passed (P = 0.1035)
W Statistic= 0.8974 Significance Level = 0.0500
Constant Variance Test Passed (P = 0.6372)

Data set: 21.00 hours, data IA (Appendix G.1 cont.)

Nonlinear Regression - Dynamic Fitting **Thursday, July 22, 2010, 6:52:23 PM**

Data Source: Data 1 in Notebook2
Equation: Ligand Binding, sigmoidal dose-response (variable slope)
f=Tc + (Th-Tc)/(1+10^((C-x)*S))

Dynamic Fit Options:

Total Number of Fits	200
Maximum Number of Iterations	500

Parameter Ranges for Initial Estimates:

	Minimum	Maximum
Tc	-6.8633	20.5900
Th	-13.6193	40.8578
C	-5.5717	16.7150
S	-1.0000	3.0000

Summary of Fit Results:

Converged	100.0%
Singular Solutions	62.5%

Results for the Overall Best-Fit Solution:

R	Rsqr	Adj Rsqr	Standard Error of Estimate
0.9998	0.9995	0.9994	0.0805

	Coefficient	Std. Error	t	P
Tc	6.9364	0.0385	180.2694	<0.0001
Th	13.5421	0.0301	449.6242	<0.0001
C	5.5474	0.0152	363.9671	<0.0001
S	1.4770	0.1289	11.4610	<0.0001

Analysis of Variance:
Analysis of Variance:

	DF	SS	MS
Regression	4	1804.3178	451.0794
Residual	10	0.0648	0.0065
Total	14	1804.3826	128.8845

Corrected for the mean of the observations:

	DF	SS	MS	F	P
Regression	3	132.3713	44.1238	6807.4166	<0.0001
Residual	10	0.0648	0.0065		
Total	13	132.4361	10.1874		

Statistical Tests:

Normality Test (Shapiro-Wilk)	Passed (P = 0.3346)
W Statistic= 0.9329	Significance Level = 0.0500
Constant Variance Test	Passed (P = 0.7499)

Data set: 22.00 hours, data IA (Appendix G.1 cont.)

Nonlinear Regression - Dynamic Fitting **Thursday, July 22, 2010, 6:54:17 PM**

Data Source: Data 1 in Sept9_DATA.JNB
Equation: Ligand Binding, sigmoidal dose-response (variable slope)
f=Tc + (Th-Tc)/(1+10^((C-x)*S))

Dynamic Fit Options:

Total Number of Fits	200
Maximum Number of Iterations	500

Parameter Ranges for Initial Estimates:

	Minimum	Maximum
Tc	-6.8498	20.5495
Th	-13.6032	40.8095
C	-6.5007	19.5021
S	-1.0000	3.0000

Summary of Fit Results:

Converged	100.0%
Singular Solutions	64.0%

Results for the Overall Best-Fit Solution:

R	Rsqr	Adj Rsqr	Standard Error of Estimate
0.9998	0.9997	0.9996	0.0678

	Coefficient	Std. Error	t	P
Tc	6.9119	0.0297	232.9510	<0.0001
Th	13.5381	0.0272	498.0271	<0.0001
C	6.5089	0.0132	494.8539	<0.0001
S	1.4096	0.0948	14.8631	<0.0001

Analysis of Variance:
Analysis of Variance:

	DF	SS	MS
Regression	4	1671.0105	417.7526
Residual	10	0.0460	0.0046
Total	14	1671.0565	119.3612

Corrected for the mean of the observations:

	DF	SS	MS	F	P
Regression	3	138.6039	46.2013	10042.3931	<0.0001
Residual	10	0.0460	0.0046		
Total	13	138.6499	10.6654		

Statistical Tests:

Normality Test (Shapiro-Wilk)	Passed (P = 0.2026)
W Statistic= 0.9175	Significance Level = 0.0500
Constant Variance Test	Passed (P = 0.8201)

<u>Data set: 23.00 hours, data IA</u> **(Appendix G.1 cont.)**

Nonlinear Regression - Dynamic Fitting **Thursday, July 22, 2010, 6:54:34 PM**

Data Source: Data 1 in Sept9_DATA.JNB
Equation: Ligand Binding, sigmoidal dose-response (variable slope)
f=Tc + (Th-Tc)/(1+10^((C-x)*S))

Dynamic Fit Options:

Total Number of Fits	200
Maximum Number of Iterations	500

Parameter Ranges for Initial Estimates:

	Minimum	Maximum
Tc	-6.8313	20.4940
Th	-13.5965	40.7894
C	-7.4377	22.3131
S	-1.0000	3.0000

Summary of Fit Results:

Converged	100.0%
Singular Solutions	68.0%

Results for the Overall Best-Fit Solution:

R	Rsqr	Adj Rsqr	Standard Error of Estimate
0.9998	0.9996	0.9995	0.0704

	Coefficient	Std. Error	t	P
Tc	6.8936	0.0282	244.1950	<0.0001
Th	13.5286	0.0301	450.0203	<0.0001
C	7.4729	0.0119	626.8686	<0.0001
S	1.7054	0.1833	9.3050	<0.0001

Analysis of Variance:
Analysis of Variance:

	DF	SS	MS
Regression	4	1539.0866	384.7717
Residual	10	0.0495	0.0050
Total	14	1539.1361	109.9383

Corrected for the mean of the observations:

	DF	SS	MS	F	P
Regression	3	140.7529	46.9176	9474.7526	<0.0001
Residual	10	0.0495	0.0050		
Total	13	140.8024	10.8310		

Statistical Tests:

Normality Test (Shapiro-Wilk)	Passed (P = 0.4704)
W Statistic= 0.9439	Significance Level = 0.0500
Constant Variance Test	Passed (P = 0.8676)

Data set: 00.00 hours, data IA (Appendix G.1 cont.)

Nonlinear Regression - Dynamic Fitting **Thursday, July 22, 2010, 6:54:51 PM**

Data Source: Data 1 in Sept9_DATA.JNB
Equation: Ligand Binding, sigmoidal dose-response (variable slope)
f=Tc + (Th-Tc)/(1+10^((C-x)*S))

Dynamic Fit Options:

Total Number of Fits	200
Maximum Number of Iterations	500

Parameter Ranges for Initial Estimates:

	Minimum	Maximum
Tc	-6.8052	20.4157
Th	-13.5845	40.7535
C	-8.3635	25.0905
S	-1.0000	3.0000

Summary of Fit Results:

Converged	99.5%
Singular Solutions	68.5%
Ill-Conditioned Solutions	0.5%
Iterations Exceeding 500	0.5%

Results for the Overall Best-Fit Solution:

R	Rsqr	Adj Rsqr	Standard Error of Estimate
0.9998	0.9996	0.9995	0.0699

	Coefficient	Std. Error	t	P
Tc	6.8724	0.0262	262.2204	<0.0001
Th	13.5050	0.0322	419.0655	<0.0001
C	8.4357	0.0153	550.2128	<0.0001
S	2.0123	0.3301	6.0951	0.0001

Analysis of Variance:
Analysis of Variance:

	DF	SS	MS
Regression	4	1405.4215	351.3554
Residual	10	0.0489	0.0049
Total	14	1405.4704	100.3907

Corrected for the mean of the observations:

	DF	SS	MS	F	P
Regression	3	136.1679	45.3893	9276.6728	<0.0001
Residual	10	0.0489	0.0049		
Total	13	136.2169	10.4782		

Statistical Tests:

Normality Test (Shapiro-Wilk) Passed (P = 0.4997)
W Statistic= 0.9459 Significance Level = 0.0500
Constant Variance Test Passed (P = 0.6155)

Data set: 01.00 hours, data IA (Appendix G.1 cont.)

Nonlinear Regression - Dynamic Fitting **Thursday, July 22, 2010, 6:55:07 PM**

Data Source: Data 1 in Sept9_DATA.JNB
Equation: Ligand Binding, sigmoidal dose-response (variable slope)
f=Tc + (Th-Tc)/(1+10^((C-x)*S))

Dynamic Fit Options:

Total Number of Fits	200
Maximum Number of Iterations	500

Parameter Ranges for Initial Estimates:

	Minimum	Maximum
Tc	-6.7818	20.3455
Th	-13.5606	40.6817
C	-9.3032	27.9097
S	-1.0000	3.0000

Summary of Fit Results:

Converged	99.5%
Singular Solutions	68.5%
Iterations Exceeding 500	0.5%

Results for the Overall Best-Fit Solution:

R	Rsqr	Adj Rsqr	Standard Error of Estimate
0.9999	0.9997	0.9997	0.0574

	Coefficient	Std. Error	t	P
Tc	6.8456	0.0203	337.8586	<0.0001
Th	13.4917	0.0296	456.3355	<0.0001
C	9.3877	0.0133	707.5220	<0.0001
S	1.8037	0.1523	11.8448	<0.0001

Analysis of Variance:
Analysis of Variance:

	DF	SS	MS
Regression	4	1271.4434	317.8609
Residual	10	0.0329	0.0033
Total	14	1271.4763	90.8197

Corrected for the mean of the observations:

	DF	SS	MS	F	P
Regression	3	125.1448	41.7149	12668.5560	<0.0001
Residual	10	0.0329	0.0033		
Total	13	125.1777	9.6291		

Statistical Tests:

Normality Test (Shapiro-Wilk)	Passed (P = 0.6557)
W Statistic= 0.9559	Significance Level = 0.0500
Constant Variance Test	Passed (P = 0.9637)

Nonlinear Regression - Dynamic Fitting **Thursday, July 22, 2010, 6:55:25 PM**

Data Source: Data 1 in Sept9_DATA.JNB
Equation: Ligand Binding, sigmoidal dose-response (variable slope)
f=Tc + (Th-Tc)/(1+10^((C-x)*S))

Dynamic Fit Options:

Total Number of Fits	200
Maximum Number of Iterations	500

Parameter Ranges for Initial Estimates:

	Minimum	Maximum
Tc	-6.7544	20.2633
Th	-13.5333	40.5998
C	-10.2075	30.6225
S	-1.0000	3.0000

Summary of Fit Results:

Converged	99.5%
Singular Solutions	70.5%
Iterations Exceeding 500	0.5%

Results for the Overall Best-Fit Solution:

R	Rsqr	Adj Rsqr	Standard Error of Estimate
0.9998	0.9997	0.9996	0.0584

	Coefficient	Std. Error	t	P
Tc	6.8264	0.0195	349.8888	<0.0001
Th	13.4618	0.0344	391.0284	<0.0001
C	10.3062	0.0161	638.4681	<0.0001
S	1.8313	0.1236	14.8139	<0.0001

Analysis of Variance:
Analysis of Variance:

	DF	SS	MS
Regression	4	1143.6628	285.9157
Residual	10	0.0341	0.0034
Total	14	1143.6969	81.6926

Corrected for the mean of the observations:

	DF	SS	MS	F	P
Regression	3	109.5495	36.5165	10708.5699	<0.0001
Residual	10	0.0341	0.0034		
Total	13	109.5836	8.4295		

Statistical Tests:

Normality Test (Shapiro-Wilk)	Passed (P = 0.5909)
W Statistic= 0.9519	Significance Level = 0.0500
Constant Variance Test	Passed (P = 0.9517)

Data set: 03.00 hours, data IA (Appendix G.1 cont.)

Nonlinear Regression - Dynamic Fitting **Thursday, July 22, 2010, 6:55:51 PM**

Data Source: Data 1 in Sept9_DATA.JNB
Equation: Ligand Binding, sigmoidal dose-response (variable slope)
f=Tc + (Th-Tc)/(1+10^((C-x)*S))

Dynamic Fit Options:

Total Number of Fits	200
Maximum Number of Iterations	500

Parameter Ranges for Initial Estimates:

	Minimum	Maximum
Tc	-6.7315	20.1946
Th	-13.5028	40.5084
C	-11.1964	33.5891
S	-1.0000	3.0000

Summary of Fit Results:

Converged	100.0%
Singular Solutions	75.5%

Results for the Overall Best-Fit Solution:

R	Rsqr	Adj Rsqr	Standard Error of Estimate
0.9998	0.9996	0.9995	0.0585

	Coefficient	Std. Error	t	P
Tc	6.8156	0.0186	366.6265	<0.0001
Th	13.4697	0.0436	308.7311	<0.0001
C	11.2802	0.0146	772.1180	<0.0001
S	1.5701	0.0750	20.9257	<0.0001

Analysis of Variance:
Analysis of Variance:

	DF	SS	MS
Regression	4	1008.3962	252.0991
Residual	10	0.0342	0.0034
Total	14	1008.4304	72.0307

Corrected for the mean of the observations:

	DF	SS	MS	F	P
Regression	3	85.3144	28.4381	8313.2956	<0.0001
Residual	10	0.0342	0.0034		
Total	13	85.3486	6.5653		

Statistical Tests:

Normality Test (Shapiro-Wilk)	Passed (P = 0.9845)
W Statistic= 0.9819	Significance Level = 0.0500
Constant Variance Test	Passed (P = 0.5834)

G.2 Data September 11, 2008

Result Summary of SIGMAPLOT Analysis Data (IB):

Charging Hour	T_c (°C)	T_h (°C)	C	S	R^2	Remarks
18:00	7.32	13.63	3.92	1.47	0.9985	Passed
19:00	7.36	13.61	4.87	1.57	0.9986	Passed
20:00	7.31	13.59	5.83	1.49	0.9987	Passed
21:00	7.27	13.59	6.77	1.34	0.9993	Passed
22:00	7.22	13.57	7.69	1.38	0.9995	Passed
23:00	7.17	13.54	8.63	1.42	0.9995	Passed
0:00	7.15	13.53	9.59	1.37	0.9996	Passed
1:00	7.12	13.50	10.49	1.26	0.9995	Passed
2:00	7.11	13.50	11.49	1.23	0.9990	Passed
3:00	7.09	13.83	12.55	1.10	0.9918	Passed
4:00	-	-	-	-	-	In-convergence
5:00	-	-	-	-	-	In-convergence
6:00	-	-	-	-	-	In-convergence
7:00	-	-	-	-	-	In-convergence

Result of SIGMAPLOT processing: September 11, 2008 (Data IB)

<u>Data set: 18.00 hours, data IB</u>

Nonlinear Regression - Dynamic Fitting **Tuesday, June 29, 2010, 2:19:08 PM**

Data Source: Data 1 in Notebook1
Equation: Ligand Binding, sigmoidal dose-response (variable slope)
f=Tc + (Th-Tc)/(1+10^((C-x)*S))

Dynamic Fit Options:

Total Number of Fits	200
Maximum Number of Iterations	500

Parameter Ranges for Initial Estimates:

	Minimum	**Maximum**
Tc	-3.7500	1.2500
Th	-13.7848	41.3543
C	-3.9603	11.8808
S	-1.0000	3.0000

Summary of Fit Results:

Converged	100.0%
Singular Solutions	45.5%

Results for the Overall Best-Fit Solution:

R	**Rsqr**	**Adj Rsqr**	**Standard Error of Estimate**
0.9993	0.9985	0.9981	0.1220

	Coefficient	**Std. Error**	**t**	**P**
Tc	7.3173	0.0727	100.6511	<0.0001
Th	13.6253	0.0410	332.0368	<0.0001
C	3.9220	0.0339	115.7509	<0.0001
S	1.4658	0.1001	14.6480	<0.0001

Analysis of Variance: **(Appendix G.2 cont.)**

Analysis of Variance:

	DF	SS	MS
Regression	4	2070.4360	517.6090
Residual	10	0.1489	0.0149
Total	14	2070.5849	147.8989

Corrected for the mean of the observations:

	DF	SS	MS	F	P
Regression	3	101.1509	33.7170	2265.0673	<0.0001
Residual	10	0.1489	0.0149		
Total	13	101.2998	7.7923		

Statistical Tests:

Normality Test (Shapiro-Wilk) Passed (P = 0.3123)

W Statistic= 0.9307 Significance Level = 0.0500

Constant Variance Test Passed (P = 0.2786)

<u>Data set: 19.00 hours, data IB</u> **(Appendix G.2 cont.)**

Nonlinear Regression - Dynamic Fitting **Tuesday, June 29, 2010, 2:19:35 PM**

Data Source: Data 1 in Notebook1
Equation: Ligand Binding, sigmoidal dose-response (variable slope)
f=Tc + (Th-Tc)/(1+10^((C-x)*S))

Dynamic Fit Options:

Total Number of Fits	200
Maximum Number of Iterations	500

Parameter Ranges for Initial Estimates:

	Minimum	Maximum
Tc	-3.6250	1.2083
Th	-13.7332	41.1995
C	-4.9275	14.7825
S	-1.0000	3.0000

Summary of Fit Results:

Converged	100.0%
Singular Solutions	48.0%

Results for the Overall Best-Fit Solution:

R	Rsqr	Adj Rsqr	Standard Error of Estimate
0.9993	0.9986	0.9982	0.1264

	Coefficient	Std. Error	t	P
Tc	7.3587	0.0644	114.2922	<0.0001
Th	13.6057	0.0450	302.3090	<0.0001
C	4.8698	0.0353	137.9451	<0.0001
S	1.5736	0.1255	12.5334	<0.0001

Analysis of Variance:
Analysis of Variance:

	DF	SS	MS
Regression	4	1943.5365	485.8841
Residual	10	0.1597	0.0160
Total	14	1943.6962	138.8354

Corrected for the mean of the observations:

	DF	SS	MS	F	P
Regression	3	113.8312	37.9437	2376.2972	<0.0001
Residual	10	0.1597	0.0160		
Total	13	113.9909	8.7685		

Statistical Tests:

Normality Test (Shapiro-Wilk)	Passed (P = 0.0510)
W Statistic= 0.8760	Significance Level = 0.0500
Constant Variance Test	Passed (P = 0.1476)

Data set: 20.00 hours, data IB (Appendix G.2 cont.)

Nonlinear Regression - Dynamic Fitting **Tuesday, June 29, 2010, 2:19:49 PM**

Data Source: Data 1 in Notebook1
Equation: Ligand Binding, sigmoidal dose-response (variable slope)
f=Tc + (Th-Tc)/(1+10^((C-x)*S))

Dynamic Fit Options:

Total Number of Fits	200
Maximum Number of Iterations	500

Parameter Ranges for Initial Estimates:

	Minimum	Maximum
Tc	-3.5000	1.1667
Th	-13.7187	41.1561
C	-5.8906	17.6717
S	-1.0000	3.0000

Summary of Fit Results:

Converged	100.0%
Singular Solutions	50.0%

Results for the Overall Best-Fit Solution:

R	Rsqr	Adj Rsqr	Standard Error of Estimate
0.9993	0.9987	0.9983	0.1272

	Coefficient	Std. Error	t	P
Tc	7.3107	0.0580	125.9718	<0.0001
Th	13.5934	0.0486	279.9471	<0.0001
C	5.8306	0.0344	169.6248	<0.0001
S	1.4949	0.1246	11.9986	<0.0001

Analysis of Variance:
Analysis of Variance:

	DF	SS	MS
Regression	4	1809.9857	452.4964
Residual	10	0.1618	0.0162
Total	14	1810.1475	129.2963

Corrected for the mean of the observations:

	DF	SS	MS	F	P
Regression	3	123.2045	41.0682	2537.5107	<0.0001
Residual	10	0.1618	0.0162		
Total	13	123.3664	9.4897		

Statistical Tests:

Normality Test (Shapiro-Wilk)	Passed (P = 0.0218)
W Statistic= 0.8494	Significance Level = 0.0500
Constant Variance Test	Passed (P = 0.1088)

Data set: 21.00 hours, data IB (Appendix G.2 cont.)

Nonlinear Regression - Dynamic Fitting **Tuesday, June 29, 2010, 2:20:52 PM**

Data Source: Data 1 in Notebook1
Equation: Ligand Binding, sigmoidal dose-response (variable slope)
f=Tc + (Th-Tc)/(1+10^((C-x)*S))

Dynamic Fit Options:

Total Number of Fits	200
Maximum Number of Iterations	500

Parameter Ranges for Initial Estimates:

	Minimum	Maximum
Tc	-3.3750	1.1250
Th	-13.6939	41.0816
C	-6.8324	20.4973
S	-1.0000	3.0000

Summary of Fit Results:

Converged	100.0%
Singular Solutions	55.0%

Results for the Overall Best-Fit Solution:

R	Rsqr	Adj Rsqr	Standard Error of Estimate
0.9997	0.9993	0.9991	0.0919

	Coefficient	Std. Error	t	P
Tc	7.2688	0.0386	188.2191	<0.0001
Th	13.5905	0.0381	356.6095	<0.0001
C	6.7725	0.0238	284.2982	<0.0001
S	1.3364	0.0822	16.2565	<0.0001

Analysis of Variance:
Analysis of Variance:

	DF	SS	MS
Regression	4	1680.2753	420.0688
Residual	10	0.0845	0.0084
Total	14	1680.3598	120.0257

Corrected for the mean of the observations:

	DF	SS	MS	F	P
Regression	3	126.7783	42.2594	5001.1470	<0.0001
Residual	10	0.0845	0.0084		
Total	13	126.8628	9.7587		

Statistical Tests:

Normality Test (Shapiro-Wilk)	Passed (P = 0.1476)
W Statistic= 0.9080	Significance Level = 0.0500
Constant Variance Test	Passed (P = 0.2715)

Data set: 22.00 hours, data IB (Appendix G.2 cont.)

Nonlinear Regression - Dynamic Fitting **Tuesday, June 29, 2010, 2:21:05 PM**

Data Source: Data 1 in Notebook1
Equation: Ligand Binding, sigmoidal dose-response (variable slope)
f=Tc + (Th-Tc)/(1+10^((C-x)*S))

Dynamic Fit Options:

Total Number of Fits	200
Maximum Number of Iterations	500

Parameter Ranges for Initial Estimates:

	Minimum	Maximum
Tc	-3.2500	1.0833
Th	-13.6634	40.9902
C	-7.7586	23.2757
S	-1.0000	3.0000

Summary of Fit Results:

Converged	100.0%
Singular Solutions	61.5%

Results for the Overall Best-Fit Solution:

R	Rsqr	Adj Rsqr	Standard Error of Estimate
0.9997	0.9995	0.9993	0.0818

	Coefficient	Std. Error	t	P
Tc	7.2158	0.0318	226.9532	<0.0001
Th	13.5667	0.0370	366.6422	<0.0001
C	7.6935	0.0201	383.4399	<0.0001
S	1.3793	0.0909	15.1799	<0.0001

Analysis of Variance:
Analysis of Variance:

	DF	SS	MS
Regression	4	1548.7478	387.1869
Residual	10	0.0669	0.0067
Total	14	1548.8146	110.6296

Corrected for the mean of the observations:

	DF	SS	MS	F	P
Regression	3	126.8398	42.2799	6321.6759	<0.0001
Residual	10	0.0669	0.0067		
Total	13	126.9067	9.7621		

Statistical Tests:
Normality Test (Shapiro-Wilk) Passed (P = 0.3852)
W Statistic= 0.9373 Significance Level = 0.0500
Constant Variance Test Passed (P = 0.3395)

Data set: 23.00 hours, data IB (Appendix G.2 cont.)

Nonlinear Regression - Dynamic Fitting **Tuesday, June 29, 2010, 2:21:20 PM**

Data Source: Data 1 in Notebook1
Equation: Ligand Binding, sigmoidal dose-response (variable slope)
f=Tc + (Th-Tc)/(1+10^((C-x)*S))

Dynamic Fit Options:

Total Number of Fits	200
Maximum Number of Iterations	500

Parameter Ranges for Initial Estimates:

	Minimum	Maximum
Tc	-3.1250	1.0417
Th	-13.6447	40.9340
C	-8.6874	26.0622
S	-1.0000	3.0000

Summary of Fit Results:

Converged	100.0%
Singular Solutions	63.0%

Results for the Overall Best-Fit Solution:

R	Rsqr	Adj Rsqr	Standard Error of Estimate
0.9998	0.9995	0.9994	0.0753

	Coefficient	Std. Error	t	P
Tc	7.1734	0.0275	261.2320	<0.0001
Th	13.5386	0.0378	358.2483	<0.0001
C	8.6282	0.0172	500.4156	<0.0001
S	1.4156	0.1016	13.9386	<0.0001

Analysis of Variance:
Analysis of Variance:

	DF	SS	MS
Regression	4	1416.1622	354.0405
Residual	10	0.0568	0.0057
Total	14	1416.2190	101.1585

Corrected for the mean of the observations:

	DF	SS	MS	F	P
Regression	3	121.2212	40.4071	7119.4173	<0.0001
Residual	10	0.0568	0.0057		
Total	13	121.2780	9.3291		

Statistical Tests:

Normality Test (Shapiro-Wilk)	Passed (P = 0.8699)
W Statistic= 0.9695	Significance Level = 0.0500
Constant Variance Test	Passed (P = 0.5940)

<u>**Data set: 00.00 hours, data IB**</u> **(Appendix G.2 cont.)**

Nonlinear Regression - Dynamic Fitting **Tuesday, June 29, 2010, 2:21:39 PM**

Data Source: Data 1 in Notebook1
Equation: Ligand Binding, sigmoidal dose-response (variable slope)
f=Tc + (Th-Tc)/(1+10^((C-x)*S))

Dynamic Fit Options:

Total Number of Fits	200
Maximum Number of Iterations	500

Parameter Ranges for Initial Estimates:

	Minimum	**Maximum**
Tc	-6.0000	2.0000
Th	-13.6248	40.8745
C	-9.6302	28.8907
S	-1.0000	3.0000

Summary of Fit Results:

Converged	100.0%
Singular Solutions	64.5%
Ill-Conditioned Solutions	0.5%

Results for the Overall Best-Fit Solution:

R	**Rsqr**	**Adj Rsqr**	**Standard Error of Estimate**
0.9998	0.9996	0.9994	0.0690

	Coefficient	**Std. Error**	**t**	**P**
Tc	7.1491	0.0238	299.7888	<0.0001
Th	13.5251	0.0396	341.2610	<0.0001
C	9.5861	0.0154	621.2670	<0.0001
S	1.3707	0.0915	14.9809	<0.0001

Analysis of Variance:
Analysis of Variance:

	DF	**SS**	**MS**
Regression	4	1284.7993	321.1998
Residual	10	0.0477	0.0048
Total	14	1284.8469	91.7748

Corrected for the mean of the observations:

	DF	**SS**	**MS**	**F**	**P**
Regression	3	109.5347	36.5116	7661.4860	<0.0001
Residual	10	0.0477	0.0048		
Total	13	109.5823	8.4294		

Statistical Tests:

Normality Test (Shapiro-Wilk)	Passed (P = 0.5526)
W Statistic= 0.9495	Significance Level = 0.0500
Constant Variance Test	Passed (P = 0.8676)

Data set: 01.00 hours, data IB (Appendix G.2 cont.)

Nonlinear Regression - Dynamic Fitting **Tuesday, June 29, 2010, 2:21:58 PM**

Data Source: Data 1 in Notebook1
Equation: Ligand Binding, sigmoidal dose-response (variable slope)
f=Tc + (Th-Tc)/(1+10^((C-x)*S))

Dynamic Fit Options:

Total Number of Fits	200
Maximum Number of Iterations	500

Parameter Ranges for Initial Estimates:

	Minimum	Maximum
Tc	-5.8750	1.9583
Th	-13.5741	40.7224
C	-10.4810	31.4430
S	-1.0000	3.0000

Summary of Fit Results:

Converged	100.0%
Singular Solutions	66.0%

Results for the Overall Best-Fit Solution:

R	Rsqr	Adj Rsqr	Standard Error of Estimate
0.9997	0.9995	0.9993	0.0685

	Coefficient	Std. Error	t	P
Tc	7.1248	0.0228	312.5994	<0.0001
Th	13.5008	0.0464	290.7041	<0.0001
C	10.4924	0.0159	658.6213	<0.0001
S	1.2565	0.0752	16.7130	<0.0001

Analysis of Variance:
Analysis of Variance:

	DF	SS	MS
Regression	4	1158.8816	289.7204
Residual	10	0.0470	0.0047
Total	14	1158.9286	82.7806

Corrected for the mean of the observations:

	DF	SS	MS	F	P
Regression	3	92.6158	30.8719	6574.1408	<0.0001
Residual	10	0.0470	0.0047		
Total	13	92.6628	7.1279		

Statistical Tests:

Normality Test (Shapiro-Wilk)	Passed (P = 0.9674)
W Statistic= 0.9788	Significance Level = 0.0500
Constant Variance Test	Passed (P = 0.6482)

Data set: 02.00 hours, data IB (Appendix G.2 cont.)

Nonlinear Regression - Dynamic Fitting **Tuesday, June 29, 2010, 2:22:12 PM**

Data Source: Data 1 in Notebook1
Equation: Ligand Binding, sigmoidal dose-response (variable slope)
f=Tc + (Th-Tc)/(1+10^((C-x)*S))

Dynamic Fit Options:

Total Number of Fits	200
Maximum Number of Iterations	500

Parameter Ranges for Initial Estimates:

	Minimum	Maximum
Tc	-5.7500	1.9167
Th	-13.4152	40.2455
C	-11.4564	34.3691
S	-1.0000	3.0000

Summary of Fit Results:

Converged	100.0%
Singular Solutions	65.0%
Ill-Conditioned Solutions	0.5%

Results for the Overall Best-Fit Solution:

R	Rsqr	Adj Rsqr	Standard Error of Estimate
0.9995	0.9990	0.9988	0.0814

	Coefficient	Std. Error	t	P
Tc	7.1128	0.0258	275.7624	<0.0001
Th	13.5007	0.0753	179.4107	<0.0001
C	11.4913	0.0205	560.7064	<0.0001
S	1.2285	0.0901	13.6330	<0.0001

Analysis of Variance:
Analysis of Variance:

	DF	SS	MS
Regression	4	1025.2366	256.3092
Residual	10	0.0663	0.0066
Total	14	1025.3029	73.2359

Corrected for the mean of the observations:

	DF	SS	MS	F	P
Regression	3	69.5151	23.1717	3497.5183	<0.0001
Residual	10	0.0663	0.0066		
Total	13	69.5814	5.3524		

Statistical Tests:
Normality Test (Shapiro-Wilk) Passed (P = 0.7529)
W Statistic= 0.9618 Significance Level = 0.0500
Constant Variance Test Passed (P = 0.4532)

Data set: 03.00 hours, data IB (Appendix G.2 cont.)

Nonlinear Regression - Dynamic Fitting **Tuesday, June 29, 2010, 2:22:27 PM**

Data Source: Data 1 in Notebook1
Equation: Ligand Binding, sigmoidal dose-response (variable slope)
f=Tc+ (Th-Tc)/(1+10^((C-x)*S))

Dynamic Fit Options:

Total Number of Fits	200
Maximum Number of Iterations	500

Parameter Ranges for Initial Estimates:

	Minimum	Maximum
Tc	-5.6250	1.8750
Th	-13.2854	39.8561
C	-12.4567	37.3702
S	-1.0000	3.0000

Summary of Fit Results:

Converged	99.0%
Singular Solutions	71.0%
Ill-Conditioned Solutions	0.5%
Iterations Exceeding 500	1.0%

Results for the Overall Best-Fit Solution:

R	Rsqr	Adj Rsqr	Standard Error of Estimate
0.9991	0.9982	0.9977	0.0864

	Coefficient	Std. Error	t	P
Tc	7.0876	0.0265	267.3137	<0.0001
Th	13.8321	0.2039	67.8335	<0.0001
C	12.5525	0.0377	333.1423	<0.0001
S	1.1023	0.1038	10.6183	<0.0001

Analysis of Variance:
Analysis of Variance:

	DF	SS	MS
Regression	4	892.0896	223.0224
Residual	10	0.0747	0.0075
Total	14	892.1642	63.7260

Corrected for the mean of the observations:

	DF	SS	MS	F	P
Regression	3	41.8394	13.9465	1868.0823	<0.0001
Residual	10	0.0747	0.0075		
Total	13	41.9140	3.2242		

Statistical Tests:

Normality Test (Shapiro-Wilk)	Passed (P = 0.3859)
W Statistic= 0.9374	Significance Level = 0.0500
Constant Variance Test	Passed (P = 0.3236)

G.3 Data September 19, 2008

Result Summary of SIGMAPLOT Analysis Data (IC)

Charging Hour	T_c (°C)	T_h (°C)	C	S	R^2	Remarks
18:00	7.73	13.54	3.19	1.11	0.9968	Passed
19:00	7.58	13.53	4.10	1.03	0.9984	Passed
20:00	7.49	13.50	5.05	1.06	0.9983	Passed
21:00	7.40	13.49	6.01	1.05	0.9989	Passed
22:00	7.34	13.49	6.98	0.99	0.9994	Passed
23:00	7.30	13.46	7.91	1.03	0.9995	Passed
0:00	7.27	13.45	8.89	1.06	0.9994	Passed
1:00	7.24	13.41	9.86	1.09	0.9990	Passed
2:00	7.20	13.43	10.78	0.92	0.9995	Passed
3:00	7.20	13.51	11.80	0.93	0.9976	Passed
4:00	-	-	-	-	-	In-convergence
5:00	-	-	-	-	-	In-convergence
6:00	-	-	-	-	-	In-convergence
7:00	-	-	-	-	-	In-convergence

Result of SIGMAPLOT processing: September 19, 2008 (Data IC)

<u>Data set: 18.00 hours, data IC</u>

Nonlinear Regression - Dynamic Fitting **Friday, July 23, 2010, 1:47:49 PM**

Data Source: Data 1 in Notebook9
Equation: Ligand Binding, sigmoidal dose-response (variable slope)
f=Tc + (Th-Tc)/(1+10^((C-x)*S))

Dynamic Fit Options:

Total Number of Fits	200
Maximum Number of Iterations	500

Parameter Ranges for Initial Estimates:

	Minimum	**Maximum**
Tc	-7.6479	22.9437
Th	-13.7291	41.1874
C	-3.1656	9.4968
S	-1.0000	3.0000

Summary of Fit Results:

Converged	100.0%
Singular Solutions	57.0%

Results for the Overall Best-Fit Solution:

R	**Rsqr**	**Adj Rsqr**	**Standard Error of Estimate**
0.9984	0.9968	0.9959	0.1488

	Coefficient	**Std. Error**	**t**	**P**
Tc	7.7339	0.1161	66.5987	<0.0001
Th	13.5444	0.0484	279.5875	<0.0001
C	3.1921	0.0494	64.5568	<0.0001
S	1.1052	0.1101	10.0382	<0.0001

Analysis of Variance: **(Appendix G.3 cont.)**

Analysis of Variance:

	DF	SS	MS
Regression	4	2161.9219	540.4805
Residual	10	0.2214	0.0221
Total	14	2162.1433	154.4388

Corrected for the mean of the observations:

	DF	SS	MS	F	P
Regression	3	69.7914	23.2638	1050.7709	<0.0001
Residual	10	0.2214	0.0221		
Total	13	70.0128	5.3856		

Statistical Tests:

Normality Test (Shapiro-Wilk) Passed (P = 0.2816)

W Statistic= 0.9275 Significance Level = 0.0500

Constant Variance Test Passed (P = 0.8676)

Data set: 19.00 hours, data IC (Appendix G.3 cont.)

Nonlinear Regression - Dynamic Fitting **Friday, July 23, 2010, 1:48:06 PM**

Data Source: Data 1 in Notebook9
Equation: Ligand Binding, sigmoidal dose-response (variable slope)
f=Tc + (Th-Tc)/(1+10^((C-x)*S))

Dynamic Fit Options:

Total Number of Fits	200
Maximum Number of Iterations	500

Parameter Ranges for Initial Estimates:

	Minimum	Maximum
Tc	-7.5313	22.5940
Th	-13.7171	41.1514
C	-4.1007	12.3020
S	-1.0000	3.0000

Summary of Fit Results:

Converged	100.0%
Singular Solutions	59.0%
Ill-Conditioned Solutions	0.5%

Results for the Overall Best-Fit Solution:

R	Rsqr	Adj Rsqr	Standard Error of Estimate
0.9992	0.9984	0.9979	0.1185

	Coefficient	Std. Error	t	P
Tc	7.5755	0.0749	101.2039	<0.0001
Th	13.5342	0.0409	330.8676	<0.0001
C	4.1009	0.0378	108.4637	<0.0001
S	1.0292	0.0706	14.5676	<0.0001

Analysis of Variance:
Analysis of Variance:

	DF	SS	MS
Regression	4	2035.0627	508.7657
Residual	10	0.1405	0.0140
Total	14	2035.2032	145.3717

Corrected for the mean of the observations:

	DF	SS	MS	F	P
Regression	3	87.9155	29.3052	2086.0444	<0.0001
Residual	10	0.1405	0.0140		
Total	13	88.0560	6.7735		

Statistical Tests:

Normality Test (Shapiro-Wilk)	Passed (P = 0.8488)
W Statistic= 0.9680	Significance Level = 0.0500
Constant Variance Test	Passed (P = 0.1835)

<u>Data set: 20.00 hours, data IC</u> **(Appendix G.3 cont.)**

Nonlinear Regression - Dynamic Fitting **Friday, July 23, 2010, 1:48:25 PM**

Data Source: Data 1 in Notebook9
Equation: Ligand Binding, sigmoidal dose-response (variable slope)
f=Tc + (Th-Tc)/(1+10^((C-x)*S))

Dynamic Fit Options:

Total Number of Fits	200
Maximum Number of Iterations	500

Parameter Ranges for Initial Estimates:

	Minimum	**Maximum**
Tc	-7.4283	22.2849
Th	-13.6765	41.0296
C	-5.0582	15.1747
S	-1.0000	3.0000

Summary of Fit Results:

Converged	100.0%
Singular Solutions	62.5%

Results for the Overall Best-Fit Solution:

R	**Rsqr**	**Adj Rsqr**	**Standard Error of Estimate**
0.9992	0.9983	0.9978	0.1303

	Coefficient	**Std. Error**	**t**	**P**
Tc	7.4853	0.0694	107.8836	<0.0001
Th	13.5047	0.0476	283.5246	<0.0001
C	5.0521	0.0397	127.3729	<0.0001
S	1.0615	0.0764	13.8878	<0.0001

Analysis of Variance:
Analysis of Variance:

	DF	**SS**	**MS**
Regression	4	1901.6078	475.4020
Residual	10	0.1697	0.0170
Total	14	1901.7775	135.8412

Corrected for the mean of the observations:

	DF	**SS**	**MS**	**F**	**P**
Regression	3	102.2105	34.0702	2007.9340	<0.0001
Residual	10	0.1697	0.0170		
Total	13	102.3802	7.8754		

Statistical Tests:

Normality Test (Shapiro-Wilk)	Passed (P = 0.7176)
W Statistic= 0.9597	Significance Level = 0.0500
Constant Variance Test	Passed (P = 0.2786)

Data set: 21.00 hours, data IC (Appendix G.3 cont.)

Nonlinear Regression - Dynamic Fitting **Friday, July 23, 2010, 1:48:44 PM**

Data Source: Data 1 in Notebook9
Equation: Ligand Binding, sigmoidal dose-response (variable slope)
f=Tc + (Th-Tc)/(1+10^((C-x)*S))

Dynamic Fit Options:

Total Number of Fits	200
Maximum Number of Iterations	500

Parameter Ranges for Initial Estimates:

	Minimum	Maximum
Tc	-7.3205	21.9616
Th	-13.6333	40.8998
C	-6.0174	18.0522
S	-1.0000	3.0000

Summary of Fit Results:

Converged	100.0%
Singular Solutions	64.5%

Results for the Overall Best-Fit Solution:

R	Rsqr	Adj Rsqr	Standard Error of Estimate
0.9995	0.9989	0.9986	0.1093

	Coefficient	Std. Error	t	P
Tc	7.3960	0.0516	143.2224	<0.0001
Th	13.4908	0.0430	314.0624	<0.0001
C	6.0113	0.0327	183.8060	<0.0001
S	1.0454	0.0615	16.9855	<0.0001

Analysis of Variance:
Analysis of Variance:

	DF	SS	MS
Regression	4	1768.7569	442.1892
Residual	10	0.1196	0.0120
Total	14	1768.8765	126.3483

Corrected for the mean of the observations:

	DF	SS	MS	F	P
Regression	3	112.0716	37.3572	3124.6535	<0.0001
Residual	10	0.1196	0.0120		
Total	13	112.1912	8.6301		

Statistical Tests:
Normality Test (Shapiro-Wilk) Passed (P = 0.4763)
W Statistic= 0.9443 Significance Level = 0.0500
Constant Variance Test Passed (P = 0.5520)

Data set: 22.00 hours, data IC **(Appendix G.3 cont.)**

Nonlinear Regression - Dynamic Fitting **Friday, July 23, 2010, 1:49:04 PM**

Data Source: Data 1 in Notebook9
Equation: Ligand Binding, sigmoidal dose-response (variable slope)
f=Tc + (Th-Tc)/(1+10^((C-x)*S))

Dynamic Fit Options:

Total Number of Fits	200
Maximum Number of Iterations	500

Parameter Ranges for Initial Estimates:

	Minimum	**Maximum**
Tc	-7.2489	21.7467
Th	-13.5899	40.7697
C	-6.9835	20.9506
S	-1.0000	3.0000

Summary of Fit Results:

Converged	100.0%
Singular Solutions	67.0%

Results for the Overall Best-Fit Solution:

R	**Rsqr**	**Adj Rsqr**	**Standard Error of Estimate**
0.9997	0.9994	0.9992	0.0818

	Coefficient	**Std. Error**	**t**	**P**
Tc	7.3402	0.0352	208.2555	<0.0001
Th	13.4863	0.0351	384.0484	<0.0001
C	6.9751	0.0247	282.7077	<0.0001
S	0.9927	0.0433	22.9193	<0.0001

Analysis of Variance:
Analysis of Variance:

	DF	**SS**	**MS**
Regression	4	1638.3229	409.5807
Residual	10	0.0669	0.0067
Total	14	1638.3898	117.0278

Corrected for the mean of the observations:

	DF	**SS**	**MS**	**F**	**P**
Regression	3	115.7808	38.5936	5772.5606	<0.0001
Residual	10	0.0669	0.0067		
Total	13	115.8476	8.9114		

Statistical Tests:

Normality Test (Shapiro-Wilk)	Passed (P = 0.3812)
W Statistic= 0.9370	Significance Level = 0.0500
Constant Variance Test	Passed (P = 0.4722)

Data set: 23.00 hours, data IC (Appendix G.3 cont.)

Nonlinear Regression - Dynamic Fitting **Friday, July 23, 2010, 1:49:23 PM**

Data Source: Data 1 in Notebook9
Equation: Ligand Binding, sigmoidal dose-response (variable slope)
f=Tc + (Th-Tc)/(1+10^((C-x)*S))

Dynamic Fit Options:

Total Number of Fits	200
Maximum Number of Iterations	500

Parameter Ranges for Initial Estimates:

	Minimum	Maximum
Tc	-7.2051	21.6152
Th	-13.5493	40.6479
C	-7.9295	23.7884
S	-1.0000	3.0000

Summary of Fit Results:

Converged	100.0%
Singular Solutions	69.0%

Results for the Overall Best-Fit Solution:

R	Rsqr	Adj Rsqr	Standard Error of Estimate
0.9998	0.9995	0.9994	0.0735

	Coefficient	Std. Error	t	P
Tc	7.3021	0.0290	251.3953	<0.0001
Th	13.4609	0.0346	388.9881	<0.0001
C	7.9114	0.0218	362.9134	<0.0001
S	1.0295	0.0412	25.0018	<0.0001

Analysis of Variance:
Analysis of Variance:

	DF	SS	MS
Regression	4	1510.3494	377.5874
Residual	10	0.0540	0.0054
Total	14	1510.4034	107.8860

Corrected for the mean of the observations:

	DF	SS	MS	F	P
Regression	3	114.6559	38.2186	7079.0717	<0.0001
Residual	10	0.0540	0.0054		
Total	13	114.7099	8.8238		

Statistical Tests:

Normality Test (Shapiro-Wilk)	Passed (P = 0.2524)
W Statistic= 0.9242	Significance Level = 0.0500
Constant Variance Test	Passed (P = 0.9396)

Data set: 00.00 hours, data IC (Appendix G.3 cont.)

Nonlinear Regression - Dynamic Fitting **Friday, July 23, 2010, 1:49:42 PM**

Data Source: Data 1 in Notebook9
Equation: Ligand Binding, sigmoidal dose-response (variable slope)
f=Tc + (Th-Tc)/(1+10^((C-x)*S))

Dynamic Fit Options:

Total Number of Fits	200
Maximum Number of Iterations	500

Parameter Ranges for Initial Estimates:

	Minimum	**Maximum**
Tc	-7.1631	21.4892
Th	-13.5276	40.5829
C	-8.9115	26.7345
S	-1.0000	3.0000

Summary of Fit Results:

Converged	100.0%
Singular Solutions	68.0%
Ill-Conditioned Solutions	0.5%

Results for the Overall Best-Fit Solution:

R	**Rsqr**	**Adj Rsqr**	**Standard Error of Estimate**
0.9997	0.9994	0.9993	0.0780

	Coefficient	**Std. Error**	**t**	**P**
Tc	7.2710	0.0286	254.0674	<0.0001
Th	13.4454	0.0413	325.2486	<0.0001
C	8.8882	0.0230	385.9494	<0.0001
S	1.0633	0.0462	23.0131	<0.0001

Analysis of Variance:
Analysis of Variance:

	DF	**SS**	**MS**
Regression	4	1379.6746	344.9187
Residual	10	0.0609	0.0061
Total	14	1379.7355	98.5525

Corrected for the mean of the observations:

	DF	**SS**	**MS**	**F**	**P**
Regression	3	108.3579	36.1193	5933.0644	<0.0001
Residual	10	0.0609	0.0061		
Total	13	108.4188	8.3399		

Statistical Tests:

Normality Test (Shapiro-Wilk)	Passed (P = 0.4880)
W Statistic= 0.9451	Significance Level = 0.0500
Constant Variance Test	Passed (P = 0.3236)

Data set: 01.00 hours, data IC (Appendix G.3 cont.)

Nonlinear Regression - Dynamic Fitting **Friday, July 23, 2010, 1:50:01 PM**

Data Source: Data 1 in Notebook9
Equation: Ligand Binding, sigmoidal dose-response (variable slope)
f=Tc + (Th-Tc)/(1+10^((C-x)*S))

Dynamic Fit Options:

Total Number of Fits	200
Maximum Number of Iterations	500

Parameter Ranges for Initial Estimates:

	Minimum	Maximum
Tc	-7.1291	21.3872
Th	-13.4859	40.4578
C	-9.8879	29.6637
S	-1.0000	3.0000

Summary of Fit Results:

Converged	100.0%
Singular Solutions	70.5%
Ill-Conditioned Solutions	0.5%

Results for the Overall Best-Fit Solution:

R	Rsqr	Adj Rsqr	Standard Error of Estimate
0.9995	0.9990	0.9987	0.0968

	Coefficient	Std. Error	t	P
Tc	7.2404	0.0333	217.3203	<0.0001
Th	13.4130	0.0599	223.7675	<0.0001
C	9.8568	0.0289	340.8787	<0.0001
S	1.0928	0.0618	17.6733	<0.0001

Analysis of Variance:
Analysis of Variance:

	DF	SS	MS
Regression	4	1248.1616	312.0404
Residual	10	0.0938	0.0094
Total	14	1248.2554	89.1611

Corrected for the mean of the observations:

	DF	SS	MS	F	P
Regression	3	96.2368	32.0789	3420.1724	<0.0001
Residual	10	0.0938	0.0094		
Total	13	96.3306	7.4100		

Statistical Tests:

Normality Test (Shapiro-Wilk)	Passed (P = 0.1163)
W Statistic= 0.9009	Significance Level = 0.0500
Constant Variance Test	Passed (P = 0.2311)

Data set: 02.00 hours, data IC (Appendix G.3 cont.)

Nonlinear Regression - Dynamic Fitting **Friday, July 23, 2010, 1:50:19 PM**

Data Source: Data 1 in Notebook9
Equation: Ligand Binding, sigmoidal dose-response (variable slope)
f=Tc + (Th-Tc)/(1+10^((C-x)*S))

Dynamic Fit Options:

Total Number of Fits	200
Maximum Number of Iterations	500

Parameter Ranges for Initial Estimates:

	Minimum	Maximum
Tc	-7.1068	21.3205
Th	-13.4108	40.2325
C	-10.7980	32.3939
S	-1.0000	3.0000

Summary of Fit Results:

Converged	100.0%
Singular Solutions	74.5%

Results for the Overall Best-Fit Solution:

R	Rsqr	Adj Rsqr	Standard Error of Estimate
0.9998	0.9995	0.9994	0.0603

	Coefficient	Std. Error	t	P
Tc	7.2042	0.0201	358.6855	<0.0001
Th	13.4320	0.0501	268.1027	<0.0001
C	10.7808	0.0206	523.9588	<0.0001
S	0.9172	0.0338	27.1143	<0.0001

Analysis of Variance:
Analysis of Variance:

	DF	SS	MS
Regression	4	1123.2739	280.8185
Residual	10	0.0364	0.0036
Total	14	1123.3103	80.2364

Corrected for the mean of the observations:

	DF	SS	MS	F	P
Regression	3	78.0147	26.0049	7140.2586	<0.0001
Residual	10	0.0364	0.0036		
Total	13	78.0511	6.0039		

Statistical Tests:

Normality Test (Shapiro-Wilk)	Passed (P = 0.6912)
W Statistic= 0.9581	Significance Level = 0.0500
Constant Variance Test	Passed (P = 0.6155)

Data set: 03.00 hours, data IC (Appendix G.3 cont.)

Nonlinear Regression - Dynamic Fitting **Friday, July 23, 2010, 1:50:35 PM**

Data Source: Data 1 in Notebook9
Equation: Ligand Binding, sigmoidal dose-response (variable slope)
f=Tc + (Th-Tc)/(1+10^((C-x)*S))

Dynamic Fit Options:

Total Number of Fits	200
Maximum Number of Iterations	500

Parameter Ranges for Initial Estimates:

	Minimum	Maximum
Tc	-7.0936	21.2807
Th	-13.2870	39.8610
C	-11.7941	35.3822
S	-1.0000	3.0000

Summary of Fit Results:

Converged	99.5%
Singular Solutions	78.0%
Iterations Exceeding 500	0.5%

Results for the Overall Best-Fit Solution:

R	Rsqr	Adj Rsqr	Standard Error of Estimate
0.9988	0.9976	0.9969	0.1152

	Coefficient	Std. Error	t	P
Tc	7.2021	0.0364	197.8757	<0.0001
Th	13.5131	0.1542	87.6516	<0.0001
C	11.8023	0.0471	250.7620	<0.0001
S	0.9292	0.0749	12.4117	<0.0001

Analysis of Variance:
Analysis of Variance:

	DF	SS	MS
Regression	4	996.7135	249.1784
Residual	10	0.1327	0.0133
Total	14	996.8463	71.2033

Corrected for the mean of the observations:

	DF	SS	MS	F	P
Regression	3	55.6822	18.5607	1398.5464	<0.0001
Residual	10	0.1327	0.0133		
Total	13	55.8149	4.2935		

Statistical Tests:
Normality Test (Shapiro-Wilk) Passed (P = 0.2989)
W Statistic= 0.9294 Significance Level = 0.0500
Constant Variance Test Passed (P = 0.0276)

G.4 Data May 8, 2009

Result Summary of SIGMAPLOT Analysis Data (IIA):

Charging Hour	T_c (°C)	T_h (°C)	C	S	R^2	Remarks
18:00	6.90	13.16	4.33	0.77	0.9952	Passed
19:00	6.95	13.12	5.65	0.84	0.9943	Passed
20:00	7.01	13.07	7.01	0.93	0.9962	Passed
21:00	7.01	12.97	8.34	1.12	0.9972	Passed
22:00	7.00	12.87	9.61	1.19	0.9978	Passed
23:00	6.98	12.71	10.84	1.12	0.9992	Passed
0:00	6.94	12.64	12.20	1.26	0.9989	Passed
1:00	-	-	-	-	-	In-convergence
2:00	-	-	-	-	-	In-convergence
3:00	-	-	-	-	-	In-convergence
4:00	-	-	-	-	-	In-convergence
5:00	-	-	-	-	-	In-convergence
6:00	-	-	-	-	-	In-convergence
7:00	-	-	-	-	-	In-convergence

Result of SIGMAPLOT processing: May 8, 2009 (Data IIA)

<u>Data set: 18.00 hours, data IIA</u>

Nonlinear Regression - Dynamic Fitting **Friday, July 23, 2010, 9:17:19 PM**

Data Source: Data 1 in Notebook10
Equation: Ligand Binding, sigmoidal dose-response (variable slope)
f=Tc + (Th-Tc)/(1+10^((C-x)*S))

Dynamic Fit Options:
Total Number of Fits 200
Maximum Number of Iterations 500

Parameter Ranges for Initial Estimates:

	Minimum	Maximum
Tc	-6.9300	20.7901
Th	-13.3201	39.9603
C	-4.3175	12.9524
S	-1.0000	3.0000

Summary of Fit Results:
Converged 100.0%
Singular Solutions 57.5%

Results for the Overall Best-Fit Solution:

R	Rsqr	Adj Rsqr	Standard Error of Estimate
0.9976	0.9952	0.9938	0.2136

	Coefficient	Std. Error	t	P
Tc	6.9013	0.1429	48.2837	<0.0001
Th	13.1627	0.0776	169.5945	<0.0001
C	4.3311	0.0754	57.4418	<0.0001
S	0.7737	0.0911	8.4902	<0.0001

Analysis of Variance: **(Appendix G.4 cont.)**

Analysis of Variance:

	DF	SS	MS
Regression	4	1860.7153	465.1788
Residual	10	0.4562	0.0456
Total	14	1861.1716	132.9408

Corrected for the mean of the observations:

	DF	SS	MS	F	P
Regression	3	95.1164	31.7055	694.9165	<0.0001
Residual	10	0.4562	0.0456		
Total	13	95.5726	7.3517		

Statistical Tests:

Normality Test (Shapiro-Wilk) Passed (P = 0.0074)

W Statistic= 0.8137 Significance Level = 0.0500

Constant Variance Test Passed (P = 0.0873)

Data set: 19.00 hours, data IIA (Appendix G.4 cont.)

Nonlinear Regression - Dynamic Fitting **Friday, July 23, 2010, 9:17:49 PM**

Data Source: Data 1 in Notebook10
Equation: Ligand Binding, sigmoidal dose-response (variable slope)
f=Tc + (Th-Tc)/(1+10^((C-x)*S))

Dynamic Fit Options:

Total Number of Fits	200
Maximum Number of Iterations	500

Parameter Ranges for Initial Estimates:

	Minimum	**Maximum**
Tc	-6.7678	20.3033
Th	-13.3014	39.9042
C	-5.6581	16.9742
S	-1.0000	3.0000

Summary of Fit Results:

Converged	100.0%
Singular Solutions	60.5%
Ill-Conditioned Solutions	0.5%

Results for the Overall Best-Fit Solution:

R	**Rsqr**	**Adj Rsqr**	**Standard Error of Estimate**
0.9971	0.9943	0.9926	0.2494

	Coefficient	**Std. Error**	**t**	**P**
Tc	6.9476	0.1290	53.8505	<0.0001
Th	13.1195	0.0987	132.9801	<0.0001
C	5.6478	0.0808	69.9199	<0.0001
S	0.8388	0.1174	7.1427	<0.0001

Analysis of Variance:
Analysis of Variance:

	DF	**SS**	**MS**
Regression	4	1691.6803	422.9201
Residual	10	0.6221	0.0622
Total	14	1692.3024	120.8787

Corrected for the mean of the observations:

	DF	**SS**	**MS**	**F**	**P**
Regression	3	108.5358	36.1786	581.5638	<0.0001
Residual	10	0.6221	0.0622		
Total	13	109.1579	8.3968		

Statistical Tests:

Normality Test (Shapiro-Wilk)	Passed (P = 0.0253)
W Statistic= 0.8542	Significance Level = 0.0500
Constant Variance Test	Passed (P = 0.6047)

Data set: 20.00 hours, data IIA (Appendix G.4 cont.)

Nonlinear Regression - Dynamic Fitting **Friday, July 23, 2010, 9:18:45 PM**

Data Source: Data 1 in Notebook10
Equation: Ligand Binding, sigmoidal dose-response (variable slope)
f=Tc + (Th-Tc)/(1+10^((C-x)*S))

Dynamic Fit Options:

Total Number of Fits	200
Maximum Number of Iterations	500

Parameter Ranges for Initial Estimates:

	Minimum	Maximum
Tc	-6.9007	20.7020
Th	-13.2685	39.8054
C	-7.0181	21.0544
S	-1.0000	3.0000

Summary of Fit Results:

Converged	100.0%
Singular Solutions	66.5%
Ill-Conditioned Solutions	0.5%

Results for the Overall Best-Fit Solution:

R	Rsqr	Adj Rsqr	Standard Error of Estimate
0.9981	0.9962	0.9950	0.2070

	Coefficient	Std. Error	t	P
Tc	7.0086	0.0899	77.9645	<0.0001
Th	13.0669	0.0899	145.2717	<0.0001
C	7.0148	0.0652	107.5497	<0.0001
S	0.9332	0.1041	8.9628	<0.0001

Analysis of Variance:
Analysis of Variance:

	DF	SS	MS
Regression	4	1521.4564	380.3641
Residual	10	0.4284	0.0428
Total	14	1521.8848	108.7061

Corrected for the mean of the observations:

	DF	SS	MS	F	P
Regression	3	111.4461	37.1487	867.0955	<0.0001
Residual	10	0.4284	0.0428		
Total	13	111.8745	8.6057		

Statistical Tests:
Normality Test (Shapiro-Wilk) Passed (P = 0.0565)
W Statistic= 0.8792 Significance Level = 0.0500
Constant Variance Test Passed (P = 0.0262)

Data set: 21.00 hours, data IIA

Nonlinear Regression - Dynamic Fitting **Friday, July 23, 2010, 9:19:08 PM**

Data Source: Data 1 in Notebook10
Equation: Ligand Binding, sigmoidal dose-response (variable slope)
f=Tc + (Th-Tc)/(1+10^((C-x)*S))

Dynamic Fit Options:

Total Number of Fits	200
Maximum Number of Iterations	500

Parameter Ranges for Initial Estimates:

	Minimum	**Maximum**
Tc	-6.9554	20.8662
Th	-13.2423	39.7268
C	-8.3084	24.9253
S	-1.0000	3.0000

Summary of Fit Results:

Converged	99.5%
Singular Solutions	66.5%
Iterations Exceeding 500	0.5%

Results for the Overall Best-Fit Solution:

R	**Rsqr**	**Adj Rsqr**	**Standard Error of Estimate**
0.9986	0.9972	0.9964	0.1713

	Coefficient	**Std. Error**	**t**	**P**
Tc	7.0148	0.0660	106.2604	<0.0001
Th	12.9740	0.0825	157.2291	<0.0001
C	8.3356	0.0477	174.7910	<0.0001
S	1.1167	0.1317	8.4780	<0.0001

Analysis of Variance:
Analysis of Variance:

	DF	**SS**	**MS**
Regression	4	1351.1699	337.7925
Residual	10	0.2935	0.0294
Total	14	1351.4634	96.5331

Corrected for the mean of the observations:

	DF	**SS**	**MS**	**F**	**P**
Regression	3	105.9490	35.3163	1203.1272	<0.0001
Residual	10	0.2935	0.0294		
Total	13	106.2425	8.1725		

Statistical Tests:

Normality Test (Shapiro-Wilk)	Passed (P = 0.9023)
W Statistic= 0.9720	Significance Level = 0.0500
Constant Variance Test	Passed (P = 0.0492)

Data set: 22.00 hours, data IIA (Appendix G.4 cont.)

Nonlinear Regression - Dynamic Fitting **Friday, July 23, 2010, 9:19:34 PM**

Data Source: Data 1 in Notebook10
Equation: Ligand Binding, sigmoidal dose-response (variable slope)
f=Tc + (Th-Tc)/(1+10^((C-x)*S))

Dynamic Fit Options:

Total Number of Fits	200
Maximum Number of Iterations	500

Parameter Ranges for Initial Estimates:

	Minimum	Maximum
Tc	-6.9380	20.8140
Th	-13.1740	39.5221
C	-9.6873	29.0619
S	-1.0000	3.0000

Summary of Fit Results:

Converged	99.5%
Singular Solutions	69.5%
Iterations Exceeding 500	0.5%

Results for the Overall Best-Fit Solution:

R	Rsqr	Adj Rsqr	Standard Error of Estimate
0.9989	0.9978	0.9971	0.1427

	Coefficient	Std. Error	t	P
Tc	6.9978	0.0497	140.8827	<0.0001
Th	12.8686	0.0839	153.3624	<0.0001
C	9.6102	0.0388	247.5425	<0.0001
S	1.1904	0.1410	8.4424	<0.0001

Analysis of Variance:
Analysis of Variance:

	DF	SS	MS
Regression	4	1185.7017	296.4254
Residual	10	0.2037	0.0204
Total	14	1185.9054	84.7075

Corrected for the mean of the observations:

	DF	SS	MS	F	P
Regression	3	91.1672	30.3891	1491.7205	<0.0001
Residual	10	0.2037	0.0204		
Total	13	91.3710	7.0285		

Statistical Tests:

Normality Test (Shapiro-Wilk)	Passed (P = 0.0434)
W Statistic= 0.8710	Significance Level = 0.0500
Constant Variance Test	Passed (P = 0.5015)

Data set: 23.00 hours, data IIA **(Appendix G.4 cont.)**

Nonlinear Regression - Dynamic Fitting **Friday, July 23, 2010, 9:20:00 PM**

Data Source: Data 1 in Notebook10
Equation: Ligand Binding, sigmoidal dose-response (variable slope)
f=Tc + (Th-Tc)/(1+10^((C-x)*S))

Dynamic Fit Options:

Total Number of Fits	200
Maximum Number of Iterations	500

Parameter Ranges for Initial Estimates:

	Minimum	**Maximum**
Tc	-6.8973	20.6920
Th	-12.8089	38.4266
C	-10.8755	32.6266
S	-1.0000	3.0000

Summary of Fit Results:

Converged	100.0%
Singular Solutions	74.5%

Results for the Overall Best-Fit Solution:

R	**Rsqr**	**Adj Rsqr**	**Standard Error of Estimate**
0.9996	0.9992	0.9990	0.0717

	Coefficient	**Std. Error**	**t**	**P**
Tc	6.9755	0.0233	299.4153	<0.0001
Th	12.7142	0.0558	227.9030	<0.0001
C	10.8388	0.0240	450.8816	<0.0001
S	1.1207	0.0541	20.7143	<0.0001

Analysis of Variance:
Analysis of Variance:

	DF	**SS**	**MS**
Regression	4	1026.6270	256.6568
Residual	10	0.0514	0.0051
Total	14	1026.6784	73.3342

Corrected for the mean of the observations:

	DF	**SS**	**MS**	**F**	**P**
Regression	3	68.0719	22.6906	4416.5451	<0.0001
Residual	10	0.0514	0.0051		
Total	13	68.1233	5.2403		

Statistical Tests:

Normality Test (Shapiro-Wilk)	Passed (P = 0.7991)
W Statistic= 0.9647	Significance Level = 0.0500
Constant Variance Test	Passed (P = 0.8676)

Data set: 00.00 hours, data IIA (Appendix G.4 cont.)

Nonlinear Regression - Dynamic Fitting **Friday, July 23, 2010, 9:20:22 PM**

Data Source: Data 1 in Notebook10
Equation: Ligand Binding, sigmoidal dose-response (variable slope)
f=Tc + (Th-Tc)/(1+10^((C-x)*S))

Dynamic Fit Options:

Total Number of Fits	200
Maximum Number of Iterations	500

Parameter Ranges for Initial Estimates:

	Minimum	Maximum
Tc	-6.8509	20.5528
Th	-12.5151	37.5453
C	-12.1240	36.3719
S	-1.0000	3.0000

Summary of Fit Results:

Converged	99.0%
Singular Solutions	80.0%
Ill-Conditioned Solutions	0.5%
Iterations Exceeding 500	1.0%

Results for the Overall Best-Fit Solution:

R	Rsqr	Adj Rsqr	Standard Error of Estimate
0.9994	0.9989	0.9985	0.0675

	Coefficient	Std. Error	t	P
Tc	6.9431	0.0206	337.1417	<0.0001
Th	12.6413	0.0822	153.8631	<0.0001
C	12.2021	0.0233	524.2921	<0.0001
S	1.2635	0.0619	20.4007	<0.0001

Analysis of Variance:
Analysis of Variance:

	DF	SS	MS
Regression	4	866.3026	216.5757
Residual	10	0.0455	0.0046
Total	14	866.3481	61.8820

Corrected for the mean of the observations:

	DF	SS	MS	F	P
Regression	3	40.2662	13.4221	2949.2537	<0.0001
Residual	10	0.0455	0.0046		
Total	13	40.3117	3.1009		

Statistical Tests:

Normality Test (Shapiro-Wilk)	Passed (P = 0.8014)
W Statistic= 0.9649	Significance Level = 0.0500
Constant Variance Test	Passed (P = 0.2064)

G.5 June 22, 2008

Result Summary of SIGMAPLOT Analysis Data (IIB):

Charging Hour	T_c (°C)	T_h (°C)	C	S	R^2	Remarks
19:00	7.59	13.97	2.83	1.17	0.9994	Passed
20:00	7.31	13.86	3.86	1.17	0.9974	Passed
21:00	7.21	13.76	4.95	1.33	0.9934	Passed
22:00	7.10	13.69	6.08	1.32	0.9959	Passed
23:00	7.03	13.65	7.27	1.26	0.9979	Passed
0:00	6.97	13.61	8.45	1.25	0.9989	Passed
1:00	6.93	13.55	9.63	1.30	0.9992	Passed
2:00	6.90	13.46	10.79	1.19	0.9994	Passed
3:00	6.88	13.48	12.13	1.23	0.9974	Passed
4:00	-	-	-	-	-	In-convergence
5:00	-	-	-	-	-	In-convergence
6:00	-	-	-	-	-	In-convergence

Result of SIGMAPLOT processing: June 22, 2008 (Data IIB)

<u>Data set: 19.00 hours, data IIB</u>

Nonlinear Regression - Dynamic Fitting **Friday, July 23, 2010, 10:21:02 PM**

Data Source: Data 1 in June22_DATA.JNB
Equation: Ligand Binding, sigmoidal dose-response (variable slope)
f=Tc + (Th-Tc)/(1+10^((C-x)*S))

Dynamic Fit Options:

Total Number of Fits	200
Maximum Number of Iterations	500

Parameter Ranges for Initial Estimates:

	Minimum	**Maximum**
Tc	-7.5609	22.6827
Th	-14.8668	44.6005
C	-2.9831	8.9493
S	-1.0000	3.0000

Summary of Fit Results:

Converged	100.0%
Singular Solutions	53.0%
Ill-Conditioned Solutions	0.5%

Results for the Overall Best-Fit Solution:

R	**Rsqr**	**Adj Rsqr**	**Standard Error of Estimate**
0.9866	0.9994	0.9654	0.4581

	Coefficient	**Std. Error**	**t**	**P**
Tc	7.5888	0.3682	20.6114	<0.0001
Th	13.9653	0.1473	94.7931	<0.0001
C	2.8326	0.1310	21.6250	<0.0001
S	1.1682	0.3147	3.7121	0.0040

Analysis of Variance: **(Appendix G.5 cont.)**

Analysis of Variance:

	DF	SS	MS
Regression	4	2327.1084	581.7771
Residual	10	2.0990	0.2099
Total	14	2329.2073	166.3720

Corrected for the mean of the observations:

	DF	SS	MS	F	P
Regression	3	76.7136	25.5712	121.8271	<0.0001
Residual	10	2.0990	0.2099		
Total	13	78.8126	6.0625		

Statistical Tests:

Normality Test (Shapiro-Wilk) Passed (P = 0.6042)

W Statistic= 0.9528 Significance Level = 0.0500

Constant Variance Test Passed (P = 0.0941)

Data set: 20.00 hours, data IIB (Appendix G.5 cont.)

Nonlinear Regression - Dynamic Fitting **Friday, July 23, 2010, 10:21:21 PM**

Data Source: Data 1 in June22_DATA.JNB
Equation: Ligand Binding, sigmoidal dose-response (variable slope)
f=Tc + (Th-Tc)/(1+10^((C-x)*S))

Dynamic Fit Options:

Total Number of Fits	200
Maximum Number of Iterations	500

Parameter Ranges for Initial Estimates:

	Minimum	Maximum
Tc	-7.2990	21.8970
Th	-14.5953	43.7859
C	-3.9824	11.9472
S	-1.0000	3.0000

Summary of Fit Results:

Converged	100.0%
Singular Solutions	56.0%
Ill-Conditioned Solutions	0.5%

Results for the Overall Best-Fit Solution:

R	Rsqr	Adj Rsqr	Standard Error of Estimate
0.9937	0.9974	0.9836	0.3645

	Coefficient	Std. Error	t	P
Tc	7.3097	0.2277	32.0997	<0.0001
Th	13.8565	0.1238	111.9582	<0.0001
C	3.8590	0.0983	39.2575	<0.0001
S	1.1692	0.2319	5.0424	0.0005

Analysis of Variance:
Analysis of Variance:

	DF	SS	MS
Regression	4	2138.5889	534.6472
Residual	10	1.3283	0.1328
Total	14	2139.9172	152.8512

Corrected for the mean of the observations:

	DF	SS	MS	F	P
Regression	3	103.9228	34.6409	260.7967	<0.0001
Residual	10	1.3283	0.1328		
Total	13	105.2510	8.0962		

Statistical Tests:

Normality Test (Shapiro-Wilk)	Passed (P = 0.2474)
W Statistic= 0.9236	Significance Level = 0.0500
Constant Variance Test	Passed (P = 0.0907)

Data set: 21.00 hours, data IIB (Appendix G.5 cont.)

Nonlinear Regression - Dynamic Fitting **Friday, July 23, 2010, 10:21:37 PM**

Data Source: Data 1 in June22_DATA.JNB
Equation: Ligand Binding, sigmoidal dose-response (variable slope)
f=Tc + (Th-Tc)/(1+10^((C-x)*S))

Dynamic Fit Options:

Total Number of Fits	200
Maximum Number of Iterations	500

Parameter Ranges for Initial Estimates:

	Minimum	Maximum
Tc	-7.1540	21.4621
Th	-14.2428	42.7283
C	-5.0182	15.0545
S	-1.0000	3.0000

Summary of Fit Results:

Converged	100.0%
Singular Solutions	58.5%

Results for the Overall Best-Fit Solution:

R	Rsqr	Adj Rsqr	Standard Error of Estimate
0.9967	0.9934	0.9914	0.2865

	Coefficient	Std. Error	t	P
Tc	7.2117	0.1480	48.7298	<0.0001
Th	13.7567	0.1028	133.8562	<0.0001
C	4.9539	0.0758	65.3563	<0.0001
S	1.3311	0.1951	6.8223	<0.0001

Analysis of Variance:
Analysis of Variance:

	DF	SS	MS
Regression	4	1957.2087	489.3022
Residual	10	0.8205	0.0821
Total	14	1958.0292	139.8592

Corrected for the mean of the observations:

	DF	SS	MS	F	P
Regression	3	123.5860	41.1953	502.0490	<0.0001
Residual	10	0.8205	0.0821		
Total	13	124.4066	9.5697		

Statistical Tests:
Normality Test (Shapiro-Wilk) Passed (P = 0.5579)
W Statistic= 0.9498 Significance Level = 0.0500
Constant Variance Test Passed (P = 0.0276)

Data set: 22.00 hours, data IIB (Appendix G.5 cont.)

Nonlinear Regression - Dynamic Fitting **Friday, July 23, 2010, 10:21:54 PM**

Data Source: Data 1 in June22_DATA.JNB
Equation: Ligand Binding, sigmoidal dose-response (variable slope)
f=Tc + (Th-Tc)/(1+10^((C-x)*S))

Dynamic Fit Options:

Total Number of Fits	200
Maximum Number of Iterations	500

Parameter Ranges for Initial Estimates:

	Minimum	Maximum
Tc	-7.0348	21.1045
Th	-14.0339	42.1017
C	-6.0882	18.2646
S	-1.0000	3.0000

Summary of Fit Results:

Converged	100.0%
Singular Solutions	61.5%

Results for the Overall Best-Fit Solution:

R	Rsqr	Adj Rsqr	Standard Error of Estimate
0.9980	0.9959	0.9947	0.2354

	Coefficient	Std. Error	t	P
Tc	7.1042	0.1078	65.9091	<0.0001
Th	13.6880	0.0907	150.9397	<0.0001
C	6.0811	0.0617	98.6205	<0.0001
S	1.3225	0.1599	8.2713	<0.0001

Analysis of Variance:
Analysis of Variance:

	DF	SS	MS
Regression	4	1778.6205	444.6551
Residual	10	0.5539	0.0554
Total	14	1779.1744	127.0839

Corrected for the mean of the observations:

	DF	SS	MS	F	P
Regression	3	135.2982	45.0994	814.1903	<0.0001
Residual	10	0.5539	0.0554		
Total	13	135.8521	10.4502		

Statistical Tests:

Normality Test (Shapiro-Wilk)	Passed (P = 0.7448)
W Statistic= 0.9613	Significance Level = 0.0500
Constant Variance Test	Passed (P = 0.0021)

Nonlinear Regression - Dynamic Fitting **Friday, July 23, 2010, 10:22:13 PM**

Data Source: Data 1 in June22_DATA.JNB
Equation: Ligand Binding, sigmoidal dose-response (variable slope)
f=Tc + (Th-Tc)/(1+10^((C-x)*S))

Dynamic Fit Options:

Total Number of Fits	200
Maximum Number of Iterations	500

Parameter Ranges for Initial Estimates:

	Minimum	Maximum
Tc	-6.9511	20.8533
Th	-13.9287	41.7860
C	-7.2356	21.7069
S	-1.0000	3.0000

Summary of Fit Results:

Converged	100.0%
Singular Solutions	66.0%

Results for the Overall Best-Fit Solution:

R	Rsqr	Adj Rsqr	Standard Error of Estimate
0.9990	0.9979	0.9973	0.1690

	Coefficient	Std. Error	t	P
Tc	7.0262	0.0702	100.0643	<0.0001
Th	13.6541	0.0716	190.8154	<0.0001
C	7.2703	0.0416	174.9612	<0.0001
S	1.2645	0.1353	9.3425	<0.0001

Analysis of Variance:
Analysis of Variance:

	DF	SS	MS
Regression	4	1600.5018	400.1255
Residual	10	0.2856	0.0286
Total	14	1600.7874	114.3420

Corrected for the mean of the observations:

	DF	SS	MS	F	P
Regression	3	138.4284	46.1428	1615.8644	<0.0001
Residual	10	0.2856	0.0286		
Total	13	138.7140	10.6703		

Statistical Tests:

Normality Test (Shapiro-Wilk)	Passed (P = 0.8717)
W Statistic= 0.9696	Significance Level = 0.0500
Constant Variance Test	Passed (P = <0.0001)

Nonlinear Regression - Dynamic Fitting **Friday, July 23, 2010, 10:22:55 PM**

Data Source: Data 1 in June22_DATA.JNB
Equation: Ligand Binding, sigmoidal dose-response (variable slope)
f=Tc + (Th-Tc)/(1+10^((C-x)*S))

Dynamic Fit Options:

Total Number of Fits	200
Maximum Number of Iterations	500

Parameter Ranges for Initial Estimates:

	Minimum	Maximum
Tc	-6.8984	20.6952
Th	-13.8664	41.5993
C	-8.4382	25.3147
S	-1.0000	3.0000

Summary of Fit Results:

Converged	99.5%
Singular Solutions	66.0%
Ill-Conditioned Solutions	0.5%
Iterations Exceeding 500	0.5%

Results for the Overall Best-Fit Solution:

R	Rsqr	Adj Rsqr	Standard Error of Estimate
0.9994	0.9989	0.9986	0.1213

	Coefficient	Std. Error	t	P
Tc	6.9700	0.0459	151.8796	<0.0001
Th	13.6089	0.0587	231.9354	<0.0001
C	8.4475	0.0266	317.1781	<0.0001
S	1.2528	0.1192	10.5136	<0.0001

Analysis of Variance:
Analysis of Variance:

	DF	SS	MS
Regression	4	1424.6394	356.1598
Residual	10	0.1470	0.0147
Total	14	1424.7864	101.7705

Corrected for the mean of the observations:

	DF	SS	MS	F	P
Regression	3	132.0835	44.0278	2994.2366	<0.0001
Residual	10	0.1470	0.0147		
Total	13	132.2305	10.1716		

Statistical Tests:

Normality Test (Shapiro-Wilk)	Passed (P = 0.3730)
W Statistic= 0.9363	Significance Level = 0.0500
Constant Variance Test	Passed (P = 0.0131)

Data set: 01.00 hours, data IIB (Appendix G.5 cont.)

Nonlinear Regression - Dynamic Fitting **Friday, July 23, 2010, 10:23:11 PM**

Data Source: Data 1 in June22_DATA.JNB
Equation: Ligand Binding, sigmoidal dose-response (variable slope)
f=Tc + (Th-Tc)/(1+10^((C-x)*S))

Dynamic Fit Options:

Total Number of Fits	200
Maximum Number of Iterations	500

Parameter Ranges for Initial Estimates:

	Minimum	Maximum
Tc	-6.8580	20.5741
Th	-13.7175	41.1526
C	-9.6937	29.0812
S	-1.0000	3.0000

Summary of Fit Results:

Converged	99.5%
Singular Solutions	70.5%
Iterations Exceeding 500	0.5%

Results for the Overall Best-Fit Solution:

R	Rsqr	Adj Rsqr	Standard Error of Estimate
0.9996	0.9992	0.9989	0.0976

	Coefficient	Std. Error	t	P
Tc	6.9349	0.0336	206.1837	<0.0001
Th	13.5477	0.0570	237.8016	<0.0001
C	9.6271	0.0227	424.6704	<0.0001
S	1.3004	0.1039	12.5118	<0.0001

Analysis of Variance:
Analysis of Variance:

	DF	SS	MS
Regression	4	1251.4363	312.8591
Residual	10	0.0952	0.0095
Total	14	1251.5314	89.3951

Corrected for the mean of the observations:

	DF	SS	MS	F	P
Regression	3	116.6008	38.8669	4084.2659	<0.0001
Residual	10	0.0952	0.0095		
Total	13	116.6959	8.9766		

Statistical Tests:
Normality Test (Shapiro-Wilk) Passed (P = 0.9846)
W Statistic= 0.9820 Significance Level = 0.0500
Constant Variance Test Passed (P = 0.0977)

Nonlinear Regression - Dynamic Fitting **Friday, July 23, 2010, 10:23:33 PM**

Data Source: Data 1 in June22_DATA.JNB
Equation: Ligand Binding, sigmoidal dose-response (variable slope)
f=Tc + (Th-Tc)/(1+10^((C-x)*S))

Dynamic Fit Options:

Total Number of Fits	200
Maximum Number of Iterations	500

Parameter Ranges for Initial Estimates:

	Minimum	Maximum
Tc	-6.8115	20.4346
Th	-13.4818	40.4454
C	-10.8322	32.4965
S	-1.0000	3.0000

Summary of Fit Results:

Converged	100.0%
Singular Solutions	73.5%
Ill-Conditioned Solutions	0.5%

Results for the Overall Best-Fit Solution:

R	Rsqr	Adj Rsqr	Standard Error of Estimate
0.9997	0.9994	0.9992	0.0725

	Coefficient	Std. Error	t	P
Tc	6.8973	0.0235	293.3831	<0.0001
Th	13.4617	0.0552	243.8163	<0.0001
C	10.7925	0.0206	523.8101	<0.0001
S	1.1850	0.0544	21.7851	<0.0001

Analysis of Variance:
Analysis of Variance:

	DF	SS	MS
Regression	4	1079.8695	269.9674
Residual	10	0.0526	0.0053
Total	14	1079.9220	77.1373

Corrected for the mean of the observations:

	DF	SS	MS	F	P
Regression	3	90.9826	30.3275	5769.7938	<0.0001
Residual	10	0.0526	0.0053		
Total	13	91.0352	7.0027		

Statistical Tests:

Normality Test (Shapiro-Wilk)	Passed (P = 0.4298)
W Statistic= 0.9409	Significance Level = 0.0500
Constant Variance Test	Passed (P = 0.6704)

Data set: 03.00 hours, data IIB (Appendix G.5 cont.)

Nonlinear Regression - Dynamic Fitting **Friday, July 23, 2010, 10:23:54 PM**

Data Source: Data 1 in June22_DATA.JNB
Equation: Ligand Binding, sigmoidal dose-response (variable slope)
f=Tc + (Th-Tc)/(1+10^((C-x)*S))

Dynamic Fit Options:

Total Number of Fits	200
Maximum Number of Iterations	500

Parameter Ranges for Initial Estimates:

	Minimum	Maximum
Tc	-6.7449	20.2347
Th	-13.3459	40.0376
C	-12.0684	36.2053
S	-1.0000	3.0000

Summary of Fit Results:

Converged	99.5%
Singular Solutions	79.0%
Iterations Exceeding 500	0.5%

Results for the Overall Best-Fit Solution:

R	Rsqr	Adj Rsqr	Standard Error of Estimate
0.9987	0.9974	0.9966	0.1215

	Coefficient	Std. Error	t	P
Tc	6.8752	0.0372	185.0389	<0.0001
Th	13.4839	0.1470	91.7554	<0.0001
C	12.1302	0.0380	319.2754	<0.0001
S	1.2332	0.0874	14.1054	<0.0001

Analysis of Variance:
Analysis of Variance:

	DF	SS	MS
Regression	4	900.2102	225.0525
Residual	10	0.1477	0.0148
Total	14	900.3579	64.3113

Corrected for the mean of the observations:

	DF	SS	MS	F	P
Regression	3	56.1792	18.7264	1267.9922	<0.0001
Residual	10	0.1477	0.0148		
Total	13	56.3269	4.3328		

Statistical Tests:

Normality Test (Shapiro-Wilk)	Passed (P = 0.0315)
W Statistic= 0.8611	Significance Level = 0.0500
Constant Variance Test	Passed (P = 0.5520)

G.6 June 24, 2008

Result Summary of SIGMAPLOT Analysis Data (IIC):

Charging Hour	T_c (^oC)	T_h (^oC)	C	S	R^2	Remarks
19:00	7.52	14.29	2.93	1.43	0.9942	Passed
20:00	7.30	14.25	4.01	1.36	0.9951	Passed
21:00	7.18	14.18	5.10	1.49	0.9968	Passed
22:00	7.05	14.14	6.18	1.31	0.9922	Passed
23:00	6.98	14.09	7.27	1.30	0.9949	Passed
0:00	6.94	14.00	8.36	1.37	0.9964	Passed
1:00	6.90	13.90	9.44	1.20	0.9986	Passed
2:00	6.87	13.77	10.52	1.25	0.9993	Passed
3:00	6.86	13.75	11.79	1.33	0.9968	Passed
4:00	-	-	-	-	-	In-convergence
5:00	-	-	-	-	-	In-convergence
6:00	-	-	-	-	-	In-convergence

Result of SIGMAPLOT processing: June 24, 2008 (Data IIC)

Data set: 19.00 hours, data IIC

Nonlinear Regression - Dynamic Fitting **Saturday, August 28, 2010, 6:10:48 PM**

Data Source: Data 1 in Notebook1
Equation: Ligand Binding, sigmoidal dose-response (variable slope)
f=Tc + (Th-Tc)/(1+10^((C-x)*S))

Dynamic Fit Options:

Total Number of Fits	200
Maximum Number of Iterations	500

Parameter Ranges for Initial Estimates:

	Minimum	**Maximum**
Tc	-7.4443	22.3328
Th	-14.6580	43.9740
C	-2.9869	8.9606
S	-1.0000	3.0000

Summary of Fit Results:

Converged	100.0%
Singular Solutions	55.0%

Results for the Overall Best-Fit Solution:

R	**Rsqr**	**Adj Rsqr**	**Standard Error of Estimate**
0.9921	0.9842	0.9794	0.3867

	Coefficient	**Std. Error**	**t**	**P**
Tc	7.5210	0.2880	26.1163	<0.0001
Th	14.2918	0.1234	115.8335	<0.0001
C	2.9331	0.1033	28.4004	<0.0001
S	1.4334	0.2893	4.9547	0.0006

Analysis of Variance: **(Appendix G.6 cont.)**

Analysis of Variance:

	DF	SS	MS
Regression	4	2414.0479	603.5120
Residual	10	1.4954	0.1495
Total	14	2415.5433	172.5388

Corrected for the mean of the observations:

	DF	SS	MS	F	P
Regression	3	92.9967	30.9989	207.2948	<0.0001
Residual	10	1.4954	0.1495		
Total	13	94.4921	7.2686		

Statistical Tests:

Normality Test (Shapiro-Wilk) Passed (P = 0.0343)

W Statistic= 0.8637 Significance Level = 0.0500

Constant Variance Test Passed (P = 0.1524)

Data set: 20.00 hours, data IIC (Appendix G.6 cont.)

Nonlinear Regression - Dynamic Fitting **Saturday, August 28, 2010, 6:11:08 PM**

Data Source: Data 1 in Notebook1
Equation: Ligand Binding, sigmoidal dose-response (variable slope)
f=Tc + (Th-Tc)/(1+10^((C-x)*S))

Dynamic Fit Options:

Total Number of Fits	200
Maximum Number of Iterations	500

Parameter Ranges for Initial Estimates:

	Minimum	Maximum
Tc	-7.2616	21.7848
Th	-14.6206	43.8617
C	-4.0404	12.1212
S	-1.0000	3.0000

Summary of Fit Results:

Converged	100.0%
Singular Solutions	54.5%

Results for the Overall Best-Fit Solution:

R	Rsqr	Adj Rsqr	Standard Error of Estimate
0.9940	0.9881	0.9845	0.3854

	Coefficient	Std. Error	t	P
Tc	7.3021	0.2312	31.5889	<0.0001
Th	14.2510	0.1301	109.5615	<0.0001
C	4.0090	0.0983	40.7975	<0.0001
S	1.3640	0.2540	5.3704	0.0003

Analysis of Variance:
Analysis of Variance:

	DF	SS	MS
Regression	4	2229.6780	557.4195
Residual	10	1.4851	0.1485
Total	14	2231.1630	159.3688

Corrected for the mean of the observations:

	DF	SS	MS	F	P
Regression	3	123.2878	41.0959	276.7277	<0.0001
Residual	10	1.4851	0.1485		
Total	13	124.7729	9.5979		

Statistical Tests:

Normality Test (Shapiro-Wilk)	Passed (P = 0.0210)
W Statistic= 0.8482	Significance Level = 0.0500
Constant Variance Test	Passed (P = 0.0778)

Data set: 21.00 hours, data IIC (Appendix G.6 cont.)

Nonlinear Regression - Dynamic Fitting **Saturday, August 28, 2010, 6:11:32 PM**

Data Source: Data 1 in Notebook1
Equation: Ligand Binding, sigmoidal dose-response (variable slope)
f=Tc + (Th-Tc)/(1+10^((C-x)*S))

Dynamic Fit Options:

Total Number of Fits	200
Maximum Number of Iterations	500

Parameter Ranges for Initial Estimates:

	Minimum	Maximum
Tc	-7.1160	21.3479
Th	-14.5652	43.6955
C	-5.1016	15.3047
S	-1.0000	3.0000

Summary of Fit Results:

Converged	100.0%
Singular Solutions	59.5%

Results for the Overall Best-Fit Solution:

R	Rsqr	Adj Rsqr	Standard Error of Estimate
0.9949	0.9898	0.9868	0.3861

	Coefficient	Std. Error	t	P
Tc	7.1800	0.1968	36.4929	<0.0001
Th	14.1823	0.1380	102.7524	<0.0001
C	5.1043	0.0969	52.6635	<0.0001
S	1.4875	0.2968	5.0119	0.0005

Analysis of Variance:
Analysis of Variance:

	DF	SS	MS
Regression	4	2041.3813	510.3453
Residual	10	1.4906	0.1491
Total	14	2042.8719	145.9194

Corrected for the mean of the observations:

	DF	SS	MS	F	P
Regression	3	145.3496	48.4499	325.0388	<0.0001
Residual	10	1.4906	0.1491		
Total	13	146.8402	11.2954		

Statistical Tests:

Normality Test (Shapiro-Wilk) Passed (P = 0.0781)
W Statistic= 0.8890 Significance Level = 0.0500
Constant Variance Test Passed (P = 0.0108)

<u>Data set: 22.00 hours, data IIC</u> **(Appendix G.6 cont.)**

Nonlinear Regression - Dynamic Fitting **Saturday, August 28, 2010, 6:11:55 PM**

Data Source: Data 1 in Notebook1
Equation: Ligand Binding, sigmoidal dose-response (variable slope)
f=Tc + (Th-Tc)/(1+10^((C-x)*S))

Dynamic Fit Options:

Total Number of Fits	200
Maximum Number of Iterations	500

Parameter Ranges for Initial Estimates:

	Minimum	Maximum
Tc	-6.9916	20.9748
Th	-14.5542	43.6625
C	-6.1690	18.5069
S	-1.0000	3.0000

Summary of Fit Results:

Converged	100.0%
Singular Solutions	62.0%

Results for the Overall Best-Fit Solution:

R	Rsqr	Adj Rsqr	Standard Error of Estimate
0.9961	0.9922	0.9899	0.3517

	Coefficient	Std. Error	t	P
Tc	7.0490	0.1608	43.8350	<0.0001
Th	14.1433	0.1360	103.9868	<0.0001
C	6.1823	0.0841	73.5224	<0.0001
S	1.3129	0.2465	5.3253	0.0003

Analysis of Variance:
Analysis of Variance:

	DF	SS	MS
Regression	4	1856.9392	464.2348
Residual	10	1.2372	0.1237
Total	14	1858.1764	132.7269

Corrected for the mean of the observations:

	DF	SS	MS	F	P
Regression	3	157.3073	52.4358	423.8205	<0.0001
Residual	10	1.2372	0.1237		
Total	13	158.5445	12.1957		

Statistical Tests:

Normality Test (Shapiro-Wilk) Passed (P = 0.2751)
W Statistic= 0.9268 Significance Level = 0.0500
Constant Variance Test Passed (P = <0.0001)

Data set: 23.00 hours, data IIC (Appendix G.6 cont.)

Nonlinear Regression - Dynamic Fitting **Saturday, August 28, 2010, 6:12:14 PM**

Data Source: Data 1 in Notebook1
Equation: Ligand Binding, sigmoidal dose-response (variable slope)
f=Tc + (Th-Tc)/(1+10^((C-x)*S))

Dynamic Fit Options:

Total Number of Fits	200
Maximum Number of Iterations	500

Parameter Ranges for Initial Estimates:

	Minimum	**Maximum**
Tc	-6.9145	20.7436
Th	-14.5437	43.6312
C	-7.2512	21.7535
S	-1.0000	3.0000

Summary of Fit Results:

Converged	100.0%
Singular Solutions	65.0%

Results for the Overall Best-Fit Solution:

R	**Rsqr**	**Adj Rsqr**	**Standard Error of Estimate**
0.9974	0.9949	0.9934	0.2863

	Coefficient	**Std. Error**	**t**	**P**
Tc	6.9821	0.1188	58.7897	<0.0001
Th	14.0942	0.1209	116.6257	<0.0001
C	7.2708	0.0653	111.4152	<0.0001
S	1.3007	0.2253	5.7723	0.0002

Analysis of Variance:
Analysis of Variance:

	DF	**SS**	**MS**
Regression	4	1676.6193	419.1548
Residual	10	0.8197	0.0820
Total	14	1677.4390	119.8171

Corrected for the mean of the observations:

	DF	**SS**	**MS**	**F**	**P**
Regression	3	159.8737	53.2912	650.1260	<0.0001
Residual	10	0.8197	0.0820		
Total	13	160.6934	12.3610		

Statistical Tests:

Normality Test (Shapiro-Wilk)	Passed (P = 0.5104)
W Statistic= 0.9467	Significance Level = 0.0500
Constant Variance Test	Passed (P = <0.0001)

Data set: 00.00 hours, data IIC (Appendix G.6 cont.)

Nonlinear Regression - Dynamic Fitting **Saturday, August 28, 2010, 6:12:30 PM**

Data Source: Data 1 in Notebook1
Equation: Ligand Binding, sigmoidal dose-response (variable slope)
f=Tc + (Th-Tc)/(1+10^((C-x)*S))

Dynamic Fit Options:

Total Number of Fits	200
Maximum Number of Iterations	500

Parameter Ranges for Initial Estimates:

	Minimum	Maximum
Tc	-6.8560	20.5681
Th	-14.5254	43.5761
C	-8.3495	25.0486
S	-1.0000	3.0000

Summary of Fit Results:

Converged	99.5%
Singular Solutions	69.0%
Iterations Exceeding 500	0.5%

Results for the Overall Best-Fit Solution:

R	Rsqr	Adj Rsqr	Standard Error of Estimate
0.9982	0.9964	0.9953	0.2355

	Coefficient	Std. Error	t	P
Tc	6.9437	0.0896	77.5170	<0.0001
Th	14.0013	0.1102	127.0042	<0.0001
C	8.3607	0.0496	168.6173	<0.0001
S	1.3722	0.2447	5.6067	0.0002

Analysis of Variance:
Analysis of Variance:

	DF	SS	MS
Regression	4	1494.8138	373.7035
Residual	10	0.5544	0.0554
Total	14	1495.3682	106.8120

Corrected for the mean of the observations:

	DF	SS	MS	F	P
Regression	3	151.6885	50.5628	911.9806	<0.0001
Residual	10	0.5544	0.0554		
Total	13	152.2429	11.7110		

Statistical Tests:
Normality Test (Shapiro-Wilk) Passed (P = 0.2699)
W Statistic= 0.9262 Significance Level = 0.0500
Constant Variance Test Passed (P = 0.0016)

Data set: 01.00 hours, data IIC **(Appendix G.6 cont.)**

Nonlinear Regression - Dynamic Fitting **Saturday, August 28, 2010, 6:12:46 PM**

Data Source: Data 1 in Notebook1
Equation: Ligand Binding, sigmoidal dose-response (variable slope)
f=Tc + (Th-Tc)/(1+10^((C-x)*S))

Dynamic Fit Options:

Total Number of Fits	200
Maximum Number of Iterations	500

Parameter Ranges for Initial Estimates:

	Minimum	**Maximum**
Tc	-6.8270	20.4809
Th	-14.2113	42.6338
C	-9.4411	28.3234
S	-1.0000	3.0000

Summary of Fit Results:

Converged	100.0%
Singular Solutions	68.5%

Results for the Overall Best-Fit Solution:

R	**Rsqr**	**Adj Rsqr**	**Standard Error of Estimate**
0.9993	0.9986	0.9982	0.1355

	Coefficient	**Std. Error**	**t**	**P**
Tc	6.8955	0.0482	143.1821	<0.0001
Th	13.9011	0.0752	184.8131	<0.0001
C	9.4354	0.0295	319.4640	<0.0001
S	1.2002	0.1137	10.5570	<0.0001

Analysis of Variance:
Analysis of Variance:

	DF	**SS**	**MS**
Regression	4	1314.2690	328.5672
Residual	10	0.1836	0.0184
Total	14	1314.4526	93.8895

Corrected for the mean of the observations:

	DF	**SS**	**MS**	**F**	**P**
Regression	3	133.0627	44.3542	2416.1200	<0.0001
Residual	10	0.1836	0.0184		
Total	13	133.2463	10.2497		

Statistical Tests:

Normality Test (Shapiro-Wilk)	Passed (P = 0.0951)
W Statistic= 0.8949	Significance Level = 0.0500
Constant Variance Test	Passed (P = 0.4254)

Data set: 02.00 hours, data IIC

Nonlinear Regression - Dynamic Fitting **Saturday, August 28, 2010, 6:13:17 PM**

Data Source: Data 1 in Notebook1
Equation: Ligand Binding, sigmoidal dose-response (variable slope)
f=Tc + (Th-Tc)/(1+10^((C-x)*S))

Dynamic Fit Options:

Total Number of Fits	200
Maximum Number of Iterations	500

Parameter Ranges for Initial Estimates:

	Minimum	Maximum
Tc	-6.7687	20.3061
Th	-13.7930	41.3791
C	-10.5286	31.5857
S	-1.0000	3.0000

Summary of Fit Results:

Converged	100.0%
Singular Solutions	72.5%

Results for the Overall Best-Fit Solution:

R	Rsqr	Adj Rsqr	Standard Error of Estimate
0.9996	0.9993	0.9991	0.0877

	Coefficient	Std. Error	t	P
Tc	6.8694	0.0291	236.2324	<0.0001
Th	13.7730	0.0605	227.8397	<0.0001
C	10.5222	0.0191	551.3108	<0.0001
S	1.2516	0.0889	14.0771	<0.0001

Analysis of Variance:

Analysis of Variance:

	DF	SS	MS
Regression	4	1140.6142	285.1535
Residual	10	0.0770	0.0077
Total	14	1140.6911	81.4779

Corrected for the mean of the observations:

	DF	SS	MS	F	P
Regression	3	107.7928	35.9309	4669.2430	<0.0001
Residual	10	0.0770	0.0077		
Total	13	107.8697	8.2977		

Statistical Tests:

Normality Test (Shapiro-Wilk)	Passed (P = 0.7553)
W Statistic= 0.9620	Significance Level = 0.0500
Constant Variance Test	Passed (P = 0.5114)

Data set: 03.00 hours, data IIC (Appendix G.6 cont.)

Nonlinear Regression - Dynamic Fitting **Saturday, August 28, 2010, 6:14:09 PM**

Data Source: Data 1 in Notebook1
Equation: Ligand Binding, sigmoidal dose-response (variable slope)
f=Tc + (Th-Tc)/(1+10^((C-x)*S))

Dynamic Fit Options:

Total Number of Fits	200
Maximum Number of Iterations	500

Parameter Ranges for Initial Estimates:

	Minimum	Maximum
Tc	-6.7358	20.2074
Th	-13.6492	40.9475
C	-11.8222	35.4666
S	-1.0000	3.0000

Summary of Fit Results:

Converged	100.0%
Singular Solutions	79.0%

Results for the Overall Best-Fit Solution:

R	Rsqr	Adj Rsqr	Standard Error of Estimate
0.9984	0.9968	0.9959	0.1523

	Coefficient	Std. Error	t	P
Tc	6.8648	0.0467	147.0387	<0.0001
Th	13.7542	0.1677	82.0183	<0.0001
C	11.7902	0.0468	252.0614	<0.0001
S	1.3257	0.1497	8.8577	<0.0001

Analysis of Variance:
Analysis of Variance:

	DF	SS	MS
Regression	4	958.8133	239.7033
Residual	10	0.2319	0.0232
Total	14	959.0451	68.5032

Corrected for the mean of the observations:

	DF	SS	MS	F	P
Regression	3	73.0454	24.3485	1050.0825	<0.0001
Residual	10	0.2319	0.0232		
Total	13	73.2772	5.6367		

Statistical Tests:

Normality Test (Shapiro-Wilk)	Passed (P = 0.0051)
W Statistic= 0.8005	Significance Level = 0.0500
Constant Variance Test	Passed (P = 0.4074)

APPENDIX H
Report of SIGMAPLOT Analysis
Verification Simulation Charging Model Type (II)

H.1 Verification September 11, 2008

Result Summary of SIGMAPLOT Analysis : Verification I B

Charging Minutes	T_c (°C)	T_h (°C)	C	S	R^2
0.0	7.32	13.63	3.92	1.47	0.9985
59.7	7.29	13.61	4.89	1.45	0.9989
119.4	7.26	13.59	5.86	1.43	0.9990
179.1	7.23	13.57	6.84	1.42	0.9990
238.8	7.21	13.54	7.81	1.42	0.9989
298.5	7.19	13.51	8.78	1.43	0.9989
358.2	7.17	13.47	9.75	1.46	0.9988
417.9	7.15	13.45	10.72	1.47	0.9983
477.6	7.14	13.44	11.70	1.46	0.9972

Result of SIGMAPLOT processing: **September 11, 2008 (Verification Data IB)**

Data set: 0.00 minutes, verification data IB

Nonlinear Regression - Dynamic Fitting **Monday, August 16, 2010, 3:52:09 PM**

Data Source: Data 1 in Notebook1
Equation: Ligand Binding, sigmoidal dose-response (variable slope)
f=Tc + (Th-Tc)/(1+10^((C-x)*S))

Dynamic Fit Options:

Total Number of Fits	200
Maximum Number of Iterations	200

Parameter Ranges for Initial Estimates:

	Minimum	**Maximum**
Tc	-7.2346	21.7037
Th	-13.7848	41.3543
C	-3.9603	11.8808
S	-1.0000	3.0000

Summary of Fit Results:

Converged	99.5%
Singular Solutions	56.0%

Results for the Overall Best-Fit Solution:

R	**Rsqr**	**Adj Rsqr**	**Standard Error of Estimate**
0.9993	0.9985	0.9981	0.1220

	Coefficient	**Std. Error**	**t**	**P**
Tc	7.3173	0.0727	100.6511	<0.0001
Th	13.6253	0.0410	332.0368	<0.0001
C	3.9220	0.0339	115.7509	<0.0001
S	1.4658	0.1001	14.6480	<0.0001

Analysis of Variance: **(Appendix H.1 cont.)**

Analysis of Variance:

	DF	SS	MS
Regression	4	2070.4360	517.6090
Residual	10	0.1489	0.0149
Total	14	2070.5849	147.8989

Corrected for the mean of the observations:

	DF	SS	MS	F	P
Regression	3	101.1509	33.7170	2265.0673	<0.0001
Residual	10	0.1489	0.0149		
Total	13	101.2998	7.7923		

Statistical Tests:

Normality Test (Shapiro-Wilk) Passed (P = 0.3123)

W Statistic= 0.9307 Significance Level = 0.0500

Constant Variance Test Passed (P = 0.2786)

Data set: 59.7 minutes, verification data IB (Appendix H.1 cont.)

Nonlinear Regression - Dynamic Fitting Monday, August 16, 2010, 3:52:30 PM

Data Source: Data 1 in Notebook1
Equation: Ligand Binding, sigmoidal dose-response (variable slope)
f=Tc + (Th-Tc)/(1+10^((C-x)*S))

Dynamic Fit Options:

Total Number of Fits	200
Maximum Number of Iterations	200

Parameter Ranges for Initial Estimates:

	Minimum	Maximum
Tc	-7.2029	21.6087
Th	-13.7256	41.1768
C	-4.9348	14.8045
S	-1.0000	3.0000

Summary of Fit Results:

Converged	100.0%
Singular Solutions	60.0%

Results for the Overall Best-Fit Solution:

R	Rsqr	Adj Rsqr	Standard Error of Estimate
0.9994	0.9989	0.9985	0.1142

	Coefficient	Std. Error	t	P
Tc	7.2876	0.0586	124.3915	<0.0001
Th	13.6056	0.0408	333.4838	<0.0001
C	4.8925	0.0311	157.5381	<0.0001
S	1.4480	0.0948	15.2723	<0.0001

Analysis of Variance:
Analysis of Variance:

	DF	SS	MS
Regression	4	1934.7563	483.6891
Residual	10	0.1304	0.0130
Total	14	1934.8868	138.2062

Corrected for the mean of the observations:

	DF	SS	MS	F	P
Regression	3	115.5992	38.5331	2953.9717	<0.0001
Residual	10	0.1304	0.0130		
Total	13	115.7297	8.9023		

Statistical Tests:

Normality Test (Shapiro-Wilk)	Passed (P = 0.1901)
W Statistic= 0.9156	Significance Level = 0.0500
Constant Variance Test	Passed (P = 0.1251)

Data set: 119.4 minutes, verification data IB **(Appendix H.1 cont.)**

Nonlinear Regression - Dynamic Fitting **Monday, August 16, 2010, 3:52:46 PM**

Data Source: Data 1 in Notebook1
Equation: Ligand Binding, sigmoidal dose-response (variable slope)
f=Tc + (Th-Tc)/(1+10^((C-x)*S))

Dynamic Fit Options:

Total Number of Fits	200
Maximum Number of Iterations	200

Parameter Ranges for Initial Estimates:

	Minimum	Maximum
Tc	-7.1480	21.4440
Th	-13.7085	41.1256
C	-5.9109	17.7328
S	-1.0000	3.0000

Summary of Fit Results:

Converged	99.5%
Singular Solutions	63.0%
Iterations Exceeding 200	0.5%

Results for the Overall Best-Fit Solution:

R	Rsqr	Adj Rsqr	Standard Error of Estimate
0.9995	0.9990	0.9986	0.1146

	Coefficient	Std. Error	t	P
Tc	7.2554	0.0524	138.4861	<0.0001
Th	13.5888	0.0438	310.0656	<0.0001
C	5.8637	0.0307	190.8044	<0.0001
S	1.4314	0.0974	14.6912	<0.0001

Analysis of Variance:

Analysis of Variance:

	DF	SS	MS
Regression	4	1799.6890	449.9223
Residual	10	0.1313	0.0131
Total	14	1799.8203	128.5586

Corrected for the mean of the observations:

	DF	SS	MS	F	P
Regression	3	124.9495	41.6498	3172.7174	<0.0001
Residual	10	0.1313	0.0131		
Total	13	125.0808	9.6216		

Statistical Tests:
Normality Test (Shapiro-Wilk) Passed (P = 0.2285)
W Statistic= 0.9212 Significance Level = 0.0500
Constant Variance Test Passed (P = 0.4532)

Data set: 179.1 minutes, verification data IB (Appendix H.1 cont.)

Nonlinear Regression - Dynamic Fitting **Monday, August 16, 2010, 3:53:00 PM**

Data Source: Data 1 in Notebook1
Equation: Ligand Binding, sigmoidal dose-response (variable slope)
f=Tc + (Th-Tc)/(1+10^((C-x)*S))

Dynamic Fit Options:

Total Number of Fits	200
Maximum Number of Iterations	200

Parameter Ranges for Initial Estimates:

	Minimum	Maximum
Tc	-7.1133	21.3399
Th	-13.6944	41.0833
C	-6.8891	20.6674
S	-1.0000	3.0000

Summary of Fit Results:

Converged	100.0%
Singular Solutions	69.5%

Results for the Overall Best-Fit Solution:

R	Rsqr	Adj Rsqr	Standard Error of Estimate
0.9995	0.9990	0.9987	0.1152

	Coefficient	Std. Error	t	P
Tc	7.2295	0.0480	150.6820	<0.0001
Th	13.5692	0.0477	284.5452	<0.0001
C	6.8355	0.0307	222.7768	<0.0001
S	1.4222	0.1021	13.9283	<0.0001

Analysis of Variance:
Analysis of Variance:

	DF	SS	MS
Regression	4	1664.6981	416.1745
Residual	10	0.1327	0.0133
Total	14	1664.8308	118.9165

Corrected for the mean of the observations:

	DF	SS	MS	F	P
Regression	3	128.6467	42.8822	3230.7412	<0.0001
Residual	10	0.1327	0.0133		
Total	13	128.7795	9.9061		

Statistical Tests:

Normality Test (Shapiro-Wilk) Passed (P = 0.3555)
W Statistic= 0.9348 Significance Level = 0.0500
Constant Variance Test Passed (P = 0.5729)

Data set: 238.8 minutes, verification data IB (Appendix H.1 cont.)

Nonlinear Regression - Dynamic Fitting **Monday, August 16, 2010, 3:53:17 PM**

Data Source: Data 1 in Notebook1
Equation: Ligand Binding, sigmoidal dose-response (variable slope)
f=Tc + (Th-Tc)/(1+10^((C-x)*S))

Dynamic Fit Options:

Total Number of Fits	200
Maximum Number of Iterations	200

Parameter Ranges for Initial Estimates:

	Minimum	Maximum
Tc	-7.0841	21.2523
Th	-13.6801	41.0403
C	-7.8673	23.6020
S	-1.0000	3.0000

Summary of Fit Results:

Converged	100.0%
Singular Solutions	66.0%

Results for the Overall Best-Fit Solution:

R	Rsqr	Adj Rsqr	Standard Error of Estimate
0.9995	0.9989	0.9986	0.1154

	Coefficient	Std. Error	t	P
Tc	7.2071	0.0444	162.2427	<0.0001
Th	13.5443	0.0524	258.2602	<0.0001
C	7.8070	0.0307	254.3794	<0.0001
S	1.4214	0.1088	13.0628	<0.0001

Analysis of Variance:

Analysis of Variance:

	DF	SS	MS
Regression	4	1529.7000	382.4250
Residual	10	0.1332	0.0133
Total	14	1529.8333	109.2738

Corrected for the mean of the observations:

	DF	SS	MS	F	P
Regression	3	126.6381	42.2127	3168.6396	<0.0001
Residual	10	0.1332	0.0133		
Total	13	126.7713	9.7516		

Statistical Tests:

Normality Test (Shapiro-Wilk) Passed (P = 0.3970)

W Statistic= 0.9383 Significance Level = 0.0500

Constant Variance Test Passed (P = 0.8438)

Data set: 298.5 minutes, verification data IB (Appendix H.1 cont.)

Nonlinear Regression - Dynamic Fitting **Monday, August 16, 2010, 3:53:32 PM**

Data Source: Data 1 in Notebook1
Equation: Ligand Binding, sigmoidal dose-response (variable slope)
f=Tc + (Th-Tc)/(1+10^((C-x)*S))

Dynamic Fit Options:

Total Number of Fits	200
Maximum Number of Iterations	200

Parameter Ranges for Initial Estimates:

	Minimum	Maximum
Tc	-7.0590	21.1771
Th	-13.6357	40.9072
C	-8.8417	26.5250
S	-1.0000	3.0000

Summary of Fit Results:

Converged	99.5%
Singular Solutions	68.0%

Results for the Overall Best-Fit Solution:

R	Rsqr	Adj Rsqr	Standard Error of Estimate
0.9995	0.9989	0.9986	0.1142

	Coefficient	Std. Error	t	P
Tc	7.1876	0.0411	175.0665	<0.0001
Th	13.5104	0.0582	232.3235	<0.0001
C	8.7774	0.0305	287.4509	<0.0001
S	1.4324	0.1181	12.1286	<0.0001

Analysis of Variance:
Analysis of Variance:

	DF	SS	MS
Regression	4	1394.7659	348.6915
Residual	10	0.1305	0.0130
Total	14	1394.8964	99.6355

Corrected for the mean of the observations:

	DF	SS	MS	F	P
Regression	3	118.8691	39.6230	3037.3894	<0.0001
Residual	10	0.1305	0.0130		
Total	13	118.9995	9.1538		

Statistical Tests:

Normality Test (Shapiro-Wilk)	Passed (P = 0.3454)
W Statistic= 0.9339	Significance Level = 0.0500
Constant Variance Test	Passed (P = 0.6482)

Data set: 358.2 minutes, verification data IB (Appendix H.1 cont.)

Nonlinear Regression - Dynamic Fitting **Monday, August 16, 2010, 3:53:47 PM**

Data Source: Data 1 in Notebook1
Equation: Ligand Binding, sigmoidal dose-response (variable slope)
f=Tc + (Th-Tc)/(1+10^((C-x)*S))

Dynamic Fit Options:

Total Number of Fits	200
Maximum Number of Iterations	200

Parameter Ranges for Initial Estimates:

	Minimum	Maximum
Tc	-7.0339	21.1016
Th	-13.5203	40.5610
C	-9.8062	29.4187
S	-1.0000	3.0000

Summary of Fit Results:

Converged	98.5%
Singular Solutions	72.0%

Results for the Overall Best-Fit Solution:

R	Rsqr	Adj Rsqr	Standard Error of Estimate
0.9994	0.9988	0.9984	0.1148

	Coefficient	Std. Error	t	P
Tc	7.1700	0.0389	184.4353	<0.0001
Th	13.4690	0.0677	198.9671	<0.0001
C	9.7469	0.0312	312.3017	<0.0001
S	1.4557	0.1353	10.7575	<0.0001

Analysis of Variance:
Analysis of Variance:

	DF	SS	MS
Regression	4	1260.6976	315.1744
Residual	10	0.1319	0.0132
Total	14	1260.8295	90.0593

Corrected for the mean of the observations:

	DF	SS	MS	F	P
Regression	3	105.5845	35.1948	2668.2835	<0.0001
Residual	10	0.1319	0.0132		
Total	13	105.7164	8.1320		

Statistical Tests:
Normality Test (Shapiro-Wilk) Passed (P = 0.3969)
W Statistic= 0.9383 Significance Level = 0.0500
Constant Variance Test Passed (P = 0.1624)

Data set: 417.9 minutes, verification data IB

Nonlinear Regression - Dynamic Fitting **Monday, August 16, 2010, 3:54:00 PM**

Data Source: Data 1 in Notebook1
Equation: Ligand Binding, sigmoidal dose-response (variable slope)
f=Tc + (Th-Tc)/(1+10^((C-x)*S))

Dynamic Fit Options:

Total Number of Fits	200
Maximum Number of Iterations	200

Parameter Ranges for Initial Estimates:

	Minimum	Maximum
Tc	-7.0124	21.0372
Th	-13.4579	40.3737
C	-10.7770	32.3310
S	-1.0000	3.0000

Summary of Fit Results:

Converged	99.5%
Singular Solutions	72.0%
Ill-Conditioned Solutions	0.5%
Iterations Exceeding 200	0.5%

Results for the Overall Best-Fit Solution:

R	Rsqr	Adj Rsqr	Standard Error of Estimate
0.9991	0.9983	0.9978	0.1231

	Coefficient	Std. Error	t	P
Tc	7.1540	0.0395	180.9786	<0.0001
Th	13.4457	0.0894	150.4034	<0.0001
C	10.7210	0.0347	309.0505	<0.0001
S	1.4677	0.1652	8.8872	<0.0001

Analysis of Variance:
Analysis of Variance:

	DF	SS	MS
Regression	4	1129.5320	282.3830
Residual	10	0.1516	0.0152
Total	14	1129.6836	80.6917

Corrected for the mean of the observations:

	DF	SS	MS	F	P
Regression	3	87.4852	29.1617	1923.6852	<0.0001
Residual	10	0.1516	0.0152		
Total	13	87.6368	6.7413		

Statistical Tests:

Normality Test (Shapiro-Wilk)	Passed (P = 0.3591)
W Statistic= 0.9351	Significance Level = 0.0500
Constant Variance Test	Passed (P = 0.2064)

Data set: 477.6 minutes, verification data IB (Appendix H.1 cont.)

Nonlinear Regression - Dynamic Fitting **Monday, August 16, 2010, 3:54:20 PM**

Data Source: Data 1 in Notebook1
Equation: Ligand Binding, sigmoidal dose-response (variable slope)
f=Tc + (Th-Tc)/(1+10^((C-x)*S))

Dynamic Fit Options:

Total Number of Fits	200
Maximum Number of Iterations	200

Parameter Ranges for Initial Estimates:

	Minimum	Maximum
Tc	-6.9839	20.9516
Th	-13.3676	40.1028
C	-11.7423	35.2269
S	-1.0000	3.0000

Summary of Fit Results:

Converged	99.0%
Singular Solutions	75.0%
Iterations Exceeding 200	1.0%

Results for the Overall Best-Fit Solution:

R	Rsqr	Adj Rsqr	Standard Error of Estimate
0.99448	0.9972	0.9964	0.1339

	Coefficient	Std. Error	t	P
Tc	7.1372	0.0410	173.8665	<0.0001
Th	13.4415	0.1397	96.1980	<0.0001
C	11.7695	0.0422	277.3351	<0.0001
S	1.4616	0.2120	6.8930	<0.0001

Analysis of Variance:
Analysis of Variance:

	DF	SS	MS
Regression	4	999.5447	249.8862
Residual	10	0.1792	0.0179
Total	14	999.7239	71.4089

Corrected for the mean of the observations:

	DF	SS	MS	F	P
Regression	3	64.3187	21.4396	1196.2674	<0.0001
Residual	10	0.1792	0.0179		
Total	13	64.4979	4.9614		

Statistical Tests:

Normality Test (Shapiro-Wilk)	Passed (P = 0.3158)
W Statistic= 0.9311	Significance Level = 0.0500
Constant Variance Test	Passed (P = 0.5316)

H.2 Verification September 19, 2008

Result Summary of SIGMAPLOT Analysis : Verification IC

Charging Minutes	T_c (°C)	T_h (°C)	C	S	R^2
0.0	7.32	13.54	3.19	1.11	0.9968
59.7	7.62	13.53	4.15	1.05	0.9983
119.4	7.56	13.51	5.12	1.00	0.9988
179.1	7.51	13.49	6.09	0.96	0.9987
238.8	7.47	13.47	7.06	0.92	0.9986
298.5	7.42	13.44	8.03	0.90	0.9985
358.2	7.39	13.42	9.00	0.87	0.9981
417.9	7.36	13.42	9.98	0.83	0.9974
477.6	7.33	13.46	10.95	0.76	0.9956

Result of SIGMAPLOT processing: **September 19, 2008 (Verification Data IC)**

Data set: 0.00 minutes, verification data IC

Nonlinear Regression - Dynamic Fitting **Thursday, July 22, 2010, 7:45:15 PM**

Data Source: Data 1 in Notebook5
Equation: Ligand Binding, sigmoidal dose-response (variable slope)
f=Tc + (Th-Tc)/(1+10^((C-x)*S))

Dynamic Fit Options:

Total Number of Fits	200
Maximum Number of Iterations	500

Parameter Ranges for Initial Estimates:

	Minimum	**Maximum**
Tc	-1.0000	1.0000
Th	-13.7291	41.1874
C	-3.1656	9.4968
S	-1.0000	3.0000

Summary of Fit Results:

Converged	100.0%
Singular Solutions	44.5%

Results for the Overall Best-Fit Solution:

R	**Rsqr**	**Adj Rsqr**	**Standard Error of Estimate**
0.9984	0.9968	0.9959	0.1488

	Coefficient	**Std. Error**	**t**	**P**
Tc	7.7239	0.1161	66.5987	<0.0001
Th	13.5444	0.0484	279.5875	<0.0001
C	3.1921	0.0494	64.5568	<0.0001
S	1.1052	0.1101	10.0382	<0.0001

Analysis of Variance: **(Appendix H.2 cont.)**

Analysis of Variance:

	DF	SS	MS
Regression	4	2161.9219	540.4805
Residual	10	0.2214	0.0221
Total	14	2162.1433	154.4388

Corrected for the mean of the observations:

	DF	SS	MS	F	P
Regression	3	69.7914	23.2638	1050.7709	<0.0001
Residual	10	0.2214	0.0221		
Total	13	70.0128	5.3856		

Statistical Tests:

Normality Test (Shapiro-Wilk) Passed (P = 0.2816)

W Statistic= 0.9275 Significance Level = 0.0500

Constant Variance Test Passed (P = 0.8676)

Data set: 59.7 minutes, verification data IC (Appendix H.2 cont.)

Nonlinear Regression - Dynamic Fitting **Thursday, July 22, 2010, 7:45:31 PM**

Data Source: Data 1 in Notebook5
Equation: Ligand Binding, sigmoidal dose-response (variable slope)
f=Tc + (Th-Tc)/(1+10^((C-x)*S))

Dynamic Fit Options:

Total Number of Fits	200
Maximum Number of Iterations	500

Parameter Ranges for Initial Estimates:

	Minimum	Maximum
Tc	-7.5790	22.7369
Th	-59.7053	179.1159
C	-4.1426	12.4279
S	-1.0000	3.0000

Summary of Fit Results:

Converged	100.0%
Singular Solutions	49.0%
Ill-Conditioned Solutions	0.5%

Results for the Overall Best-Fit Solution:

R	Rsqr	Adj Rsqr	Standard Error of Estimate
0.9992	0.9983	0.9978	0.1204

	Coefficient	Std. Error	t	P
Tc	7.6224	0.0753	101.2911	<0.0001
Th	13.5261	0.0416	325.4951	<0.0001
C	4.1537	0.0382	108.6343	<0.0001
S	1.0500	0.0761	13.7929	<0.0001

Analysis of Variance:
Analysis of Variance:

	DF	SS	MS
Regression	4	2029.8281	507.4570
Residual	10	0.1449	0.0145
Total	14	2029.9730	144.9981

Corrected for the mean of the observations:

	DF	SS	MS	F	P
Regression	3	87.3295	29.1098	2008.8900	<0.0001
Residual	10	0.1449	0.0145		
Total	13	87.4744	6.7288		

Statistical Tests:
Normality Test (Shapiro-Wilk) Passed (P = 0.7034)
W Statistic= 0.9588 Significance Level = 0.0500
Constant Variance Test Passed (P = 0.0977)

Data set: 119.4 minutes, verification data IC (Appendix H.2 cont.)

Nonlinear Regression - Dynamic Fitting **Thursday, July 22, 2010, 7:45:57 PM**

Data Source: Data 1 in Notebook5
Equation: Ligand Binding, sigmoidal dose-response (variable slope)
f=Tc + (Th-Tc)/(1+10^((C-x)*S))

Dynamic Fit Options:

Total Number of Fits	200
Maximum Number of Iterations	500

Parameter Ranges for Initial Estimates:

	Minimum	Maximum
Tc	-7.4466	22.3399
Th	-119.4106	358.2318
C	-5.1028	15.3084
S	-1.0000	3.0000

Summary of Fit Results:

Converged	100.0%
Singular Solutions	46.5%
Ill-Conditioned Solutions	1.5%

Results for the Overall Best-Fit Solution:

R	Rsqr	Adj Rsqr	Standard Error of Estimate
0.9994	0.9988	0.9984	0.1114

	Coefficient	Std. Error	t	P
Tc	7.5624	0.0597	126.6411	<0.0001
Th	13.5056	0.0411	328.5230	<0.0001
C	5.1216	0.0350	146.1490	<0.0001
S	1.0023	0.0638	15.7032	<0.0001

Analysis of Variance:
Analysis of Variance:

	DF	SS	MS
Regression	4	1898.4411	474.6103
Residual	10	0.1241	0.0124
Total	14	1898.5652	135.6118

Corrected for the mean of the observations:

	DF	SS	MS	F	P
Regression	3	99.3922	33.1307	2670.3582	<0.0001
Residual	10	0.1241	0.0124		
Total	13	99.5162	7.6551		

Statistical Tests:
Normality Test (Shapiro-Wilk) Passed (P = 0.1235)
W Statistic= 0.9027 Significance Level = 0.0500
Constant Variance Test Passed (P = 0.2858)

Data set: 179.1 minutes, verification data IC (Appendix H.2 cont.)

Nonlinear Regression - Dynamic Fitting **Thursday, July 22, 2010, 7:46:19 PM**

Data Source: Data 1 in Notebook5
Equation: Ligand Binding, sigmoidal dose-response (variable slope)
f=Tc + (Th-Tc)/(1+10^((C-x)*S))

Dynamic Fit Options:

Total Number of Fits	200
Maximum Number of Iterations	500

Parameter Ranges for Initial Estimates:

	Minimum	Maximum
Tc	-7.3662	22.0987
Th	-179.1159	537.3477
C	-6.0729	18.2186
S	-1.0000	3.0000

Summary of Fit Results:

Converged	100.0%
Singular Solutions	52.5%
Ill-Conditioned Solutions	1.5%

Results for the Overall Best-Fit Solution:

R	Rsqr	Adj Rsqr	Standard Error of Estimate
0.9994	0.9987	0.9984	0.1161

	Coefficient	Std. Error	t	P
Tc	7.5141	0.0554	135.5722	<0.0001
Th	13.4850	0.0463	291.0380	<0.0001
C	6.0915	0.0368	165.6649	<0.0001
S	0.9563	0.0616	15.5147	<0.0001

Analysis of Variance:
Analysis of Variance:

	DF	SS	MS
Regression	4	1767.2386	441.8096
Residual	10	0.1349	0.0135
Total	14	1767.3735	126.2410

Corrected for the mean of the observations:

	DF	SS	MS	F	P
Regression	3	106.5051	35.5017	2631.7986	<0.0001
Residual	10	0.1349	0.0135		
Total	13	106.6400	8.2031		

Statistical Tests:

Normality Test (Shapiro-Wilk)	Passed (P = 0.0964)
W Statistic= 0.8953	Significance Level = 0.0500
Constant Variance Test	Passed (P = 0.5316)

<u>Data set: 238.8 minutes, verification data IC</u> **(Appendix H.2 cont.)**

Nonlinear Regression - Dynamic Fitting **Thursday, July 22, 2010, 7:46:39 PM**

Data Source: Data 1 in Notebook5
Equation: Ligand Binding, sigmoidal dose-response (variable slope)
f=Tc + (Th-Tc)/(1+10^((C-x)*S))

Dynamic Fit Options:

Total Number of Fits	200
Maximum Number of Iterations	500

Parameter Ranges for Initial Estimates:

	Minimum	**Maximum**
Tc	-7.2981	21.8942
Th	-238.8212	716.4637
C	-7.0457	21.1370
S	-1.0000	3.0000

Summary of Fit Results:

Converged	100.0%
Singular Solutions	55.0%
Ill-Conditioned Solutions	2.0%

Results for the Overall Best-Fit Solution:

R	**Rsqr**	**Adj Rsqr**	**Standard Error of Estimate**
0.9993	0.9986	0.9982	0.1227

	Coefficient	**Std. Error**	**t**	**P**
Tc	7.4686	0.0533	140.1547	<0.0001
Th	13.4654	0.0536	251.0381	<0.0001
C	7.0608	0.0393	179.5224	<0.0001
S	0.9194	0.0616	14.9277	<0.0001

Analysis of Variance:
Analysis of Variance:

	DF	**SS**	**MS**
Regression	4	1636.3791	409.0948
Residual	10	0.1507	0.0151
Total	14	1636.5297	116.8950

Corrected for the mean of the observations:

	DF	**SS**	**MS**	**F**	**P**
Regression	3	108.9280	36.3093	2410.0620	<0.0001
Residual	10	0.1507	0.0151		
Total	13	109.0787	8.3907		

Statistical Tests:

Normality Test (Shapiro-Wilk)	Passed (P = 0.3112)
W Statistic= 0.9306	Significance Level = 0.0500
Constant Variance Test	Passed (P = 0.1251)

Data set: 298.5 minutes, verification data IC (Appendix H.2 cont.)

Nonlinear Regression - Dynamic Fitting **Thursday, July 22, 2010, 7:46:57 PM**

Data Source: Data 1 in Notebook5
Equation: Ligand Binding, sigmoidal dose-response (variable slope)
f=Tc + (Th-Tc)/(1+10^((C-x)*S))

Dynamic Fit Options:

Total Number of Fits	200
Maximum Number of Iterations	500

Parameter Ranges for Initial Estimates:

	Minimum	Maximum
Tc	-7.2449	21.7346
Th	-298.5265	895.5796
C	-8.0155	24.0464
S	-1.0000	3.0000

Summary of Fit Results:

Converged	96.0%
Singular Solutions	61.0%
Ill-Conditioned Solutions	0.5%
Iterations Exceeding 500	4.0%

Results for the Overall Best-Fit Solution:

R	Rsqr	Adj Rsqr	Standard Error of Estimate
0.9993	0.9985	0.9981	0.1248

	Coefficient	Std. Error	t	P
Tc	7.4247	0.0500	148.6161	<0.0001
Th	13.4397	0.0608	221.1416	<0.0001
C	8.0303	0.0405	198.0570	<0.0001
S	0.8975	0.0609	14.7463	<0.0001

Analysis of Variance:
Analysis of Variance:

	DF	SS	MS
Regression	4	1504.7623	376.1906
Residual	10	0.1557	0.0156
Total	14	1504.9181	107.4941

Corrected for the mean of the observations:

	DF	SS	MS	F	P
Regression	3	106.4821	35.4940	2279.4304	<0.0001
Residual	10	0.1557	0.0156		
Total	13	106.6378	8.2029		

Statistical Tests:
Normality Test (Shapiro-Wilk) Passed (P = 0.9283)
W Statistic= 0.9743 Significance Level = 0.0500
Constant Variance Test Passed (P = 0.0663)

<u>Data set: 358.2 minutes, verification data IC</u> **(Appendix H.2 cont.)**

Nonlinear Regression - Dynamic Fitting **Thursday, July 22, 2010, 7:48:42 PM**

Data Source: Data 1 in Notebook5
Equation: Ligand Binding, sigmoidal dose-response (variable slope)
f=Tc + (Th-Tc)/(1+10^((C-x)*S))

Dynamic Fit Options:

Total Number of Fits	200
Maximum Number of Iterations	500

Parameter Ranges for Initial Estimates:

	Minimum	Maximum
Tc	-7.1997	21.5991
Th	-358.2318	1074.6955
C	-8.9766	26.9298
S	-1.0000	3.0000

Summary of Fit Results:

Converged	98.0%
Singular Solutions	63.0%
Ill-Conditioned Solutions	3.0%
Iterations Exceeding 500	2.0%

Results for the Overall Best-Fit Solution:

R	Rsqr	Adj Rsqr	Standard Error of Estimate
0.9991	0.9981	0.9976	0.1365

	Coefficient	Std. Error	t	P
Tc	7.3905	0.0510	144.7931	<0.0001
Th	13.4174	0.0765	175.3274	<0.0001
C	8.9996	0.0457	196.9107	<0.0001
S	0.8687	0.0649	13.3847	<0.0001

Analysis of Variance:
Analysis of Variance:

	DF	SS	MS
Regression	4	1374.8958	343.7239
Residual	10	0.1862	0.0186
Total	14	1375.0820	98.2201

Corrected for the mean of the observations:

	DF	SS	MS	F	P
Regression	3	98.7436	32.9145	1767.2957	<0.0001
Residual	10	0.1862	0.0186		
Total	13	98.9299	7.6100		

Statistical Tests:
Normality Test (Shapiro-Wilk) Passed (P = 0.9589)
W Statistic= 0.9777 Significance Level = 0.0500
Constant Variance Test Passed (P = 0.0018)

Data set: 417.9 minutes, verification data IC (Appendix H.2 cont.)

Nonlinear Regression - Dynamic Fitting **Thursday, July 22, 2010, 7:49:04 PM**

Data Source: Data 1 in Notebook5
Equation: Ligand Binding, sigmoidal dose-response (variable slope)
f=Tc + (Th-Tc)/(1+10^((C-x)*S))

Dynamic Fit Options:

Total Number of Fits	200
Maximum Number of Iterations	500

Parameter Ranges for Initial Estimates:

	Minimum	Maximum
Tc	-7.1664	21.4992
Th	-417.9371	1253.8114
C	-9.9561	29.8684
S	-1.0000	3.0000

Summary of Fit Results:

Converged	98.0%
Singular Solutions	68.0%
Ill-Conditioned Solutions	1.5%
Iterations Exceeding 500	2.0%

Results for the Overall Best-Fit Solution:

R	Rsqr	Adj Rsqr	Standard Error of Estimate
0.9987	0.9974	0.9966	0.1505

	Coefficient	Std. Error	t	P
Tc	7.3597	0.0531	138.6275	<0.0001
Th	13.4218	0.1031	130.1731	<0.0001
C	9.9753	0.0532	187.6238	<0.0001
S	0.8337	0.0702	11.8830	<0.0001

Analysis of Variance:
Analysis of Variance:

	DF	SS	MS
Regression	4	1247.5134	311.8784
Residual	10	0.2264	0.0226
Total	14	1247.7398	89.1243

Corrected for the mean of the observations:

	DF	SS	MS	F	P
Regression	3	86.4320	28.8107	1272.6609	<0.0001
Residual	10	0.2264	0.0226		
Total	13	86.6584	6.6660		

Statistical Tests:

Normality Test (Shapiro-Wilk)	Passed (P = 0.8888)
W Statistic= 0.9709	Significance Level = 0.0500
Constant Variance Test	Passed (P = 0.0907)

Data set: 477.6 minutes, verification data IC (Appendix H.2 cont.)

Nonlinear Regression - Dynamic Fitting **Thursday, July 22, 2010, 7:49:22 PM**

Data Source: Data 1 in Notebook5
Equation: Ligand Binding, sigmoidal dose-response (variable slope)
f=Tc + (Th-Tc)/(1+10^((C-x)*S))

Dynamic Fit Options:

Total Number of Fits	200
Maximum Number of Iterations	500

Parameter Ranges for Initial Estimates:

	Minimum	Maximum
Tc	-7.1332	21.3997
Th	-477.6424	1432.9273
C	-10.9207	32.7622
S	-1.0000	3.0000

Summary of Fit Results:

Converged	94.5%
Singular Solutions	71.0%
Ill-Conditioned Solutions	1.0%
Iterations Exceeding 500	5.5%

Results for the Overall Best-Fit Solution:

R	Rsqr	Adj Rsqr	Standard Error of Estimate
0.9978	0.9956	0.9943	0.1745

	Coefficient	Std. Error	t	P
Tc	7.3318	0.0589	124.4666	<0.0001
Th	13.4619	0.1702	79.0924	<0.0001
C	10.9513	0.0717	152.6749	<0.0001
S	0.7640	0.0794	9.6279	<0.0001

Analysis of Variance:
Analysis of Variance:

	DF	SS	MS
Regression	4	1121.4815	280.3704
Residual	10	0.3044	0.0304
Total	14	1121.7859	80.1276

Corrected for the mean of the observations:

	DF	SS	MS	F	P
Regression	3	68.6134	22.8711	751.3597	<0.0001
Residual	10	0.3044	0.0304		
Total	13	68.9178	5.3014		

Statistical Tests:

Normality Test (Shapiro-Wilk)	Passed (P = 0.3320)
W Statistic= 0.9326	Significance Level = 0.0500
Constant Variance Test	Passed (P = 0.5834)

H.3 Verification June 22, 2008

Result Summary of SIGMAPLOT Analysis : Verification II B

Charging Minutes	T_c (°C)	T_h (°C)	C	S	R^2
0.0	7.59	13.97	2.83	1.17	0.9934
59.7	7.31	13.86	3.84	1.19	0.9977
119.4	7.20	13.76	4.94	1.36	0.9937
179.1	7.07	13.69	6.06	1.30	0.9959
238.8	7.01	13.66	7.25	1.25	0.9982
298.5	6.96	13.61	8.45	1.27	0.9989
358.2	6.91	13.55	9.62	1.27	0.9993
417.9	6.87	13.47	10.78	1.16	0.9994
477.6	6.86	13.50	12.12	1.20	0.9974

Result of SIGMAPLOT processing: **June 22, 2008 (Verification Data IIB)**

Data set: 0.0 minutes, verification data IIB

Nonlinear Regression - Dynamic Fitting **Friday, July 30, 2010, 10:56:52 AM**

Data Source: Data 1 in Notebook2
Equation: Ligand Binding, sigmoidal dose-response (variable slope)
f=Tc + (Th-Tc)/(1+10^((C-x)*S))

Dynamic Fit Options:

Total Number of Fits	200
Maximum Number of Iterations	200

Parameter Ranges for Initial Estimates:

	Minimum	Maximum
Tc	-7.6000	22.8000
Th	-14.8668	44.6005
C	-2.9750	8.9251
S	-1.0000	3.0000

Summary of Fit Results:

Converged	100.0%
Singular Solutions	54.5%

Results for the Overall Best-Fit Solution:

R	Rsqr	Adj Rsqr	Standard Error of Estimate
0.9868	0.9934	0.9660	0.4524

	Coefficient	Std. Error	t	P
Tc	7.5888	0.3604	21.1368	<0.0001
Th	13.9653	0.1452	96.1647	<0.0001
C	2.8326	0.1276	22.0905	<0.0001
S	1.1682	0.3272	3.6698	0.0043

Analysis of Variance: **(Appendix H.3 cont.)**

Analysis of Variance:

	DF	SS	MS
Regression	4	2331.3547	582.8387
Residual	10	2.0468	0.2047
Total	14	2333.4015	166.6715

Corrected for the mean of the observations:

	DF	SS	MS	F	P
Regression	3	76.1626	25.3875	124.0327	<0.0001
Residual	10	2.0468	0.2047		
Total	13	78.2094	6.0161		

Statistical Tests:

Normality Test (Shapiro-Wilk) Passed (P = 0.4332)

W Statistic= 0.9411 Significance Level = 0.0500

Constant Variance Test Passed (P = 0.0690)

Data set: 59.7 minutes, verification data IIB (Appendix H.3 cont.)

Nonlinear Regression - Dynamic Fitting **Friday, July 30, 2010, 10:57:05 AM**

Data Source: Data 1 in Notebook2
Equation: Ligand Binding, sigmoidal dose-response (variable slope)
f=Tc + (Th-Tc)/(1+10^((C-x)*S))

Dynamic Fit Options:

Total Number of Fits	200
Maximum Number of Iterations	200

Parameter Ranges for Initial Estimates:

	Minimum	Maximum
Tc	-7.2990	21.8970
Th	-14.5953	43.7859
C	-4.0249	12.0748
S	-1.0000	3.0000

Summary of Fit Results:

Converged	100.0%
Singular Solutions	56.0%
Ill-Conditioned Solutions	0.5%

Results for the Overall Best-Fit Solution:

R	Rsqr	Adj Rsqr	Standard Error of Estimate
0.9955	0.9977	0.9845	0.3511

	Coefficient	Std. Error	t	P
Tc	7.3112	0.2243	32.8098	<0.0001
Th	13.8653	0.1202	115.3718	<0.0001
C	3.8218	0.1006	38.9846	<0.0001
S	1.1536	0.1938	5.4376	0.0003

Analysis of Variance:
Analysis of Variance:

	DF	SS	MS
Regression	4	2135.9153	533.9788
Residual	10	1.2325	0.1232
Total	14	2137.1478	152.6534

Corrected for the mean of the observations:

	DF	SS	MS	F	P
Regression	3	102.2066	34.0689	276.4317	<0.0001
Residual	10	1.2325	0.1232		
Total	13	103.4390	7.9568		

Statistical Tests:

Normality Test (Shapiro-Wilk)	Passed (P = 0.3434)
W Statistic= 0.9337	Significance Level = 0.0500
Constant Variance Test	Passed (P = 0.0610)

Data set: 119.4 minutes, verification data IIB **(Appendix H.3 cont.)**

Nonlinear Regression - Dynamic Fitting **Friday, July 30, 2010, 10:57:17 AM**

Data Source: Data 1 in Notebook2
Equation: Ligand Binding, sigmoidal dose-response (variable slope)
f=Tc + (Th-Tc)/(1+10^((C-x)*S))

Dynamic Fit Options:

Total Number of Fits	200
Maximum Number of Iterations	200

Parameter Ranges for Initial Estimates:

	Minimum	Maximum
Tc	-7.1540	21.4621
Th	-14.2428	42.7283
C	-5.0685	15.2055
S	-1.0000	3.0000

Summary of Fit Results:

Converged	100.0%
Singular Solutions	60.5%
Ill-Conditioned Solutions	0.5%

Results for the Overall Best-Fit Solution:

R	Rsqr	Adj Rsqr	Standard Error of Estimate
0.9874	0.9937	0.9928	0.2618

	Coefficient	Std. Error	t	P
Tc	7.1958	0.1406	50.9548	<0.0001
Th	13.7614	0.0959	143.7906	<0.0001
C	4.9429	0.0732	68.4734	<0.0001
S	1.3563	0.1352	7.6399	<0.0001

Analysis of Variance:
Analysis of Variance:

	DF	SS	MS
Regression	4	1947.6125	486.9031
Residual	10	0.6853	0.0685
Total	14	1948.2978	139.1641

Corrected for the mean of the observations:

	DF	SS	MS	F	P
Regression	3	122.6908	40.8969	596.7963	<0.0001
Residual	10	0.6853	0.0685		
Total	13	123.3760	9.4905		

Statistical Tests:

Normality Test (Shapiro-Wilk)	Passed (P = 0.5797)
W Statistic= 0.9512	Significance Level = 0.0500
Constant Variance Test	Passed (P = 0.0131)

Data set: 179.1 minutes, verification data IIB (Appendix H.3 cont.)

Nonlinear Regression - Dynamic Fitting **Friday, July 30, 2010, 10:57:28 AM**

Data Source: Data 1 in Notebook2
Equation: Ligand Binding, sigmoidal dose-response (variable slope)
f=Tc + (Th-Tc)/(1+10^((C-x)*S))

Dynamic Fit Options:

Total Number of Fits	200
Maximum Number of Iterations	200

Parameter Ranges for Initial Estimates:

	Minimum	Maximum
Tc	-7.0000	21.0000
Th	-14.0339	42.1017
C	-6.1650	18.4949
S	-1.0000	3.0000

Summary of Fit Results:

Converged	100.0%
Singular Solutions	62.5%

Results for the Overall Best-Fit Solution:

R	Rsqr	Adj Rsqr	Standard Error of Estimate
0.9918	0.9959	0.9962	0.1987

	Coefficient	Std. Error	t	P
Tc	7.0714	0.0943	74.7340	<0.0001
Th	13.6884	0.0796	172.5181	<0.0001
C	6.0589	0.0557	110.8098	<0.0001
S	1.3040	0.0973	9.8914	<0.0001

Analysis of Variance:
Analysis of Variance:

	DF	SS	MS
Regression	4	1764.3900	441.0975
Residual	10	0.3950	0.0395
Total	14	1764.7849	126.0561

Corrected for the mean of the observations:

	DF	SS	MS	F	P
Regression	3	134.1337	44.7112	1132.0499	<0.0001
Residual	10	0.3950	0.0395		
Total	13	134.5287	10.3484		

Statistical Tests:

Normality Test (Shapiro-Wilk)	Passed (P = 0.9554)
W Statistic= 0.9772	Significance Level = 0.0500
Constant Variance Test	Passed (P = 0.0023)

Data set: 238.8 minutes, verification data IIB **(Appendix H.3 cont.)**

Nonlinear Regression - Dynamic Fitting **Friday, July 30, 2010, 10:57:53 AM**

Data Source: Data 1 in Notebook2
Equation: Ligand Binding, sigmoidal dose-response (variable slope)
f=Tc + (Th-Tc)/(1+10^((C-x)*S))

Dynamic Fit Options:

Total Number of Fits	200
Maximum Number of Iterations	200

Parameter Ranges for Initial Estimates:

	Minimum	**Maximum**
Tc	-6.9511	20.8533
Th	-13.9287	41.7860
C	-7.2937	21.8811
S	-1.0000	3.0000

Summary of Fit Results:

Converged	99.5%
Singular Solutions	68.5%
Iterations Exceeding 200	0.5%

Results for the Overall Best-Fit Solution:

R	**Rsqr**	**Adj Rsqr**	**Standard Error of Estimate**
0.9964	0.9982	0.9987	0.1197

	Coefficient	**Std. Error**	**t**	**P**
Tc	7.0144	0.0504	139.0987	<0.0001
Th	13.6616	0.0524	261.4633	<0.0001
C	7.2537	0.0311	235.3061	<0.0001
S	1.2489	0.0707	14.6654	<0.0001

Analysis of Variance:
Analysis of Variance:

	DF	**SS**	**MS**
Regression	4	1598.8968	399.7242
Residual	10	0.1433	0.0143
Total	14	1599.0401	114.2171

Corrected for the mean of the observations:

	DF	**SS**	**MS**	**F**	**P**
Regression	3	138.1735	46.0578	3214.0145	<0.0001
Residual	10	0.1433	0.0143		
Total	13	138.3168	10.6398		

Statistical Tests:

Normality Test (Shapiro-Wilk)	Passed (P = 0.9221)
W Statistic= 0.9737	Significance Level = 0.0500
Constant Variance Test	Passed (P = 0.0223)

Data set: 298.5 minutes, verification data IIB (Appendix H.3 cont.)

Nonlinear Regression - Dynamic Fitting **Friday, July 30, 2010, 10:58:05 AM**

Data Source: Data 1 in Notebook2
Equation: Ligand Binding, sigmoidal dose-response (variable slope)
f=Tc + (Th-Tc)/(1+10^((C-x)*S))

Dynamic Fit Options:

Total Number of Fits	200
Maximum Number of Iterations	200

Parameter Ranges for Initial Estimates:

	Minimum	Maximum
Tc	-6.8984	20.6952
Th	-13.8664	41.5993
C	-8.4255	25.2765
S	-1.0000	3.0000

Summary of Fit Results:

Converged	99.5%
Singular Solutions	68.5%
Iterations Exceeding 200	0.5%

Results for the Overall Best-Fit Solution:

R	Rsqr	Adj Rsqr	Standard Error of Estimate
0.9978	0.9989	0.9986	0.1178

	Coefficient	Std. Error	t	P
Tc	6.9635	0.0447	155.8355	<0.0001
Th	13.6144	0.0570	239.0816	<0.0001
C	8.4462	0.0263	320.1571	<0.0001
S	1.2737	0.1091	11.2678	<0.0001

Analysis of Variance:
Analysis of Variance:

	DF	SS	MS
Regression	4	1426.8754	356.7188
Residual	10	0.1387	0.0139
Total	14	1427.0140	101.9296

Corrected for the mean of the observations:

	DF	SS	MS	F	P
Regression	3	132.5909	44.1970	3186.7934	<0.0001
Residual	10	0.1387	0.0139		
Total	13	132.7295	10.2100		

Statistical Tests:

Normality Test (Shapiro-Wilk)	Passed (P = 0.5551)
W Statistic= 0.9496	Significance Level = 0.0500
Constant Variance Test	Passed (P = 0.2248)

Data set: 358.2 minutes, verification data IIB (Appendix H.3 cont.)

Nonlinear Regression - Dynamic Fitting **Friday, July 30, 2010, 10:58:17 AM**

Data Source: Data 1 in Notebook2
Equation: Ligand Binding, sigmoidal dose-response (variable slope)
f=Tc + (Th-Tc)/(1+10^((C-x)*S))

Dynamic Fit Options:

Total Number of Fits	200
Maximum Number of Iterations	200

Parameter Ranges for Initial Estimates:

	Minimum	Maximum
Tc	-6.8580	20.5741
Th	-13.7175	41.1526
C	-9.5800	28.7399
S	-1.0000	3.0000

Summary of Fit Results:

Converged	100.0%
Singular Solutions	71.5%

Results for the Overall Best-Fit Solution:

R	Rsqr	Adj Rsqr	Standard Error of Estimate
0.9986	0.9993	0.9992	0.0876

	Coefficient	Std. Error	t	P
Tc	6.9117	0.0304	226.4536	<0.0001
Th	13.5502	0.0493	274.2570	<0.0001
C	9.6156	0.0175	545.0508	<0.0001
S	1.2748	0.1251	11.2779	<0.0001

Analysis of Variance:
Analysis of Variance:

	DF	SS	MS
Regression	4	1254.2023	313.5506
Residual	10	0.0767	0.0077
Total	14	1254.2790	89.5914

Corrected for the mean of the observations:

	DF	SS	MS	F	P
Regression	3	118.9512	39.6504	5169.5965	<0.0001
Residual	10	0.0767	0.0077		
Total	13	119.0279	9.1560		

Statistical Tests:
Normality Test (Shapiro-Wilk) Passed (P = 0.0738)
W Statistic= 0.8872 Significance Level = 0.0500
Constant Variance Test Passed (P = 0.0046)

Data set: 417.9 minutes, verification data IIB (Appendix H.3 cont.)

Nonlinear Regression - Dynamic Fitting **Friday, July 30, 2010, 10:58:29 AM**

Data Source: Data 1 in Notebook2
Equation: Ligand Binding, sigmoidal dose-response (variable slope)
f=Tc + (Th-Tc)/(1+10^((C-x)*S))

Dynamic Fit Options:

Total Number of Fits	200
Maximum Number of Iterations	200

Parameter Ranges for Initial Estimates:

	Minimum	Maximum
Tc	-6.8000	20.4000
Th	-13.4818	40.4454
C	-10.7005	32.1015
S	-1.0000	3.0000

Summary of Fit Results:

Converged	99.5%
Singular Solutions	73.5%
Iterations Exceeding 200	0.5%

Results for the Overall Best-Fit Solution:

R	Rsqr	Adj Rsqr	Standard Error of Estimate
0.9988	0.9994	0.9994	0.0660

	Coefficient	Std. Error	t	P
Tc	6.8721	0.0217	314.9093	<0.0001
Th	13.4664	0.0498	269.7214	<0.0001
C	10.7804	0.0182	585.6693	<0.0001
S	1.1589	0.0496	22.1771	<0.0001

Analysis of Variance:
Analysis of Variance:

	DF	SS	MS
Regression	4	1085.8393	271.4598
Residual	10	0.0436	0.0044
Total	14	1085.8829	77.5631

Corrected for the mean of the observations:

	DF	SS	MS	F	P
Regression	3	93.0539	31.0180	7115.4697	<0.0001
Residual	10	0.0436	0.0044		
Total	13	93.0975	7.1613		

Statistical Tests:
Normality Test (Shapiro-Wilk) Passed (P = 0.7819)
W Statistic= 0.9636 Significance Level = 0.0500
Constant Variance Test Passed (P = 0.3158)

Data set: 477.6 minutes, verification data IIB (Appendix H.3 cont.)

Nonlinear Regression - Dynamic Fitting **Friday, July 30, 2010, 10:58:42 AM**

Data Source: Data 1 in Notebook2
Equation: Ligand Binding, sigmoidal dose-response (variable slope)
f=Tc + (Th-Tc)/(1+10^((C-x)*S))

Dynamic Fit Options:

Total Number of Fits	200
Maximum Number of Iterations	200

Parameter Ranges for Initial Estimates:

	Minimum	Maximum
Tc	-6.7449	20.2347
Th	-13.3459	40.0376
C	-11.8566	35.5699
S	-1.0000	3.0000

Summary of Fit Results:

Converged	98.5%
Singular Solutions	77.0%
Iterations Exceeding 200	1.5%

Results for the Overall Best-Fit Solution:

R	Rsqr	Adj Rsqr	Standard Error of Estimate
0.9948	0.9974	0.9980	0.0960

	Coefficient	Std. Error	t	P
Tc	6.8640	0.0301	226.5246	<0.0001
Th	13.4981	0.1304	103.5095	<0.0001
C	12.1219	0.0370	320.9996	<0.0001
S	1.1972	0.0588	16.2284	<0.0001

Analysis of Variance:
Analysis of Variance:

	DF	SS	MS
Regression	4	920.8469	230.2117
Residual	10	0.0922	0.0092
Total	14	920.9390	65.7814

Corrected for the mean of the observations:

	DF	SS	MS	F	P
Regression	3	60.5516	20.1839	2190.0447	<0.0001
Residual	10	0.0922	0.0092		
Total	13	60.6438	4.6649		

Statistical Tests:
Normality Test (Shapiro-Wilk) Passed (P = 0.8395)
W Statistic= 0.9674 Significance Level = 0.0500
Constant Variance Test Passed (P = 0.1524)

H.4 Verification June 24, 2008

Result Summary of SIGMAPLOT Analysis : Verification IIC

Charging Minutes	T_c (°C)	T_h (°C)	C	S	R^2
0.0	7.52	14.29	2.93	1.43	0.9918
59.7	7.40	14.28	4.11	1.57	0.9969
119.4	7.37	14.28	5.15	1.37	0.9935
179.1	7.24	14.28	6.32	1.21	0.9960
238.8	7.01	14.18	7.42	1.19	0.9979
298.5	6.99	14.11	8.41	1.30	0.9989
358.2	6.81	14.00	9.47	1.29	0.9992
417.9	6.77	13.87	10.60	1.45	0.9994
477.6	6.74	13.70	11.65	1.07	0.9975

Result of SIGMAPLOT processing: **June 24, 2008 (Verification Data IIC)**

Data set: 0.0 minutes, verification data IIC

Nonlinear Regression - Dynamic Fitting **Friday, July 30, 2010, 11:08:03 AM**

Data Source: Data 1 in Notebook3
Equation: Ligand Binding, sigmoidal dose-response (variable slope)
f=Tc + (Th-Tc)/(1+10^((C-x)*S))

Dynamic Fit Options:

Total Number of Fits	200
Maximum Number of Iterations	200

Parameter Ranges for Initial Estimates:

	Minimum	**Maximum**
Tc	-7.5609	22.6827
Th	-14.8668	44.6005
C	-2.9990	8.9969
S	-1.0000	3.0000

Summary of Fit Results:

Converged	100.0%
Singular Solutions	53.5%
Ill-Conditioned Solutions	0.5%

Results for the Overall Best-Fit Solution:

R	**Rsqr**	**Adj Rsqr**	**Standard Error of Estimate**
0.9837	0.9918	0.9634	0.4718

	Coefficient	**Std. Error**	**t**	**P**
Tc	7.5210	0.3810	19.9073	<0.0001
Th	14.2918	0.1519	91.8586	<0.0001
C	2.9331	0.1372	20.7822	<0.0001
S	1.4334	0.3114	3.6750	0.0043

Analysis of Variance: **(Appendix H.4 cont.)**

Analysis of Variance:

	DF	SS	MS
Regression	4	2321.0688	580.2672
Residual	10	2.2257	0.2226
Total	14	2323.2945	165.9496

Corrected for the mean of the observations:

	DF	SS	MS	F	P
Regression	3	76.7556	25.5852	114.9521	<0.0001
Residual	10	2.2257	0.2226		
Total	13	78.9813	6.0755		

Statistical Tests:

Normality Test (Shapiro-Wilk) Passed (P = 0.7339)

W Statistic= 0.9607 Significance Level = 0.0500

Constant Variance Test Passed (P = 0.1128)

Data set: 59.7 minutes , verification data IIC (Appendix H.4 cont.)

Nonlinear Regression - Dynamic Fitting **Friday, July 30, 2010, 11:08:17 AM**

Data Source: Data 1 in Notebook3
Equation: Ligand Binding, sigmoidal dose-response (variable slope)
f=Tc + (Th-Tc)/(1+10^((C-x)*S))

Dynamic Fit Options:

Total Number of Fits	200
Maximum Number of Iterations	200

Parameter Ranges for Initial Estimates:

	Minimum	Maximum
Tc	-7.2990	21.8970
Th	-14.5953	43.7859
C	-4.0572	12.1715
S	-1.0000	3.0000

Summary of Fit Results:

Converged	100.0%
Singular Solutions	55.5%
Ill-Conditioned Solutions	0.5%

Results for the Overall Best-Fit Solution:

R	Rsqr	Adj Rsqr	Standard Error of Estimate
0.9938	0.9969	0.9838	0.3629

	Coefficient	Std. Error	t	P
Tc	7.4021	0.2324	31.3809	<0.0001
Th	14.2810	0.1246	111.2514	<0.0001
C	4.1090	0.1044	37.8936	<0.0001
S	1.5720	0.1931	5.3516	0.0003

Analysis of Variance:
Analysis of Variance:

	DF	SS	MS
Regression	4	2124.2701	531.0675
Residual	10	1.3173	0.1317
Total	14	2125.5874	151.8277

Corrected for the mean of the observations:

	DF	SS	MS	F	P
Regression	3	104.4022	34.8007	264.1923	<0.0001
Residual	10	1.3173	0.1317		
Total	13	105.7195	8.1323		

Statistical Tests:

Normality Test (Shapiro-Wilk)	Passed (P = 0.2907)
W Statistic= 0.9285	Significance Level = 0.0500
Constant Variance Test	Passed (P = 0.1383)

Data set: 119.4 minutes, verification data IIC (Appendix H.4 cont.)

Nonlinear Regression - Dynamic Fitting **Friday, July 30, 2010, 11:08:50 AM**

Data Source: Data 1 in Notebook3
Equation: Ligand Binding, sigmoidal dose-response (variable slope)
f=Tc + (Th-Tc)/(1+10^((C-x)*S))

Dynamic Fit Options:

Total Number of Fits	200
Maximum Number of Iterations	200

Parameter Ranges for Initial Estimates:

	Minimum	Maximum
Tc	-7.1540	21.4621
Th	-14.2428	42.7283
C	-5.1394	15.4183
S	-1.0000	3.0000

Summary of Fit Results:

Converged	99.5%
Singular Solutions	60.0%
Iterations Exceeding 200	0.5%

Results for the Overall Best-Fit Solution:

R	Rsqr	Adj Rsqr	Standard Error of Estimate
0.9870	0.9935	0.9929	0.2589

	Coefficient	Std. Error	t	P
Tc	7.3663	0.1397	51.3290	<0.0001
Th	14.2837	0.0957	144.0289	<0.0001
C	5.1539	0.0740	68.9963	<0.0001
S	1.3708	0.1291	7.5898	<0.0001

Analysis of Variance:
Analysis of Variance:

	DF	SS	MS
Regression	4	1936.2331	484.0583
Residual	10	0.6705	0.0670
Total	14	1936.9035	138.3503

Corrected for the mean of the observations:

	DF	SS	MS	F	P
Regression	3	122.7318	40.9106	610.1789	<0.0001
Residual	10	0.6705	0.0670		
Total	13	123.4023	9.4925		

Statistical Tests:
Normality Test (Shapiro-Wilk) Passed (P = 0.7776)
W Statistic= 0.9633 Significance Level = 0.0500
Constant Variance Test Passed (P = 0.0306)

Data set: 179.1 minutes, verification data IIC (Appendix H.4 cont.)

Nonlinear Regression - Dynamic Fitting **Friday, July 30, 2010, 11:09:33 AM**

Data Source: Data 1 in Notebook3
Equation: Ligand Binding, sigmoidal dose-response (variable slope)
f=Tc + (Th-Tc)/(1+10^((C-x)*S))

Dynamic Fit Options:

Total Number of Fits	200
Maximum Number of Iterations	200

Parameter Ranges for Initial Estimates:

	Minimum	Maximum
Tc	-7.0496	21.1487
Th	-14.0339	42.1017
C	-6.2725	18.8176
S	-1.0000	3.0000

Summary of Fit Results:

Converged	100.0%
Singular Solutions	63.0%

Results for the Overall Best-Fit Solution:

R	Rsqr	Adj Rsqr	Standard Error of Estimate
0.9920	0.9960	0.9966	0.1861

	Coefficient	Std. Error	t	P
Tc	7.2412	0.0874	81.0862	<0.0001
Th	14.2756	0.0752	182.6895	<0.0001
C	6.3185	0.0513	122.6070	<0.0001
S	1.2110	0.0976	9.9022	<0.0001

Analysis of Variance:
Analysis of Variance:

	DF	SS	MS
Regression	4	1753.9535	438.4884
Residual	10	0.3462	0.0346
Total	14	1754.2997	125.3071

Corrected for the mean of the observations:

	DF	SS	MS	F	P
Regression	3	133.6245	44.5415	1286.6595	<0.0001
Residual	10	0.3462	0.0346		
Total	13	133.9707	10.3054		

Statistical Tests:

Normality Test (Shapiro-Wilk)	Passed (P = 0.9850)
W Statistic= 0.9820	Significance Level = 0.0500
Constant Variance Test	Passed (P = 0.0016)

<u>Data set: 238.8 minutes, verification data IIC</u> **(Appendix H.4 cont.)**

Nonlinear Regression - Dynamic Fitting **Friday, July 30, 2010, 11:09:46 AM**

Data Source: Data 1 in Notebook3
Equation: Ligand Binding, sigmoidal dose-response (variable slope)
f=Tc + (Th-Tc)/(1+10^((C-x)*S))

Dynamic Fit Options:

Total Number of Fits	200
Maximum Number of Iterations	200

Parameter Ranges for Initial Estimates:

	Minimum	Maximum
Tc	-6.9748	20.9245
Th	-13.9287	41.7860
C	-7.4092	22.2275
S	-1.0000	3.0000

Summary of Fit Results:

Converged	99.5%
Singular Solutions	69.5%
Iterations Exceeding 200	0.5%

Results for the Overall Best-Fit Solution:

R	Rsqr	Adj Rsqr	Standard Error of Estimate
0.9958	0.9979	0.9981	0.1407

	Coefficient	Std. Error	t	P
Tc	7.0130	0.0582	121.2273	<0.0001
Th	14.1836	0.0620	220.9694	<0.0001
C	7.4213	0.0340	218.2587	<0.0001
S	1.1859	0.1041	10.7244	<0.0001

Analysis of Variance:
Analysis of Variance:

	DF	SS	MS
Regression	4	1585.4284	396.3571
Residual	10	0.1979	0.0198
Total	14	1585.6263	113.2590

Corrected for the mean of the observations:

	DF	SS	MS	F	P
Regression	3	136.4210	45.4737	2298.3564	<0.0001
Residual	10	0.1979	0.0198		
Total	13	136.6188	10.5091		

Statistical Tests:

Normality Test (Shapiro-Wilk)	Passed (P = 0.6484)
W Statistic= 0.9555	Significance Level = 0.0500
Constant Variance Test	Passed (P = 0.0560)

Data set: 298.5 minutes, verification data IIC (Appendix H.4 cont.)

Nonlinear Regression - Dynamic Fitting **Friday, July 30, 2010, 11:09:59 AM**

Data Source: Data 1 in Notebook3
Equation: Ligand Binding, sigmoidal dose-response (variable slope)
f=Tc + (Th-Tc)/(1+10^((C-x)*S))

Dynamic Fit Options:

Total Number of Fits	200
Maximum Number of Iterations	200

Parameter Ranges for Initial Estimates:

	Minimum	Maximum
Tc	-6.8984	20.6952
Th	-13.8664	41.5993
C	-8.5669	25.7008
S	-1.0000	3.0000

Summary of Fit Results:

Converged	99.5%
Singular Solutions	70.0%
Iterations Exceeding 200	0.5%

Results for the Overall Best-Fit Solution:

R	Rsqr	Adj Rsqr	Standard Error of Estimate
0.9978	0.9989	0.9985	0.1238

	Coefficient	Std. Error	t	P
Tc	6.9900	0.0461	150.4271	<0.0001
Th	14.1149	0.0607	224.0396	<0.0001
C	8.4086	0.0250	341.6492	<0.0001
S	1.3004	0.1537	8.8159	<0.0001

Analysis of Variance:
Analysis of Variance:

	DF	SS	MS
Regression	4	1409.2612	352.3153
Residual	10	0.1534	0.0153
Total	14	1409.4146	100.6725

Corrected for the mean of the observations:

	DF	SS	MS	F	P
Regression	3	133.8093	44.6031	2908.2366	<0.0001
Residual	10	0.1534	0.0153		
Total	13	133.9626	10.3048		

Statistical Tests:

Normality Test (Shapiro-Wilk)	Passed (P = 0.5816)
W Statistic= 0.9513	Significance Level = 0.0500
Constant Variance Test	Passed (P = <0.0001)

Data set: 358.2 minutes, verification data IIC

Nonlinear Regression - Dynamic Fitting **Friday, July 30, 2010, 11:10:12 AM**

Data Source: Data 1 in Notebook3
Equation: Ligand Binding, sigmoidal dose-response (variable slope)
f=Tc + (Th-Tc)/(1+10^((C-x)*S))

Dynamic Fit Options:

Total Number of Fits	200
Maximum Number of Iterations	200

Parameter Ranges for Initial Estimates:

	Minimum	**Maximum**
Tc	-6.8580	20.5741
Th	-13.7175	41.1526
C	-9.7146	29.1439
S	-1.0000	3.0000

Summary of Fit Results:

Converged	99.5%
Singular Solutions	71.0%
Iterations Exceeding 200	0.5%

Results for the Overall Best-Fit Solution:

R	**Rsqr**	**Adj Rsqr**	**Standard Error of Estimate**
0.9984	0.9992	0.9991	0.0897

	Coefficient	**Std. Error**	**t**	**P**
Tc	6.8110	0.0309	222.9880	<0.0001
Th	13.9957	0.0528	256.1377	<0.0001
C	9.4709	0.0215	449.6441	<0.0001
S	1.2934	0.0877	14.4428	<0.0001

Analysis of Variance:
Analysis of Variance:

	DF	**SS**	**MS**
Regression	4	1240.9201	310.2300
Residual	10	0.0805	0.0081
Total	14	1241.0006	88.6429

Corrected for the mean of the observations:

	DF	**SS**	**MS**	**F**	**P**
Regression	3	116.3536	38.7845	4815.1023	<0.0001
Residual	10	0.0805	0.0081		
Total	13	116.4341	8.9565		

Statistical Tests:

Normality Test (Shapiro-Wilk)	Passed (P = 0.3848)
W Statistic= 0.9373	Significance Level = 0.0500
Constant Variance Test	Passed (P = 0.0101)

Data set: 417.9 minutes, verification data IIC (Appendix H.4 cont.)

Nonlinear Regression - Dynamic Fitting **Friday, July 30, 2010, 11:10:26 AM**

Data Source: Data 1 in Notebook3
Equation: Ligand Binding, sigmoidal dose-response (variable slope)
f=Tc + (Th-Tc)/(1+10^((C-x)*S))

Dynamic Fit Options:

Total Number of Fits	200
Maximum Number of Iterations	200

Parameter Ranges for Initial Estimates:

	Minimum	Maximum
Tc	-6.8000	20.4000
Th	-13.4818	40.4454
C	-10.8295	32.4886
S	-1.0000	3.0000

Summary of Fit Results:

Converged	99.5%
Singular Solutions	73.5%
Iterations Exceeding 200	0.5%

Results for the Overall Best-Fit Solution:

R	Rsqr	Adj Rsqr	Standard Error of Estimate
0.9988	0.9994	0.9995	0.0588

	Coefficient	Std. Error	t	P
Tc	6.7698	0.0191	360.1620	<0.0001
Th	13.8739	0.0447	300.4378	<0.0001
C	10.5960	0.0167	647.4669	<0.0001
S	1.4530	0.0446	26.7049	<0.0001

Analysis of Variance:
Analysis of Variance:

	DF	SS	MS
Regression	4	1074.7832	268.6958
Residual	10	0.0346	0.0035
Total	14	1074.8178	76.7727

Corrected for the mean of the observations:

	DF	SS	MS	F	P
Regression	3	91.3264	30.4421	8792.4139	<0.0001
Residual	10	0.0346	0.0035		
Total	13	91.3610	7.0278		

Statistical Tests:

Normality Test (Shapiro-Wilk)	Passed (P = 0.7367)
W Statistic= 0.9608	Significance Level = 0.0500
Constant Variance Test	Passed (P = 0.4346)

Data set: 477.6 minutes, verification data IIC (Appendix H.4 cont.)

Nonlinear Regression - Dynamic Fitting **Friday, July 30, 2010, 11:10:40 AM**

Data Source: Data 1 in Notebook3
Equation: Ligand Binding, sigmoidal dose-response (variable slope)
f=Tc + (Th-Tc)/(1+10^((C-x)*S))

Dynamic Fit Options:

Total Number of Fits	200
Maximum Number of Iterations	200

Parameter Ranges for Initial Estimates:

	Minimum	Maximum
Tc	-6.7741	20.3224
Th	-13.3459	40.0376
C	-11.9525	35.8574
S	-1.0000	3.0000

Summary of Fit Results:

Converged	99.0%
Singular Solutions	78.0%
Ill-Conditioned Solutions	0.5%
Iterations Exceeding 200	1.0%

Results for the Overall Best-Fit Solution:

R	Rsqr	Adj Rsqr	Standard Error of Estimate
0.9975	0.9975	0.9990	0.0689

	Coefficient	Std. Error	t	P
Tc	6.7393	0.0211	323.6221	<0.0001
Th	13.6988	0.0820	163.8337	<0.0001
C	11.6542	0.0231	518.2881	<0.0001
S	1.0700	0.0492	24.2827	<0.0001

Analysis of Variance:
Analysis of Variance:

	DF	SS	MS
Regression	4	914.2459	228.5615
Residual	10	0.0475	0.0047
Total	14	914.2934	65.3067

Corrected for the mean of the observations:

	DF	SS	MS	F	P
Regression	3	60.5753	20.1918	4253.2324	<0.0001
Residual	10	0.0475	0.0047		
Total	13	60.6228	4.6633		

Statistical Tests:
Normality Test (Shapiro-Wilk) Passed (P = 0.0283)
W Statistic= 0.8577 Significance Level = 0.0500
Constant Variance Test Passed (P = 0.0338)

REFERENCES

[1] ASHRAE, *HVAC Applications Handbook*, 1999.

[2] T. K, "Co-generation and the New Era of Absorption Chiller," *[online]* www.ashraethailand.org, August 2010.

[3] N. L. Minh, "Modeling and Analysis of Cogeneration-Based District Energy System," in *Mechanical Engineering*. vol. MSc: University of Western Ontario, 1996.

[4] F. DP, "Case Study of a Large, Naturally Stratified Chilled-Water Thermal Storage Systems," *ASHRAE Transaction,* vol. II, pp. 1161-1169, 1991.

[5] G. DP, "Succesfull Thermal Storage," *ASHRAE Transaction,* vol. IB, pp. 843-855, 1985.

[6] H. JH, *Cogeneration--combined heat and power (CHP): thermodynamics and economics*: Pergamon, Oxford, England, 1987.

[7] K. BF, *Small-scale Cogeneration Handbook*, 3rd ed.: Fairmont Press Inc, 2008.

[8] C. S, "The Perfect Match: Combined Cycles and District Heating/Cooling," *Power,* vol. 135, pp. 117-120, 1991.

[9] S. E. R. Institute, "Economic Aspect of District Heating and Cooling," *Heating/Piping/Air Conditioning,* vol. 59, No. 9, pp. 47-56, 1987.

[10] G. C, "District Energy Trend: Opportunities and Issues," *World Bank Technical Paper No. 493,* 2001.

[11] M. Fallek, "Absorption Chillers for Cogeneration Applications," *ASHRAE Transactions SF 1B,* vol. 92 (2), pp. 321-327, 1986.

[12] P. K. a. S. Devotta, "Study of an Absorption Refrigeration System for Simultaneous " *ASHRAE Transactions,* vol. 96 Part 2, pp. 291-298, 1990.

[13] R. M. Tozer, "Absorption Refrigeration (Principles, Cycles and Applications to Cogeneration)," *Conference Cogeneracion 92, Madrid 28-30,* pp. 170-175, 1992.

[14] R. M. T. a. R. W. James, "Absorption Chillers Applied to CHP Systems," *Building Services Engineering Research and Technology* vol. 16 (4), pp. 175–188, 1995.

[15] P. E. Hufford, "Absorption Chillers Maximize Cogeneration Value," *ASHRAE Transactions,* vol. 2(3) pp. 428-433, 1991.

[16] P. Hufford, "Absorption Chillers Improve Cogeneration Energy Efficiency," *ASHRAE Journals,* vol. 34, No.3, pp. 46-53
1992.

[17] A. Abedin, "Cogeneration : Balancing Heat Power ratio," *ASHRAE Journals,* pp. 23-37, 2003.

[18] A. OE, *Storage of Thermal Energy, in Energy Storage Systems*: Encyclopedia of Life Support System (EOLSS), Eolss Publishers, Oxford, UK, 2006.

[19] I. D. a. M. A. Rosen, "Energetic, Environmental and Economic Aspects of Thermal Energy Storage System for Cooling Capacity," *Applied Thermal Engineering,* vol. 21, pp. 1105-1107, 2001.

[20] T. K. G. t. C. Fitting, *[Online]. Available : http://www.synergy.com/Tools/curvefitting.pdf*, August 2009.

[21] ASHRAE, *Handbooks HVAC Applications*, 2003.

[22] E. M. a. G. Reeves, "Stratified Chilled Water Storage Design Guide," Electric Power Research Institute 1988.

[23] Y. Z. a. A. Ghajar, *Heat Transfer and Stratification in Sensible Heat Storage System, in Thermal energy Storage System and Applications, Eds, I Dincer and M Rosen*: John Willey and Sons 2002.

[24] N. T. a. J. Kreider, "Field Measurement of Chilled Water Storage Thermal Performance," *ASHRAE,* vol. 95 (1), pp. 1106-1112, 1989.
[25] EPRI, *Commercial Cool Storage Design Guide* Springer-Verlag, 1987.
[26] W. MW, "Diffuser Design for Naturally Startified Thermal Storage " *ASHRAE Transaction,* vol. I, pp. 1094-1101, 1990.
[27] D. I. a. R. MA, *Thermal Energy storage Systems and Applications*: John Wiley and Sons Ltd, 2001.
[28] A. Musser, "Field Measured and Modeled Performance of Full Scale Cylindrical Sttratified Chilled Water Stoerage Tanks," in *Graduate School*. vol. PhD: The Pennsylvania State University, 1998.
[29] W. SK, *Handbook of Air Conditioning and Refrigeration*, 2nd Edition ed.: Mc Graw Hill Company, 2000.
[30] C. E. Dorgan, Elleson and James S, *Design Guide for Cool Thermal Storage*: Atlanta, GA, 1994.
[31] ASHRAE, *HVAC Applications Handbook*, 2007.
[32] M. W. W. a. C. R. Truman., "Performance of Stratified Vertical Cylindrical Thermal Storage Tanks—Part 1: Scale Model Tank," *ASHRAE Transactions* vol. 95 (1), pp. 1086-1095, 1989.
[33] M. E. a. H. W. Wildin MW, "Thermal Storage Forum - Stratified Thermal Storage : A New/Old Technology," *ASHRAE Journal* vol. 32(4), pp. 29 - 39, 1990.
[34] A. M. a. W. Bahnfleth, "Evolution of Temperature Distributions in a Full-Scale Stratified Chilled-Water Storage Tank with Radial Diffusers," *ASHRAE Transaction,* vol. 104 (1), pp. 55-67, 1998.
[35] A. M. a. W. P. Bahnfleth, "Field-Measured Performance of Four Full-Scale Cylindrical Stratified Chilled-Water Thermal Storage Tanks," *ASHRAE Transaction* vol. 105 (2), pp. 218-230, 1998.
[36] J. S. a. C. J. Bahnfleth WP, "Measured and Modeled Charging of Stratified Chilled Water thermal Storage Tank with Slotted Pipe Diffusers," *HVAC&R Research,* vol. 9, No. 4, pp. 467-491, 2003.
[37] A. M. a. W. Bahnfleth, "Parametric Study of Charging Inlet Diffuser Performance in Stratified Chilled Water Storage Tanks with radial Diffusers: Part 2-Dimensional Analysis, Parametric Simulations and simplified Model Development," *HVAC&R Research,* vol. Vol. 7, No. 2, pp. 205-221, 2001.
[38] M. A. a. W. Bahnfleth, "Parametric Study of Charging Inlet Diffuser Performance in Stratified Chilled Water Storage Tanks with Radial Diffusers: Part 1-Model Development and Validation," *HVAC&R Research* vol. 7 No.1, pp. 31-49, 2001.
[39] J. S. a. W. Bahnfleth, "Parametric Study of Single-Pipe Diffusers in Stratified Chilled Water Storage Tanks," *HVAC&R Research,* vol. Vol. 10, No. 3, pp. 345-364, 2004.
[40] J. S. a. W. Bahnfleth, "Constant Flowrate Charging Characteristics of a Full-Scale Stratified Chilled Water Storage Tank with Double-Ring Slotted pipe Diffusers," *Applied Thermal Engineering* pp. 3067-3082, 2005.
[41] J. C. a. W. Bahnfleth, "Identification of Mixing Effects in Stratified Chilled-Water Storage Tanks by Analysis of Time Series Temperature Data," *ASHRAE Transaction,* vol. 104 (2), pp. 366-376, 1998.
[42] A. B. a. S. S. M. JEB Nelson, "Experiments on Stratified Chilled-Water Tanks," *International Journal of Refrigeration,* vol. 22, pp. 216-234, 1999.

[43] M. Karim, "Performance Evaluation of A Stratified Chilled-Water Thermal Storage System," *World Academy of Science Engineering and Technology,* vol. 53, pp. 328-334, 2009.

[44] M. J. A. a. J. R. M.R.W. Walmsley, "Thermocline Management of Stratified Tanks for Thermal Storage," *Proceedings of 12th International Conference on Process Integration, Modelling and Optimisation for Energy Saving and Pollution Reduction. AIDIC, Rome, Italy; 10-13 May,* pp. 231-236, 2009.

[45] W. M. a. T. C. Yoo J, "Initial Formation of Thermocline in Stratified Thermal Storage tanks," *ASHRAE Transaction,* vol. 92(2A), pp. 280-292, 1986.

[46] S. a. S. Homan K, "Thermal Performance of Stratified Chilled Water Storage Tanks," *HVAC&R Research,* vol. 2, pp. 158-170, 1996.

[47] W. B. a. A. Musser, "Thermal Performance of a Full Scale Stratified Chilled Water Storage Tank," *ASHRAE Transaction* vol. 104(2), pp. 377-388, 1998.

[48] J. W. a. M. A. A. Majid, "Temperature Profile and Thermocline Thickness Evaluation of a Stratified Thermal Energy Storage Tank," *International Journal of Mechanical & Mechatronics Engineering IJMME-IJENS* vol. 10, No.1, pp. 7-12, 2010.

[49] M. A. a. W. Joko, "Thermocline Thickness Evaluation on Stratified Thermal Energy Storage Tank of Co-generated District Cooling Plant," *Journal of Energy and Power Engineering,* vol. 4, No.2 pp. 28-33, 2010.

[50] J. W. a. M. A. A. Majid, "Performance Evaluation of Stratified TES using Sigmoid Dose Response Function," *International Conference on Plant Equipment and Reliability, 15-17 June 2010, Kuala Lumpur, Malaysia,* 2010.

[51] A. B. a. S. S. M. JEB Nelson, "Parametric Studies on Thermally Startified Chilled Water Storage Systems," *Applied Thermal Engineering,* vol. 19, pp. 89-115, 1999.

[52] W. MW, "Flow Near the Inlet and Design Parameter for Stratified Chilled Water Storage," *ASME 91-HT-27,* 1991.

[53] H. C. a. M. CW, "An Experimental and Numerical Study on the Effect of the Wall in a Cylindrical Exposure," *Solar energy,* vol. 28, pp. 145-152, 1982.

[54] J. Y. a. G. SK, "Decay of of Thermal Stratification in water Body for Solar Energy Storage," *Solar energy,* vol. 28, pp. 137-143, 1982.

[55] R. G. a. H. K. Lighsone MF, "Numerical Simulation of the charging of Liquid Storage Tanks; Comparison with experiment," *Journal of Solar Energy Engineering* vol. Vol 111, pp. 225-231, 1989.

[56] S. C. a. S. S. Homan K, "Thermal Performance of Stratified Chilled Water Storage Tanks " *HVAC&R Research,* vol. Vol. 2, pp. 158-170, 1996.

[57] A. G. a. P. M. YH Zurigat, "A Comparison Study of One-Dimensional Models for Stratified Thermal Storage Tanks," *Transaction of ASME,* vol. 111, pp. 204-210, 1989.

[58] M. W. a. C. Truman, "A Summary of Experience with Stratified Chilled Water Tanks " *ASHRAE Transactions* vol. 91 (1b), pp. 956-976, 1985.

[59] Y. J. a. K. Thomas, *Computational Heat Transfer*, 2nd ed., 2003.

[60] G. RJ, "An Experimental Study of Single Medium Thermocline Thermal Energy Storage," *ASME Paper 82-HT-53,* 1982.

[61] W. B. a. S. K. EM Kleinback, "Performance Study of One-Dimensional Moels for Stratified Thermal Storage Tanks," *Solar Energy,* vol. 50, pp. 155-166, 1993.

[62] V. Badescu, "Optimal Operation of Thermal Energy Storage Units Based on Stratified and Fully Mixed Water Tanks," *Applied Thermal Engineering 24,* pp. 2101-2116, 2004.

[63] P. C. a. S. R. Gretarsson SP, "Development of Fundamentally Based Stratified Thermal Storage Tank Model for Energy Calculation," *ASHRAE Transaction,* vol. Vol. 100 pp. 1213-1220, 1994.

[64] J. D. a. N. Farnum, *Applied Statistics for Engineers and Scientist*, 2nd ed.: Thomson Learning Inc, 2005.

[65] Y. J. a. K. Homan, "On Simplified Models for the Rate and Time Dependent Performance of Stratified Thermal Storage," *Transaction of ASME,* vol. 129, pp. 214-222, 2007.

[66] J. Y, *Design and Optimization of Thermal Systems*: CRC Press, 2008.

[67] I. F. a. D. DP, *Introduction to Heat Transfer*: John Wiley and Sons, 2002.

[68] N. A.-N. N. El-Refaee, "A Numerical Study for the Prediction of Turbulent Mixing factor in Thermal Storage Tank," *Applied Thermal Engineering,* vol. Vol. 17, No. 12, pp. 1173-1181, 1997.

[69] O. MN, *Heat Conduction*, 2nd ed.: John Wiley and Sons, Inc., 1993.

[70] C. S. a. C. RP, *Numerical Methods for Engineers*, 6 ed.: Mc Graw Hill International Edition, 2009.

[71] H. JP, *Heat Transfer*, 10 ed.: Mc Graw Hill Higher Education, 2009.

[72] J. Y. a. T. KE, *Computational Heat Transfer*, 2 ed.: Taylor and Francis, 2003.

[73] G. C. a. W. PO, *Applied Numerical Analysis* 7th ed.: Addison-Wesley Publishing Company, 2004.

[74] O. MN, *Finite Difference Methods in Heat Transfer*: CRC Press Inc, 1994.

[75] M. A. A. M. a. C. R. J. Waluyo, "Analysis of Temperature Distribution of Chilled-Water Thermal Storage Tank," *National Postgraduate Conference, Universiti Teknologi PETRONAS, 25-26 March 2009,* pp. 1-5, 2009

[76] A. G. a. P. M. FJ Oppel, "Computer Simulation of Stratified Heat Storage," *Applied Energy,* vol. 23, pp. 293-, 1986.

[77] A. G. a. P. M. FJ Oppel, "A Numerical and Experiment Study of Stratified Thermal Storage," *ASHRAE Transaction,* vol. 92, No. 2, pp. 293-309, 1986.

[78] C. N. D. a. T. F. Dupont, "Explicit/implicit Conservative Domain Decomposition Procedures for Parabolic Problems Based on bBlock-Centered Finite Differences," *SIAM Journal on Numerical Analysis,* vol. 31. no. 4, pp. 1045-1061, 1994.

[79] W. M. a. T. CR, "Evaluation of Stratified Chilled Water Storage Technique," EPRI Report 1985.

[80] A. G. a. P. M. YH Zurigat, "Stratified Thermal Storage Inlet Mixing Characterization," *Applied Energy,* vol. 30, pp. 99-111, 1988.

[81] T. S. Votsis PP, Wilson DR and Marquand CJ, "Experimental and Theoretical of Mixed and Stratified Water Storage Tanks," *Proceedings of the Institution of Mechanical Engineers, Part-C Journal of Mechanical Engineering Science* vol. Vol. 202, pp. 187-193, 1988.

[82] W. MW, "Performance of Stratifified Vertical Cylindrical Thermal Storage tank, Part 2; Prototype Tank," *ASHRAE Transaction 95(1),* pp. 1096-1105, 1989.

[83] J. W. a. T. J. Whitman WC, *Refrigeration and Air Conditioning Technology* 5th ed.: Thompson Delmar Learning 2005.

[84] W. S. a. J. Jones, *Refrigeration and Air Conditioning*, 2 ed.: Mc Graw Hill International Editions, 1982.
[85] D. Ibrahim, *Refrigeration Systems and Applications*: John Wiley and Sons 2003.
[86] C. HR, *HVAC System Evaluation*. New York: RS Means, 1990.
[87] K. JF, *Handbook of Heating, Ventilating and Air Conditioning*: CRC Press, 2001.
[88] K. EA, "The Modeling, Performance and Optimal Control of Commercial Absorption Chillers," in *Mechanical Department* vol. MSc: University of Wisconsin, 1994.
[89] ASHRAE, *ASHRAE Refrigeration Handbook*, 2002.
[90] R. R. a. S. K. KE Herold, *Absorption Chillers and Heat Pumps*: CRC Press. Inc, 1996.
[91] V. M. Izquierdo M, Rodriquez P and Leucona A, "Crystallization as a Limit to develop Solar Air-Cooled LiBr-H2O Absorption System Using Low-Grade Heat," *Solar Energy Materials and Solar Cells,* vol. 81, pp. 205-216, 2004.
[92] K. S. GA Florides, Tassou SA and Wrobel LC, "Design and Construction of a LiBr-Water Absorption Machine," *Energy Conversion and management,* vol. Vol. 44, pp. 483-2508, 2003.
[93] R. R. Xiaohong Liaoa, "Absorption chiller crystallization control strategies for integrated cooling heating and power systems," *International Journal of Refrigeration* vol. 30, pp. 904-911, 2007.
[94] S. C. Sugarman, *HVAC Fundamentals*: Fairmont Press Inc, 2005.
[95] A. A. Bell, *HVAC equations, data and ruleof thumbs*, 2 ed.: Mc Graw Hill Book
2008.
[96] F. Kreith, *Handbook of Thermal Engineering*: Springer, 2000.
[97] C. C. a. Marshal, "Simulation of Refrigerating and Air Conditioning Equipment Based on Experiment Data," *ASHRAE Transaction,* vol. 97, pp. 388-393, 1991.
[98] G. J. a. N. KC, "Thermodynamic Modeling for Reciprocating Chillers," *Journal of Applied Physics,* vol. 75 (6), pp. 2769-2774, 1994.
[99] P. C. a. C. G. Strand RK, "Development of Direct and Indirect Ice-Storage for Energy Calculations," *ASHRAE Transaction,* vol. 100, Part. 1, pp. 1230-1244, 1994.
[100] M. M. Figuera LE, Cathey M and Nutre DW, "Modification and Validation of a Universal Thermodynamic Chiller Model Used to Evaluate the Performance of Water Cooled Centrifugal Chillers," *The Eleventh Symposium on Improving Building Systems in Hot nd Humid Climates, Texas,* pp. 57-65, 1998.
[101] R. D. a. K. S. Jahing DI, "A Semi Empirical Method for Representing Domestic Refrigerator/Freezer Compressor Calorimeter Test Data," *ASHRAE Transaction,* vol. 106 (2), pp. 122-130, 2000.
[102] M. J. a. B. A. McIntosh IIBD, "Fault Detection and Diagnosis Part (I), Model Development and Application," *ASHRAE Transaction,* vol. 106 (2), pp. 268-282, 2000.
[103] G. G. a. Michelson, "A Modular Computer Simiulation of Absorption Systems," *ASHRAE Transaction,* vol. 91 (2B), pp. 1808-1827, 1985.

[104] G. K. a. G. D. Grossman G, "Computer Model for Simulation of Absorption Systems in Flexible and Modular Form," *ASHRAE Transaction,* vol. 93 (2), pp. 1590-1598, 1987.
[105] G. K. a. G. G, "Performance of Staged Absorption Heat Pumps : Water-Lithium Bromide Systems," *ASHRAE Transaction,* vol. 96 (1), pp. 1590-1598, 1990.
[106] W. M. a. D. R. Grossman G, "Simulation and Performance Analysis of Triple-Effect Absorption Chiller Cycles," *ASHRAE Transaction,* vol. 100 Part.1, pp. 452-462, 1994.
[107] S. J. a. P.-B. H, "Simple Model for Calculating Performance of Lithium Bromide/Water Coil Absorber " *ASHRAE Transaction,* vol. 100 Part. 2, pp. 318-328, 1999.
[108] H. H. a. Z. FF, "Simple Absorption Heat Pump Modules for System Simulation Program," *ASHRAE Transaction,* vol. 105 Part. 1, pp. 780-787, 1999.
[109] M. A. A. M. a. C. R. Joko Waluyo, "Simulation of Generated Chilled Water of a Cogeneration Plant," *International Conference on Plant Equipment and Reliability, 27-28 March 2008, Selangor, Malaysia,* 2008.
[110] ASHRAE, "ASHRAE Fundamental Handbooks," ASHRAE, 2005.
[111] W. Stoecker, *Design of Thermal System*, 3rd ed.: Mc. Graw Hill International Editions, 1989.
[112] 1994, *Practical Handbook of Curve Fitting*: CRC Press, 1994.
[113] J. R. Hauser, *Numerical Methods for Nonlinear Engineering Models*: Springer, 2009.
[114] E. N. Virtanen, *Applied Mathematical Modeling*: Nova Publishers, 2008.
[115] S. S. Inc, "Regression Equation Library," in *SIGMAPLOT User's Guide*, Systat Software Inc. ed, 2008.
[116] S. G. a. W. CJ, *Non Linear Regression* John Wiley and Sons, 2003.
[117] B. D. a. W. DG, *Non Linear Regression Analysis and Its Applications*, 2nd ed.: John Wiley and Sons Inc., 2007.
[118] D. E. a. M. Little, "Nonlinear Regression Analysis and Nonlinear Simulation Models," *SAS Institute Inc.*
[119] S. S. Inc, "SigmaPlot 11 User's Guide," 2008.